# SHORT TITLE

CHEN "LIQUID-LIQUID EXTRACTION UNDER ULTRASONIC VIBRATION"

# LIQUID-LIQUID EXTRACTION IN A SPRAY COLUMN UNDER ULTRASONIC VIBRATION

bу

ERH-CHUN CHEN, B.Sc., M. Eng.

A thesis submitted to the Faculty of Graduate Studies and Research in partial fulfilment of the requirements for the degree of Doctor of Philosophy

Chemical Engineering Department,

March, 1968

McGill University,

Montreal.

# LIQUID-LIQUID EXTRACTION IN A SPRAY COLUMN UNDER ULTRASONIC VIBRATION

by

#### ERH-CHUN CHEN

#### ABSTRACT

Experiments were carried out to investigate the effect of ultrasonic vibration on the liquid-liquid extraction in a spray-type column. The ultrasonic source was at the bottom of the column and water-acetic acid-methyl isobutyl ketone was used as a test system. The results indicated that there was an appreciable increase in the extraction efficiency when the system was subjected to ultrasonic vibration. The increase was found to be due to either a reduction in the average droplet size or an increase in turbulence at the aqueous-organic interface, depending on whether the light or the heavy phase was dispersed.

Empirical correlations have been developed for predicting the increase in the capacity coefficient and the decrease in the average drop diameter due to ultrasonic vibration. Methods for correlating the interfacial area of contact and overall mass transfer coefficient in a spraytype liquid-liquid extraction column under ultrasonic vibration have also been proposed.

## ACKNOWLEDGEMENTS

The author wishes to express his sincere appreciation to Dr. W.Y. Chon for his continued interest in directing this research. He is also indebted to:

Dr. I. Pliskin for many of his valuable suggestions.

The Eldorado Mining and Refining Company, Ltd., Port Hope, Ontario, for its financial support of this investigation.

Mr. B.B. Pruden for reviewing the manuscript.

Mr. A. Nowacki for his assistance in the photographic work.

His parents for their constant encouragement, and his wife for her untiring perseverence throughout these past years.

# TABLE OF CONTENTS

**ACKNOWLE DGEMENTS** 

TABLES OF CONTENTS			
LIST OF ILLUSTRATIONS			
LIST OF TABLES			
GENERAL INTRODUCTION  LITERATURE SURVEY	1		
INTRODUCTION	3		
EXTRACTION IN A SPRAY COLUMN	4		
(1) Column Performance	4		
(2) Holdup	8		
(3) Axial Mixing and Concentration Gradient	10		
(4) Mass Transfer Correlation	11		
DROPLET BEHAVIOUR IN A SPRAY COLUMN	19		
(1) Size	19		
(2) Velocity	21		
(3) Shape	24		
(4) Coalescence at the Interface	26		
PULSED COLUMNS PERFORMANCE	29		
(1) Sieve-Plate Type	29		
(2) Packed Type	33		
(3) Spray Type	35		

BACKGROUND INFORMATION ON ULTRASONIC VIBRATION	37
(1) Cavitation	38
(2) Intensity Measurement	41
(3) Threshold Intensity	44
GENERAL COMMENTS	47
NOMENCLATURE	51
REFERENCES	55
EXPERIMENTAL SECTION	
PART I. EFFECTS OF ULTRASONIC VIBRATION ON THE EXTRACTION EF	FICIENCY
INTRODUCTION	61
APPARATUS AND PROCEDURE	62
CALCULATION OF THE EXTRACTION EFFICIENCY	71
EXPERIMENTAL RESULTS	73
ANALYSIS AND DISCUSSION OF RESULTS	86
CONCLUSIONS	103
NOMENCLATURE	105
REFERENCES	107
PART II. EFFECTS OF ULTRASONIC VIBRATION ON THE DROPLET SIZE COALESCENCE AT THE INTERFACE	AND
INTRODUCTION	108
APPARATUS AND PROCEDURE	109
EXPERIMENTAL RESULTS	111
ANALYSIS AND DISCUSSION OF RESULTS	111

CONCLUSIONS	127
NOMENCLATURE	128
REFERENCES	129
PART III. THE MECHANISM OF EXTRACTION UNDER ULTRASONIC VIBRATION	
INTRODUCTION	130
APPARATUS AND PROCEDURE	131
METHODS OF CALCULATION	132
RESULTS AND DISCUSSION	134
CONCLUSIONS	152
NOMENCLATURE	154
REFERENCES	156
APPENDICES	
A. RESULTS OF THE PRELIMINARY INVESTIGATION	157
B. TRANSDUCERS USED IN THIS WORK	158
C. ROTAMETER CALIBRATION CURVES	159
D. PHYSICAL PROPERTIES OF THE SYSTEM:	
WATER-ACETIC AGID-METHYL ISOBUTYL KETONE	160
E. EXPERIMENTAL AND CALCULATED DATA	161
F. ANALYSIS OF ERROR IN THE MATERIAL BALANCE FOR ACETIC ACID	162
SUMMARY AND CONTRIBUTIONS TO KNOWLEDGE	163
SUGGESTIONS FOR FUTURE WORK	166

# LIST OF ILLUSTRATIONS

# EXPERIMENTAL SECTION

PART I.	EFFECTS OF ULTRASONIC VIBRATION ON THE EXTRACTION EFFICIENCY	
FIGURE 1	. FLOW DIAGRAM OF EXPERIMENTAL SYSTEM	63
fïgurë 2	PHOTOGRAPH OF THE EXTRACTION COLUMN	64
FIGURE 3	. PHOTOGRAPH OF THE TRANSDUCERS	66
FIGURE 4	. PHOTOGRAPH OF THE INSTRUMENTATION	68
FIGURE 5	THERMOCOUPLE PROBE	70
FIGURE 6	EFFECT OF ULTRASONIC VIBRATION ON $K_{W}$ a FOR MIBK PHASE DISPERSED $(F_{m}/F_{W} = 2.158)$	78
FIGURE 7	EFFECT OF ULTRASONIC VIBRATION ON $K$ a FOR MIBK PHASE DISPERSED $(F_m/F_w = 1.147)$	79
FIGURE 8	EFFECT OF ULTRASONIC VIBRATION ON $K_{\mathbf{w}}$ FOR MIBK PHASE DISPERSED $(F_{\mathbf{m}}/F_{\mathbf{w}} = 0.462)$	80
FIGURE 9	EFFECT OF ULTRASONIC VIBRATION ON $_{\rm W}^{\rm K}$ a FOR WATER PHASE DISPERSED ( $_{\rm m}^{\rm F}/_{\rm W}^{\rm F}=2.158$ )	81
FIGURE 1	0 EFFECT OF ULTRASONIC VIBRATION ON $K_{\mathbf{w}}$ a FOR WATER PHASE DISPERSED $(F_{\mathbf{m}}/F_{\mathbf{w}} = 1.147)$	82
FIGURE 1	1 EFFECT OF ULTRASONIC VIBRATION ON $K_{W}$ a FOR WATER PHASE DISPERSED $(F_{m}/F_{W} = 0.462)$	83
FIGURE 1	2 EFFECT OF NOZZLE SIZE ON THE PERCENT INCREASE IN  K a FOR MIBK PHASE DISPERSED  W	84
FIGURE 1	3 EFFECT OF NOZZLE SIZE ON THE PERCENT INCREASE IN K a FOR WATER PHASE DISPERSED	85

FIGURE	14	AXIAL INTENSITY PROFILE FOR THE 20 kc TRANSDUCER	87
FIGURE	15	AXIAL INTENSITY PROFILE FOR THE 40 kc TRANSDUCER	88
FIGURE	16	AXIAL INTENSITY PROFILE FOR THE 100 kc TRANSDUCER	89
FIGURE	17	K a VERSUS I/I' FOR MIBK PHASE DISPERSED	
	(	$(F_{\rm m}/F_{\rm w} = 2.158)$	91
FIGURE	18	K <sub>w</sub> a VERSUS I/I' FOR MIBK PHASE DISPERSED (F <sub>m</sub> /F <sub>w</sub> = 1.147)	92
FIGURE	19	K a VERSUS I/I' FOR MIBK PHASE DISPERSED	
		$(F_{\rm m}/F_{\rm w}=0.462)$	93
FIGURE	20	K a VERSUS I/I' FOR WATER PHASE DISPERSED	
		$(F_{\rm m}/F_{\rm w} = 2.158)$	94
FIGURE	21	K a VERSUS I/I' FOR WATER PHASE DISPERSED	
		$(F_{\rm m}/F_{\rm w} = 1.147)$	95
FIGURE	22	K a VERSUS I/I' FOR WATER PHASE DISPERSED	
		$(F_{\rm m}/F_{\rm w} = 0.462)$	96
FIGURE	23	CORRELATION FOR MIBK PHASE DISPERSED	99
FIGURE	24	CORRELATION FOR WATER PHASE DISPERSED	100
PART II	<u>.</u>	EFFECTS OF ULTRASONIC VIBTRAION ON THE DROPLET SIZE AND COALESCENCE AT THE INTERFACE	
FIGURE	1	SAMPLE DROP PHOTOGRAPHS	112
FIGURE	2	EFFECT OF ULTRASONIC VIBRATION ON D FOR MIBK DROPLETS IN WATER ( $D_{N} = 0.079$ cm)	113
FIGURE	3	EFFECT OF ULTRASONIC VIBRATION ON D FOR MIBK DROPLETS IN WATER ( $D_{N} = 0.163$ cm)	114
FIGURE	4	EFFECT OF ULTRASONIC VIBRATION ON D FOR MIBK DROPLETS IN WATER ( $D_{N} = 0.316$ cm)	115
FIGURE	5	EFFECT OF ULTRASONIC VIBRATION ON D FOR WATER DROPLETS IN MIBK ( $D_N = 0.163$ cm)	116

FIGURE	6	EFFECT OF ULTRASONIC VIBRATION ON D FOR WATER DROPLETS IN MIBK ( $D_{N} = 0.316$ and 0.079 cm)	117
FIGURE	7	EFFECT OF ULTRASONIC VIBRATION ON D FOR WATER DROPLETS IN TCE ( $D_N = 0.163$ cm)	118
FIGURE	8	EFFECT OF ULTRASONIC VIBRATION ON D FOR WATER DROPLETS IN TCE ( $D_N = 0.316$ and 0.079 cm)	119
FIGURE	9	EFFECT OF ULTRASONIC VIBRATION ON tr FOR WATER-3.49% ACETIC ACID-MIBK SYSTEM	120
FIGURE	10	EFFECT OF ULTRASONIC VIBRATION ON t FOR TCE-WATER SYSTEM	121
FIGURE	11	DROP SIZE CORRELATION	125
PART 11	i.	THE MECHANISM OF EXTRACTION UNDER ULTRASONIC VIBRATION	
			1
FIGURE	1	a VERSUS I/I' FOR MIBK PHASE DISPERSED (D <sub>N</sub> = 0.079 cm)	136
FIGURE	2	a VERSUS I/I' FOR MIBK PHASE DISPERSED $(D_N^{\perp} = 0.163 \text{ cm})$	137
FIGURE	3	a VERSUS I/I' FOR MIBK PHASE DISPERSED (DN = 0.316 cm)	138
FIGURE	4	K VERSUS I/I' FOR MIBK PHASE DISPERSED (Fm/Fw = 2.158)	139
FIGURE	5	Kw VERSUS I/I' FOR MIBK PHASE DISPERSED  (Fm/Fw = 1.147)	140
FIGURE	6	$K_{w}$ VERSUS I/I' FOR MIBK PHASE DISPERSED $(F_{m}/F_{w} = 0.462)$	141
FIGURE	7	K VERSUS I/I' FOR WATER PHASE DISPERSED  (F F = 2.158)	142
FIGURE	8	K VERSUS I/I' FOR WATER PHASE DISPERSED  (F M/F = 1.147)	143

٠.

•-

FIGURE		VERSUS I/I' FOR WATER PHASE DISPERSED $F_{m}/F_{w} = 0.462)$	<sup>"</sup> 144
APPEND	<u>ICES</u>		
		DETAILS OF THE CERAMIC DISTRIBUTOR	A-2
FIGURE	A-2	EFFECT OF ULTRASONIC INTENSITY ON K a	A-5
FIGURE	A-3	EFFECT OF ULTRASONIC FREQUENCY ON K a	A-6
FIGURE	A-4	RADIAL INTENSITY PROFILES FOR THE 20 kc TRANSDUCER	A-7
FIGURE	A-5	RADIAL INTENSITY PROFILES FOR THE 100 kc TRANSDUCER	A-8
FIGURE	C-1	ROTAMETER CALIBRATION CURVE FOR DISTILLED WATER AT 25°C	C-1
FIGURE	C-2	ROTAMETER CALIBRATION CURVE FOR 10% ACETIC ACID- MIBK SOLUTION	C-2
FIGURE	<b>D-1</b>	EQUILIBRIUM CURVE FOR WATER-ACETIC ACID-MIBK SYSTEM AT 25°C	D-1
FIGURE	D-2	DENSITY OF ACETIC ACID-MIBK SOLUTION AT 25°C	D- 2
FIGURE	D-3	VISCOSITY OF ACETIC ACID-MIBK SOLUTION AT 25°C	D-3
FIGURE	D-4	INTERFACIAL TENSION OF WATER-ACETIC ACID-MIBK SYSTEM AT 25°C	D-4

# LIST OF TABLES

# EXPERIMENTAL SECTION

	EFFECTS OF ULTRASONIC VIBRATION ON THE EXTRACTION EFFICIENCY	
TABLE 1	DETAILS OF THE TRANSDUCERS	65
TABLE 2	SUMMARY OF EXPERIMENTAL RESULTS (1)	74
TABLE 3	SUMMARY OF EXPERIMENTAL RESULTS (2)	76
	VALUES OF THE THRESHOLD INTENSITY FOR THE SYSTEM STUDIED AT 25°C	86
	EFFECTS OF ULTRASONIC VIBRATION ON THE DROPLET SIZE AND COALESCENCE AT THE INTERFACE	
TABLE 1	PHYSICAL PROPERTIES OF THE LIQUIDS USED AT 25°C	110
PART III.	THE MECHANISM OF EXTRACTION UNDER ULTRASONIC VIBRATION	ī. ·
TABLE 1	SUMMARY OF RESIDENCE TIME DATA	135
TABLE 2	INTERFACIAL AREA FOR WATER PHASE DISPERSED	146
TABLE 3	VALUES OF $lpha$	148
rable 4	VALUES OF β	149
TABLE 5	FRACTION EXTRACTED DATA	150
APPENDICES		
TABLE A-1	EXPERIMENTAL RESULTS (PRELIMINARY INVESTIGATION)	A-3.
TABLE B-1	IMPORTANT CONSTANTS FOR FERROXCUBE 7A2	B 2
TABLE B-2	IMPORTANT CONSTANTS FOR BARIUM TITANATE	B-3
TABLE E-1	CAPACITY COEFFICIENT DATA	E-1
TABLE E-2	AXIAL INTENSITY PROFILE DATA	E-10

CABLE E-3	MASS TRANSFER CORRELATION DATA	E-11
rable e-4	DROP SIZE DATA	E-18
TABLE E-5	REST TIME DATA	E-22
TABLE E-6	DROPLET CORRELATION DATA	E-24
TABLE E-7	INTERFACIAL AREA DATA	E-26
rable e-8	MASS TRANSFER COEFFICIENT DATA	E-28
TABLE F-1	ERROR IN THE MATERIAL BALANCE FOR ACETIC ACID	F- 2
TABLE F-2	ERROR IN THE MATERIAL BALANCE IF F IS INCREASED	
	BY A FACTOR OF 1.22	F- 6

#### GENERAL INTRODUCTION

Continuous countercurrent liquid-liquid extraction is a unit operation of chemical engineering which has occupied a position of increasing importance in recent years. Many difficult or expensive separations performed previously by using the more common methods such as evaporation, distillation, absorption and chemical precipitation can now be carried out more efficiently and cheaply by this operation. The process involves dispersion of one liquid as drops into an immiscible liquid and transfer of solutes from one phase to the other. It is usually carried out in columns provided there is a sufficient difference in density between the two liquid phases. Sieve-plate, packed and spray columns are the types encountered most frequently.

The extraction efficiency of the above mentioned columns is primarily dependent on the degree of turbulence imparted to the system and the interfacial area available for mass transfer. In practice, it can be increased by supplying additional energy for dispersion and agitation. The purpose of this study was to accumulate some knowledge for determining whether ultrasonic vibration, whose application to industrial processes has received considerably attention recently, could be used as a means of accomplishing this. A spray column was chosen for experimentation because of its simplicity of construction and operation, and because in this system the inter-

facial area could easily be calculated. Moreover, the dissipation of ultrasonic energy in a spray column was thought to be much less than in any other type of extractor.

LITERATURE SURVEY

### INTRODUCTION

In the past decades, the use of liquid-liquid extraction has increased rapidly and a great number of papers dealing with both theoretical and applied aspects of extraction have been published. Also, a sizable literature in the field of ultrasonic vibration and its application has appeared. It is, therefore, neither possible nor desirable to report all of these publications in this survey.

A knowledge of the extraction and droplet behaviour in a spray column is essential for this study, since the spray column was chosen for experimentation. It is also necessary to know about the performance of pulsed columns because the original idea of the present investigation was drawn from the successful development of such extractors. Accordingly, literature concerning the extraction and droplet behaviour in a spray column as well as the performance of pulsed columns is surveyed in the following parts. The background information on ultrasonic vibration is, of course, required, and in addition, general comments for all the papers reviewed are given at the end of the chapter.

## EXTRACTION IN A SPRAY COLUMN

## (1) Column Performance

In a spray column, mass transfer occurs between dispersed liquid drops and a continuous liquid phase. The rate of mass transfer, N, is governed by an equation of the type (1)

$$N = K \cdot a \cdot Z \cdot \Delta C \tag{1}$$

where K is the overall mass transfer coefficient, and "a" the interfacial area of contact between the phases. Whereas  $\Delta$  C is the concentration difference. The product of K and "a" is usually called a capacity coefficient and is often used to express the overall extraction efficiency of the column. Alternatively, the extraction efficiency of a spray column can be expressed in terms of the overall height of a transfer unit, HTU. The following is the relationship between Ka and HTU<sup>(2)</sup>

$$HTU = v/Ka$$
 (2)

where v is the superficial velocity and Ka is calculated from concentrations in the same phase to which v refers.

The first systematic study of a spray column was done by Elgin and Browning<sup>(3)</sup>, using the system of water-acetic acid-isopropyl ether. They found that Ka was affected by flow rates of both dispersed and continuous phases, direction of solute transfer, and drop size of the dispersed phase. In studying extraction from single drops, Sherwood

and coworkers (4) reported that Ka increased roughly in proportion to the dispersed phase flow rate and went through a maximum as the continuous phase flow rate was increased. They also determined the amount of extraction during drop formation by making a semilog plot of fraction extracted versus column height and extrapolating the line back to zero abscissa. The amount of extraction during drop formation, i.e., the ordinate intercept, was found to be about 40% of the total extraction.

Licht and Conway<sup>(5)</sup> separated the extraction process in a spray column into three stages, namely, drop formation, free rise or fall, and coalescence at the interface. For the extraction of acetic acid from water droplets by isopropyl ether, methyl isobutyl ketone and ethyl acetate, they found the extraction during drop formation to be 5,8 and 17% respectively, irrespective of drop size and formation time. These values are much less than that reported by Sherwood. The discrepancy was explained to be due to the difference in the direction of solute transfer.

Licht and Pansing<sup>(6)</sup> studied the effect of drop diameter on the extraction efficiency. The results of their investigation were presented graphically as logarithm fraction unextracted versus fall time of the drops using drop diameter as a parameter. The total extraction was found to increase with decrease of drop diameter. Nevertheless, the amount of extraction during the drop coalescence period was proportional to the drop diameter as well as to the entering concentration

of the drops. Since the plot was not a straight line all the way back to zero fall time, they claimed that the method of determining the amount of extraction during drop formation by extrapolation was incorrect.

Johnson and Bliss<sup>(7)</sup> carried out experimental work in a 1.824"I.D. spray column and concluded that Ka increased with both dispersed and continuous phase flow rates. The effect of dispersed phase flow rate on Ka was found to be due to the increase in the interfacial area. However, the effect of continuous phase flow rate was thought to be due partly to the reduction of effective film thickness, and also partly to the retarding effect on the rate of rise or fall of the drops which would result in an increase in the holdup and therefore the interfacial area. They also reported that Ka increased slightly with increase in entering solute concentration, and that mass transfer rate was greater when extraction was from continuous to dispersed phase. The effect of column height on Ka was found to be small. Other investigators<sup>(8,9)</sup>, however, reported an increase in HTU when the column height was increased.

Coulson and Skinner<sup>(10)</sup> transferred propionic and benzoic acid from solution in water to benzene drops and measured the transfer coefficient, K, during drop formation by forming a drop and then collapsing it. Assuming that the transfer rate was the same during formation and subsequent collapse, they showed K to be inversely proportional to formation time but independent of drop size. The overall

mass transfer coefficient, K, increased with drop size during free rise of the drops, but decreased with increasing interfacial tension. They also concluded that it was the time of contact rather than the height of rise which was important.

The internal circulation within a drop, which is induced by the relative motion of the continuous phase, has a remarkable effect on the extraction efficiency of a spray column. This was first recognized by Sherwood, Evans and Longcor (4). They found that extraction of a solute from liquid drops was far in excess of that predicted by the theoretical relation for mass transfer by molecular diffusion, and concluded that this was due to the movement of the fluid within the drops which maintained a higher concentration gradient at the interface than would exist if the interior was stagnant. West et al. (11) attempted to repeat the work of Sherwood but observed a much lower rate of extraction. The discrepancy was thought to be due to differences in the purity of the chemicals used with the resultant reduction in the internal circulation in the drops. Garner, Foord and Tayeban (12) stated that internal circulation might lead to a thinning of the boundary layer and a consequent reduction in the interfacial resistance to mass transfer. However, Calderbank and Korchinski (13) found that internal circulation raised the effective diffusivity to a value of several times the molecular diffusivity. Thorsen and Terjesen  $^{(14)}$ , on the other hand, did not agree that internal circulation could directly assist mass transfer, and suggested that it might do so indirectly by altering the hydrodynamic conditions outside the drops.

# (2) Holdup.

Holdup is defined as the fractional volume in the column occupied by the dispersed phase at steady-state operation. It is, in general, linear with the dispersed phase flow rate and is expressed by the equation (3)

$$H = (\Theta/V_e) L_d$$
 (3)

Moreover, H is related directly to the interfacial area of contact, a, by

$$a = H \cdot S/V_D \tag{4}$$

Knowing the forming frequency of the drops (15) or the average drop diameter (16) and the holdup value, the interfacial area of contact in a spray column may be calculated.

Holdup in a spray column can be measured (7) directly by shutting off the feed and effluent simultaneously and noting the fall or rise of the interface as the dispersed phase droplets cleared the column and accumulated at the interface. This measurement is not accurate, however, since the change in interface level is small and subject to considerable error.

Lapidus and Elgin<sup>(17)</sup> proposed that the holdup for all types of vertical fluidized systems was a unique function of the slip velocity between the two phases. Weaver, Lapidus and Elgin<sup>(18)</sup> extended this concept to include the case of liquid drops moving through a quiscent continuous liquid phase in a spray column. They investigated the holdup for organic liquid drops in a static water phase, and presented their

results as a plot of holdup versus  $(v_S/v_T)$ . Later, Beyaert, Lapidus and Elgin<sup>(19)</sup> further extended the work of Weaver et al. to cover the case of countercurrent flow of both liquid phases. The slip velocity for countercurrent flow in a spray column given by them is

$$v_S = (v_d/H) + v_c/(1 - H)$$
 (5)

Thornton<sup>(20)</sup> correlated the holdup and superficial velocities of the two phases in a spray column by the function

$$(v_d/H) + v_c/(1 - H) = v_0 (1 - H)$$
 (6)

where  $v_0$  is a characteristic velocity, obtained by extrapolating the mean relative velocity of the drops to zero flow rate. They derived an equation for calculating  $v_0$  for any given system and nozzle geometry with an accuracy of  $\pm$  20%.

Based on Weaver's data (21), Hughmark developed the following equations for the holdup value at zero continuous phase velocity

$$H = v_d/v_T$$
, for  $v_d/v_T < 0.02$  (7a)

$$H = -0.0023 + 1.11 (v_d/v_T), \text{ for } 0.02 < v_d/v_T < 0.05 (7b)$$

$$H = -0.00285 + 1.36(v_d/v_T) + 2.98(v_d/v_T)^2, \text{ for } 0.05 < v_d/v_T$$

(7c)

## (3) Axial Mixing and Concentration Gradient.

Ideally each phase in a liquid-liquid extraction column should be in plug flow, i.e., elements of the fluid which enter the column should move through it with constant and equal velocity on parallel paths. However, in practice, perfect plug flow will never occur, and there will always be some axial mixing due to viscous effects and molecular diffusion. In a spray column, owing to the absence of internal structure over the active portion of the column, the continuous phase is relatively free to circulate and this leads to an appreciable degree of axial mixing. The effect of axial mixing is to reduce the extraction rates by destruction of the true countercurrent concentration differences between the liquids.

Pratt<sup>(23)</sup>, and Morello and Poffenberger<sup>(24)</sup> were among the earliest workers to recognize axial mixing in a spray column and its effect upon extraction efficiency. Geankoplis and Hixson<sup>(25)</sup>, and Geankoplis et al.<sup>(26)</sup> developed a method for sampling the continuous phase at different levels and determined the concentration gradient throughout the column. The results revealed a large change in concentration for the continuous phase at the inlet. The significance of this was explained by Newman<sup>(27)</sup> to be due to the dilution of the extensively axial mixed continuous phase by the incoming liquid.

Gier and Hougen (28) determined the concentration profiles for both the continuous and dispersed phase. They observed considerable axial

mixing in the continuous phase, and stated that the normal material balance was inadequate in correlating the local phase compositions in the spray column. However, the concentration profile obtained by them for the dispersed phase indicates little axial mixing in that phase. The latter finding was thought to be reasonable (29) if the drops of the dispersed phase are uniform in size and do not collide, and the continuous phase velocity profile is flat. Gier and Hougen also reported that the continuous phase axial mixing was affected by the relative velocity of the two phases with respect to each other, and increased with the column diameter to length ratio. However, Cavers and Ewanchyna (30) found it increased with decreased continuous phase flow rate.

The axial mixing is characterized by the axial eddy diffusivity which can be determined by using either a standard tracer-injection technique (31,32) or a radiotracer technique (33).

#### (4) Mass Transfer Correlation

In a spray column, the overall mass transfer coefficients based on the continuous and dispersed phase,  $K_{\rm c}$  and  $K_{\rm d}$ , are characterized by the following equations (34)

$$1/K_c = 1/k_c + m/k_d, 1/K_d = 1/k_d + 1/\frac{mk}{c}$$
 (8a)

or

$$1/K_{d} = 1/k_{d} + m/k_{c}, 1/K_{c} = 1/k_{c} + 1/mk_{d}$$
 (8b)

depending on which phase is dispersed, provided the equilibrium

curve is straight.  $k_{\rm c}$  and  $k_{\rm d}$  are the individual film mass transfer coefficients for the continuous and dispersed phase respectively.

For solute transfer to or from the dispersed phase, a differential material balance on the drop results (35)

$$\frac{d}{d\theta} \qquad (v_D^c) = k_d (c_i - c)s \qquad (9)$$

This is integrated to give an expression for kd.

$$k_d = -(v_D/S\theta) \ln [(c_i - c_0)/(c_i - c_0)]$$
 (10)

Since

$$E = (C_0 - C_0)/(C_1 - C_0),$$

then

$$k_d = -(V_D/S\theta) \ln (1 - E)$$
 (11)

where E is the fraction extracted and is referred to as the extraction rate. By knowing E,k, can be determined.

As suggested by Licht and Conway<sup>(5)</sup>, there are three major periods in the droplet life during which mass transfer takes place: (1) during formation, (2) during free rise or fall, and (3) during coalescence at the end of the column. Period (2) is of prime importance in a spray column, and considerable work has been reported on the correlations of mass transfer during this period.

For drops which are internally stagnant and with no resistance in

the continuous phase, Newman (36) derived an expression for the fraction extracted during period (2)

$$E_2 = 1 - \frac{6}{\pi^2} \sum_{n=1}^{\infty} \frac{1}{n^2} \exp(-4\pi^2 n^2 \otimes \theta/D^2)$$
 (12)

Vermeulen (37) showed that this result could be represented by the empirical equation

$$E_2 = [1 - \exp(-4\pi^2 \delta \theta/D^2)]^{1/2}$$
 (13)

When the drop Reynolds number is less than unity and negligible resistance in the continuous phase is assumed, Kronig and Brink's (38) theoretical expression leads to

$$E_2 = 1 - \frac{3}{8} \sum_{n=1}^{\infty} B_n^2 \exp(-64 \lambda_n \Theta \theta/D^2)$$
 (14)

 $B_n$  and  $\lambda_n$  were given by Heertjes et al. (39) for  $1 \le n \le 7$  and Elzinga and Banchero (40) for  $1 \le n \le 3$ . Equation (14) was found (13) to be well represented by the following empirical equation.

$$E_2 = [1 - \exp(-9.0 \pi^2 8 \theta/D^2)]^{1/2}$$
 (15)

For high drop Reynolds number and negligible resistance in the continuous phase, Handlos and Baron $^{(41)}$  proposed a circulation model which yields

$$E_{2} = 1 - 2 \sum_{n=1}^{\infty} B_{n} \exp \left[-16 \lambda_{n} \partial \theta U/2048 D(1 + \mu_{d}/\mu_{c})\right]$$
 (16)

The above equation may be rearranged by considering only the first term in the series as follows

$$k_d = 2.88 \, \text{U}/768 \, (1 + \mu_d/\mu_c)$$
 (17)

Johnson and Hamielec $^{(42)}$  used a factor R as a multiplier of the molecular diffusivity to modify the transfer equation for a stagnant drop and obtained

$$E_2 = 1-6 \sum_{n=1}^{\infty} B_n \exp(-4 \lambda_n^2 R \partial \Theta/D^2)$$
 (18)

For low values of  $E_2$ ,i.e.,  $E_2 < 0.5$ , the following equation was found to fit the above expression

$$E_2 = 1.81 (\pi^2 R \partial \Theta/D^2)^{1/2} + 0.189$$
 (19)

The overall fraction extracted  $E_{t}$  for this is then

$$E_t = 1.81 (1 - E_f) (\pi^2 R_0 9 \theta / D^2)^{1/2} + (0.0189 + 0.981 E_f)..(20)$$

since

$$E_2 = (E_t - E_f)/(1 - E_f)$$

 $E_f$  is the fraction extracted during drops formation and coalescence, i.e., the combined E for periods (1) and (3). At high values of  $E_2$ , all but the first term of the series on the right hand side of Equation (18) are negligible. The equation is therefore reduced to

$$\ln (1 - E_2) = -10.96 R \Re \theta / D^2 + \ln 7.74$$
 (21)

and consequently

$$\ln (1 - E_f) = -10.96 \text{ R} \cdot 90/\text{D}^2 + \ln 7.74 (1-E_f)$$
 (22)

A plot of  $E_t$  against the square root of the contact time  $\theta$  for  $E_2 < 0.5$ , or  $\ln(1 - E_t)$  versus  $\theta$  for higher  $E_2$  should yield a straight line in which the intercept and slope may be used to determine  $E_f$  and R.

Skelland and Wellek  $^{(35)}$  studied the resistance to mass transfer inside droplets and developed correlations for  $k_d$  in the form of dimensionless groups. For non-oscillating droplets, the expression is

$$N_{Sh,d} = 31.4 N_{Tm}^{-0.338} N_{Sc}^{-0.125} N_{We}^{0.371}$$
 (23)

where  $N_{\rm Tm}$  is a dimensionless time group which appears in the theoretical expression for  $E_2^{(36,38,41,42)}$ ; and for oscillating droplets, both of the following equations fit equally well

$$N_{Sh,d} = 0.320 N_{Tm}^{-0.141} N_{Re}^{0.683} N_{p}^{0.10}$$
 (24a)

$$N_{Sh,d} = 0.142 N_{Tm}^{-0.141} N_{We}^{0.769} N_{O}^{0.285}$$
 (24b)

N is the  $\rho$  group which was used with success by Hu and Kintner (43) in correlating droplet fall-velocity with a variety of variables.

In a later publication (44), Wellek and Skelland modified the Handlos-Baron's (41) turbulence model for circulating drops by considering the effect of a finite continuous phase resistance in the boundary conditions of the original equation. Their correlation is given by the following

$$E_2 = 1 - 2 \sum_{n=1}^{\infty} B_n^2 \exp(-\lambda_n' b \theta)$$
 (25)

where b = U/128 (1 +  $\mu_d/\mu_c$ ) and  $\lambda_n^i$  is a function of  $k_c$ . When  $k_c$ 

is infinite,  $\lambda_n^{\prime}$  is equal to  $\lambda_n^{\prime}$  of Equation (16).

All the above mentioned correlations for E and  $\mathbf{k}_{d}$  are based on the assumption of spherical drops, constant molecular diffusivity, and uniform initial concentration.

The transfer coefficient for periods (1) or (3), i.e., during drop formation or coalescence of the droplets at the end of the column, may be estimated by Higbie Equation (45).

$$k_d = 2 \left( \sqrt{8} / \pi \Theta \right)^{1/2} \tag{26}$$

This equation was derived for unsteady-state diffusion of a solute through a stagnant film of infinite thickness, and was used by several investigators  $^{(6,10,11,39,44)}$  to calculate the transient mass transfer film coefficient in a spray column.

Based on Equation (26) Heertjes et al. (39) developed the following expression for the fraction extracted during the formation period

$$E_1 = (20.6/D)(690/\pi)^{1/2}$$
 (27)

In addition, the extraction rate during the coalescence period was found by Johnson and Hamielec $^{(42)}$  to be

$$E_3 = (2S/V_D)(00/\pi)^{1/2}$$
 (28)

The combined extraction rate for periods (1) and (3),  $E_f$ , may be determined by the method mentioned earlier (42).

The development of a correlation for predicting  $k_c$  in a spray column has been the subject of several publications. Based on the successful correlation of mass transfer in a solid-liquid batch fluidized system (46), Ruby and Elgin (15) fitted their experimental data on one line by use of a j'-Reynolds number plot which gives

$$j' = 0.725 (N_{Re})^{-0.43}$$
 (29)

where j' is a modified j-factor, and is equal to  $[(k_{\rm c}/v_{\rm c}){\rm N_{Sc}}^{0.58}]$  .

Generally,  $k_{_{\mbox{\scriptsize C}}}$  is correlated with the physical and flow properties of the system from the functional relationship

$$N_{Sh,c} = \emptyset(N_{Re}, N_{Sc})$$

Garner, Foord, and Tayeban (12) obtained data for systems with low interfacial tension. Thorsen and Terjesen (14) carried out experimental work for four systems with high interfacial tension. Data from these two investigations were fitted with the following equations, respectively

Garner: 
$$N_{Sh,c} = -126 + 1.8 N_{Re} N_{Sc}^{-0.42}$$
 (30)

Thorsen: 
$$N_{Sh,c} = -178 + 3.62 N_{Re} N_{Sc}$$
 (31)

The latter equation was found not to be affected by variations in  $\mu_{\rm d}$  from 0.72 to 1.32 cp, and to be applicable to non-circulating as well as to circulating drops.

By using the Higbie concepts  $^{(45)}$  and assuming potential flow across the drops, Heertjes, Holve and Talsma $^{(39)}$  derived an equation for  $k_c$ 

$$N_{Sh,c} = h N_{Re}^{1/2} N_{Sc}^{1/2}$$
 (32)

where h was reported to depend on the thickness of the layer around the drops and to be a function of  $\mu_c/(\mu_c + \mu_d)$ .

Griffith (47) presented a correlation for several systems. Experimental data for isobutyl alcohol drops in water, ethyl acetate drops in water, and water drops in isobutyl alcohol were fitted with the equation

$$N_{Sh,c} = 2 + 1.13 (N_{Re})^{1/2} (N_{Sc})^{1/2} w^{1/2}$$
 (33)

where w is a function of  $(\mu_c/\mu_d)N_{Re}^{1/2}$ . Garner and Keely suggested that a dependence of  $N_{Sh,c}$  on  $N_{Gr,c}$  should be noticed when  $N_{Gr,c}^{1/4} = N_{Sc}^{-1/4} > 0.4$ . However, in Griffith's work no dependence of  $N_{Sh,c}^{N}$  on  $N_{Gr,c}^{N}$  was found.

The experimental data of Thorsen and Terjesen (14), and of Garner et al. (12) were fitted by Hughmark (22) with the equation

$$N_{Sh,c} = 2 + 0.084[(N_{Re})^{0.484} (N_{Sc})^{0.339} (Dg^{1/3}/65^{2/3})]^{3/2}$$
(34)

He also proposed that  $N_{Sh,c}$  for liquid drops might be estimated from  $N_{Sh,c}$  for rigid spheres by multiplying by a factor F, i.e.,

where 
$$(N_{Sh,c}) \text{ circulating drops} = F(N_{Sh,c}) \text{ rigid sphere}$$
 (35) 
$$F = 0.281 + 1.615 (x) + 3.73 (x)^2 - 1.874 (x)^3,$$
 
$$x = (N_{Re})^{1/8} (\mu_c/\mu_d)^{1/4} (\sigma^*/\mu_c v_s)^{1/6}.$$

# 2. DROPLET BEHAVIOUR IN A SPRAY COLUMN

#### (1) <u>Size</u>

As mentioned earlier, the interfacial area of contact between the two phases in a spray column is directly proportional to the surface area of the individual droplets which, in turn, is a function of drop size. If the drop sizes and holdup are known, the interfacial area, a, can easily be calculated.

Hayworth and Treybal (49) studied drop formation in a spray column for a static continuous phase. They found that drop size was increased by increased interfacial tension, decreased difference in density between the phases, increased viscosity of the continuous phase, and increased nozzle diameter. However, it was independent of whether light or heavy liquid is dispersed, and practically unaffected by viscosity of the dispersed phase. They also reported that drop size was uniform and increased with velocity through the nozzle up to 10 cm/sec, decreased and became less uniform from 10 to 30 cm/sec, and was erratic and unreproducible at higher velocities. By considering the forces acting upon the drop during formation, they derived a semitheoretical equation for estimating the drop sizes in a liquid-liquid system. The equation is as follows

$$v_{D} + 4.11 (10^{-4}) v_{D}^{2/3} (\rho_{d} v_{N}^{2} / \Delta \rho)$$

$$= 21 (10^{-4}) (\sigma D_{N} / \Delta \rho)$$

$$+ 1.069 (10^{-2}) (D_{N}^{0.747} v_{N}^{0.365} \mu_{c}^{0.186} / \Delta \rho)^{3/2}$$
(36)

Based on the above equation, and the assumption of spherical drops, a chart was prepared from which the drop diameter could be calculated directly without the necessity of trial-and-error computations.

Null and Johnson  $^{(50)}$  also developed a method for predicting the drop volume, and thus the drop diameter in a spray column for flow rates in the range of  $0 \le (D_N^2 \, v_N^2 \, \rho_d^2/\sigma)^{0.5} \le 1.4$ . Knowing physical properties of the system, the drop volume,  $V_D^2$ , may be computed from a series of charts given by them.

After studying drop formation in liquid-liquid systems, Keith and Hixson (51) concluded that (1) at low flow rates, drops form individually at the nozzle tip and grow in size until the buoyant force overcomes the interfacial tension and the drop is released; (2) at increased flow rate, a point is reached where a liquid jet exists between the nozzle tip and the point of drop detachment; (3) further increase in the flow rate rapidly lengthen the jet till a maximum value is reached; (4) increasing the flow rate further decreases the jet length and increases drop non-uniformity until the jet breakup point retreats to the nozzle tip. Keith and Hixson also reported that the continuous phase velocity had no effect on the drop size for values ordinarily encountered.

Christiansen and Hixson<sup>(52)</sup> investigated the disintegration of organic liquid jets in water for the conditions in which the interfacial area produced by the drops is at a maximum. They were able to relate the nozzle velocity at which the maximum area occurs with the properties

of the system. The resultant expression is

$$v_{N,M} = 2.27 (10^{-2}) (D_j/D_N)^2 [(\sigma/D_j)/(0.5137 \rho_d+0.4719 \rho_c)]^{0.5}$$
 (37)

where  $D_{N}/D_{i}$  was given empirically by

$$\begin{split} & D_{N}/(\sigma/g\Delta\rho)^{0.5} < 5.73 \ (10^{-2}): \\ & D_{N}/D_{j} = 0.258 \ (10^{-2}) \left[ D_{N}/(\sigma/g\Delta\rho)^{0.5} \right]^{2} + 1 \ , \\ & D_{N}/(\sigma/g\Delta\rho)^{0.5} > 5.73 \ (10^{-2}) : \\ & D_{N}/D_{j} = 0.12 \ D_{N}/(\sigma/g\Delta\rho)^{0.5} + 0.12 \ . \end{split}$$

The drop diameter corresponding to  $v_{N_{\bullet}M}$  was found to be

$$D_{M} = 2 D_{j}$$

Christiansen-Hixson's correlation was found (22) to be suitable only for systems in which the continuous phase properties were similar to water.

#### (2) Velocity

Correlations available on the fall or rise velocities of rigid spheres in liquids do not always apply to liquid droplets in a spray column. The discrepancy is due to the deformation and oscillation as well as the internal circulation of the drop. The internal circulation is known to be caused by the relative motion of the continuous phase. In studying factors affecting droplet behaviour in liquid-liquid systems, Garner and Skelland found that internal

circulation substantially increased the drop velocity while prolateoblate type oscillation reduced the velocity. However, the deformation of the drops causes an increase in the total surface area, gives rise to a higher drag coefficient, and thus a smaller velocity.

Hu and Kintner (43) studied the steady motion of single drops of ten organic liquids falling through a stationary water phase and presented a correlation for predicting the terminal velocity of the drop. The correlation is in the form of a single curve relating the drag coefficient, Weber number, Reynolds number, and physical property group. It can be expressed in the following manner

$$N_{Ph} = (\rho_c^2 \sigma^3)/(g \Delta \rho \mu_c^4) = 4 (N_{Re}^{'})^4/3c_D (N_{we}^{'})^3$$
 (38)

The terminal velocities of fall of liquid droplets in a stationary continuous phase without mass transfer between the phases was studied by Licht and Narasimhamurty  $^{(54)}$ . They concluded that, for any given system, as the drop size was increased the fall velocity of the droplets first increased to a maximum, and then fell off asymptotically. However, a lower interfacial tension would lower the fall velocity of the drop. They also proposed the following correlation for  $\beta \geq 0.4$ 

$$\left(\frac{C_{D}}{C_{D}^{s}}\right) = 1.87 \beta + 0.423$$
 (39)

where

$$\beta = (g D'^2 \Delta \rho)/4\sigma$$

Klee and Treybal<sup>(55)</sup> measured the terminal velocity of liquid drops immersed in an insoluble liquid for eleven systems which covered a wide range of physical properties. The velocity-drop diameter relationship was found to be different in two separate regions, i.e., region I where the velocity increased with the drop diameter and region II where the velocity remained substantially constant with increasing drop diameter. Correlations were developed for each of the two regions. For region I, the equation is

$$v_T = 38.3 \rho_c^{-0.45} \Delta \rho^{0.58} \mu_c^{-0.11} D'^{0.70}$$
 (40a)

and for region II

$$v_T = 17.6 \rho_c^{-0.55} \Delta \rho^{0.28} \mu_c^{0.10} \sigma^{0.18}$$
 (40b)

At high Reynolds number, as reported by Harmathy (56), the terminal velocity of the drop is practically independent of the drop size but depends only on the shape of the drop which turns out to be solely a function of the Eötvös number. From a chart prepared by Harmathy, it is possible to calculate the terminal velocity of liquid droplets moving in liquid media for a Reynolds number greater than 500.

It has been shown<sup>(13)</sup> that the terminal velocity of drops in a spray column is attained at a point very close to the dispersing nozzle, and that the effect of column diameter is negligible when the column diameter is about ten times that of the drop.

# (3) <u>Shape</u>

The shape of a drop moving in a continuous liquid phase is determined by the forces acting along the drop surface. Drops of small volume are usually spherical because the interfacial forces are sufficient to make the drop a sphere. On the other hand, for large drops, the inertial forces tend to cause a distortion from the spherical shape (56,57).

Drop shape is generally characterized by the term "eccentricity", i.e., the ratio of horizontal to vertical diameters of the drop. Eccentricity data are usually presented as a plot of  $E_e$  versus D'. The relationship has been reported to be essentially linear  $^{(51,55)}$ . The slope of the lines, as indicated by Keith and Hixson  $^{(51)}$ , is related to the quantity  $\Delta \rho / \sigma$  whereas Klee and Treybal  $^{(55)}$  found it to be proportional to  $(\Delta \rho)^{0.5} / \sigma$ .

Hughes and Gilliland (58) proposed a method of predicting the eccentricity of drops in the range of intermediate and high Reynolds numbers. The development was based on the suggestion of Spilhaus (59) that the force tending to separate the drop laterally could be considered to be proportional to the area over which it acts and to the kinetic head  $\rho_c v_c^2/2$  of the continuous phase. The dimensionless proportionality factor,  $\gamma$ , was termed the distortion coefficient. They obtained the relation

$$\frac{1}{4} \gamma N_{We}' = \psi(h) \tag{41}$$

where the function  $\psi(h)$  was presented in Table 1 of Reference 58.

Harmathy (56) attempted to describe the shape of the drop by means of a force balance at the drop surface. However, rather than solving the force balance relation for the drop shape, he suggested that the unknown relation be left as

$$E_e = \emptyset (N_{We}^i, N_{Eo}^i)$$

In the turbulent region,  $N_{Eo}^{I}$  was found to be directly proportional to  $N_{We}^{I}$ , and the eccentricity was, therefore, a function of  $N_{Eo}^{I}$  only.

Wellek, Agrawal, and Skelland  $^{(60)}$  investigated the effects of physical properties, drop size, and drop velocity on the shape of non-oscillating drops moving in liquid media. They found the eccentricity of the drop to be a function only of  $N_{We}'$  and  $\mu_c/\mu_d$  over the entire range of  $N_{Re}'$  (6 to 1345). The following correlation was obtained with an average absolute deviation of 6.0%.

$$E_e = 1.0 + 0.093 \text{ NWe}^{10.98} (\mu_c/\mu_d)^{0.07}$$
 (42)

They also found that the Hughes-Gilliland model (58) applied only to liquid drops in a gas continuous phase and could not be used for a liquid-liquid system.

### (4) Coalescence at the Interface

In a spray column, when droplets of the dispersed phase reach the phase boundary, they do not normally coalesce immediately with their homo-phase but restrat the interface for some time. This phenomenon was first reported by Mahajan (61). The magnitude of the rest time is dependent on several factors such as temperature, drop size, physical properties, purity of the system, and disturbances at the interface. Such a rest time arises from a thin film of the continuous phase which is trapped between the drop and the interface when the drop first arrives there. This film drains under the gravitational force of the drop until it becomes very thin and ultimately ruptures as reported in Reference 62.

Several investigators (63,64,65) have revealed that coalescence may take place in several stages, i.e., the primary drop will coalesce with the subsequent formation of a secondary droplet which also exists at the interface for a certain time before coalescing and giving rise to yield another droplet, and so on, until the drop is smaller than a critical size. Charles and Mason (63) found that the chief factor in determining whether the coalescence would take place in single or several stages was the ratio of the viscosities of the phases. They concluded that single stage coalescene usually occurs if the viscosity ratio (dispersed/continuous) is less than 0.02 or greater than about 9.

This was roughly corroborated by Jeffreys and Hawksley (65), who also

investigated the effects of physical properties on drop coalescence at the interface, correlating the average rest time with interfacial tension, continuous phase viscosity, drop size, and length of fall. Whereas Linton and Sutherland (66) reported that the rest time of the drop was proportional to the drop size.

It has been shown (67,68,69) that high energy electric fields promote coalescence in liquid-liquid systems. In other words, electric fields will reduce the rest time of the drops at the interface. Charles and Mason (67) employed a system consisting of water drops coalescing at a plane benzen-water or heptane-water interface. An electrostatic field was applied to the system in a direction perpendicular to the interface. They found that, with increasing potential, the rest times of primary and secondary drops decreased. In addition, the primary drop gave rise to a smaller secondary drop on coalescing. For the heptane-water system, no secondary drop was found at a potential of approximately 450 volts DC. At 900 volts, coalescence became instantaneous.

Allan and Mason (68) investigated the effect of DC fields on coalescence at liquid-liquid interfaces. They observed the effect of increasing field strength on the mean rest time of the primary and the first two secondary drops. A plot of their results showed an inverse linear relationship between the strength of the applied field and the mean rest time of drops. By extrapolation, it was possible to arrive at a critical field strength at which coalescence is instantaneous.

Brown and Hanson (69) carried out work similar to that of the above investigation but used high energy AC fields with frequencies ranging from 1 to 10 kc/sec. They found that high frequency oscillating fields reduced the rest time of aqueous drops at an oil-water interface. Using the system kerosene-water, they obtained results for the critical field strength which were in good agreement with those of Allan and Mason. They also indicated that it was the field strength at the interface which affected the rest time of drops, and that the rest time was virtually insensitive to frequency.

The mechanism by which electric fields promote coalescence is not yet clear. However, the increased disturbance at the boundary, and the polarization of the drops may be responsible for the reduction of rest time  $^{(62)}$ .

#### PULSED COLUMNS PERFORMANCE

The "pulsed column" concept was first introduced by Van Dijck (70) in 1935. It involved the use of mechanical device to superimpose a pulsating motion in a conventional liquid-liquid extraction column in order to obtain a higher efficiency and mass transfer rate. Pulsed columns have been applied successfully in the nuclear energy industry because the increase of efficiency by pulsation will lead eventually to a reduction in the column height, and hence a decrease in the expense of massive radiation shielding.

The two most common pulsing devices are; a reciprocating pump with the check valves removed, and a flexible bellows or diaphragm being pulsed mechanically. Such devices provide adjustable pulse amplitude and frequency, and are usually attached directly to the bottom of the column (71).

Most of the studies on pulsed columns concern the sieve-plate and packed type columns, and only a few published papers deal with the spray type pulsed column. However, literature on the performance of all types of pulsed columns will be reviewed in the following.

#### (1) Sieve-Plate Type

The first systematic study on a sieve-plate type pulsed column was made by Belaga and  $Bigelow^{(72)}$ , who used the system water-acetic

acid-methyl isobutyl ketone, and a column 45" long by 1-1/2" in.diameter. The plates were drilled with 1/32" holes, giving a free area of approximately 23%, and were spaced at 1" intervals. Pulsing was carried out by means of a positive displacement plunger pump with the check valves removed. These workers reported HTU values varying from 2.63" to 6.25", depending upon the frequency and amplitude employed. During the course of their work, the amplitude was varied from 1/8" to 2" and the frequency from 20 to 80 cycles/min. The product of frequency and amplitude was considered to be a measure of the rate of pulsing, and an empirical correlation was obtained by plotting this quantity against HTU. The authors pointed out, however, that the relationship so obtained might well depend upon the influence of physical properties and the wave form of the pulse and may not, therefore, hold for other systems.

Cohen and Beyer (73) studied the aqueous extraction of boric acid from isoamyl alcohol. They used a 1" I.D. sieve-plate column, 20" long. The plates, which were 1 mm thick and spaced at 2" intervals, were drilled with 53 holes of 0.040" diameter, giving a free area of 9%. Two types of pulsing mechanism were used: a 4.7" diameter bellows driven by means of a lever and cam and a diaphragm-proportional pump with the valves removed. They suggested that flooding was caused by inadequate pulsing capacity at low frequencies and amplitudes. On the other hand, at very high frequencies and amplitudes, a considerable degree of back mixing occured. They also correlated their mass transfer data with the product of the amplitude and the frequency.

Sege and Woodfield (74) examined the effects of pulse frequency and amplitude on the performance of a pulsed sieve-plate column using the system of water-uranyl nitrate-tributyl phosphate. They found that at low frequencies, the capacity of the column was equal to the product of the frequency and the pulse volume displacement, and the capacity thus increased in proportion to fA until flooding occurred. Accordingly, they concluded that the frequency-amplitude product, fA, represented a useful simple means of correlating the pulsing conditions with column performance. However, they further suggested that f<sup>n'</sup> A might be a more exact correlator than fA, where the exponent n' would have some values between 1 and 2 and might not be the same for all systems or for all ranges of the amplitude.

Goldberger and Benenati<sup>(75)</sup> carried out experimental work to examine the efficiency of a pulsed sieve-plate column. They used a unit consisting of two 12" sections of glass tubing, having an inside diameter of 2-23/32", which were separated by a perforated plate. The plate included a circular downcomer of 0.497" I.D. and 15 holes of 0.046" diameter. Cyclic pulsations were developed by a reciprocating plunger operating within a cylinder, and controlled by a variable-speed motor. The system consisting of toluene-benzoic acid-water was used. It was observed that at frequencies greater than 150 cycles/min the column performance was apparently improved. They concluded that the extraction efficiency of a conventional sieve-plate column might be significantly increased by applying pulsation to the system, if the degree of pulsation was sufficient to alter the mechanism of the phase dispersacon.

Several investigators  $^{(76,77,78)}$  have proposed empirical correlations for predicting HTU in a sieve-plate type pulsed column. Thornton's  $^{(76)}$  correlation is as follows

$$\frac{(HTU)_{c}}{(\mu_{c}^{2}/g\rho_{c}^{2})^{1/3}} = \alpha \left(\frac{\mu_{c}g}{F_{e}^{3} v_{o}^{3}(1-H)^{3} \rho_{c}}\right)^{2m^{*}/3} \left(\frac{\Delta \rho}{\rho_{c}}\right)^{2(m^{*}-1)/3}$$

$$\left(\frac{v_{d}}{v_{c}}\right)^{0.50} \left(\frac{v_{c}^{3} \rho_{c}}{g \mu_{c}^{H}}\right)^{0.33}$$
(43)

where the constant  $\alpha$ , the exponent m', and the enhancement factor  $F_e$  are characteristics of the system and to be determined empirically, while the characteristic velocity of the drop  $v_o$  can be calculated from an equation given by the authors.

By dimensional analysis and analysing the experimental data available in the literature, Smoot, Mar, and Babb $^{(77)}$  presented an equation as follows

$$\frac{\text{(HTU)}_{c}}{\ell} = 0.20 \quad \left(\frac{\text{fA} \quad D_{h} \cdot \rho_{d}}{\epsilon \mu_{d}}\right)^{-0.434} \quad \left(\frac{\Delta \rho}{\rho_{d}}\right)^{1.04} \quad \left(\frac{\mu_{d}}{\rho_{d}}\right)^{0.865}$$

$$\left(\frac{\sigma}{\mu_{c}v_{c}}\right)^{0.096} \left(\frac{v_{d}}{v_{d}}\right)^{-0.636} \left(\frac{D_{c}}{\ell}\right)^{0.317} \left(\frac{\mu_{c}}{\mu_{d}}\right)^{4.57}$$

(44)

This equation was reported to be valid only for extraction in a sieveplate type pulsed column where mass transfer occurs from the dispersed phase to the aqueous continuous phase, and where the major resistance to mass transfer is in the dispersed phase.

Also, by dimensional analysis, Smooth and Babb $^{(78)}$  developed the following expression for the system water-acetic acid-methyl isobutyl ketone

$$\frac{\text{(HTU)}_{w}}{\ell} = 504 \quad \left(\frac{\text{fA} \cdot D_{h} \rho_{m}}{\mu_{m}}\right)^{-0.40} \quad \left(\frac{v}{\text{fA}}\right)^{0.43} \quad \left(\frac{v}{v_{m}}\right)^{0.56} \left(\frac{D_{h}}{\ell}\right)^{0.62}$$
(45)

#### (2) Packed Type

Feick and Anderson<sup>(79)</sup> studied the extraction of benzoic acid from toluenes by means of water, the latter being the continuous phase throughout. The column was 1-7/16" in diameter and 36" long. Two types of column packing were used, 1/2" stainless steel McMahon Saddles, and 3/8" ceramic Raschig rings. It was noted that the packing tended to settle on pulsing, and therefore the column was operated until no more settling occurred. Pulsing was carried out by means of a reinforced neoprene diaphragm attached near the bottom of the column, operated by an eccentric, and giving amplitudes ranging from 1/16" to 1/4" at frequencies from 200 to 1000 cycles/min. They reported that Ka was increased by a factor of 3.4 when the column liquids were pulsed. In an

attempt to determine whether this increase was due to an increase in the interfacial area or to the increased turbulence and its resultant effects upon K, they carried out additional experiments using a solute whose major resistance to mass transfer lay in the toluene instead of the water phase, namely, acetic acid. On pulsing, an increase in Ka was observed of the same order of magnitude as in the benzoic acid case. They, therefore, concluded that the main effect of pulsing on Ka was to increase the interfacial area of contact.

Chantry, Von Berg, and Wiegandt (80) studied the application of pulsation to an extraction column of 1-1/2" I.D. and 4' height packed with 1/4" Raschig rings. The pulser was a pair of copper bellows driven by an electric motor. Two systems were used; water-acetic acid-methyl isobutyl ketone and ethyl acetate-acetic acid-water. On a pulse frequency of 74 cycles/min and an amplitude of 1/4", they observed a five-fold decrease in HETS, but the maximum throughput was found to be reduced by 5-10%.

Potvis and coworkers (81) used a variable stroke, reciprocating plunger pump to provide a pulsation in a column of 1-1/4" I.D., 30" long packed with 0.25" glass Raschig rings. The system studied was benzene-acetic acid-water, the transfer of solute being from the continuous aqueous to the dispersed benzene phase. They proposed that at any fixed value of HTU, pulse frequency f, and amplitude A, were related as follows

$$f = p + s \log A \tag{46}$$

and the general equation relating pulse characteristics to HTU was given as

$$f = q (r-HTU) + s \log A$$
 (47)

where p,q,r and s are constants. The values of these constants for the system studied were 125, 76.5, 6.92 and -150.0 respectively.

Karpacheva et al. (82) found that mass transfer rate in a packed type pulsed column were fairly constant with increased pulse frequency but increased with pulse amplitude. Nevertheless, Moon and coworkers (83) reported that doubling the frequency gave a greater reduction in HTU than doubling the amplitude.

#### (3) Spray Type

The earliest report on a spray type pulsed column was made by Lurie and Shaver (84) who indicated that pulsing had little effect on the efficiency of a spray column. However, in attempting to check this conclusion, O'Brien (85) found that there was a definite decrease in HTU at frequencies above 200 cycles/min.

Billerback et al. (86) carried out a detailed investigation on a pulsed spray column using the system water-acetic acid-methyl isobutyl ketone. The extraction column was 1.5" I.D. with an effective height of 85.6". Throughout their experimental runs, the organic phase was dispersed and used as a solvent to extract acetic acid from water. The pulser consisted of a circular offset cam driven by an electric motor. The cam drove

a cam follower which pulsed a brass bellows attached to the bottom of the column. Runs were made without pulsing, and at pulse frequencies of 200, 300, 400, and 500 cycles/min. Their results indicated that the effect of pulse on HTU was small up to approximately 200 cycles/min, after which HTU decreased significantly with increasing pulse frequency. In addition, the drap size decreased and the droplets became more spherical in shape with increasing pulse frequency. The above effects would lead to a larger interfacial area of contact. However, increasing the frequency also appeared to increase the turbulence within the column, thus achieving a greater mass transfer coefficient, K.

#### BACKGROUND INFORMATION ON ULTRASONIC VIBRATION

The term "ultrasonic vibration" is used to denote vibrational waves with a frequency above the hearing range of the normal human ear. The upper frequency limit of audible sound may range from 10 to 20 kilocycles per second (kc/sec) depending on the age and health of a person. However, in general, "ultrasonic" refers to frequencies greater than about 16 kc/sec (87).

Ultrasonic waves can be propagated in any substance which posesses elastic properties. Two types of ultrasonic waves are usually observed, i.e., longitudinal and shear waves. Longitudinal waves exist when the motion of the particles in a medium is parallel to the direction of wave progagation, and shear waves exist when particle oscillations take place in a direction perpendicular to the direction of wave propagation. Shear waves will not travel in liquids or gases because fluids have low shear strength. Therefore, the only type of wave of importance in liquids is longitudinal waves.

It is known that the laws of sound valid for the audible range are also true for the ultrasonic range (88). However, in the latter case, some phenomena appear, such as cavitation, degassing, erosion etc., which are not usually observed in the audible range. Ultrasonic cavitation is a well known phenomenon, and actually plays an important role in most applications of ultrasonic vibration.

#### (1) Cavitation

When ultrasonic waves of suitable frequency and intensity pass through a liquid, bubbles or cavities may be formed at certain points. This reaction is referred to as ultrasonic cavitation. The phenomenon of ultrasonic cavitation is rather complex. However, its cause may be explained as follows (89):

As mentioned above, the only type of ultrasonic wave that can be propagated in liquids is a longitudinal wave which consists of alternate rarefactions and compressions along the axis of propagation. As the intensity is increased beyond a certain point, the local pressure in the liquid may be reduced to the vapor pressure, which will lead to the formation of vapor. Alternatively, if the local pressure is reduced to a value so low that the gases dissolved in the liquid will emerge, cavitation will also occur. The minimum intensity required to produce cavitation is called the threshold intensity.

With water and using a frequency of 60 kc/sec, Blake (90) reported that there were three distinct types of ultrasonic cavitation. At very, low intensity, large visible bubbles were formed in gassy water. This was termed quiet degassing. At higher intensity, a continuous stream of small gas bubbles, which were accompanied by a soft hissing sound, was observed. This second type of cavitation was called gaseous cavitation. The threshold intensities, in terms of the pressure amplitude (I'p) for these two types of cavitation, were found to be 0.25 and 1.25 atm.

respectively. In degassed water, and at higher intensities, vaporous cavitation occurred. This was characterized by sporadic nuptures of cavities and sharp snapping sounds. According to Blake, the small explosive ruptures could be observed when I'<sub>p</sub> was about 4 atm. Quiet degassing and gaseous cavitation have been combined and termed simply as gaseous cavitation by many investigators (91,92,93). Barger (93) was able to achieve this type of cavitation in water with a gas content of half the saturation value. The value of I'<sub>p</sub> found by him for frequencies smaller than 200 kc/sec was bout 3 atm. However, Degrois (94) reported that vaporous cavitation was produced at low frequencies while gaseous cavitation occurred at high frequencies.

Two theoretical papers on "Cavitation Produced by Ultrasonics" were written by Noltingk and Neppiras (95,96). They assumed that the liquid was incompressible, the mass of the gas in the bubble was constant, and that there was no vapor in it. The applied ultrasonic waves were taken to be sinusoidal. Although their differential equations of motion were insoluble analytically, they were able to obtain numerical solutions for a number of specific sets of parameters, i.e., pressure amplitude, frequency, and initial bubble radius. All calculations were for an ambient pressure of 1 atm. Their results, which were presented in curves of radius versus time for growth and collapse of the bubble, showed that the bubble initially increased in size to a maximum radius during the rarefaction period of the ultrasonic waves, and then collapsed during the

compression period. At the end of the first complete wave cycle, the bubble radius was calculated to be equal to or less than the initial radius. They reported that the maximum radius of the bubble was inversely proportional to the frequency but directly proportional to the intensity. It was also concluded that for a specified frequency and intensity, there existed a minimum and maximum bubble radius for which cavitation could set in.

When calculated by Noltingk-Neppiras's method, the lifetime of a cavitation bubble is less than a wave cycle. But this is found to be contradictory to experimental observations (91,93). Using a high-speed photographic method, Willard (91) as well as Barger (93), observed that the lifetime of a cavitation bubble was hundreds of times longer than the ultrasonic wave cycles. Nevertheless, the numerical solutions given by Noltingk and Neppiras are of great help in picturing the possibilities of the growth and collapse of a cavitation bubble in an ultrasonic field.

By making use of high-speed photographs, Rozenberg (97) was able to distinguish between two stages in the cavitation process; stage 1 was the formation of gas or vapor bubbles and their subsequent movement and oscillation, and stage 2 was the violent collapse or breakup of these bubbles with shock wave generation. Both stages 1 and 2 create strong agitation, and form the basis of many of the phenomena associated with ultrasonic vibration, such as disruption, erosion, dispersion, emulsification, and chemical reaction (98).

# (2) Intensity Measurement

It has always been found difficult to measure the absolute values of the ultrasonic intensity in liquids. However, a number of methods have been proposed for the measurement of relative ultrasonic intensities in liquids. Generally, the intensity of an ultrasonic field is expressed as the output power of the transducer working into a typical load. The output power of the transducer is obtained by multiplying the electric power input to the transducer by the transducer efficiency, where the transducer efficiency may be obtained from the measurements of the transducer output for loaded and unloaded conditions (99). Nevertheless, this method does not lead to a reliable indication of the actual intensity in the liquids, especially when different frequencies are used.

A calorimetric method is suitable for measuring the overall ultrasonic energy in a finite medium. It was first used by Dunn and Fry (100) to measure ultrasonic intensities in liquids. This method is based on the assumption that all the dissipated ultrasonic energy appears eventually as heat. The intensity of an ultrasonic field may thus be determined by noting the temperature rise in the vessel after a given time interval under adiabatic conditions.

Teumin (101) developed a mechanical wattmeter for determining ultrasonic intensities in solids and liquids. This method involves mechanical measurements on the transducer. The ultrasonic intensity measured by

this wattmeter was expressed as the mechanical impedance which might be obtained by measuring force, velocity and their phase difference at frequencies through resonance by means of force-sensitive and velocity-sensitive probes or pick-ups attached to the transducer at suitable points.

The hot-wire microphone is the earliest instrument for measuring the local intensity at any point in an ultrasonic field. Richardson (102) used such a microphone to determine the intensity distribution in gases at frequencies up to 600 kc/sec. The principle of this method is as follows: When a wire heated to just below redness is placed in a fluid stream, the resultant cooling causes a drop in its electrical resistance. The particle velocity amplitude in an ultrasonic field, which is directly proportional to the intensity, may be determined by measuring this fall in resistance. However, such a microphone has not met with much success for liquids because of the low sensitivity due to convection losses.

Blitz<sup>(103)</sup> used a piezoelectric crystal probe to measure the local intensity in water in which ultrasonic waves were generated at a frequency of 40 kc/sec. The probe acted in the following way: When a wave met the piezoelectric crystal in one of its vibration directions, the crystal was set in mechanical vibration, and the resultant mechanical deformation caused electric charges to be liberated. The intensity was thus determined by detecting the amount of electric charges released, to which the intensity is directly proportional.

Blitz's probe involved the immersion of a small fragile element, the piezoelectric crystal, into the ultrasonic field. It will be easily damaged if the intensity is high, especially when cavitation occurs. The probe microphone designed by Saneyoshi, Okujima, and Ide (104) eliminates this disadvantage. They used a slim brass rod as a reflection-less transmission line of the ultrasonic pressure, immersed only one end of this rod in the liquid, and thus avoided direct contact of the fragile microphone receiver with the ultrasonic field.

The use of thermocouples enclosed in a sound-absorbing envelope for the intensity measurement was first proposed by Richards (105). He investigated the passage of ultrasonic waves through plates of different material and thickness, making use of a thermopile surrounded by ebonite, fibre, bakelite, or pitch. Such an envelope absorbed the ultrasonic energy and gave a temperature rise which was a linear function of the intensity. His thermopile was reported to respond to ultrasonic intensities as low as 0.01 watts/cm<sup>2</sup>. This thermocouple method is rather simple and can be used for low as well as high intensity measurement. It was used recently with success by Weber and Chon (106) for measuring the distribution of ultrasonic cavitation intensities in a liquid and liquid-solid system.

When a metal piece is exposed to an intense ultrasonic field, its surface will be eroded by the cavitation bubbles. The erosion loss has been found to increase with the square of the ultrasonic intensity,

and to be a linear function of time (107,108). The erosion rate may, therefore, be used as a measure of intensities which are above the cavitation level. Based on this, Crawford (109) proposed a method for measuring cavitation intensities in an ultrasonic cleaning tank. Aluminium, tin, or lead foils under a slight tension with suitable thickness were used. The erosion loss was measured by a densitometer. His method provides a simple means of comparing the intensity levels in ultrasonic vessels where constant conditions are applied.

Relying also on the erosive nature of cavitation bubbles, Chon and Wong (110) developed a method for measuring ultrasonic cavitation intensities in liquids. They suspended a copper wire of 1-1/2" long, and 0.0403" O.D., coated with cobalt-60, in the ultrasonic field for a suitable time, and calculated the cavitation intensities in terms of the percentage decrease in the radioactivity of the wire.

# (3) Threshold Intensity

The gas content of the liquid is an important variable affecting the threshold intensity. A study of this variable was made by Galloway (92). His results were presented in graphical form for distilled water and petroleum ether with frequencies ranging from 20 to 40 kc/sec. He reported that the threshold intensity depended very much on the gas content of the liquid for gas contents greater than 5% of the saturation value. He also found that if the gas content was less than 10% of the

saturation value, vaporous cavitation would occur, otherwise gaseous cavitation would produced. Strasberg (111) also studied the effect of gas content on the threshold intensity. He proposed the following empirical equation

$$I_p^1 = 2 + 4.8 (1-G_c/200)$$
 (48)

Several studies (90,92,112) have been made to investigate the effect of temperature on the threshold intensity. With distilled water, synthetic seawater, petroleum ether, and a 0.1 mole fraction dioxanewater mixture over a temperature range of 0° to 50° C, Galloway (92) reported that the threshold intensity decreased linearly with increasing temperature. Similar results for water between temperatures of 10° to 50° C were obtained by Blake (90), whereas, Connolly and Fox (112) found that the threshold intensity was not a linear function of temperature between 0° and 30° C. Empirical equations given by these investigators are listed in the following

Galloway I'<sub>p</sub> = I'<sub>po</sub> (1-T/273) (frequency = 20-40 kc/sec) (49 Black I'<sub>p</sub> = 0.07 (
$$T_s$$
-T) + 1 (frequency = 60 kc/sec) (50 Connolly and Fox I'<sub>p</sub> = 1.75 + 0.0176( $G_{cs}$ - $G_c$ ) (frequency = 1000 kc/sec)(51

Briggs et al. (113) studied the effect of viscosity on the threshold intensity in liquids at a frequency of 25 kc/sec. Although the threshold intensity was found to increase with the viscosity, the effect was rather small. (The threshold intensity changed by less than a factor of 3 over a

range of viscosities from 0.007 to 8.0 poise.) However, it has been shown (114) that the ability of the liquids to withstand cavitation increases with increasing viscosity.

Generally, as the ultrasonic frequency is increased, the production of cavitation in liquids becomes more difficult, and thus a greater value of the threshold intensity is necessary (114). For example, the threshold intensity for water has been found to remain constant for frequencies up to 10 kc/sec and then to increase steadily up to 50 kc/sec, and finally to increase rapidly as the frequency is raised still further (115,116).

A complete study on the frequency-dependency of the threshold intensity was made by Barger (93) who used water at seven different frequencies varying from 27 to 1,160 kc/sec. The gas content of water covered a very wide range and the suspended particle size was carefully controlled. He reported that the threshold intensity increased rapidly and the effect of gas content became negligible when the frequency was greater than 350 kc/sec. The suspended particle size, however, was found not to be an important factor.

The effect of the hydrostatic pressure was studied by Galloway (92). He found that for liquids saturated with air, the threshold intensity was directly proportional to the hydrostatic pressure, while for unsaturated liquids, it was independent of the hydrostatic pressure.

#### GENERAL COMMENTS

Spray column extraction has continuously held the interest of chemical engineering researchers, despite of the fact that spray columns comprise a small portion of the commercial extraction equipment. It is relatively simple to study, yet a knowledge of it helps greatly in predicting the behaviour of other continuous countercurrent liquid-liquid extraction columns.

The number of publications relating to the operation, design, and performance of a spray column is considerably large. However, results obtained from individual investigators are sometimes inconsistent, because most of the experimental work is centered around specific systems and is for particular operating conditions.

All the correlations developed for determining the mass transfer rate in a spray column are empirical or semi-empirical, and are based on certain simplifying assumptions. It appears that studies on the fundamental mechanism of mass transfer between droplets and the continuous phase still remains a challenging field of research in liquid-liquid extraction.

The droplet size, velocity, and shape in a spray column operating with common liquid systems can be predicted well by correlations available in the literature, since drop Reynolds numbers for this case are usually low. Actually, the great majority of spray column operations

have been found (15) to be in a drop Reynolds number range of 4 to 200, since the kinematic viscosities of common liquids fall in a narrow range, and the diameter and velocity terms are limited by the operating conditions. However, at higher drop Reynolds numbers, droplets are subjected to a higher degree of nonideality, induced internal circulation and distortion, and the oscillation of the drops are more appreciable, and the prediction of the droplet behaviour accordingly becomes more difficult.

For droplet coalescene at the interface, the number of papers reviewed in this section is rather limited and emphasis was given to methods of improving coalescence. A high electric field has been found to be an effective means for promoting the drop coalescene at the interface. However, the mechanism of this has not yet been fully understood. Most work on coalescene studies was carried out with simple binary systems, and hence little is known about the relationship between mass transfer and the coalescence process.

From the performance of pulsed columns, it may be concluded that pulsating motion, increases the degree of turbulence in the liquids as well as the interfacial area of contact between the two phases, and thus increases the extraction efficiency. On the other hand, pulsating also increases the tendency toward emulsification, and at high amplitudes, increases the degree of axial mixing. The best performance seems to be with a combination of low amplitude and high frequency. Because of the

complexity of the problem, all correlations for predicting the mass transfer rate in a pulsed column were obtained by dimensional analysis of the variables involved and determining the constants empirically.

Although considerable amount of work has been done for the understanding of ultrasonic cavitation, the fundamental mechanism of this phenomenon has not yet been clear. However, it is generally believed that the formation and collapse of cavitation bubbles may create strong agitation in liquids, and bring about drastic effects such as dispersion, emulsification, erosion, and chemical reaction. In the study of ultrasonic cavitation, the gas content of the liquid, frequency of the ultrasonic waves, temperature, and hydrostatic pressure are important variables. The effects of these variables on the threshold intensity have been well studied.

For the measurement of ultrasonic intensity in liquids, a calorimetric method is reliable for determining the overall intensity in a vessel, while the absorption thermocouple probe offers a simple means for mapping the ultrasonic field. Nevertheless, the calorimetric method is not convenient to use, since it requires isolation of the system to avoid heat gain or loss from and to its environment. On the other hand, the thermocouple probe may not be reliable at high intensities because of the surface discontinuity which may encourage gases to come out of the liquid and adhere to the probe.

The use of the empirical equations given for determining the threshold intensity in liquids is limited, because all of them are based on experimental data for narrow temperature and frequency ranges. Moreover, the vapor pressure of the liquid, which seems to be an important factor, has not been taken into consideration.

# NOMENCLATURE

# Roman Symbols

- a interfacial area of contact, cm<sup>2</sup>/unit volume
- A amplitude, cm
- b constant, dimensionless
- B\_ coefficients in series expansion, dimensionless
- C average solute concentration, g/cm<sup>3</sup>
- $c_{D}^{2}$  drag coefficient,  $4g\Delta\rho D'/3 \rho_{c}^{2} v_{T}^{2}$ , dimensionless
- $c_{
  m D}^{
  m s}$  value of  $c_{
  m D}^{
  m c}$  for a rigid sphere, dimensionless
- D drop diameter, cm
- $\mathbf{D}_{\mathbf{C}}$  column diameter, cm
- $\mathbf{D_{h}}$  sieve-plate hole diameter, cm
- D; liquid jet diameter, cm
- $D_{M}$  drop diameter corresponding to  $v_{N,M}$ , cm
- D, nozzle diameter, cm
- D' equivalent spherical drop diameter,  $(6 \text{ V}_{\text{D}}/\pi)^{1/3}$ , cm
- 🙈 molecular diffusivity, cm<sup>2</sup>/sec
- E fraction extracted, dimensionless
- E drop eccentricity, dimensionless
- E f fraction extracted during drop formation and coalescence at the interface, dimensionless
- E overall fraction extracted, dimensionless
- f pulse frequency, cycles/min
- F correlation factor, dimensionless
- F enhancement factor, dimensionless
- g acceleration of gravity, cm/sec<sup>2</sup>

G - gas content, vol.%

G - saturation gas content, vol.%

h - fineness ratio, 1/E<sub>e</sub>, dimensionless

H - dispersed phase holdup, vol.%

HETS - height equivalent to a theoretical stage, cm

HTU - overall height of a transfer unit, cm

I' - threshold intensity in terms of the pressure amplitude, atm

 $I_{po}^{\dagger}$  -  $I_{p}^{\dagger}$  evaluated at  $0^{\circ}$ C, atm

k - individual mass transfer film coefficient, cm/sec

K - overall mass transfer coefficient, cm/sec

sieve-plate spacing, cm

L - volume flow rate, cm<sup>3</sup>/sec

m - phase-distribution ratio, dimensionless

m' - exponential constant, dimensionless

n - integer, dimensionless

n' - exponential constant, dimensionless

N - rate of mass transfer, g/sec-cm<sup>2</sup>

p,q,r,s- constants, dimensionless

S - drop surface area, cm<sup>2</sup>

T - temperature, OC

T - saturation temperature, OC

U - drop velocity, cm/sec

 $v_{_{
m N}}$  - nozzle velocity, cm/sec

v<sub>N,M</sub> - nozzle velocity at which the maximum interfacial area is produced, cm/sec

v - characteristic velocity, cm/sec.

v - slip velocity, cm/sec

v<sub>m</sub> - terminal velocity, cm/sec

V<sub>D</sub> - drop volume, cm<sup>3</sup>

V - effective column volume, cm<sup>3</sup>

w - dimensionless quantity, a function of  $(\mu_c/\mu_d)N_{Re}^{1/2}$ , dimensionless

Z - effective column height, cm.

#### Greek Symbols

~ - constant, dimensionless

γ - distortion coefficient, dimensionless

 $\Delta$  - finite difference

€ - fractional free space per plate, dimensionless

0 - contact time, sec

 $\lambda_n, \lambda_n'$  - eigenvalues, dimensionless

 $\mu$  - viscosity, poise

 $\pi$  - 3.1416

 $\rho$  - density, g/cm<sup>3</sup>

σ - interfacial tension, dynes/cm

 $\phi_{,\psi}$  - function

#### Dimensionless Groups

j' - modified j-factor,  $(k_c/L_c)N_{Sc}^{0.58}$ 

 $N_{Eo}^{\prime}$  - Eötvös number based on D',  $g \triangle \rho D^{\prime 2}/\sigma$ 

 $N_{Cr}$ - Grashof number,  $D^3 g \Delta \rho \rho / \mu^2$ 

 $N_{Ph}$  - Physical properties group,  $\rho_c^2 \sigma^3/g \Delta \rho \mu_c^4$ 

 $N_{Re}$  - Reynolds number,  $DU\rho_c/\mu_c$ 

 $N_{Re}^{\prime}$  - Reynolds number based on D', D'U $\rho_{c}/\mu_{c}$ 

N<sub>Sc</sub> - Schmidt number, μ/ρ<sub>2</sub>S

N<sub>Sh</sub> - Sherwood number, k/D.

 $N_{Tm}$  - Time group, 4.89/D

 $N_{We}$  - Weber number,  $DU^2 \rho / \sigma$ 

 $N_{We}^{1}$  - Weber number based on  $D^{1}$ ,  $D^{1}U^{2}\rho/\sigma$ 

 $N_{\rho}$  -  $\rho$  group,  $\sigma^3 \rho_c^3/g \mu_c^4 \Delta \rho$ 

 $_{x}$  -  $(N_{Re})^{1/8} (\mu_{c}/\mu_{d})^{1/4} (\sigma^{*})^{1/6}$ 

 $\beta$  -  $g D'^2 \Delta \rho/4\sigma$ 

 $\sigma^*$  -  $\sigma/\mu_c v_s$ 

# Subscripts

c - continuous phase

d - dispersed phase

i - interface

m - MIBK phase

w - water phase

 $\theta$  - at time  $\theta$ 

0 - at time zero

1 - during drop formation

2 - during drop rise or fall

3 - during drop coalescence at the interface

#### REFERENCES

- 1. Treybal, R.E., "Liquid Extraction", Second Edition, p.352, McGraw-Hill, New York (1963)
- Sherwood, T.K., and R.L. Pigford, "Absorption and Extraction", p.425, McGraw-Hill, New York (1965)
- 3. Elgin, J.C., and F.M. Browning, Trans./Am..Inst. Engrs. 31 639 (1935)
- 4. Sherwood, T.K., Evans, J.E., and J.V.A. Longcor, Ind. Eng. Chem. 31 1144 (1939)
- 5. Licht, W., and J.B. Conway, Ind. Eng. Chem. <u>42</u> 1151 (1950)
- 6. Licht, W., and W.F. Pansing, Ind. Eng. Chem. 45 1885 (1953)
- 7. Johnson, H.F., and H. Bliss, Trans. Am. Inst. Chem. Engrs. <u>42</u> 331 (1946)
- 8. Nandi, S.K., and T.R. Viswanathan, Current Sci. (India) 15 162 (1946)
- 9. Kreager, R.M., and C.J. Geankoplis, Ind. Eng. Chem. 45 2156 (1953)
- 10. Coulson, J.M., and S.J. Skinner, Chem. Eng. Sci. <u>1</u> 197 (1952)
- 11. West, F.B., Robinson, P.A., Morgenthaler, A.C., Beck, T.R., and D.K. McGregor, Ind. Eng. Chem. 43 234 (1951)
- 12. Garner, F.H., Foord, A., and M.J. Tayeban, J. Appl. Chem. 9 315 (1959)
- 13. Calderbank, P.H., and I.J.D. Korchinski, Chem. Eng. Sci. 6 65 (1956)
- 14. Thorsen, G., and S.G. Terjesen, Chem. Eng. Sci. 17 137 (1962)
- 15. Ruby, C.L., and J.C. Elgin, Chem. Eng. Progr. Symp. Ser. <u>51</u> (15): 17 (1955)
- 16 Seltzer, E., and B. Williams, Paper presented at the A.I.Ch. E. Atlanta meeting (March, 1952)
- 17. Lapidus, L., and J.C. Elgin, A.I.Ch.E. Journal <u>3</u> 63 (1957)

- 18. Weaver, R.E.C., Lapidus, L., and J.C. Elgin, A.I.Ch.E. Journal 5 533 (1959)
- 19. Beyaert, B.O., Lapidus, L., and J.C. Elgin, A.I.Ch.E. Journal 7 46 (1961)
- 20. Thornton, J.D., Chem. Eng. Sci. <u>5</u> 201 (1956)
- 21. Weaver, R.E.C., Ph.D. dissertation, Princeton University, Princeton, N.J., U.S.A. (1955)
- 22. Hughmark, G.A., Ind. Eng. Chem. Fundamentals 6 (3) 408 (1967)
- 23. Pratt, H.R.C., Trans. Inst. Chem. Eng. (London) 29 195 (1951)
- 24. Morello, V.S., and N. Poffenberger, Ind. Eng. Chem. <u>42</u> 1021 (1950)
- 25. Geankoplis, C.J., and A.N. Hixson, Ind. Eng. Chem. 42 1141 (1950)
- 26. Geankoplis, C.J., Wells, P.L., and E.L. Hawk, Ind. Eng. Chem. <u>43</u> 1848 (1951)
- 27. Newman, M.L., Ind. Eng. Chem. 44 2457 (1952)
- 28. Gier, T.E., and J.D. Hougen, Ind. Eng. Chem. 45 1362 (1953)
- 29. Hazlebeck, D.E., and C.J. Geankoplis, Ind. Eng. Chem. Fundamentals 2 310 (1963)
- 30. Cavers, S.D., and J.E. Ewanchyna, Can. J. Chem. Eng. 35 113 (1957)
- 31. Mar, B.W., and A.L. Babb, Ind. Eng. Chem. <u>51</u> 1011 (1959)
- 32. Bibaud, R.E., and R.E. Treybal, A.I.Ch.E. Journal 12 472 (1966)
- 33. Mixon, F.O., Whitaker, D.R., and J.C. Orcutt, A.I.Ch.E. Journal 13 21 (1967)
- 34. Treybal, R.E., "Liquid Extraction", Second Edition, p.176, McGraw-Hill, New York (1963)
- 35. Skelland, A.H.P., and R.M. Wellek, A.I.Ch.E. Journal, 10 491 (1964)
- 36. Newman, A.B., Trans. Am. Inst. Chem. Engrs. 27 203 (1931)
- 37. Vermeulen, T., Ind. Eng. Chem., 45 1664 (1953)
- 38. Kronig,, R., and J.C. Brink, Appl. Sci. Res. A-2, 142 (1950)

- 39. Heertjes, P.M., Holve, W.A., and H. Talsma, Chem. Eng. Sci. <u>3</u> 122 (1954)
- 40. Elzinga, E.R., and T.J. Banchero, Chem. Eng. Progr. Symp. Ser. <u>55</u> (29) 149 (1959)
- 41. Handlos, A.E., and T. Baron. A.I.Ch.E. Journal 3 127 (1957)
- 42. Johnson, A.I., and A.E. Hamielec, A.I.Ch.E. Journal, <u>6</u> 145 (1960)
- 43. Hu, S.G., and R.C.Kintner, A.I.Ch.E. Journal 1 42 (1955)
- 44. Wellek, R.M., and A.H.P. Skelland, A.I.Ch.E. Journal <u>3</u> 557 (1965)
- 45. Higbie, R., Trans. Inst. Am. Chem. Engrs. 31 365 (1935)
- 46. McCune, L.K., and R.H. Whilhelm, Ind. Eng. Chem. 41 1124 (1949)
- 47. Griffith, R.M., Chem. Eng. Sci. 12 198 (1960)
- 48. Garner, F.H., and R.B., Keely, Chem. Eng. Sci. 9 119 (1958)
- 49. Hayworth, C.B., and R.E. Treybal, Ind. Eng. Chem. 42 1174 (1950)
- 50. Null, H.R., and H.F. Johnson, A.I.Ch.E. Journal 4 273 (1958)
- 51. Keith, F.W., and A.N. Hixson, Ind. Eng. Chem. 47 258 (1955)
- 52. Christiansen and A.N. Hixson, Ind. Eng. Chem. 49 1017 (1957)
- 53. Garner, F.H., and A.H.P. Skelland, Chem. Eng. Sci. 4 149 (1955)
- 54. Licht, W., and G.S.R. Narasimhamurty, A.I.Ch.E. Journal 1 366 (1955)
- 55. Klee, A.J., and R.E. Treybal, A.I.Ch.E. Journal 2 444 (1956)
- 56. Harmathy, T.Z., A.I.Ch.E. Journal 6 281 (1960)
- 57. Kintner, R.C., Drew, T.B., Hoopes, J.W., and T. Vermeulen, "Advances in Chemical Engineering", Vol. 4, p.51, Academic Press, New York (1963)
- 58. Hughes, R.R., and E.R. Gilliland, Chem. Eng. Progr. 48 497 (1952)
- 59. Spilhaus, A.H.P., J. Meteor. 5 108 (1948)
- 60. Wellek, R.M., Agrawal, A.K., and A.H.P. Skelland, A.I.Ch.E. Journal 12 854 (1966)

- 61. Mahajan, L.D., Phil.Mag. 10 383 (1930)
- 62. Brown, A.H., and C. Hanson, Brit. Chem. Eng. <u>11</u> 695 (1966)
- 63. Charles, G.E., and S.G. Mason, J. Golloid Sci. 15 105 (1960)
- 64. Jeffreys, G.V., and J.L. Hawksley, J. Appl. Chem. 12 329 (1962)
- 65. Jeffreys, G.V., and J.L. Hawksley, A.I.Ch.E. Journal 11 413 (1965)
- 66. Linton, M., and K.L. Sutherland, J.Colloid Sci. 11 391 (1956)
- 67. Charles, G.E., and S.G. Mason, J. Colloid Sci. 15 236 (1960)
- 68. Allan, R.S., and S.G. Mason, Trans. Far. Soc. <u>57</u> 2027 (1961)
- 69. Brown, A.H., and C. Hanson, Trans. Far. Soc. 61 1754 (1965)
- 70. Van Dijck, W.J.D., U.S. Patent 2,001,186 (1935)
- 71. Treybal, R.E., "Liquid-Liquid Extraction", Second Edition, p.523, McGraw-Hill, New York (1963)
- 72. Belaga, M.W., and J.E. Bigelow, U.S.A.E.C. Declass, Doc. KT-133 (1952)
- 73. Cohen, R.M., and G.H. Beyer, Chem. Eng. Progr. 49 279 (1953)
- 74. Sege, G., and F. Woodfield, Chem. Eng. Progr. <u>50</u> 396 (1954)
- 75. Goldberger, W.M., and R.F. Benenati, Ind. Eng. Chem. 51 641 (1959)
- 76. Thornton, J.D., Brit. Chem. Eng. 3 247 (1958)
- 77. Smoot, L.D., Mar, B.W., and A.L. Babb, Ind. Eng. Chem. <u>51</u> 1005 (1959)
- 78. Smoot, L.D., and A.L. Babb, Ind. Eng. Chem. Fundamentals <u>1</u> (2) 93 (1962)
- 79. Feick, G., and H.M. Anderson, Ind. Eng. Chem. 44 404 (1952)
- 80. Chantry, W.A., Von Berg, R.L., and H.F. Wiegandt, Ind. Eng. Chem. 47 1153 (1955)
- 81. Pontnis, G.V., Bijawat, H.C., and L.K. Doraiswamy, Ind. Eng. Chem. 51 645 (1959)

- 82. Karpacheva, S.M. Rodienov, E.P., and G.M. Popova, C.A. <u>55</u> 8963 f (1960)
- 83. Moon, J. S., Hennico, A., and T. Vermeulen, Lawrence Radiation Laboratory, University of California, Report UCRL-10928 (1963)
- Lurie, R.M., and R.G. Shaver, Carbide and Carbon Chemicals Co. Memo. EPS-K-184 (1952)
- 85. O'Brien, D.C., S.M. Dissertation, Massachusetts Institute of Technology, Cambridge, Mass (1954)
- 86. Billerbeck, C.J., Farquhar, J., Reid, R.C., Bresee, J.C., and A.S. Hoffman, Ind. Eng. Chem. 48 183 (1956)
- 87. Brown, B., and J.E. Goodman, "High-Intensity Ultrasonics, Industrial Applications", p.1 Iliffe, London (1965)
- 88. Ibid p. 1-29
- 89. Ibid .p.31
- 90. Blake, F.G., Acoustic Research Lab., Harvard University, Tech. Memo. No. 12 (1949)
- 91. Willard, G.W., & J. Acoust. Soc. Am. <u>25</u> 669 (1953)
- 92. Galloway, J.E., J. Acoust. Soc. Am. 26 849 (1954)
- 93. Barger, J.E., Acoustic Research Lab., Harvard University, Tech. Memo. No. 57 (1962)
- 94. Degrois, M., Ultrasonics <u>4</u> 38 (1966)
- 95. Noltingk, B.E., and E.A. Neppiras, Proc. Phys. Soc. (London) B<u>63</u> 674 (1950)
- 96. Ibid B64 1032 (1951)
- 97. Rozenberg, L.D., Ultrasonic News <u>4</u> 16 (1960)
- 98. Goldman, R., "Ultrasonic Technology", p.113-166, Reinhold, New York (196
- 99. Hueter, T.F., and R.H. Bolt, "Sonics" p.120, John Wiley, New York (1955)
- 100. Dunn, F., and W.J. Fry, Trans. I.R.E. <u>5</u> 59 (1957)

- 101. Teumin, I.I., Soviet Physics-Acoustics 8 291 (1963)
- 102. Richardson, E.G., Proc. Royal Soc. (London) A146 56 (1934)
- 103. Blitz, J., "Fundamentals in Ultrasonics", p.60 Butterworths, London (1963)
- 104. Saneyoshi, J., Okujima, M., and M. Ide, Ultrasonics 4 64 (1966)
- 105. Richards, W.T., Sicence, New York 76 36 (1932)
- 106. Weber, M.E., and W.Y. Chon, Can. J. Chem. Eng. 45 238 (1967)
- 107. Bebchuk, A.S., Soviet Physics-Acoustics 3 95 (1957)
- 108. Bebchuk, A.S., Borisov, I.I., and L.D. Rosenberg, Soviet Physics-Acoustics 4 372 (1958)
- 109. Crawford, A.E., Ultrasonics 2 120 (1964)
- 110. Chon, W.Y., and S.W. Wong, Paper presented at the European Convention of Chem. Eng., Frankfurt am Main, Germany (June 25, 1967)
- 111. Strasberg, M., J. Acoust. Soc. Am. <u>33</u> 359 (1961)
- 112. Connolly, W., and F.E. Fox, J. Acoust. Soc. Am. <u>26</u> 843 (1954)
- 113. Briggs, H.B., Johnson, J.B., and W.P.M. Mason, J. Acoust. Soc. Am. 19 664 (1947)
- Brown, B., and J.E. Goodman, "High-Intensity Ultrasonics, Industrial Applications", p.33, Iliffe, London (1965)
- 115. Heuter, T.F., and R.H. Bolt, "Sonics", p.230, John Wiley, New York (1955)
- 116. Blitz, J. "Fundamentals in Ultrasonics" p.200, Butterworths, London (1963)

EXPERIMENTAL SECTION

#### PART I.

## EFFECTS OF ULTRASONIC VIBRATION ON THE EXTRACTION EFFICIENCY

#### INTRODUCTION

It has been established from the performance of pulsed columns that pulsating motion, when imposed to an extraction column, increases the degree of turbulence and the interfacial area of contact between the phases. Vibrations caused by the ultrasonic waves may be considered as a form of high frequency pulsating motion. Therefore, it seems reasonable to assume that ultrasonic vibration may increase the extraction efficiency of a liquid-liquid extraction column. However, since no previous work has been done in this field, a preliminary investigation was carried out to experimentally confirm the above assumption. Results of the preliminary investigation are given in Appendix A.

The main experimental work, which followed the preliminary investigation, was devoted to single drop extractions, in order to simplify the measurements of interfacial area and contact time, so that a later study of the extraction mechanism was made feasible.

The ternary system studied was water-acetic acid-methyl isobutyl ketone (MIBK) which is one of the most frequently used systems in liquid-liquid extraction studies.

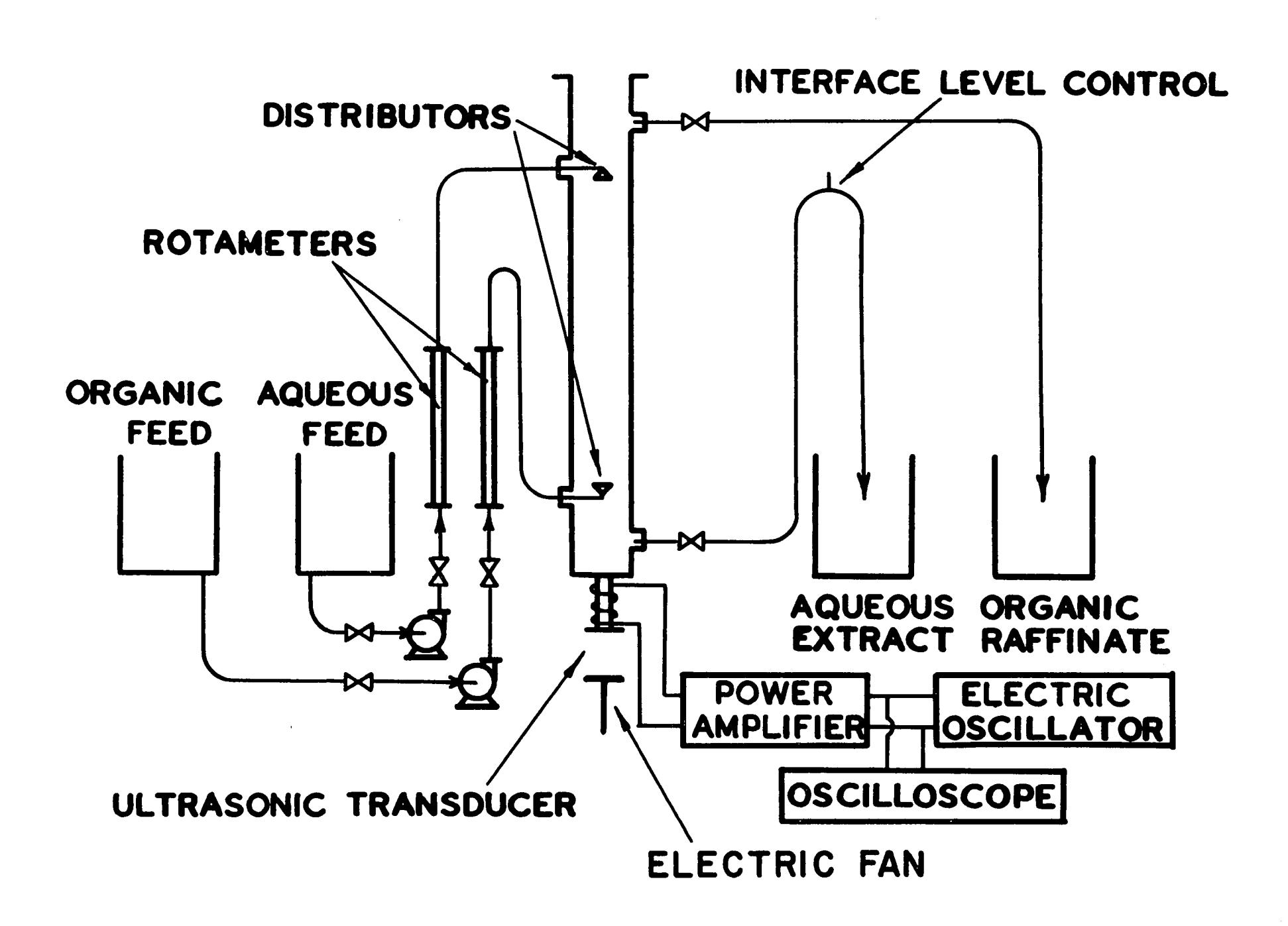
### APPARATUS AND PROCEDURE

The experimental apparatus was arranged as shown in Figure 1. The extraction column consisted of a Quickfit Pyrex glass cylinder, 3.81 cm I.D., 45.72 cm in length, and with a 9 x 9 cm rectangular plexiglass jacket. During the operation, cooling water was passed through the jacket to remove the heat generated by the transducer and keep the temperature in the column at  $25 \pm 0.5^{\circ}$ C. The inlet and outlet pipes at both ends of the column were 0.48 cm I.D., and the dispersing distributor was a single glass nozzle. Three different sizes of nozzles were used, i.e., 0.079, 0.163 and 0.316 cm. Figure 2 is a photograph of the column.

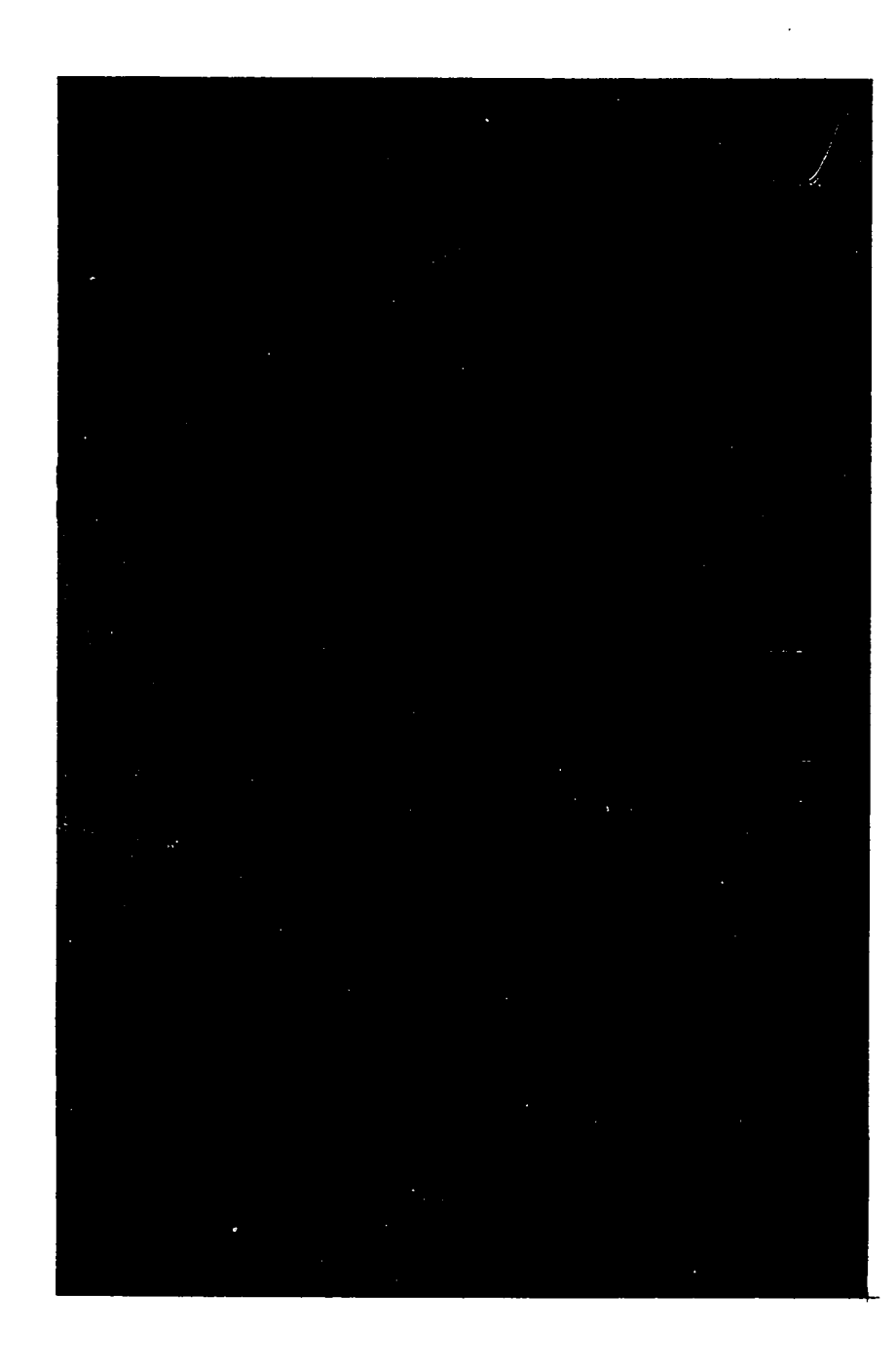
Using Armstrong Al2T epoxy, the ultrasonic transducer was cemented onto a 0.079 cm thick stainless steel plate which was attached immediately under the bottom of the column. The center of the transducer was located along the axis of the column. All the transducers were operated at their resonant frequency in order to obtain a stable and maximum output. Details of the transducers used in this work are summarized in Table 1, and a photograph of them is shown in Figure 3. Brief information on the materials of transducers is given in Appendix B.

The transducer was cooled by an electric fan, and was driven by a sine-wave form electric oscillator (Heathkit Model IG-82) whose output was amplified by a custom-built power amplifier.

FLOW DIAGRAM OF EXPERIMENTAL SYSTEM

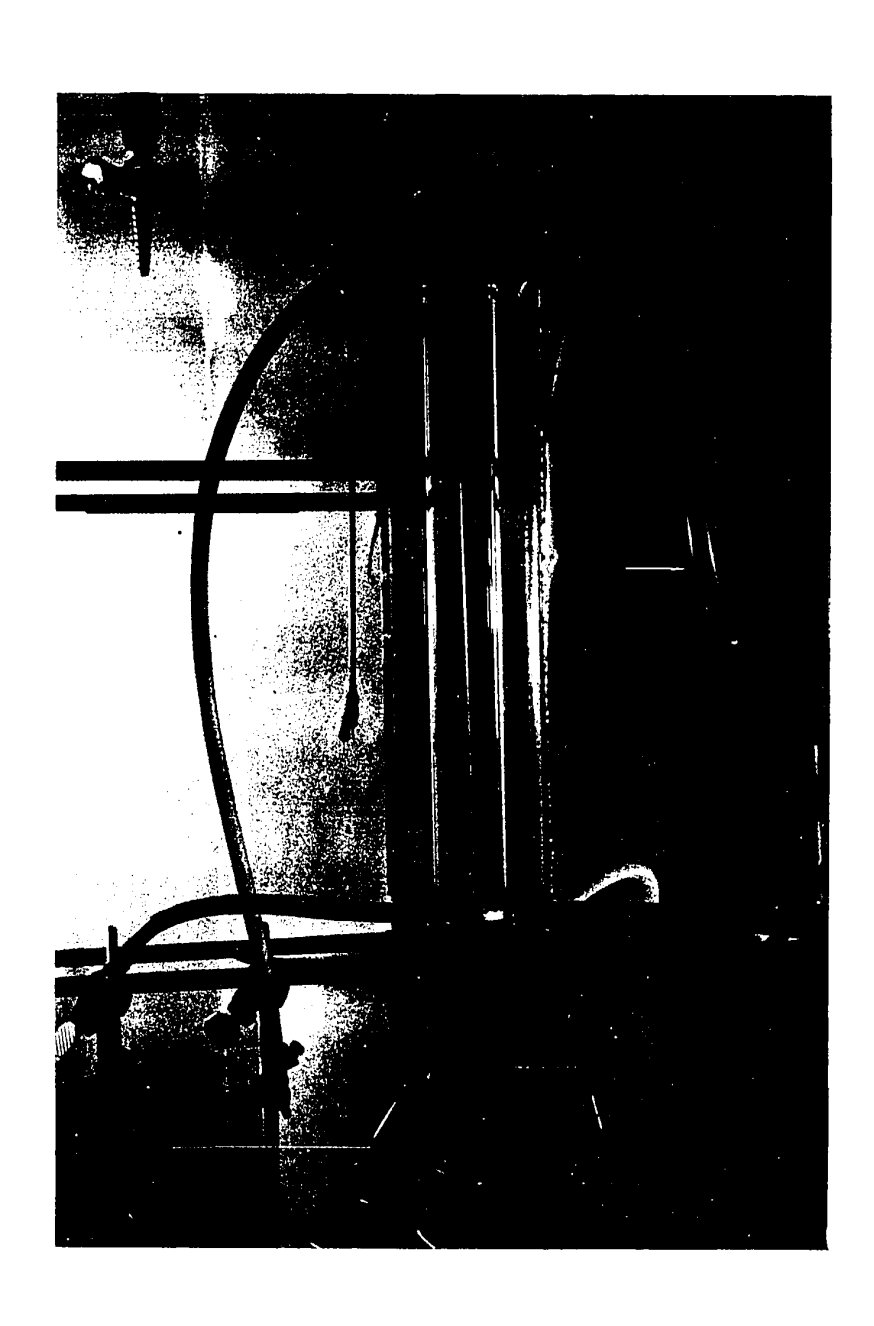


PHOTOGRAPH OF THE EXTRACTION COLUMN



.





è

1

TABLE 1. DETAILS OF THE TRANSDUCERS

No.	Туре	Shape	Material	Manufac- turer	Dimensions cm	Resonant Frequency
1	Magnetostrictive	Square Bar	Ferroxcube 7A2	_	Base: 4.13 x 3.97 Length: 9.53	20
2	Magnetostrictive	Square Bar	Ferroxcube 7A2	•	Base: 3 x 2.95 Length: 5	40
3	Piezoelectric	<b>Ņisc</b>	Barium Titanate	Gulton Indus- tries	Diameter: 3.81 Thickness: 1.98	100

PHOTOGRAPH OF THE TRANSDUCERS

No. 3

No. 1

No. 2



1

()

こととというできるのでは、

これによるとのではないのではないのではないとうと

The amplifier had a frequency range of 15 to 200 kc/sec, and a maximum power output of 300 watts. The wave form as well as the vibration frequency during the operation were checked regularly by a Tektronix Type 502A oscilloscope. Figure 4 is the photograph of the instrumentation.

The feed storage and effluent receiving tanks were both 25-gallon barrels, made of polyethylene. Two stainless steel centrifugal pumps, built by Eastern Engineering Company, were used to transport the aqueous and organic solutions. The pump motors were 1/15 H.P.. Each feed line included a Manostat Model FM1044B rotameter, and flow rates of each phase were regulated by a stainless steel globe valve (Crane 222 F-8) on the pump outlet line. Calibration curves of the rotameters for distilled water and 10% acetic acid-MIBK solution are given in Appendix C. All of the lines were of 0.95 cm I.D. Teflon tubing.

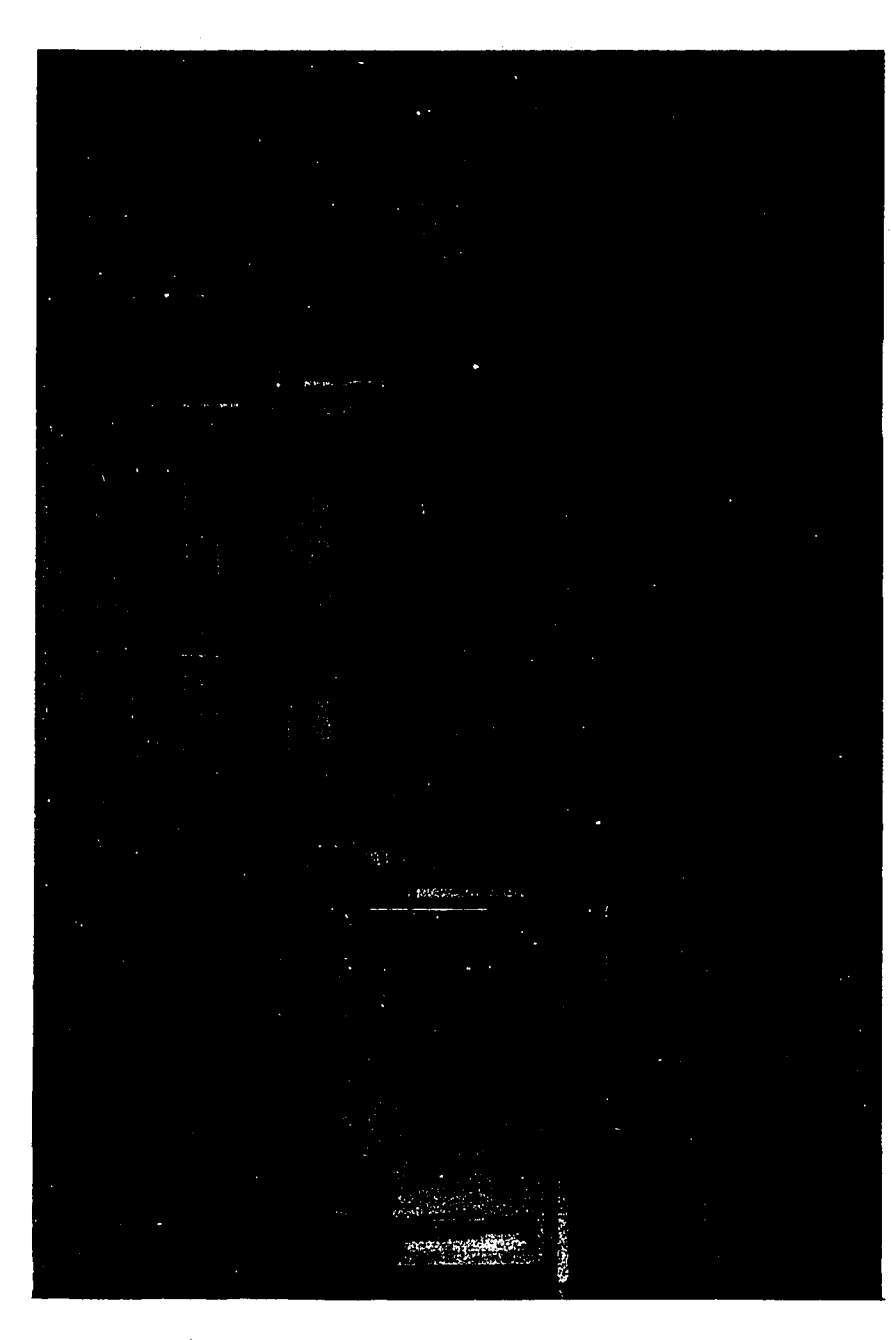
As for the chemicals, U.S.P. glacial (99%) acetic acid, commercial MIBK from J.T. Baker Chemicals Company, and laboratory distilled water were used. Equilibrium data were taken from the literature (1), and are given in Appendix D. Density, viscosity, and interfacial tension as a function of the concentration of the acetic acid-MIBK solution were measured by a hydrometer, Cannon-Fenske Viscometer, and a Ring-Type Tensiometer respectively, and are also given in Appendix D.

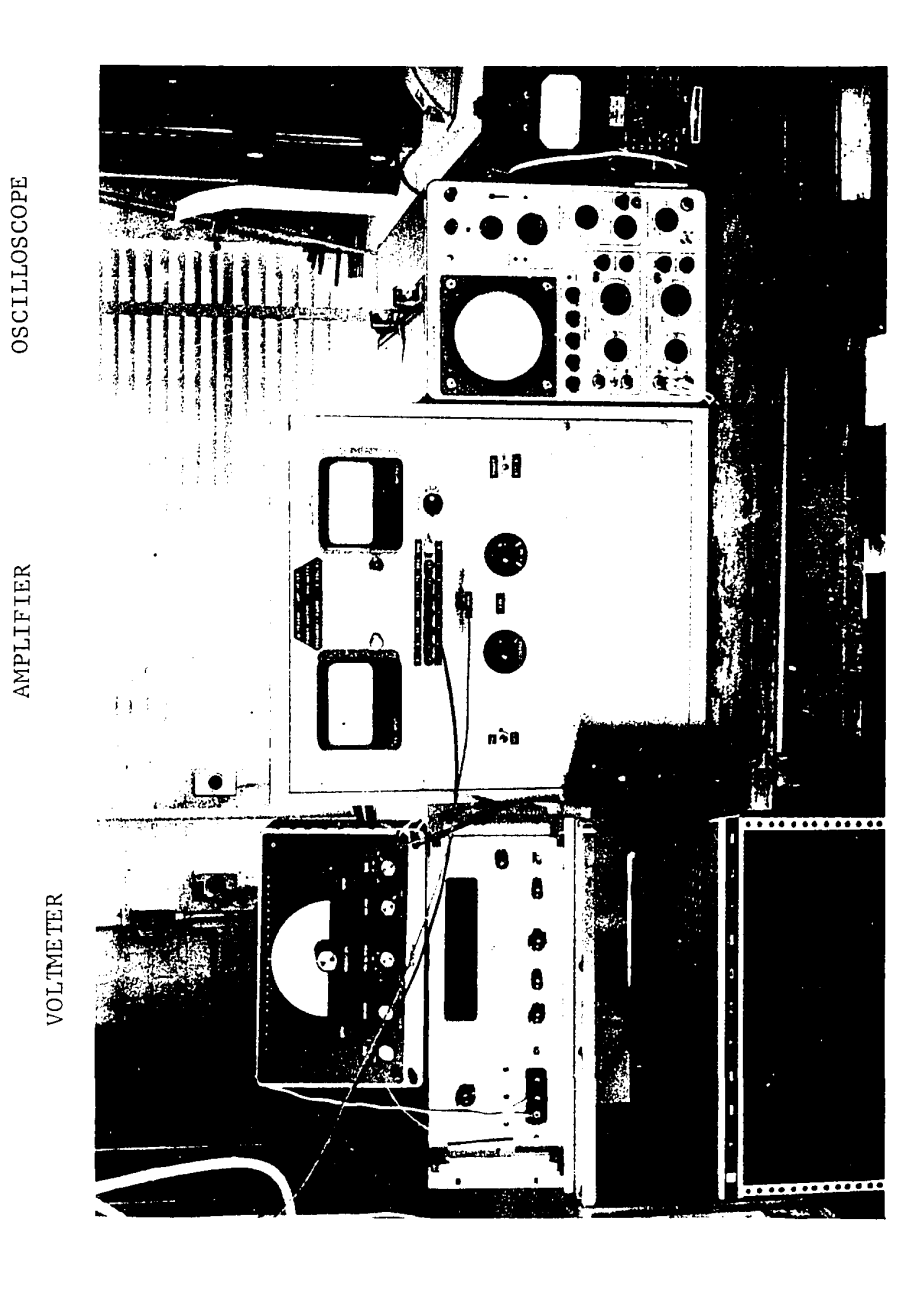
PHOTOGRAPH OF THE INSTRUMENTATION

OSCILLATOR
AMPLIFIER

VOL IME TER

OSCILLOSCOPE





OSCILLATOR

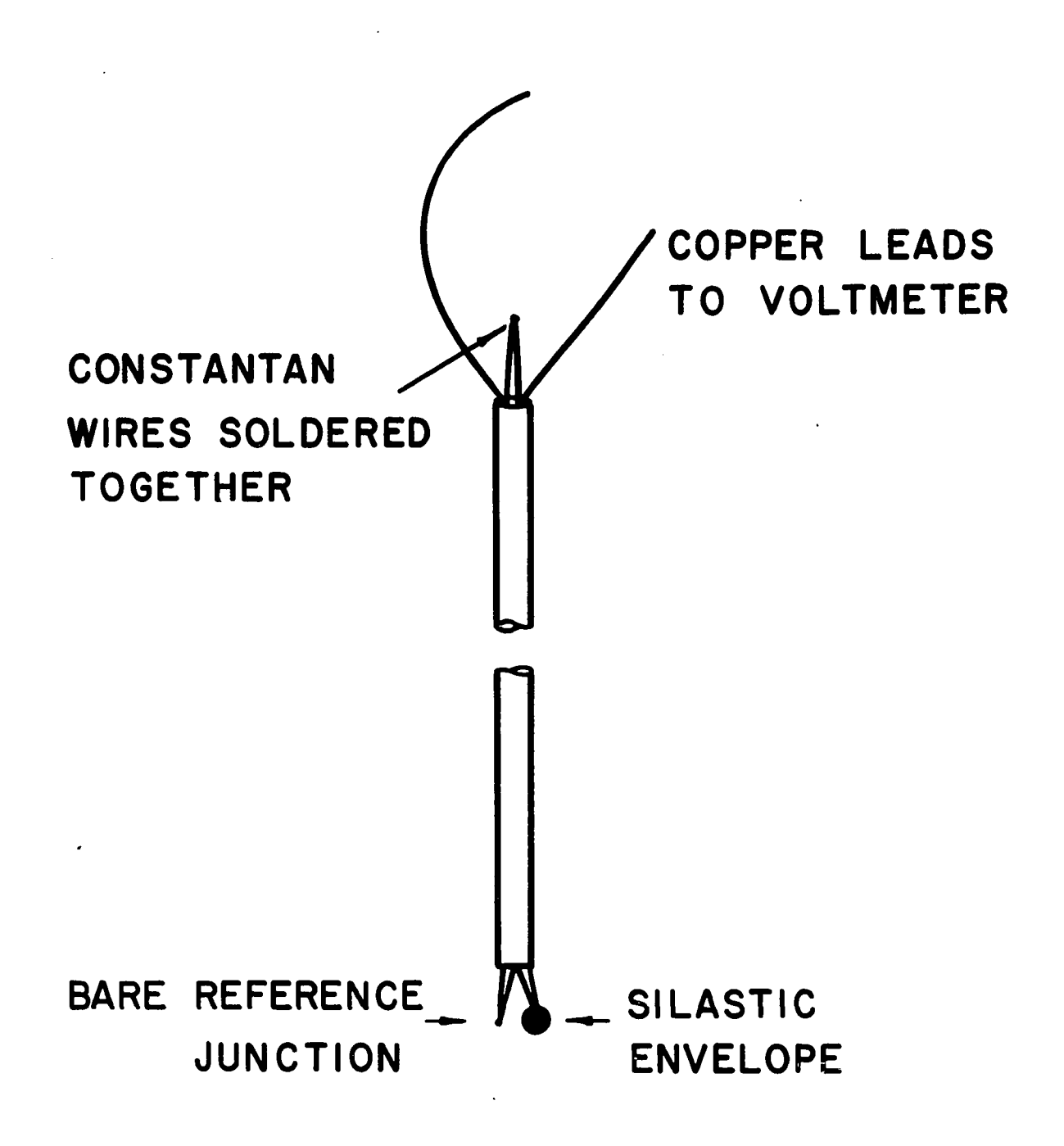
In making a run, feed solutions were first mutually saturated with respect to water and MIBK, and the organic feed was made up to the desired acid concentration. The column, after washing, was filled with the phase which was to be continuous during the run. The run was then started by opening the valves in the aqueous and organic lines. The rotameters were set to give the desired flow rate while the height of the aqueous-organic interface was adjusted to the desired level by regulating the hydrostatic head of the aqueous outlet line. The frequency and intensity of vibrations were set to the desired values. Samples were withdrawn and analysed after the whole system reached a steady state.

The acid concentration of each phase was determined by titrating the feed and exit stream samples with standard sodium hydroxide solution using phenolphthalein as an indicator.

The relative ultrasonic intensity in liquids was measured by an absorbed thermocouple probe similar to that used by Weber and Chon<sup>(2)</sup>. Referring to Figure 5, the thermocouple has one junction bare and the other enclosed in a small silastic (Dow Corning RTV 502) ball of 0.64 cm in diameter, and the two junctions positioned about 0.2 cm apart. The silastic envelope absorbs ultrasonic energy and gives a temperature difference between the two junctions which is proportional to the local

THERMOCOUPLE PROBE





ultrasonic intensity<sup>(3,4)</sup>. The probe output was read on a Hewlett Packard Model 2401C digital voltmeter which is shown in Figure 4 together with other insturments used.

### CALCULATION OF THE EXTRACTION EFFICIENCY

The extraction efficiency was calculated in terms of the capacity coefficient, Ka. The water and MIBK were mutually saturated before the run, and they may be considered as immiscible for low acid concentrations. A mass balance for the water phase across a differential element of column height is then written as

$$F_{\omega}d C_{\omega} = K_{\omega} (C_{\omega}^{*} - C_{\omega}) dA$$
 (1)

or

$$\frac{d C_{w}}{C_{w}^{*} - C_{w}} = \frac{K_{w}}{F_{w}} dA \qquad (2)$$

Integrating both sides gives

$$\int \frac{d C_w}{C_w^* - C_w} = \int \frac{K_w}{F_w} dA$$
 (3)

$$\int \frac{d C_{w}}{C_{w}^{*} - C_{w}} = \frac{K_{w}}{F_{w}} \int dA$$
 (4)

Since  $dA = a \times dV$ ,

$$\int \frac{d C_w}{C_w^* - C_w} = \frac{K_w a}{F_w} \int dV = \frac{K_w a V}{F_w}$$
 (5)

If the equilibrium curve is straight over the range of concentrations involved, which may be considered true for the system of water-acetic acid-MIBK with concentrations of less than 10%, a log-mean concentration driving force can be used. Equation (5) becomes

$$\frac{\Delta C_{w}}{(C_{w}^{*}-C_{w})_{\ell n}} = \frac{K_{w}^{a} V}{F_{w}}$$
 (6)

The overall capacity coefficient based on the water phase,  $K_{_{\!\!\!\!U}}a$ , then is

$$K_{w}a = \frac{F_{w}}{V} \times \frac{\Delta C_{w}}{(C_{w}^{*} - C_{w})_{\ell n}}$$
(7)

where

$$\Delta C_{w} = C_{w2} - C_{w1},$$

and

$$(C_{w}^{*} - C_{w})_{\ell n} = \frac{(C_{w1}^{*} - C_{w1}) - (C_{w2}^{*} - C_{w2})}{\ell n \frac{(C_{w1}^{*} - C_{w1})}{(C_{w2}^{*} - C_{w2})}}$$

The variation in  $K_W$  a values due to ultrasonic vibration was expressed in terms of the "% increase in  $K_W$  a" which was defined by the following equation

% Increase in 
$$K_{w}^{a} = \frac{(K_{w}^{a})_{1} - (K_{w}^{a})_{0}}{(K_{w}^{a})_{0}} \times 100$$
 (8)

#### EXPERIMENTAL RESULTS

For this investigation, one hundred and twenty experiments were performed. Half were with the MIBK phase dispersed and the water phase continuous, and the other half with the water phase dispersed and the MIBK phase continuous. In both cases, the transfer of acetic acid was from MIBK to water. The results are summarized in Tables 2 and 3, and are shown through Figures 6 to 13. Figures 6 to 11 are plots of  $K_w$  a versus the solute concentration of the MIBK feed, using the vibrational conditions as parameters. In Figure 12 and 13, the % increase in  $K_w$  a was plotted against the nozzle diameter in a log-log scale, where the parameter was the flow rate ratio defined as  $F_m/F_w$ . Values of  $K_w$  and the % increase in  $K_w$  a were calculated by Equations (7) and (8) respectively.

The measuring point for I, the ultrasonic intensity, was 7.62 cm from the bottom and near the center of the column which was either the center of the aqueous-organic interface level or the dispersing nozzle tip, depending on whether MIBK phase was continuous or dispersed. The axial intensity profiles for the three different transducers used were

TABLE 2. SUMMARY OF EXPERIMENTAL RESULTS (1)

DISPERSED PHASE: MIBK CONTINUOUS PHASE: Water

SOLUTE: Acetic Acid TRANSFER OF SOLUTE: From MIBK to Water

LOCATION OF DISPERSING NOZZLE: 7.62 cm from the LOCATION OF INTERFACE LEVEL: 38.10 cm from the

Bottom

Bottom

EFFECTIVE COLUMN HEIGHT: 30.48 cm COLUMN DIAMETER: 3.81 cm

TEMPERATURE: 24.5 - 25.5°C PRESSURE: Atmosphere

(K <sub>w</sub> a) <sub>0</sub> x 10 <sup>4</sup>	$(K_w^a)_I \times 10^4$	$(K_w^a)_I \times 10^4$	$(K_w^a)_1 \times 10^4$				
1/sec	1/sec	1/sec	1/sec	F <sub>m</sub> /F <sub>w</sub>	c <sub>m2</sub>	D <sub>N</sub>	
I = 0 mv $f = 0 kc/sec$	I = 0.17  mV f = 100  kc/sec	I = 0.36  mV $c f = 40  kc/sec$	I = 0.64 mv f = 20 kc/sec		wt.%	cm	
· · · · · · · · · · · · · · · · · · ·			1 - 20 KC/ SeC		**************************************		<del></del>
0.336	0.366	0.410	0.454	0.462	.5.91	0.079	
0.318	0.345	0.379	0.433	0.462	4.73	0.079	
0.304	0.330	0.352	0.376	0.462	3.49	0.079	
0.250	0.268	0.296	0.313	0.462	2.47	0.079	
0.412	0.443	0.487	0.563	1.147	5.91	0.079	
0.402	0.443	0.476	0.504	1.147	4.73	0.079	
0.375	0.410	0.449	0.517	1.147	3.49	0.079	
0.321	0.353	0.398	0.444	1.147	2.47	0.079	
0.557	0.606	0.680	0.766	2.158	5.91	0.079	
0.537	0.588	0.648	0.750	2.158	4.73	0.079	74
0.492	0.539	0.605	0.682	2.158	3.49	0.079	•
0.424	0.463	0.519	0.594	2.158	2.47	0.079	



TABLE 2. (continued)

0.445	-	0.525	-	2.158	3.49	0.316
0.475	-	0.569	•	2.158	3.49	0.163
0.342	-	0.378	-	1.147	3.49	0.316
0.364	-	0.421	-	1.147	3.49	0.163
0.272	-	0.290	•	0.462	3.49	0.316
0.302	-	0.335	-	0.462	3.49	0.163

TABLE 3. SUMMARY OF EXPERIMENTAL RESULTS (2)

DISPERSED PHASE: Water CONTINUOUS PHASE: MIBK

SOLUTE: Acetic Acid TRANSFER OF SOLUTE: From MIBK to Water

LOCATION OF DISPERSING NOZZLE: 38.10 cm from LOCATION OF INTERFACE LEVEL: 7.62 cm from the

Bottom

the Bottom
EFFECTIVE COLUMN HEIGHT: 30.48 cm COLUMN DIAMETER: 3.81 cm

DITECTIVE COLOUR INTENT. 30.40 Cm Colour Branches. 3.01 Cm

TEMPERATURE: 24.5 - 25.5°C PRESSURE: Atmosphere

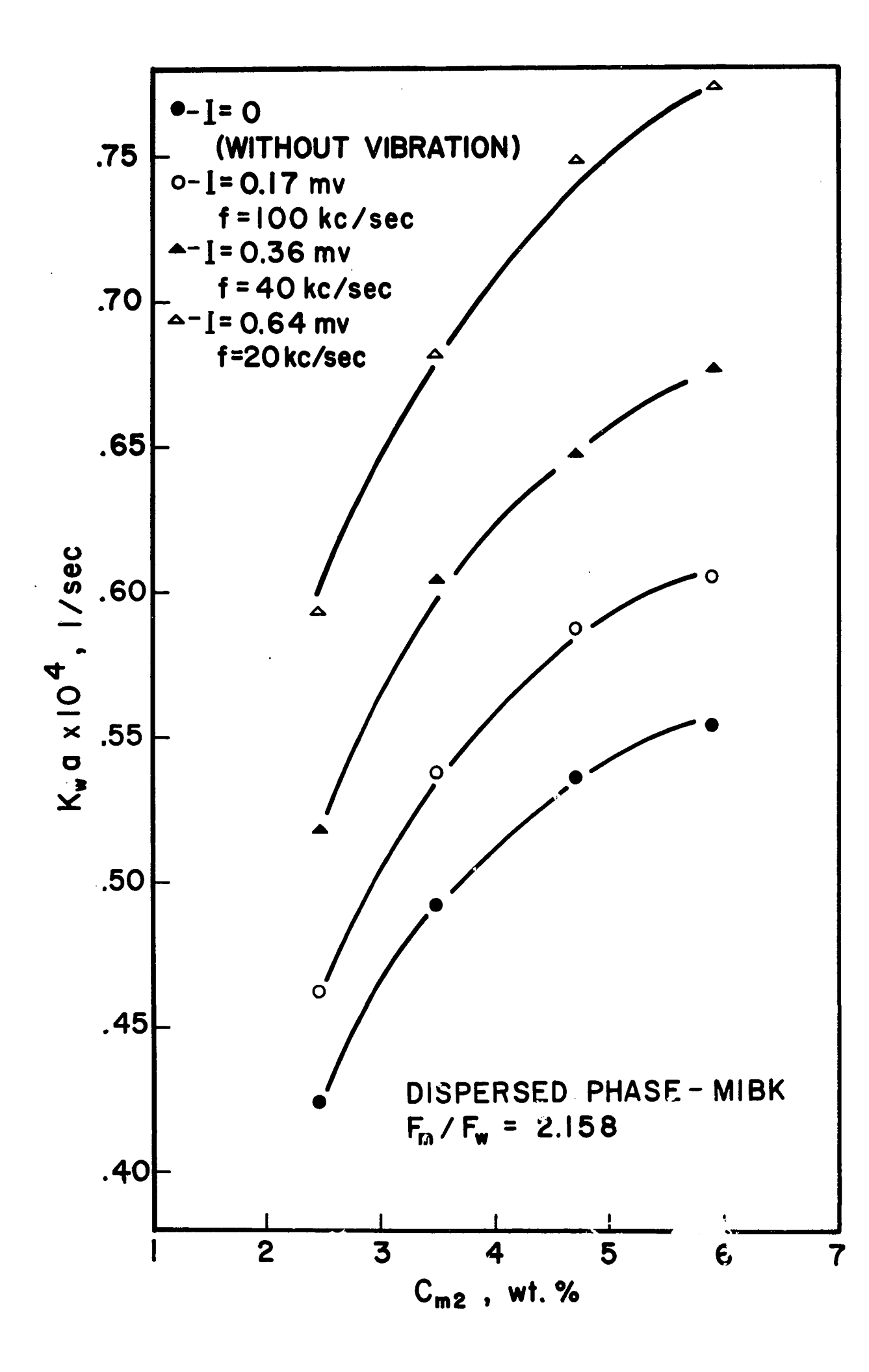
(K <sub>w</sub> a) <sub>0</sub> x 10 <sup>4</sup>	(Kwa) <sub>I</sub> x 10 <sup>4</sup>	(K`a) <sub>I</sub> x 10 <sup>4</sup> 1/sec	(K <sub>w</sub> a) <sub>I</sub> x 10 <sup>4</sup>	F <sub>m</sub> /F <sub>w</sub>	C <sub>m2</sub>	D <sub>N</sub>	. <del></del>
I.= 0	I =. 0.17 mv	I = 0.36 mv.	I = 0.64 mv		wt.%	cm	
f = 0	f = 100 kc/sec	f = 40 kc/sec	f = 20 kc/sec	<b>.</b>			
0.196	0.206	0.219	0.235	0.462	5.91	0.079	
0.191 0.182	0.203 0.190	0.218 0.199	0.230 0.214	0.462 0.462	4.73 3.49	0.079 0.079	
0.175	0.183	0.195	0.210	0.462	2.47	0.079	
0.318 0.311	0.344 0.331	0.375 0.369	0.413 0.392	1.147 1.147	5.91 4.73	0.079 0.079	
0.295	0.316	0.341	0.374	1.147	3.49	0.079	
0.282 0.471	0.299 0.504	0.333 0.559	0.361 0.629	1.147	2.47	0.079	_
0.461	0.493	0.539	0.608	2.158 2.158	5.91 4.73	0.079 0.079	à
0.424	0.451	0.494	0.565	2.158	3.49	0.079	



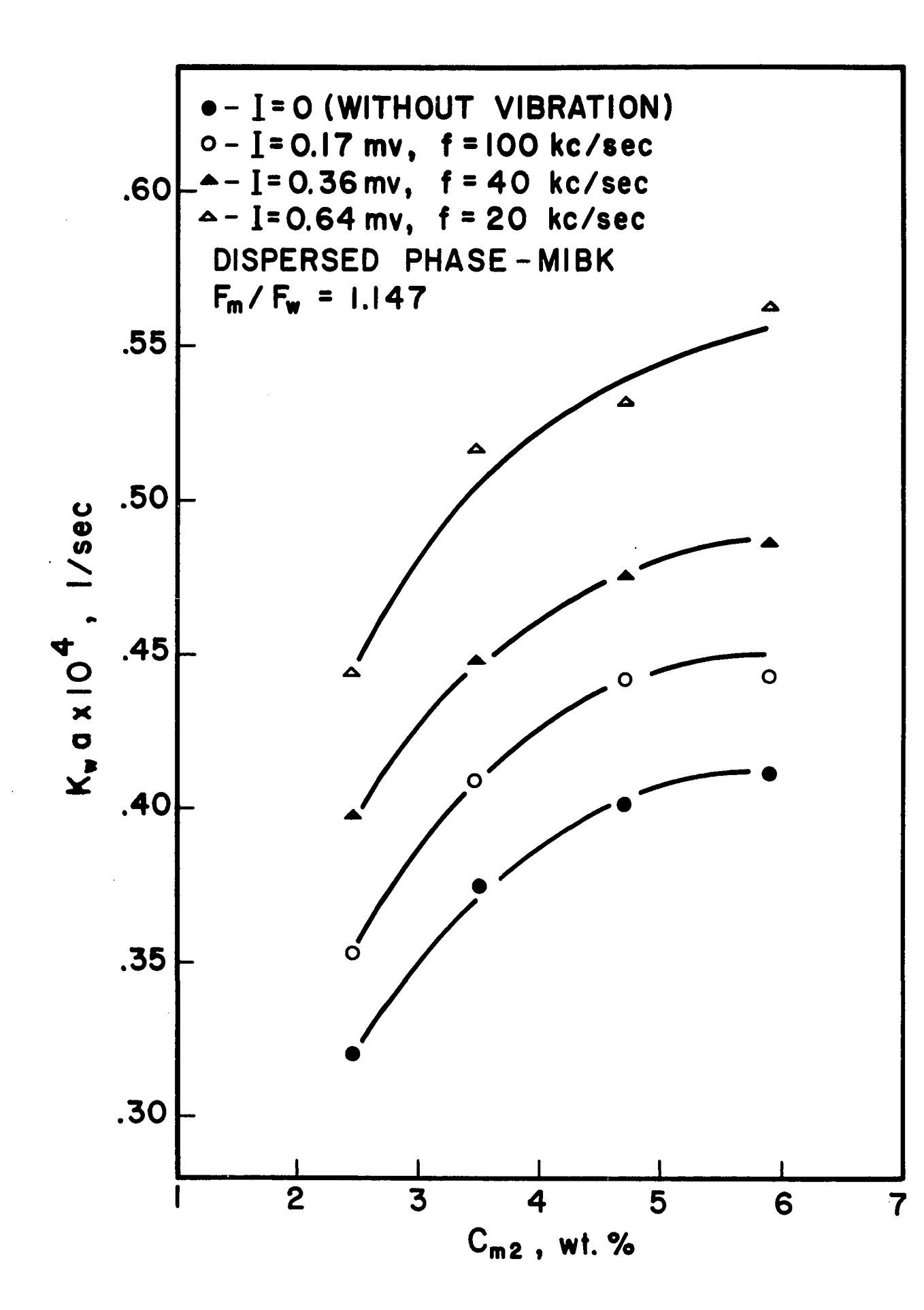
TABLE 3 (continued)

0.353	0.376	0.428	0.477	2.158	2.47	0.079
0.423	`. <b>-</b>	0.498	-	2.158	3.49	0.31
0.425	•	0.492	-	2.158	3.49	0.16
0.289	-	0.325	-	1.147	3.49	0.31
0.286	-	0.331	•	1.147	3.49	0.16
0.182	•	0.194	-	0.462	3.49	0.31
0.187	_	0.200	-	0.462	3.49	0.16

EFFECT OF ULTRASONIC VIBRATION ON  $_{\rm W}^{\rm A}$  FOR MIBK PHASE DISPERSED ( $_{\rm m}^{\rm F}/_{\rm W}^{\rm C}$  = 2.158)

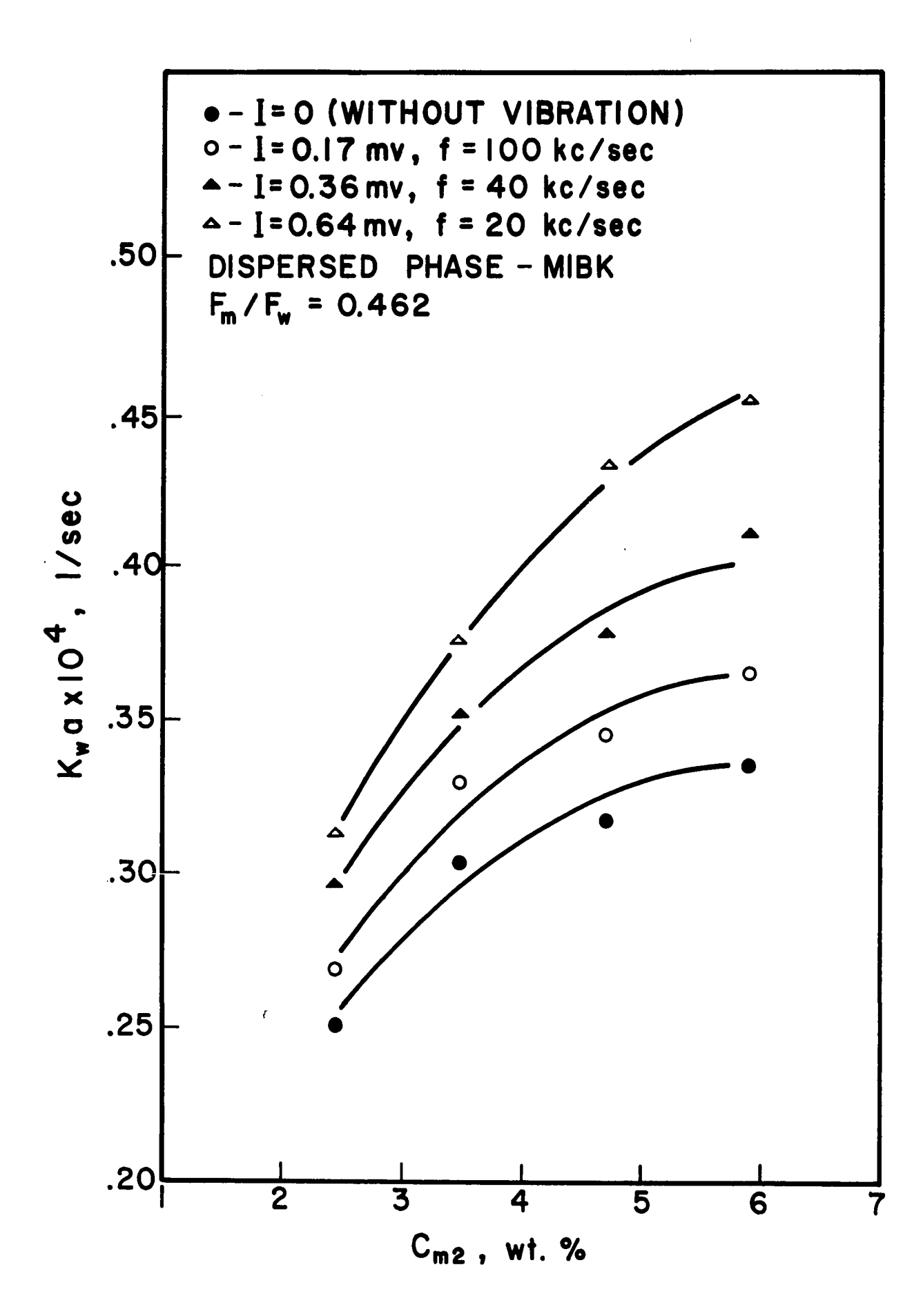


EFFECT OF ULTRASONIC VIBRATION ON  $K_w a$ FOR MIBK PHASE DISPERSED  $(F_m/F_w = 1.147)$ 

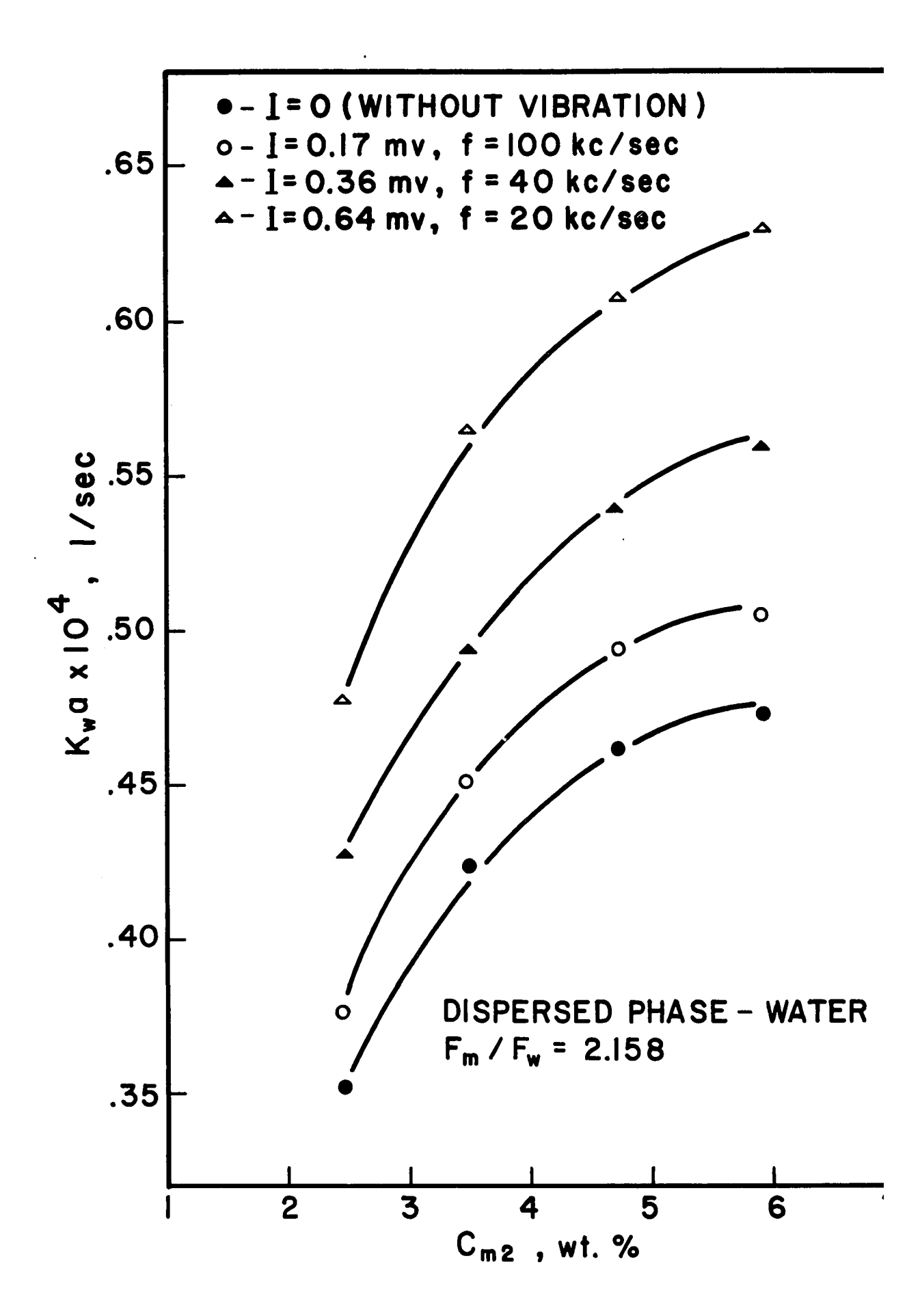




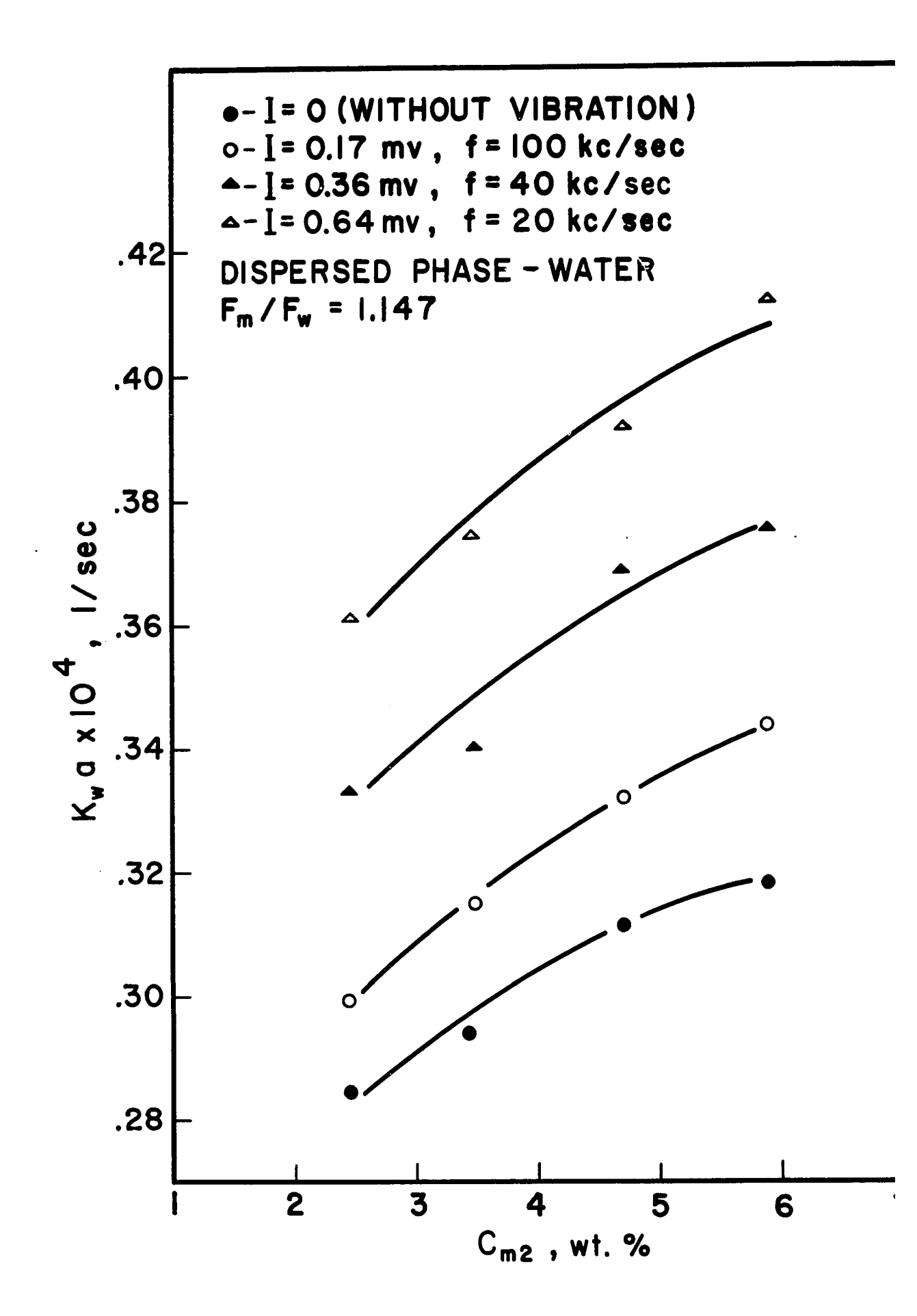
EFFECT OF ULTRASONIC VIBRATION ON  $K_w^a$ FOR MIBK PHASE DISPERSED  $(F_m/F_w^a = 0.462)$ 



EFFECT OF ULTRASONIC VIBRATION ON  $K_w^a$ FOR WATER PHASE DISPERSED  $(F_m/F_w^a = 2.158)$ 

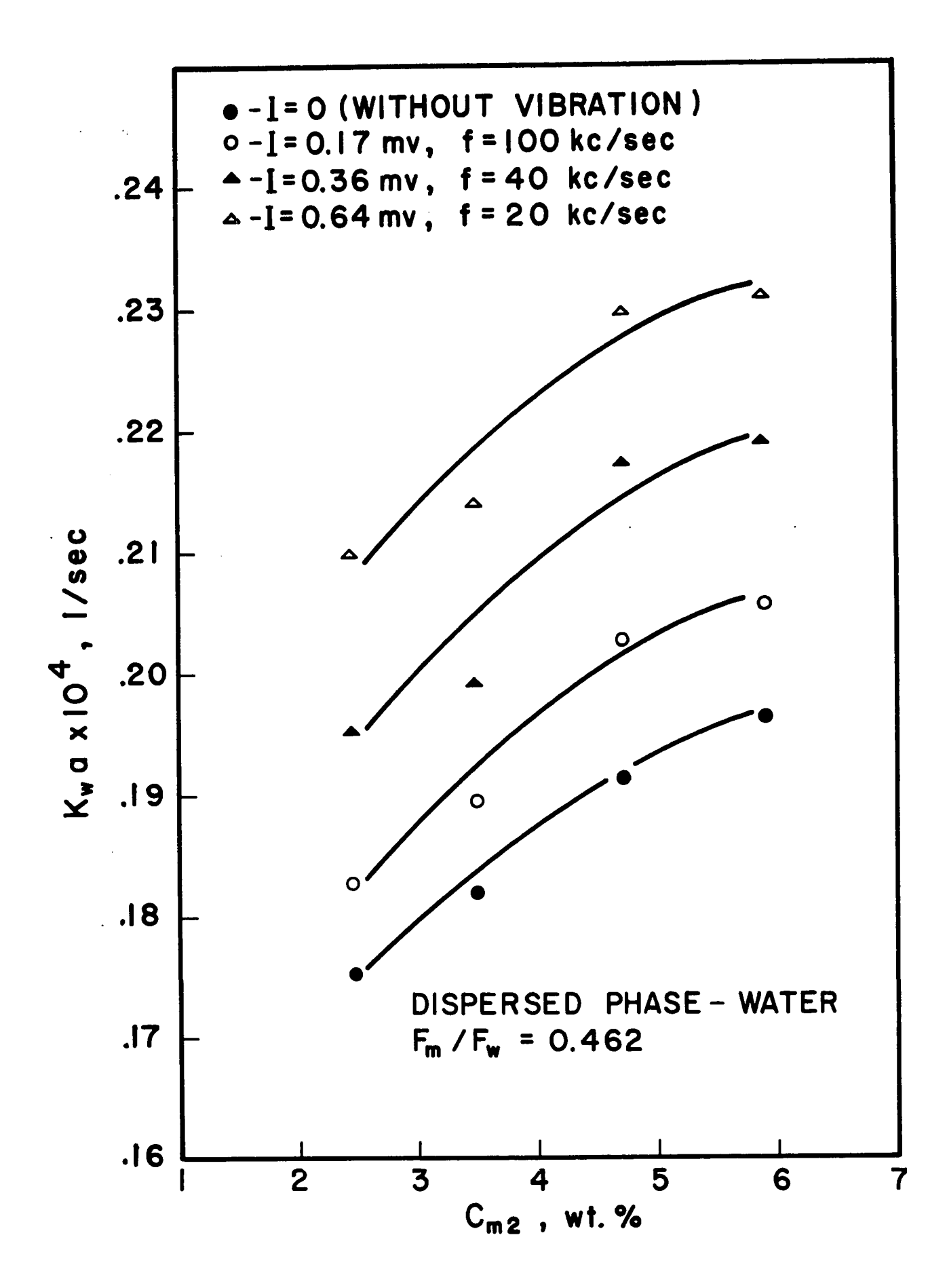


EFFECT OF ULTRASONIC VIBRATION ON  $K_w$ a FOR WATER PHASE DISPERSED  $(F_m/F_w = 1.147)$ 

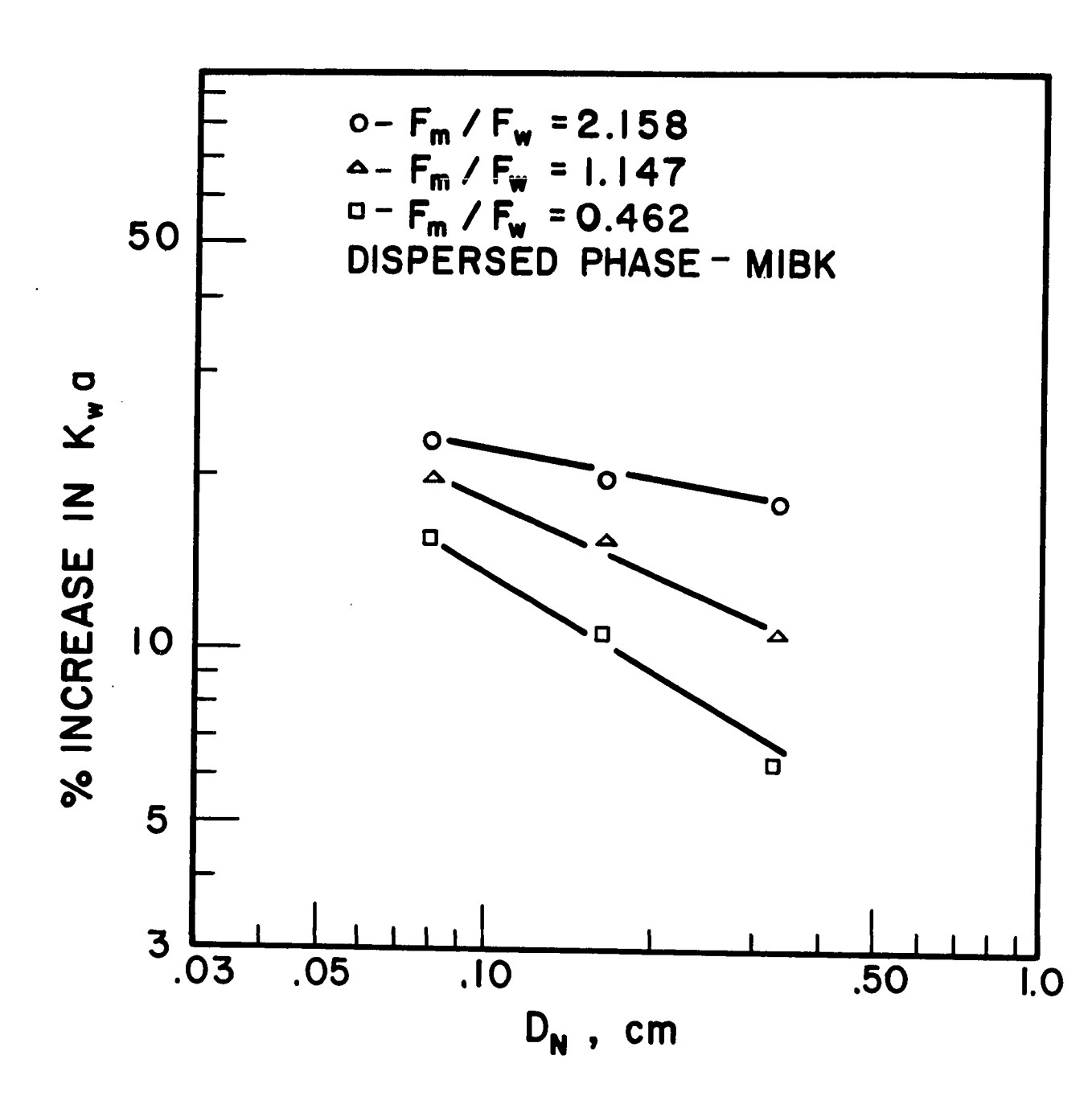


EFFECT OF ULTRASONIC VIBRATION ON  $K_w^a$ FOR WATER PHASE DISPERSES  $(F_m^f/F_w^f = 0.462)$ 



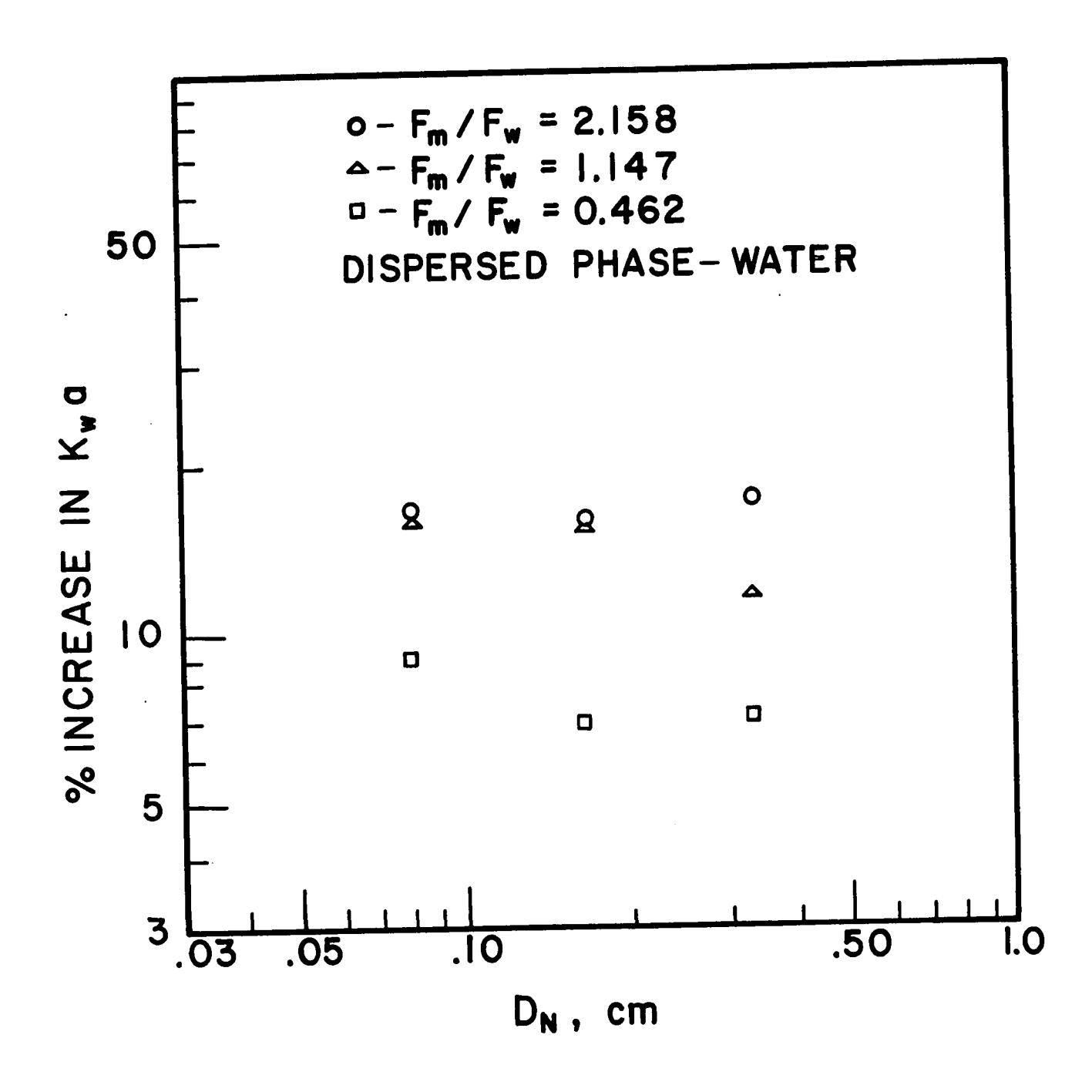


EFFECT OF NOZZLE SIZE ON THE PERCENT INCREASE  $\hbox{ in $K_{\bf w}$ a for Mibk Phase Dispersed }$ 





EFFECT OF NOZZLE SIZE ON THE PERCENT INCREASE  $\hbox{In $K_{\bf w}$ a for water phase dispersed }$ 



measured, and are shown in Figures 14,15 and 16 respectively. In addition, values of the threshold intensity, i.e., the minimum intensity required to cause cavitation in the system, were determined by the thermocouple probe at the measuring point, and are given in Table 4. Detailed experimental data of this investigation are presented in Appendix E.

TABLE 4. VALUES OF THE THRESHOLD INTENSITY FOR THE SYSTEM STUDIED AT 25°C

Ultrasonic Frequency f kc/sec	20	40	100
Threshold Intensity I' mv	.0.11	0.10	0.15

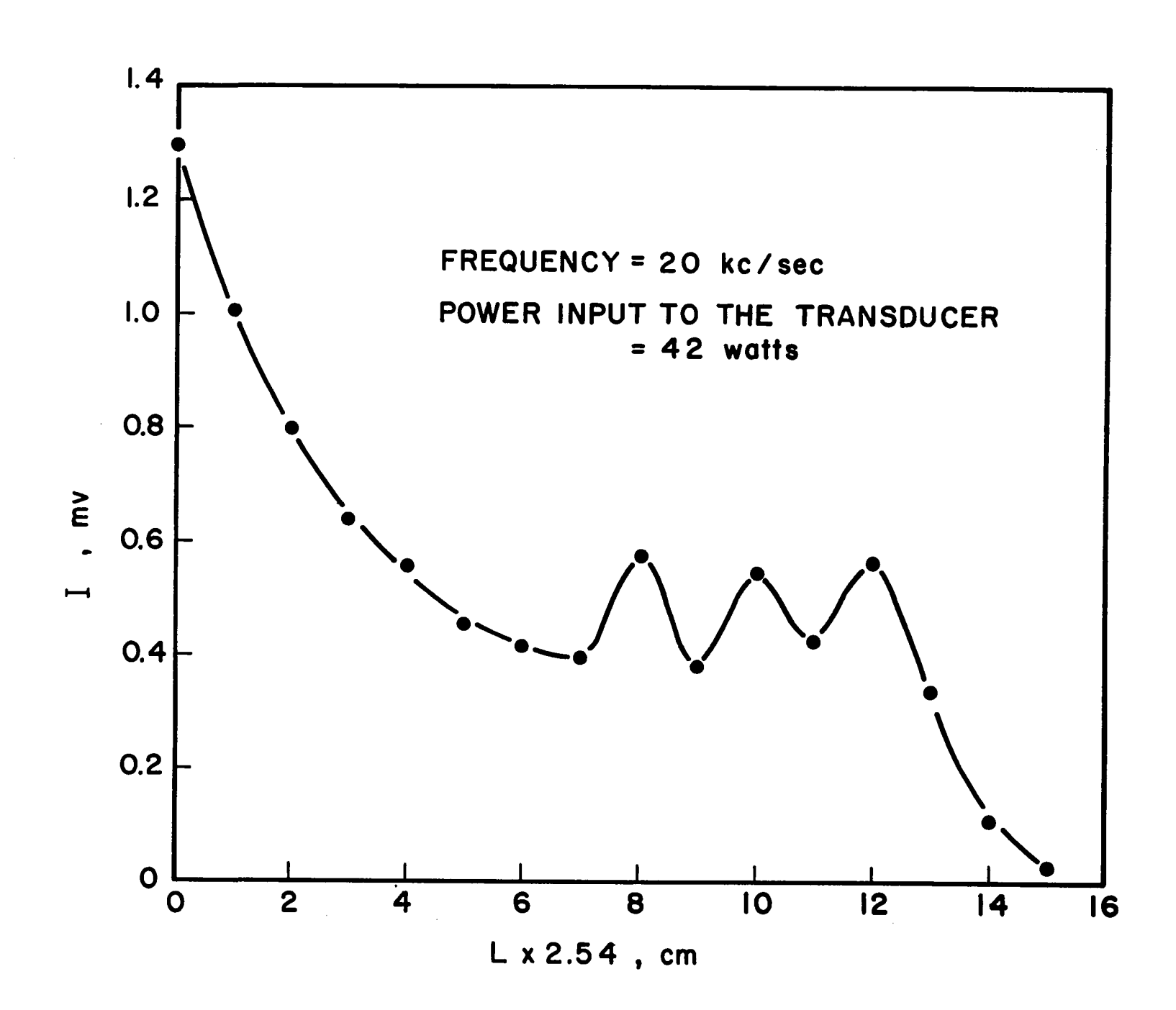
#### ANALYSIS AND DISCUSSION OF RESULTS

It is seen through Figures 6 to 11 that ultrasonic vibration increases the capacity coefficient, Ka, and hence the extraction efficiency of a spray column. It has also been shown that Ka increases with increasing ultrasonic intensity. All the plots are consistent in this trend. However, there is a practical limit in the intensity when ultrasonic energy is applied to a liquid-liquid system, since emulsification will occur if the intensity is greater than a critical value. The maximum

AXIAL INTENSITY PROFILE FOR THE

20 ke TRANSDUCER

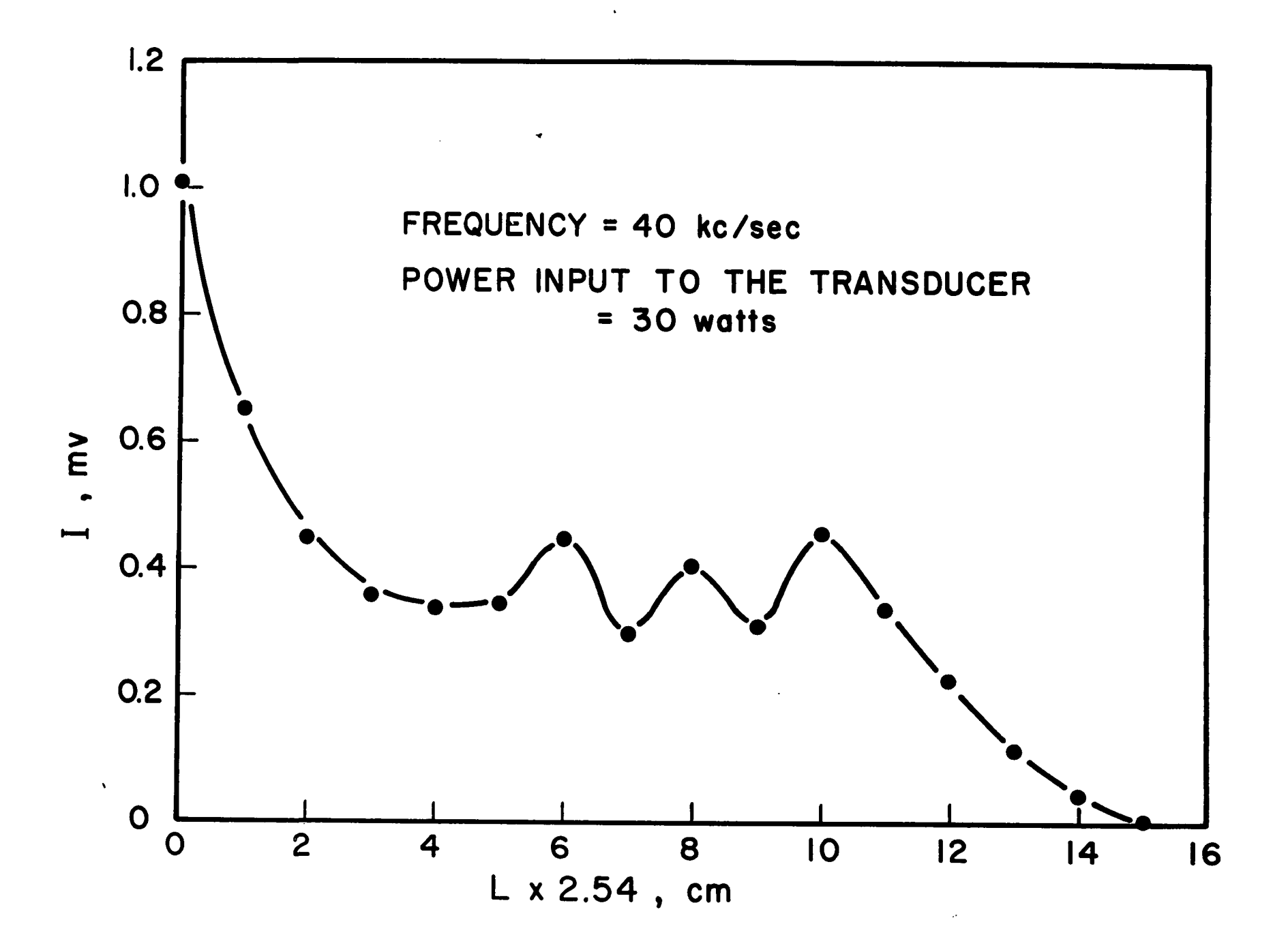




AXIAL INTENSITY PROFILE FOR THE

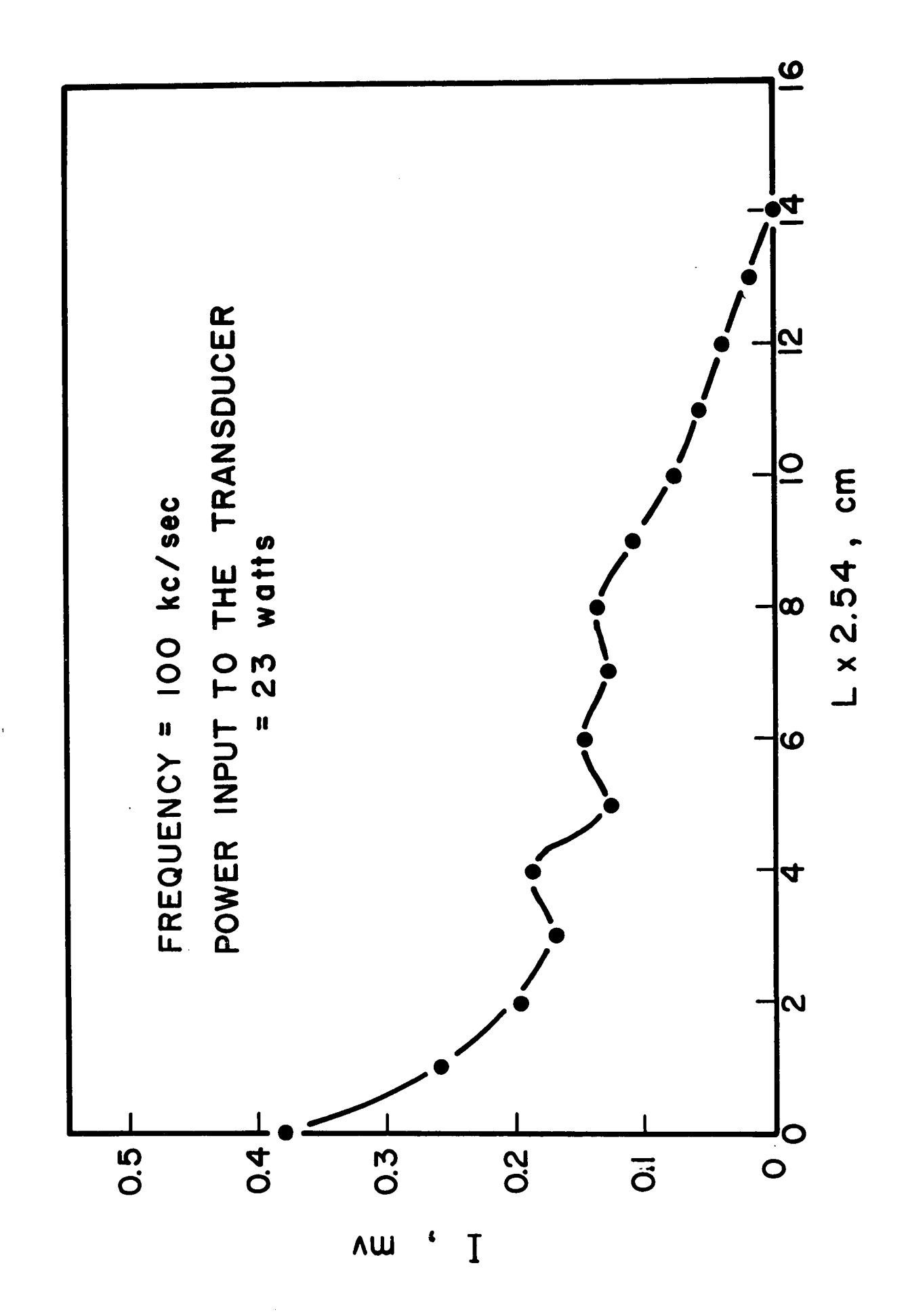
40 kc TRANSDUCER





AXIAL INTENSITY PROFILE FOR THE

100 ke transducer



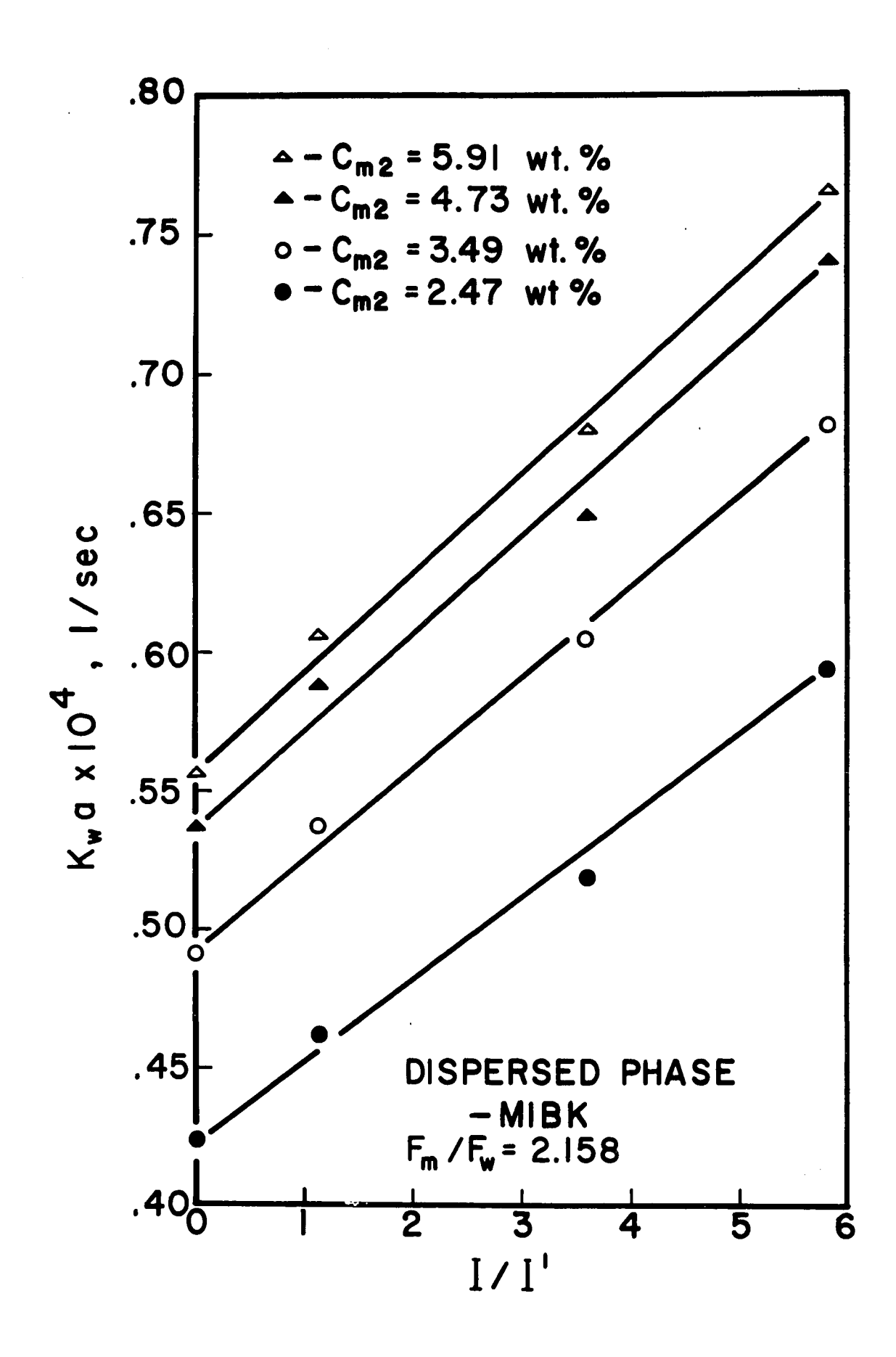
intensity applied to the system without causing emulsification is termed critical intensity,  $I_{\rm c}$ . In this investigation, the value of  $I_{\rm c}$  was found to be about 0.71 mv, measured by the thermocouple probe at the measuring point. Emulsification is undesirable for a liquid-liquid extraction process, and hence the ultrasonic intensity employed should be always less than  $I_{\rm c}$ .

From Figure 12, it is seen that for the case where MIBK phase was dispersed, the % increase in  $K_{\rm w}$  a decreased with increasing nozzle diameter. On the other hand, when the water phase was dispersed, the nozzle size had no significant effect.

Although the frequency of ultrasonic vibration might not directly affect the mass transfer rate in a spray column as concluded from the preliminary investigation, it may have an indirect effect on  $K_w$ a, since the threshold intensity of cavitation is a function of the frequency (5), and cavitation is believed to play an important role in the enhancement of  $K_w$ a in the column. An intensity ratio, defined as I/I', was used to correlate the  $K_w$ a data, where I', the threshold intensity, is a function of the frequency. Plots of  $K_w$ a versus I/I' are shown through Figures 17 to 22. It is observed that the relationship between  $K_w$ a and I/I' for all the plots can be represented by a straight line. Therefore, the use of I/I' as a combining term for both effects of the intensity and frequency seems to be justified. Furthermore, since I/I' is dimensionless, the use of this quantity gives a great advantage, namely, the independence of the measuring method.

 ${\tt K}_{\tt W}$ a VERSUS I/I¹ FOR MIBK PHASE DISPERSED

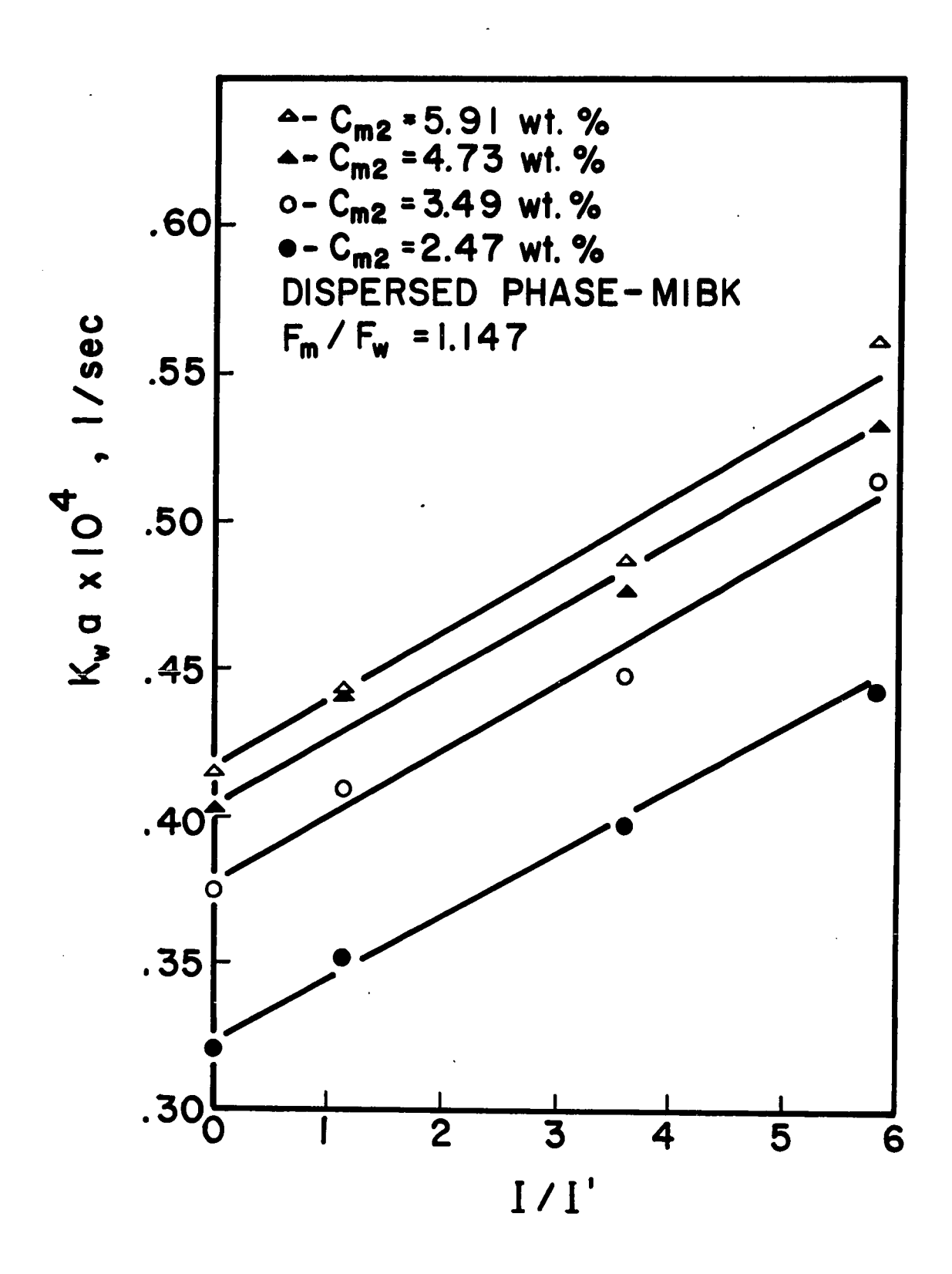
$$(F_{\rm m}/F_{\rm w} = 2.158)$$



 ${\tt K}_{\tt W}$ a VERSUS I/I¹ FOR MIBK PHASE DISPERSED

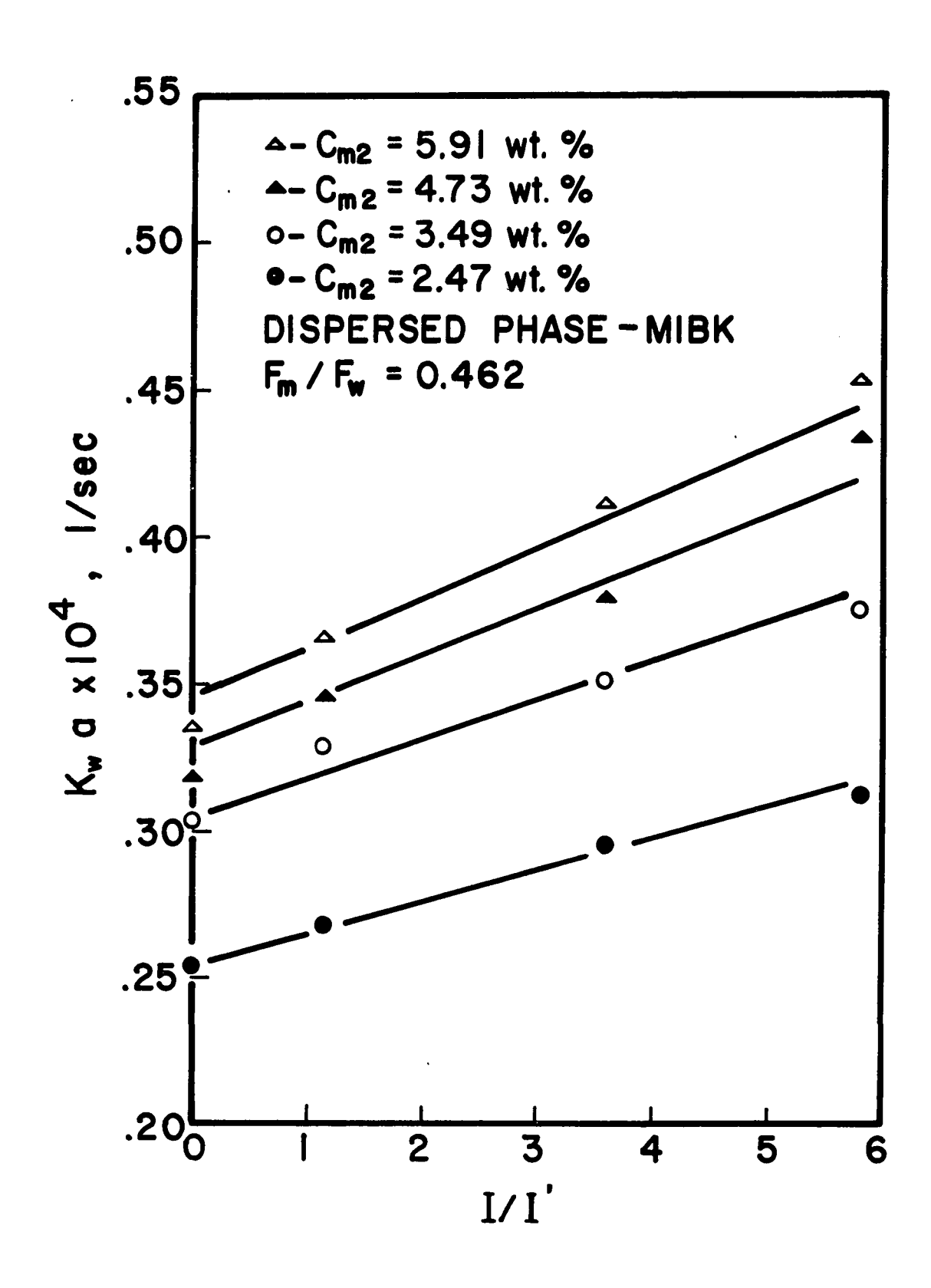
 $(F_{m}/F_{w} = 1.147)$ 



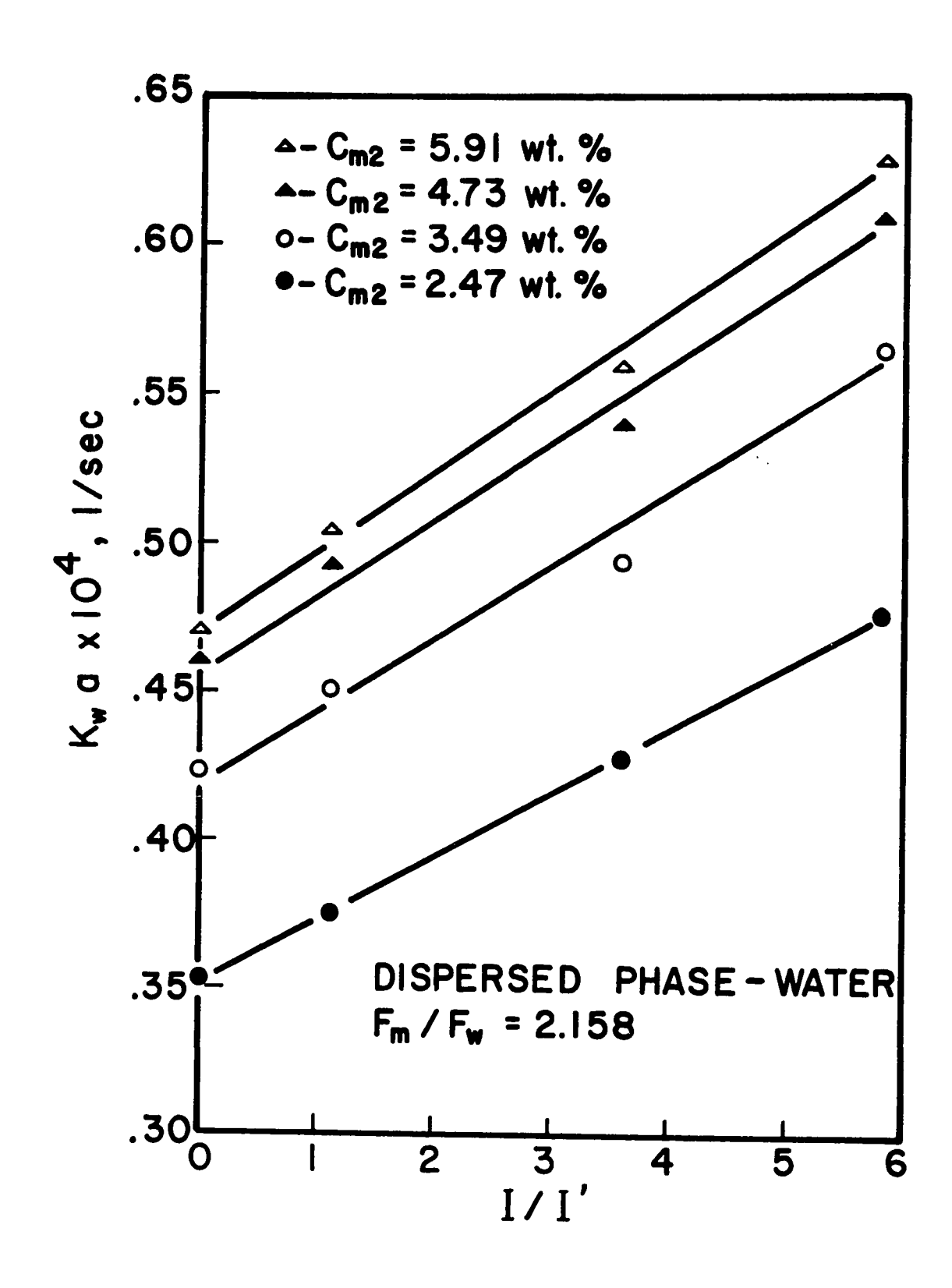




 $K_w^a$  VERSUS I/I' FOR MIBK PHASE DISPERSED  $(F_m/F_w = 0.462)$ 

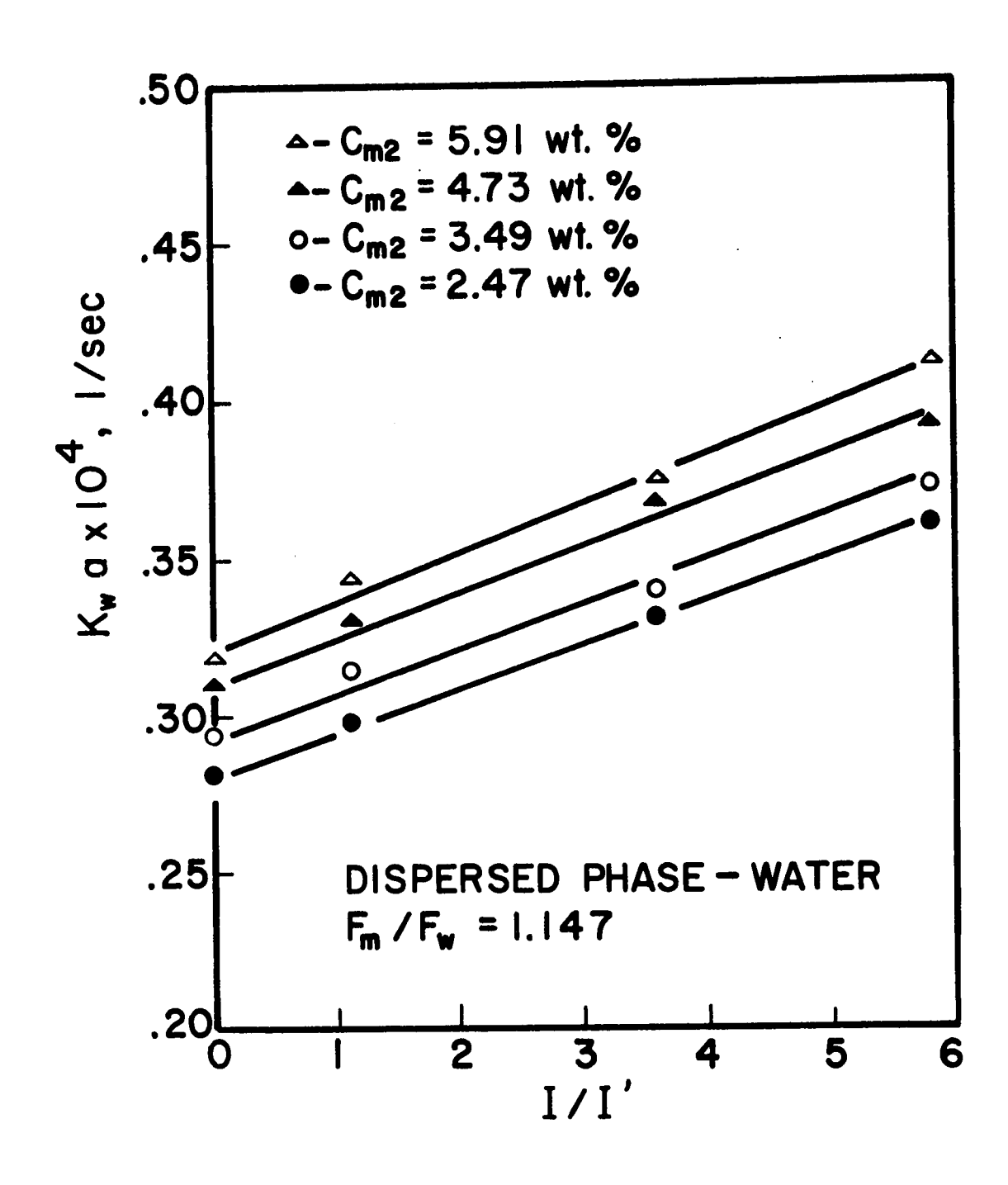


 $K_{W}^{a}$  VERSUS I/I' FOR WATER PHASE DISPERSED  $(F_{m}/F_{W}^{} = 2.158)$ 

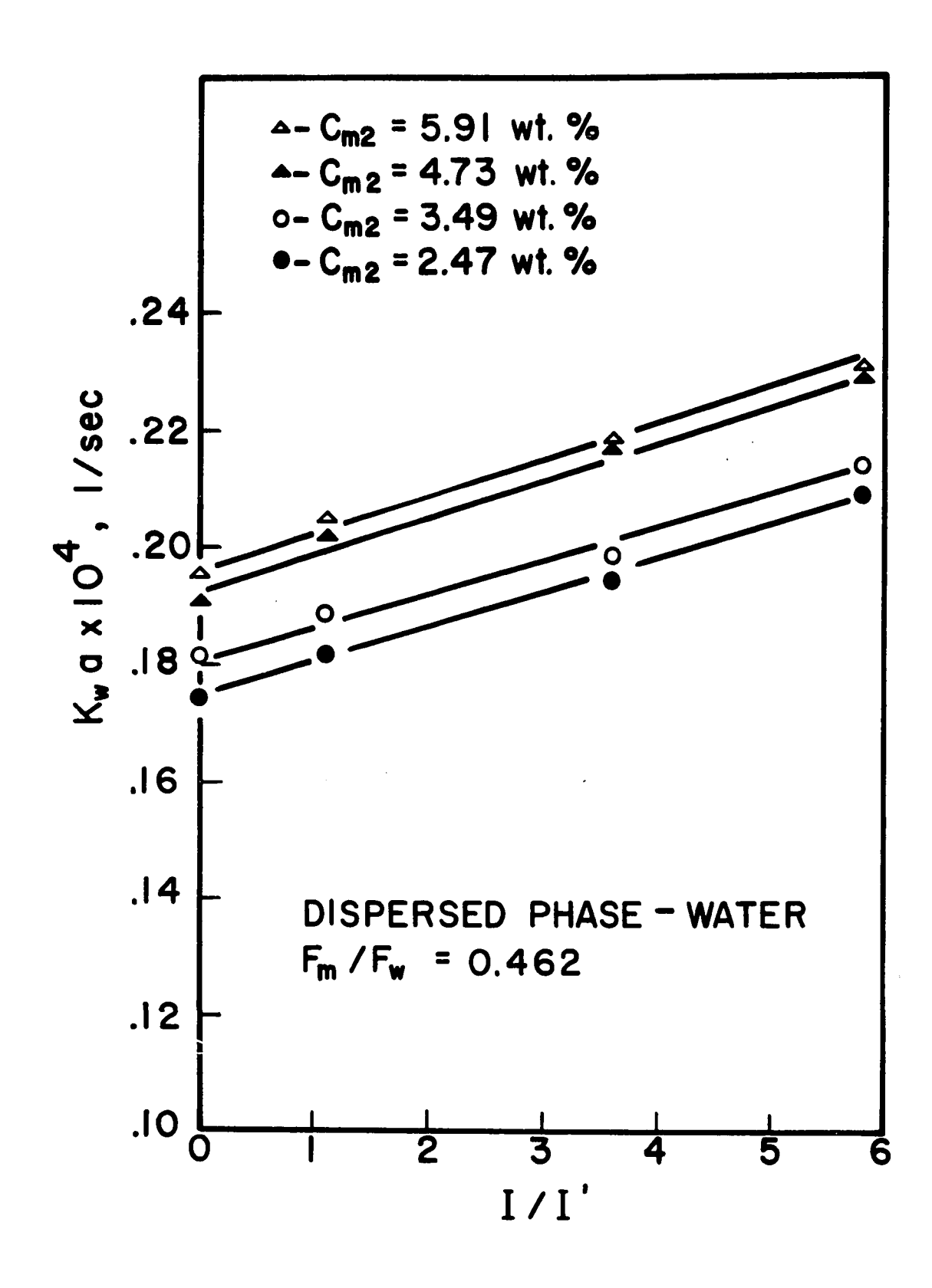


 $K_w^a$  VERSUS I/I' FOR WATER PHASE DISPERSED'  $(F_m^{}/F_w^{} = 1.147)$ 





 $K_{w}$ a VERSUS I/I' FOR WATER PHASE DISPERSED  $(F_{m}/F_{w} = 0.462)$ 



Variables affecting the % increase in Ka based either on the aqueous or organic phase are thought to be the intensity ratio, the superficial velocities, densities and viscosities of both aqueous and organic phases, the interfacial tension, distribution coefficient, diffusivity of the system, the nozzle diameter, and the initial solute concentration of the solution. At low flow rates, the effect of column height on Ka is small as reported by Johnson and Bliss (6). The effective column height is thus assumed not to have any significant effect on the % increase in Ka. It may then be written

% Increase in 
$$K_x^a$$
 or  $K_y^a$ 

$$= \phi(I/I', v_x, v_y, \rho_x, \rho_y, \mu_x, \mu_y, \sigma, m, \delta, D_N, C_i, \rho_i) \qquad (9)$$

Application of the techniques of dimensional analysis to the variables of Equation (9), combined with the assumption that the correlation can be represented by an exponential function, yields

% Increase in 
$$K_x^a$$
 or  $K_y^a = b_0(\frac{1}{1})^{b_1}(\frac{v_y}{v_x})^{b_2}(\frac{c_1^{\rho_1}}{\rho_x})^{b_3}$ 

$$\left(\frac{\mu_{x}}{\rho_{x}v_{x}D_{N}}\right)^{b_{4}}\left(\frac{\mu_{y}}{\mu_{x}}\right)^{b_{5}}\left(\frac{\rho_{y}}{\rho_{x}}\right)^{b_{6}}\left(m\right)^{b_{7}}\left(\frac{\mu_{x}}{\rho_{x}\partial}\right)^{b_{8}}\left(\frac{\sigma}{\mu_{x}v_{x}}\right)^{b_{9}}$$

(10)

For systems having the values of physical properties similar to water-acetic acid-MIBK, the last five groups in Equation (10) may be dropped, and the equation becomes

% Increase in K.a

$$= b_{0} (I/I')^{b_{1}} (v_{m}/v_{w})^{b_{2}} (c_{i} \rho_{i}/\rho_{w})^{b_{3}} (\mu / \rho_{w} v_{w} D_{N})^{b_{4}}$$
 (11)

By analysing the experimental results obtained, the constants in Equation (11) were found. For the case where MIBK was dispersed,

% Increase in K.a

= 5.06 
$$(I/I')^{0.94} (v_m/v_w)^{0.16} (c_i \rho_i/\rho_w)^{0.17}$$
  
 $(\mu/\rho_w v_w D_N)^{0.23}$  (12)

When MIBK was used as the continuous phase, i.e., the water phase was dispersed,

% Increase in 
$$K_w^a = 7.44 (I/I')^{1.00} (v_m/v_w)^{0.36}$$

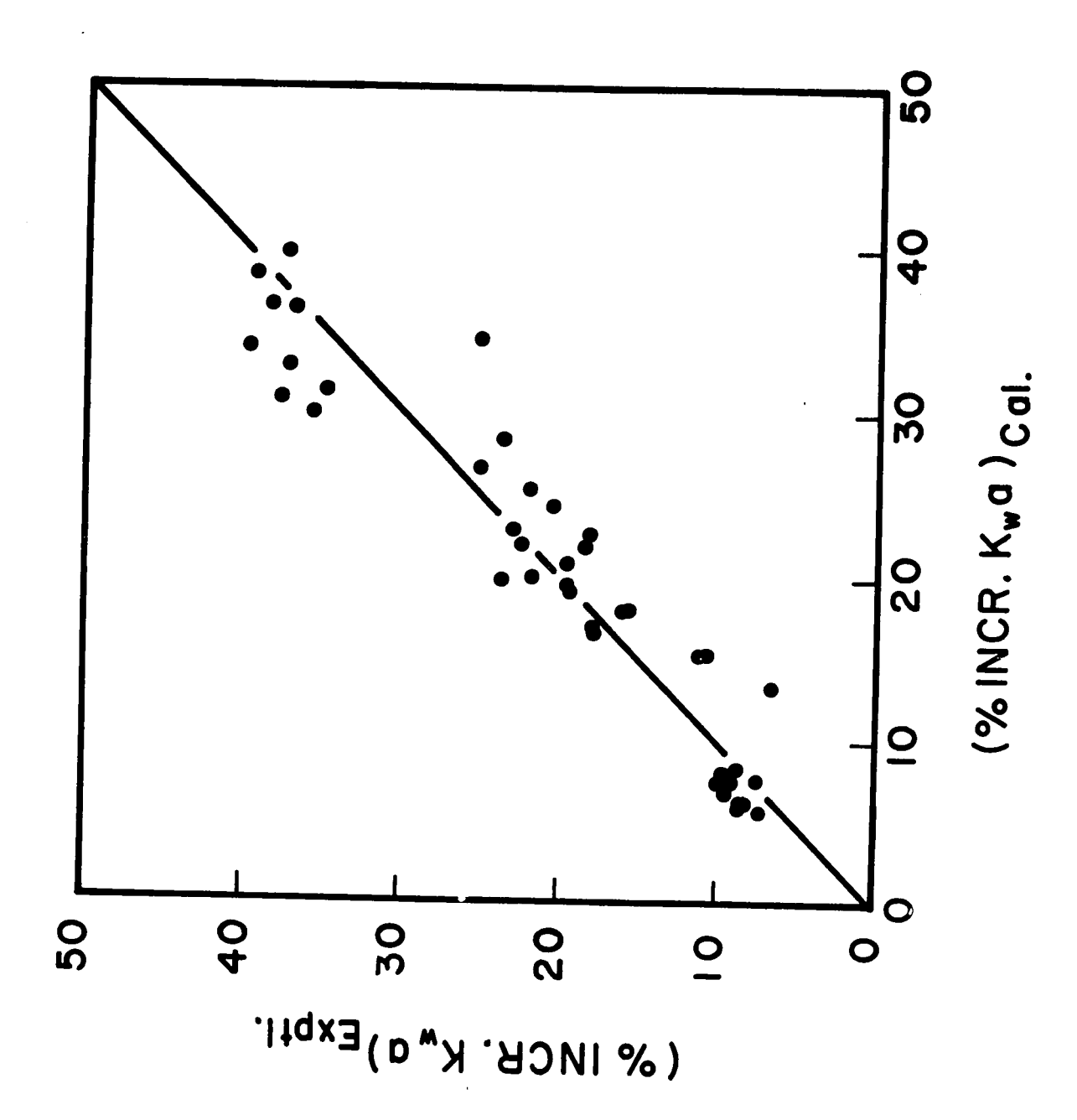
$$(C_i \rho_i/\rho_w)^{0.17} (\mu_w/\rho_w v_w^D)^{0.001}$$
(13)

The last group in Equation (13) is negligible because its exponential constant is small; the effect of nozzle size on the % increase in K a for this case is insignificant as can be seen in Figure 13. The correlations for both these cases are presented in Figures 23 and 24, and the calculated data are given in Appendix E. The average deviations are 17.9 and 21.6% respectively. Data from the preliminary investigation, where the effective column height, column diameter and distributor geometry were different from the present investigation, were included in Figure 24.

A material balance for each run was calculated by comparing the amount of acetic acid picked up by the aqueous phase to the amount extracted from the organic phase. It has been found that the average error is 18.9%. Generally, in a spray column operation, when the system has reached a steady state, the error in the material balance should not be greater than 5%. The source of such a high error may be due to an inaccuracy either in the analytical technique or in the control of flow rates. The analytical method employed in this work for determining the acid concentration of each phase, i.e., by direct titration with standard 0.05 N sodium hydroxide solution using phenolphthalein as an indicator, is fairly accurate. As mentioned by Smoot and Babb (7), the maximum analytical error incurred in this titration was only about 3%. From the analysis of data, it can be seen that the amount of acetic acid transferred to the aqueous phase is always greater than the amount extracted from the organic phase. This fact suggests that the discrepancy in the above mentioned material balance may be due to either a higher aqueous flow rate or a lower organic flow rate. The individual K a value reported may be thus higher than the actual value. However, values of the "% increase in K\_a" as calculated by Equation (8) will not be affected, since the experimental error may be cancelled out. Detailed analysis of the error is given in Appendix F.

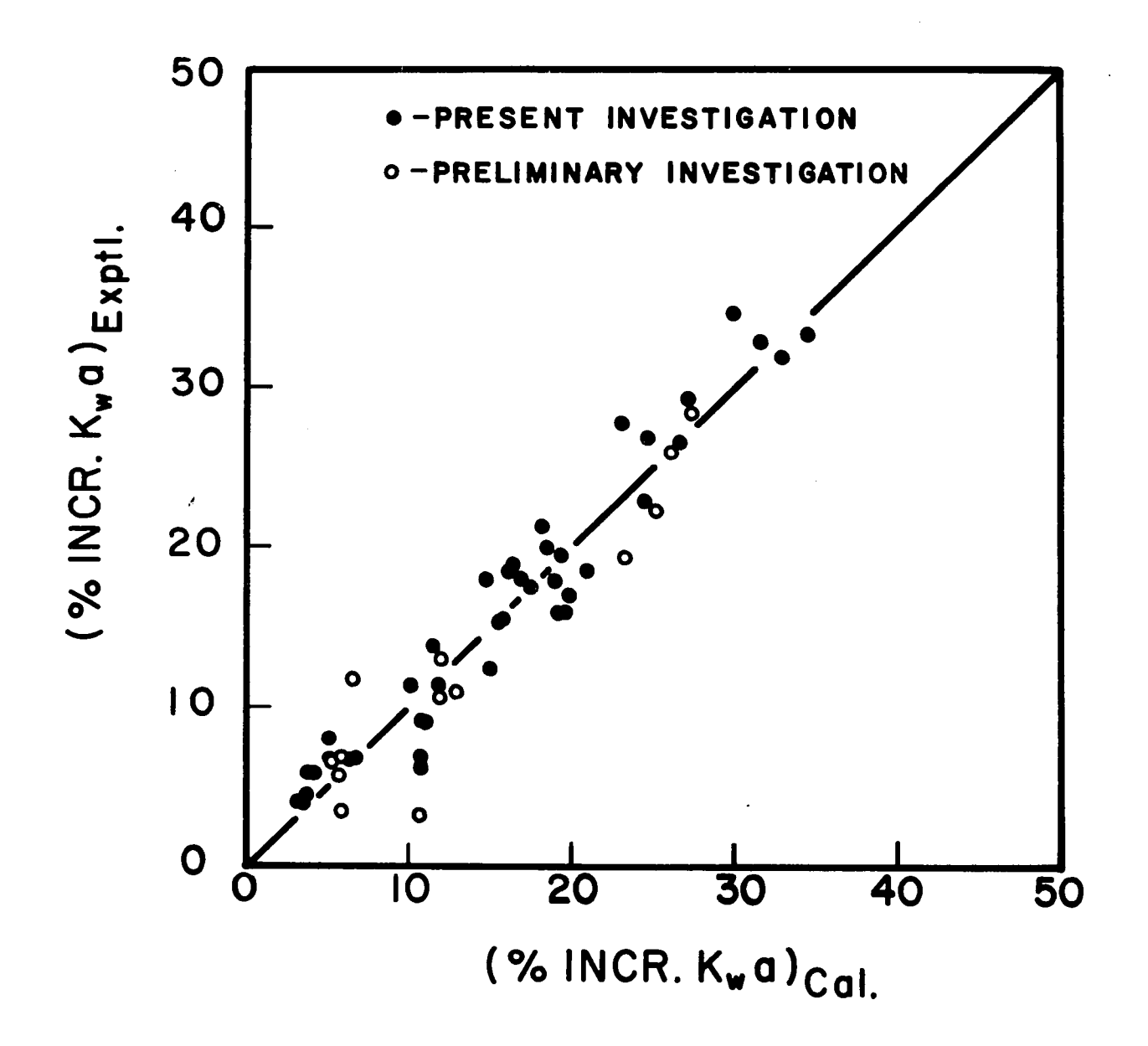
CORRELATION FOR MIBK PHASE DISPERSED





CORRELATION FOR WATER PHASE DISPERSED





An increase in the capacity coefficient, Ka, is due to an increase in either K, the overall mass transfer coefficient, or a, the interfacial area of contact, or both these quantities. The formation and collapse of cavitation bubbles caused by ultrasonic vibration is known to create agitation in liquids (8,9), and obviously will increase the degree of turbulence in the liquids. In a spray column, this increase of turbulence may be accomplished in either the continuous or the dispersed phase, or in both these phases, with a consequent reduction in the resistance to mass transfer. The higher the intensity, the greater is the increase in the turbulence, and hence in K.

As Hayworth and Treybal (10) pointed out, there are several forces acting on a drop when it is being formed at a nozzle tip. The force acting in the direction toward the nozzle is the interfacial tension force, and the force acting in the direction away from the nozzle is the buoyant force. In addition, a certain amount of kinetic energy is supplied to the drop acting also in the direction away from the nozzle. When the drop is subjected to an intense ultrasonic field, an additional force in the direction away from the nozzle may be created. In other words, ultrasonic vibration would cause the drop to leave the nozzle prematurely and make it become smaller. The higher the intensity, the

greater the additional force and the smaller the drop. A decrease in the drop size means an increase in the total surface area, and thus the interfacial area of contact.

The difference in the values of constants between Equation (12) and Equation (13) suggests that the mechanism of increase in K a for these two cases are not the same. For the case where MIBK, the light liquid, was dispersed, the dispersing nozzle was close to the bottom and the interface level was held at the top of the column. On the other hand, when water, the heavy liquid, was dispersed, the interface level was near the bottom and the dispersing nozzle was at the top. As seen from Figures 14, 15 and 16, the ultrasonic intensity near the top of the column is much less than that close to the bottom. Therefore, for the latter case, the increase in  $K_{\overline{\nu}}a$  would be mainly due to the increase in the mass transfer coefficient, K,, because the interface level was close to the ultrasonic source. The vibration would primarily affect the lower section, increasing the degree of turbulence there and thus reducing the resistance to mass transfer. Also, the mass transfer during drop coalescence may be increased by the increasing turbulence at the interface. The fact that the group containing  $\boldsymbol{D}_{\!\!N}$  is negligible in Equation (13) supports the assumption that ultrasonic vibration has little effect on the droplet size, and hence the interfacial area of contact, when the dispersing nozzle is far away from the source. On the contrary, when the dispersing nozzle is near the source, the effect of ultrasonic vibration would be principally on the drop formation process, reducing

the drop size, and hence increasing ,a, the interfacial area of contact. It might also increase the mass transfer coefficient,  $K_{\rm w}$ , during the drop formation period due to the induced turbulence near the nozzle. A study on the mechanism involved was undertaken and the results were presented in Part III of this thesis.

#### CONCLUSIONS

The efficiency of a spray-type liquid-liquid extraction column may be improved by the imposition of ultrasonic vibration to the system. Such increases in the extraction efficiency depend mainly on the ultrasonic intensity, and are thought to be caused by the cavitation phenomenon which induces turbulence in the liquids. However, the intensity should not be in excess of a critical value, otherwise severe cavitation will cause emulsification in the system, making the separation difficult in the column. The optimum condition would be attained by setting the intensity at such a level that a controlled cavitation condition is realized within the system without introducing an excess degree of emulsification.

An intensity ratio defined as the ratio of the ultrasonic intensity to the threshold intensity of cavitation, the latter being a function of the frequency, was used to correlate the capacity coefficient data. The capacity coefficient increases with this intensity ratio in a linear fashion, and the linear relationship hold for all different operating conditions.

Correlations have been developed to predict the increase in mass transfer rate by ultrasonic vibration in a spray column. Separate correlation must be used depending on whether the dispersing nozzle or the interface level is closely located to the ultrasonic source. The correlations obtained would be applicable to systems having values of physical properties similar to the system of water-acetic acid-MIBK.

#### NOMENCLATURE

#### Roman Symbols

- a interfacial area of contact, cm<sup>2</sup>/unit volume
- A total transfer area. cm<sup>2</sup>
- b<sub>1</sub>-b<sub>Q</sub> empirical constants, dimensionless
  - C solute concentration, wt.%
  - C\* equilibrium solute concentration, wt.%
  - C, initial solute concentration of the solution, wt.%
- ΔC change in solute concentration, wt.%
- (C\*-C) log-mean concentration driving force, wt.%
  - $\mathbf{D}_{\mathbf{N}}$  nozzle diameter, cm
  - ob diffusivity, cm<sup>2</sup>/sec
  - f frequency, kc/sec
  - F flow rate, ml/sec
  - I ultrasonic intensity measured by the thermocouple probe, my
  - I' threshold intensity measured by the thermocouple probe, my
  - I critical intensity measured by the thermocouple probe, mv
  - K overall mass transfer coefficient, cm/sec
  - Ka capacity coefficient, 1/sec
  - L distance from the bottom of the column, cm
  - m solute distribution coefficient, dimensionless
  - v superficial velocity, cm/sec
  - V effective column, cm<sup>3</sup>
  - Z effective column height, cm

#### Greek Symbols

- $\mu$   $\mu$  viscosity, poise
- $\rho$  density,  $g/cm^3$
- $\sigma$  interfacial tenstion, dynes/cm

### Subscripts

- I at an intensity I
- m MIBK phase
- o at zero intensity
- w water phase
- x aqueous phase
- y organic phase
- feed or effluent: at the top of the column
- 2 feed or effluent at the bottom of the column

#### REFERENCES

- Sherwood, T.K., Evans, J.E., and J.V.A. Longcor, Ind. Eng. Chem. 31 1144 (1939)
- 2. Weber, M.E., and W.Y.Chon, Can. J. Chem. Eng. 45 238 (1967)
- 3. Richards, W.T., Science, New York <u>76</u>] 36 (1932)
- 4. Degrois, M. Ultrasonics  $\underline{4}$  38 (1966)
- Blitz, L., "Fundamentals of Ultrasonics," p.200, Butterworths, London (1963)
- 6. Johnson, H.F., and H. Bliss, Trans. Am. Inst. Chem. Engrs. 42 331 (1946)
- Smoot, L.D., and A.L.Babb, Ind. Eng. Chem. Fundamentals
   (2) 93 (1962)
- 8. Nottingk, B.E., and E.A. Neppiras, Proc. Phys. Soc. (London) B63 674 (1950)
- 9. Carlin, B. "Ultrasonics" p. 200, McGraw-Hill, New York (1949)
- 10. Hayworth, C.B., and R.E. Treybal, Ind. Eng. Chem. 42 1174 (1950)

#### PART II

# EFFECTS OF ULTRASONIC VIBRATION ON THE DROPLET SIZE AND COALESCENCE AT THE INTERFACE

#### INTRODUCTION

In a spray column the interfacial area of contact between the phases, and thus the extraction efficiency, is directly proportional to the average surface area of the individual drops, which, in turn, is a function of the droplet size. A study of the droplet formation, therefore, is the logical first step towards predicting the interficial area available for extraction.

As concluded from the previous experiments, the overall extraction efficiency of a spray column can be increased by applying ultrasonic vibration to the system. However, whether such an increase is due to the increase in the mass transfer coefficient, the interfacial area of contact, or possible due to both of these quantities, is open to investigation. A study of the droplet size under the influence of ultrasonic vibration was designed to provide basic information for the understanding of this problem.

In addition, the coalescence of droplets at the interface is also an important phenomenon in a spray column. A study of this phenomenon as the column liquids are subjected to ultrasonic vibration was thought to be necessary in explaining the mechanism of extraction, and was also undertaken.



#### APPARATUS AND PROCEDURE

The experimental apparatus and equipment are the same as described in the previous part. In addition, a 35-mm, f-3.5 Nikon FT camera was used for taking the photographs of the drops, and a high-speed motion picture camera (Hycam Model K2001 of Red Lake Labs,Inc.) with a Micro-Switar 50 mm lens was employed to record the motion of the droplets at the aqueous-organic interface. In either case, the camera was placed in front of the column at a distance of about 25 cm. Flood lamps surrounding the column were used as a light source.

In this investigation, a rectangular plexiglass jacket of the column, when filled with water, eliminated the optical distortion caused by the curvature of the column wall and also maintained the temperature of the column within  $25 + 0.5^{\circ}$ C.

Most of the experiments were performed using water and 3.49% acetic acid-MIBK solution. The chemicals used were the same as in Part I. Supplemental experiments were carried out with water and 1,1,2-trichloroethane (TCE), where the TCE was obtained from Matheson Company Inc.. There was no transfer of solute between the phases for the TCE-water system.

Both water-MIBK and water-TCE were mutually saturated before the runs were made. Densities and viscosities of the liquids used were determined by a hydrometer and a Cannon-Fenske Viscosimeter respectively,

while interfacial tensions of the systems were measured with a Ringtype Tensiometer. The values obtaind are presented in Table 1. The density and viscosity of distilled water, saturated with MIBK or TCE, 1.0 g/ml and 0.90 cp are not tabulated.

TABLE 1. PHYSICAL PROPERTIES OF THE LIQUIDS USED AT 25°C

Liquid	Density g/ml	Viscositý y x 10 <sup>2</sup> poise	Interfacial Tension (with water) dynes/cm
3.49% Acetic acid- MIBK solution (MIBK saturated with water)	0.801	0.588	8.6*
1,1,2 Trichloroethane (Saturated with water)	1.435	1.278	20.3

<sup>\*</sup> Mean value of 9.9 (MIBK with water) and 7.2 (3.49% acetic acid-MIBK solution in equilibrium with an aqueous phase)

For a typical run in the drop size experiment, flow rates of both continuous and dispersed phases, and the frequency and intensity of the ultrasonic vibration were adjusted to the desired values, and the system was allowed to reach a steady state. The camera was set at a lens opening of f-8 and 1/125 second exposure time, and was focused on the dispersing nozzle tip. Photographs of the drop were then taken. The negative film of the droplet photographs were projected onto a screen, and the drop

1. . . .

sizes were measured by a divider, using the nozzle opening as a reference to calculate the enlargement factor.

Similarly for the coalescence experiments, the flow rates, frequency, and intensity were set, and the system was allowed to reach a steady state. The camera was set at a lens opening of f-11, and motion pictures of the drops at the interface were taken with a speed of 200 frames/sec. The rest times of the drop at the interface were determined by counting the number of frames between the first arrival and the final disappearance of the drop at the interface.

#### EXPERIMENTAL RESULTS

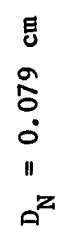
The experimental results are shown in Figures 2 to 10. Detailed experimental data are given in Appendix E. Figure 1 is a sample of the droplet photographs. Figures 2 to 8 are semi-log plots of the average drop diameter versus the nozzle velocity, where the intensity ratio, I/I', was used as a parameter. The nozzle velocity was defined as the dispersed phase flow rate divided by the cross-sectional area of the nozzle opening. Figures 9 and 10 are plots of t<sub>r</sub>, the average rest time of the drop at the interface, against I/I'.

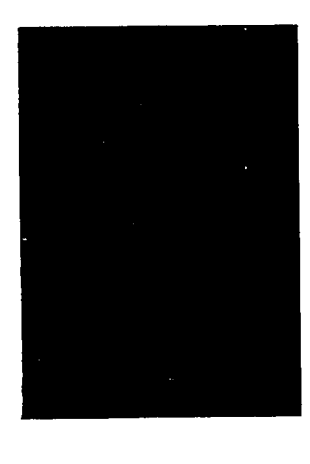
#### ANALYSIS AND DISCUSSION OF RESULTS

In this investigation, the drop size data are presented as a semilog plot of D versus  $\,v_{_{N}}$ . The existence of a maximum drop diameter in

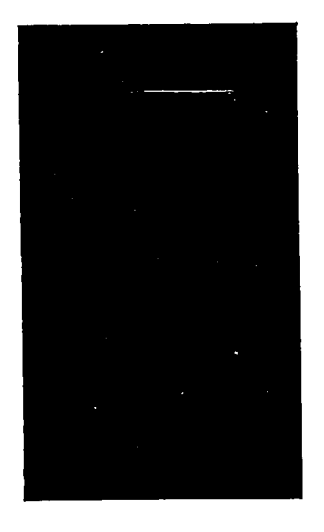
SAMPLE DROP PHOTOGRAPHS







$$D_N = 0.163$$
 cm



 $D_N = 0.316$  cm



0

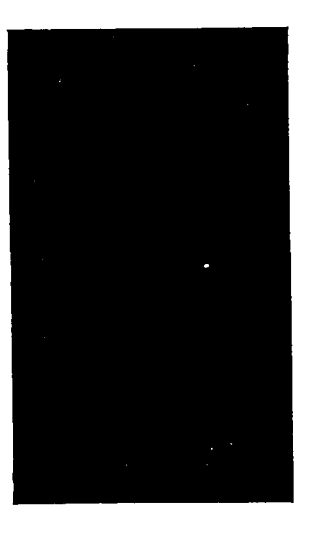








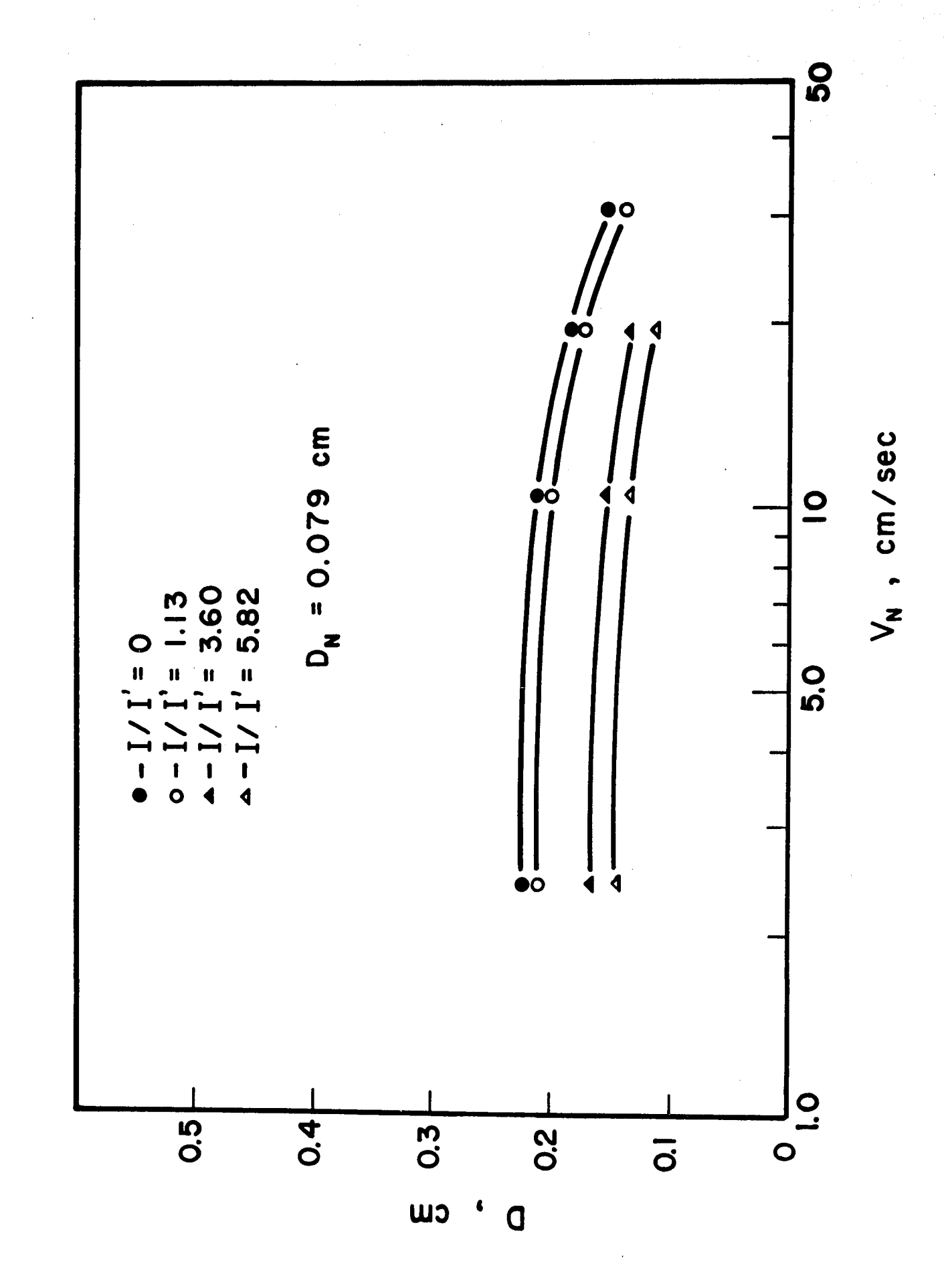


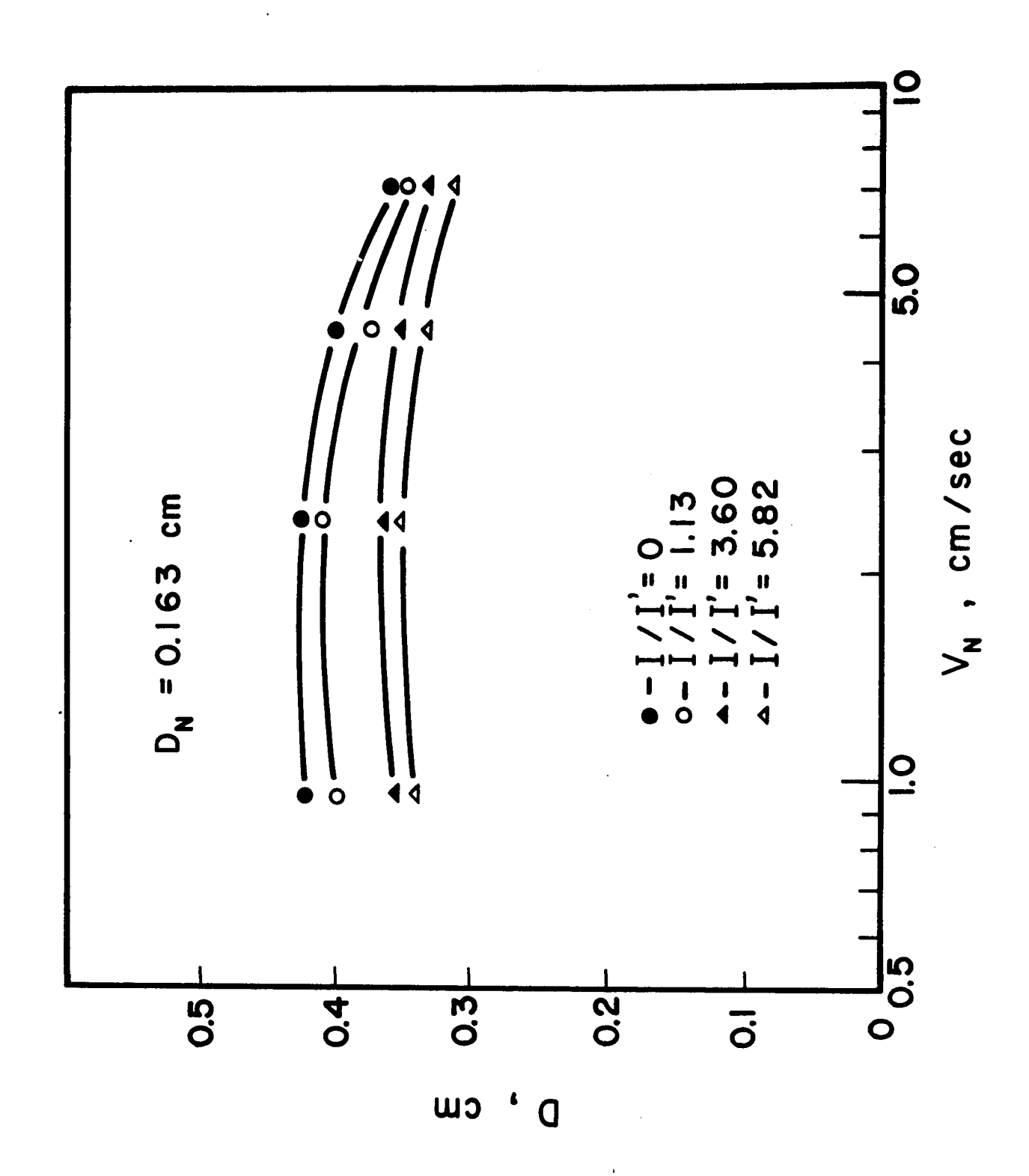


$$D_N = 0.316$$
 cm

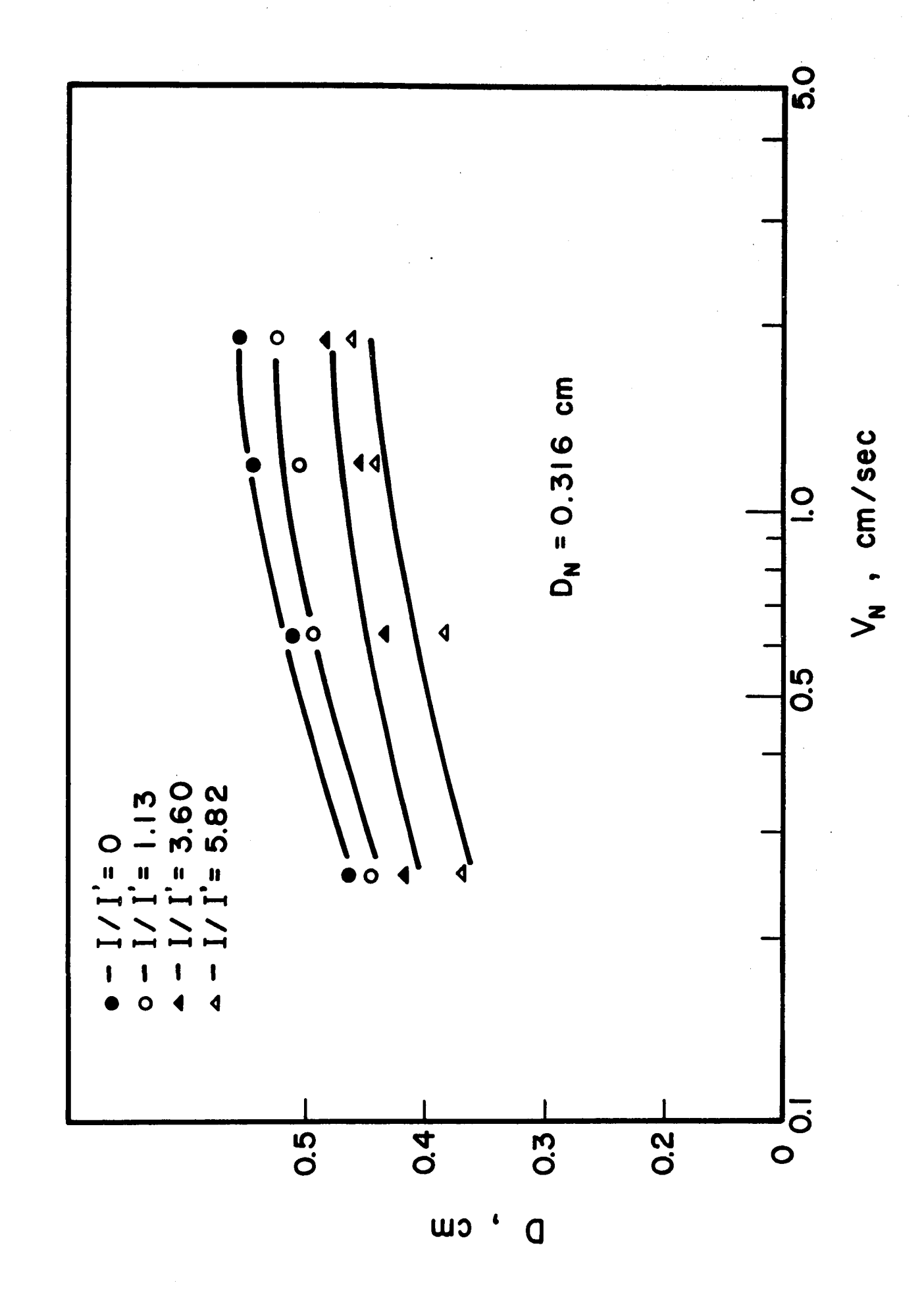
 $D_{\rm N}$  = 0.163 cm

EFFECT OF ULTRASONIC VIBRATION ON D FOR MIBK DROPLETS IN WATER  $(D_{N} = 0.079 \text{ cm})$ 

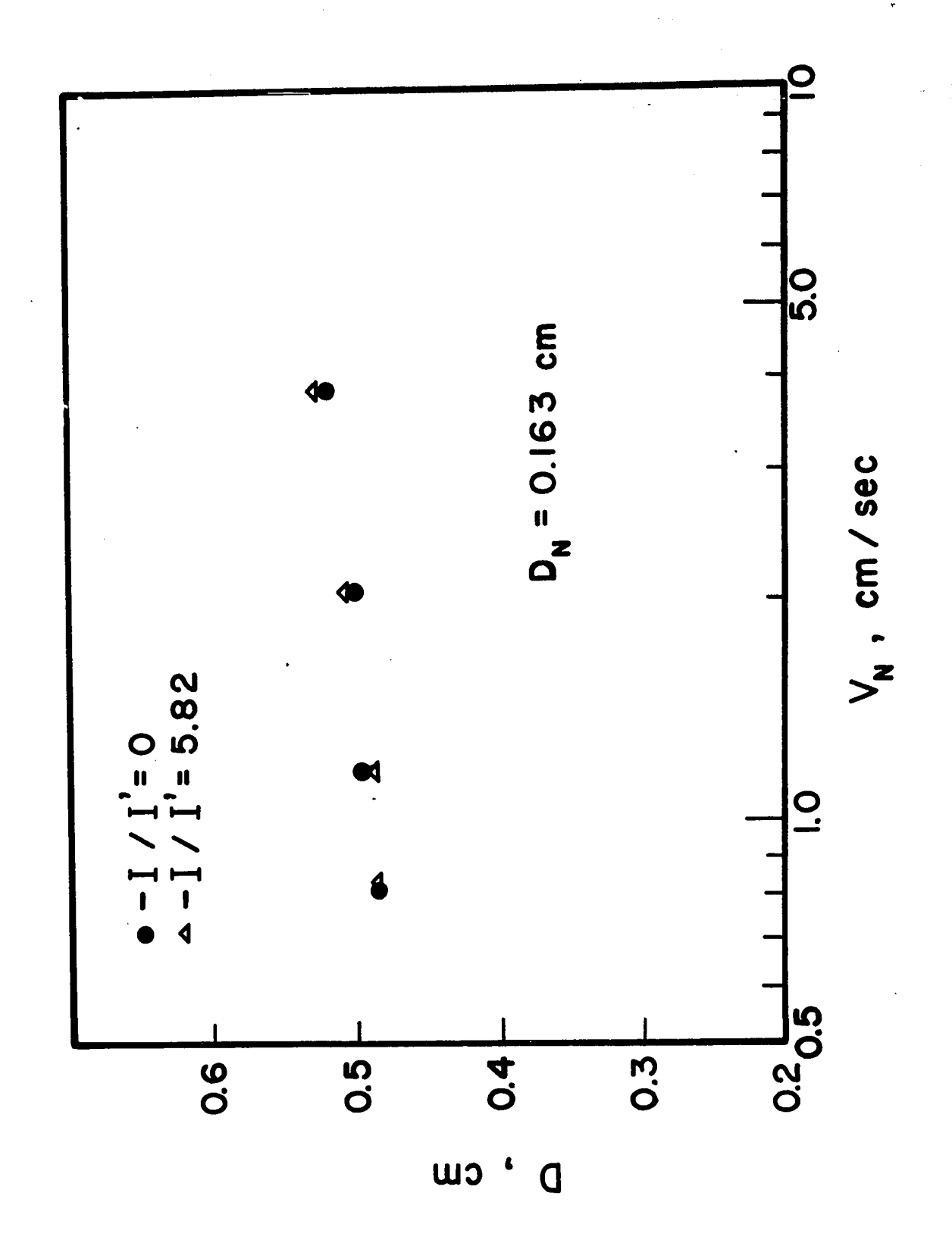




EFFECT OF ULTRASONIC VIBRATION ON D FOR MIBK DROPLETS IN WATER ( $D_{N} = 0.316$  cm)

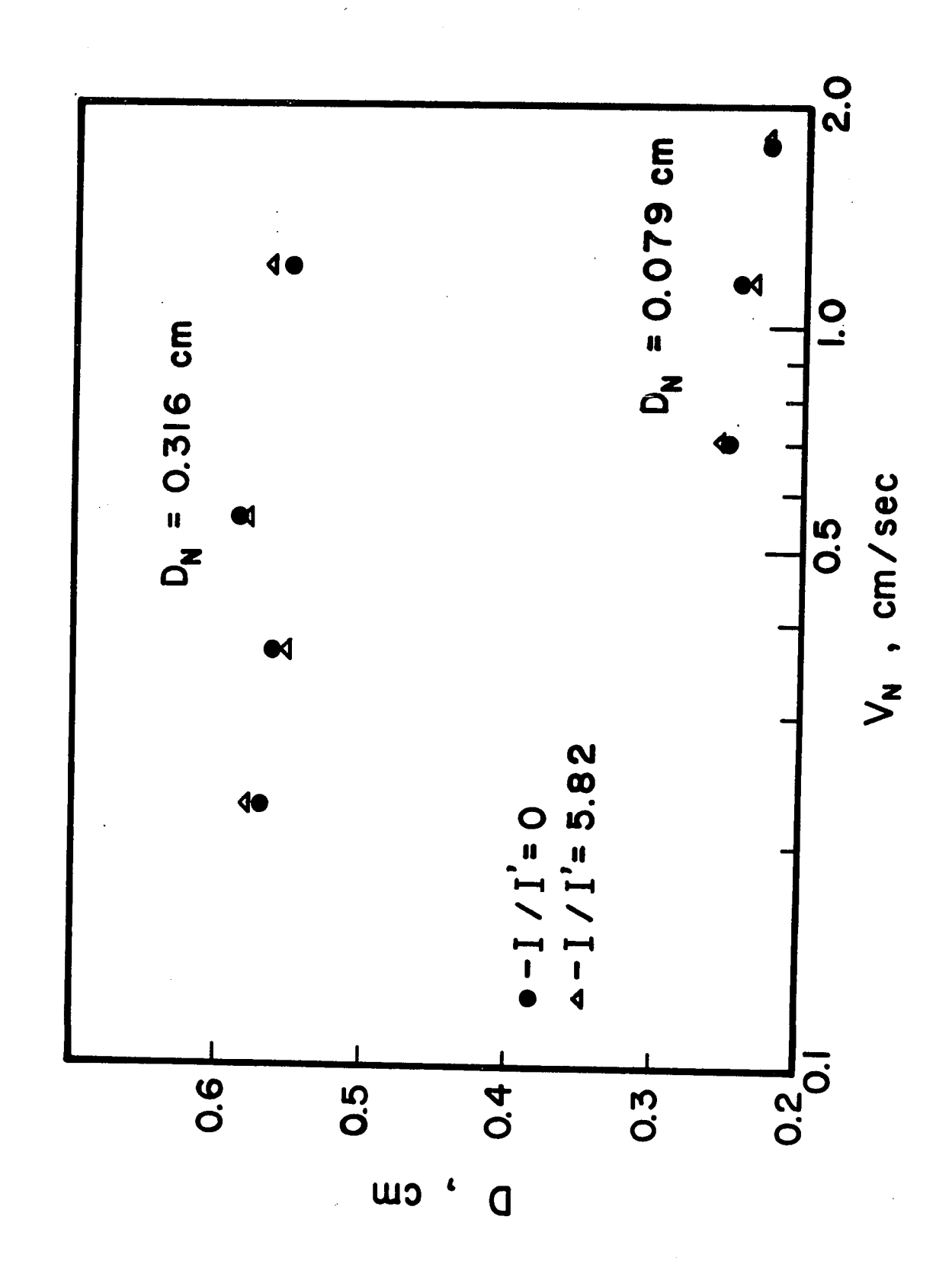


EFFECT OF ULTRASONIC VIBRATION ON D FOR WATER DROPLETS IN MIBK (D<sub>N</sub> = 0.163 cm)



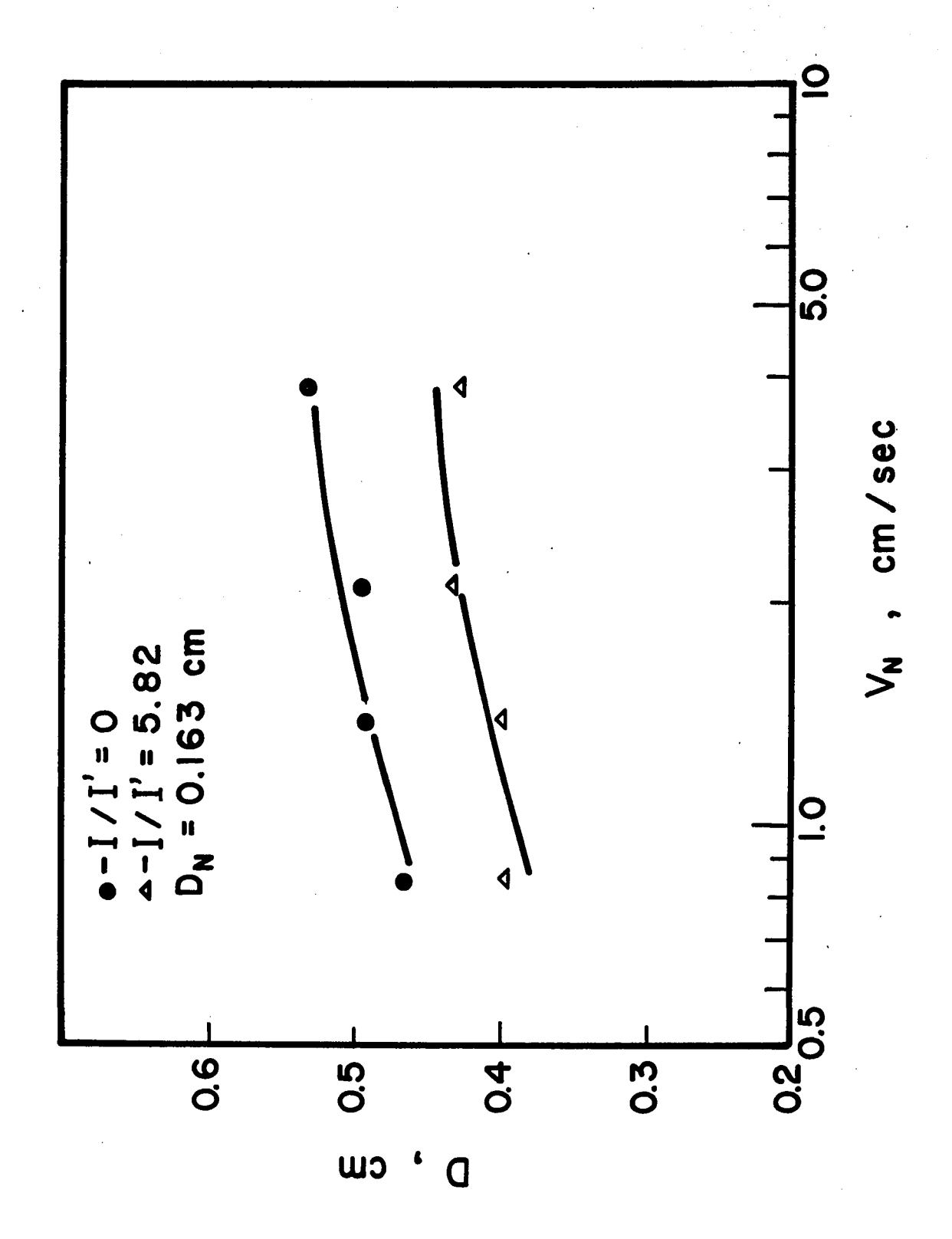
EFFECT OF ULTRASONIC VIBRATION ON D FOR

WATER DROPLETS IN MIBK ( $D_N = 0.316$  and 0.079 cm)

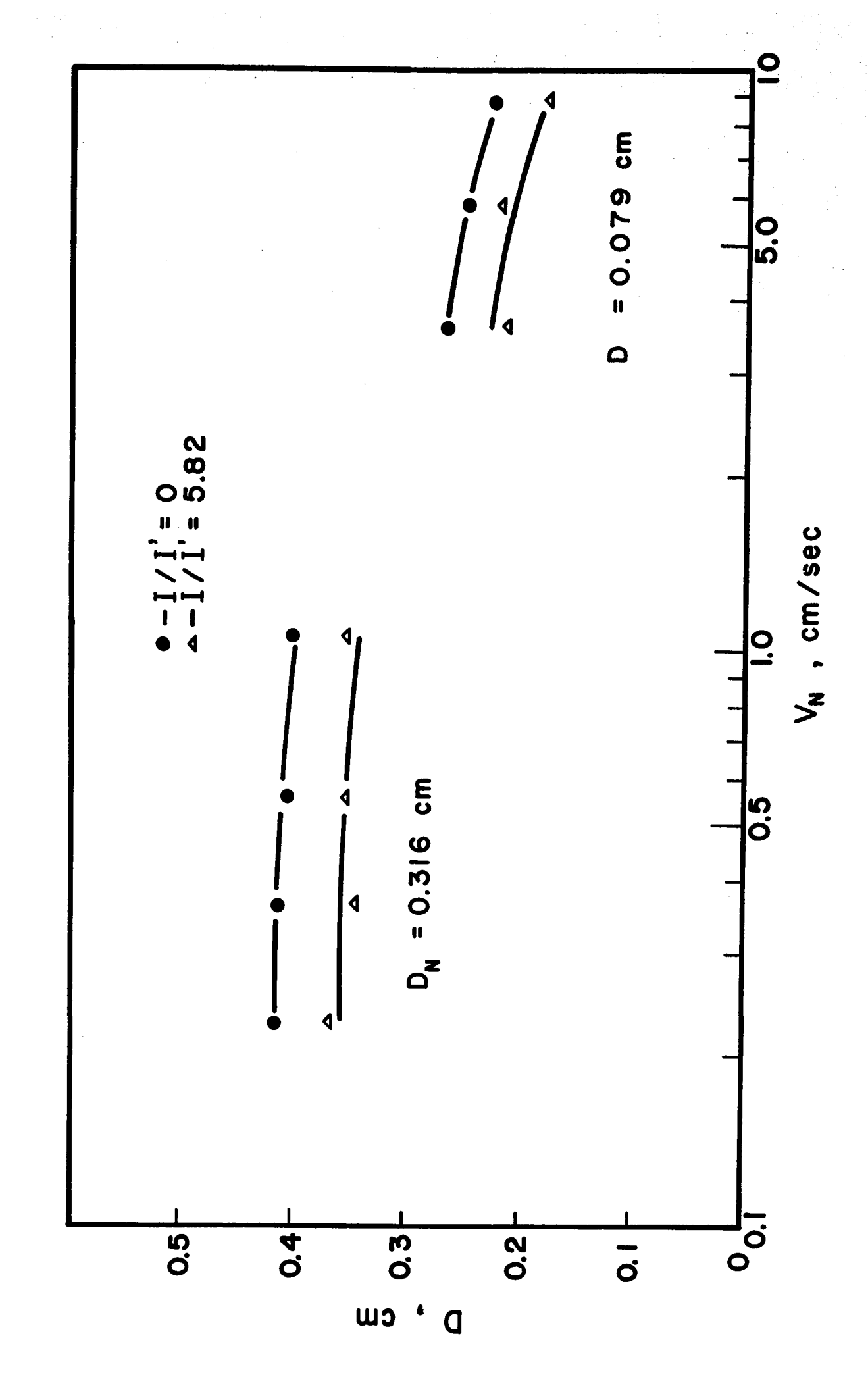


EFFECT OF ULTRASONIC VIBRATION ON D FOR

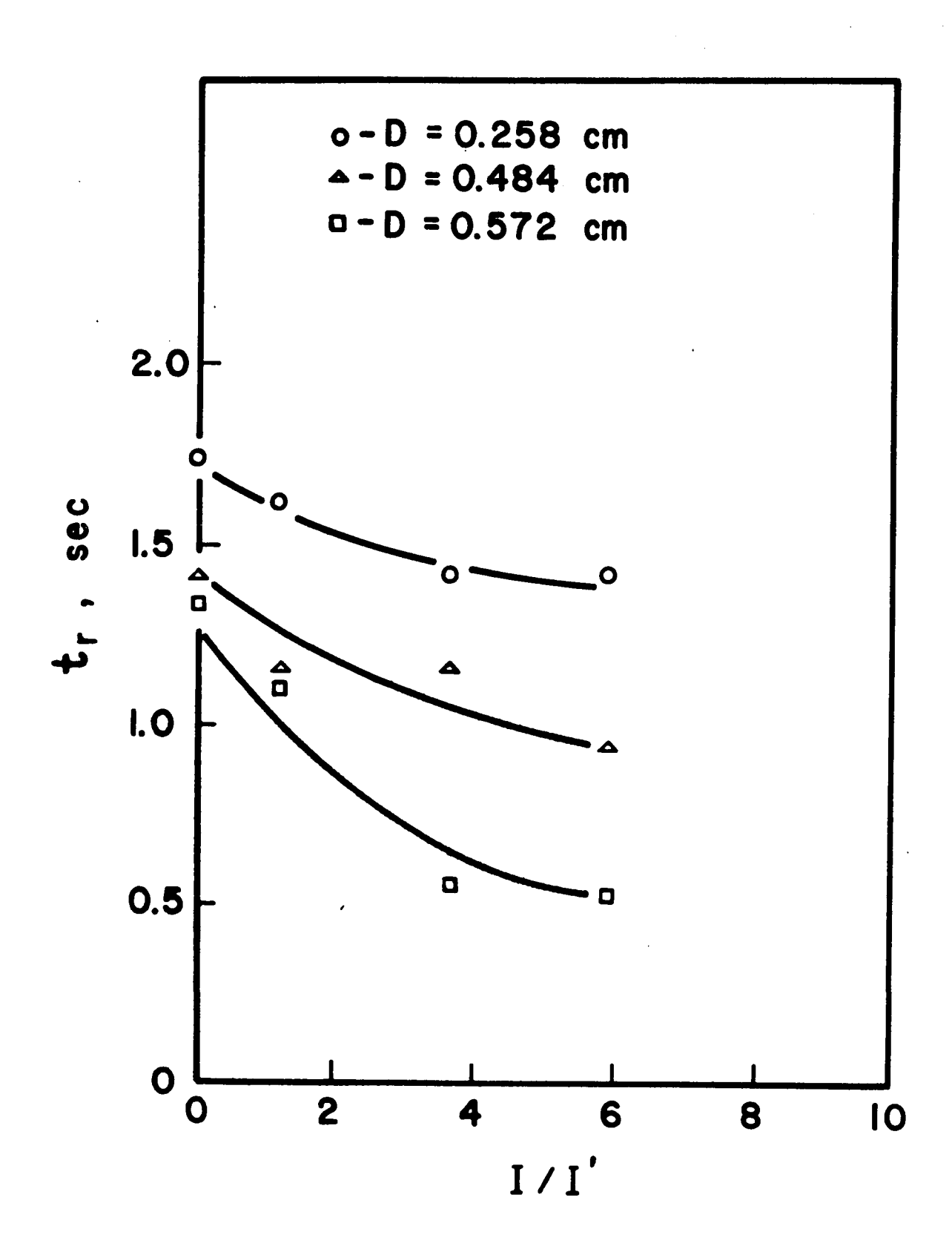
WATER DROPLETS IN TCE ( $D_{N} = 0.163$  cm)



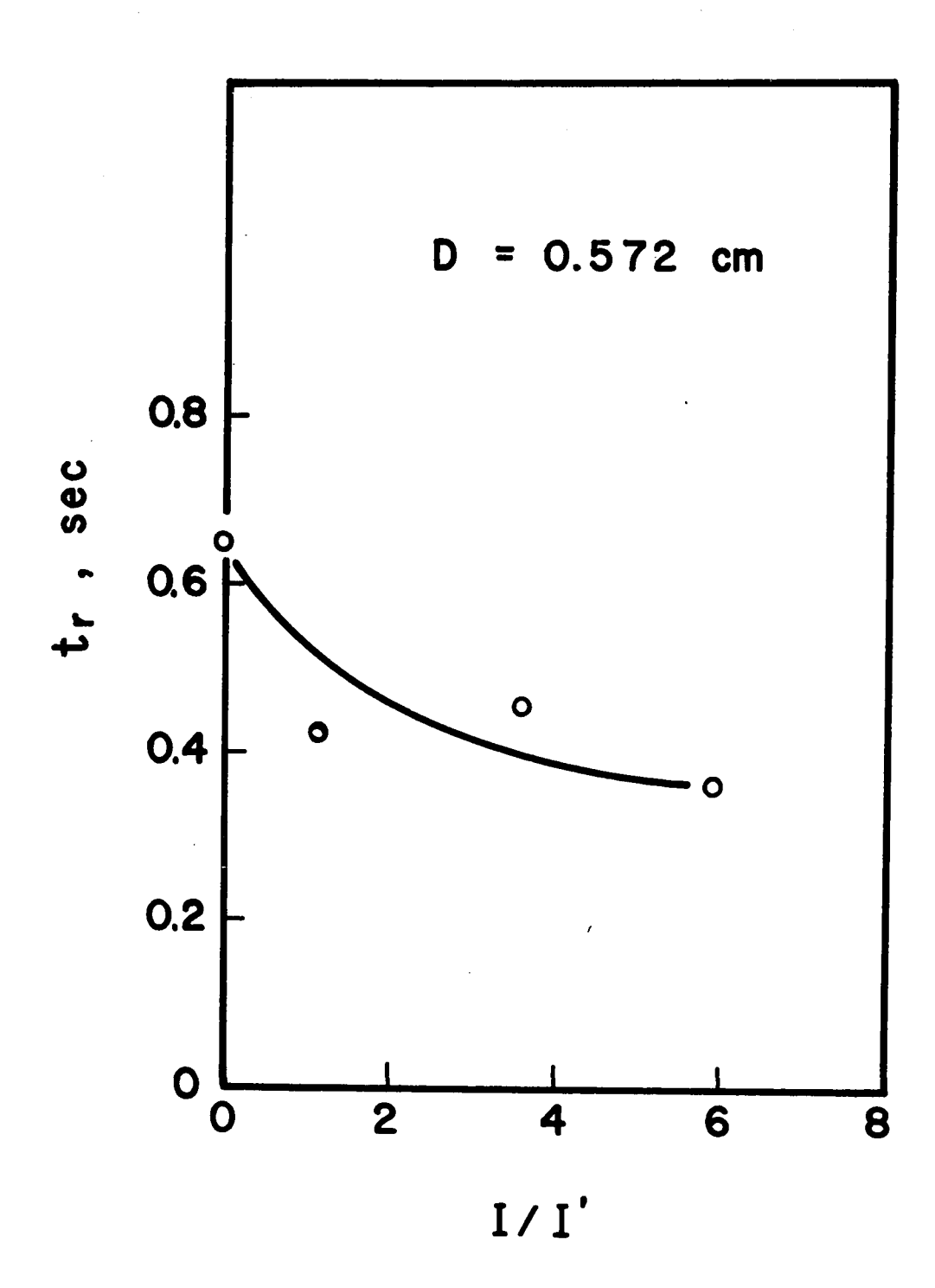
EFFECT OF ULTRASONIC VIBRATION ON D FOR WATER DROPLETS IN TCE ( $D_{N} = 0.316$  and 0.079 cm)



EFFECT OF ULTRASONIC VIBRATION ON tr FOR WATER-3.49% ACETIC ACID-MIBK SYSTEM



EFFECT OF ULTRASONIC VIBRATION ON  $t_{\mathbf{r}}$ FOR TCE-WATER SYSTEM



such a plot is in agreement with the prediction of Hayworth and Treybal (1).

It is seen from Figures 2 to 4 that the average diameter of MIBK drops in water is decreased as the intensity ratio, I/I', is increased. On the other hand, the size of water drops in MIBK is not affected by ultrasonic vibration as seen from Figures 5 and 6. Results of the latter case are expected, because when water, the heavy phase, was dispersed, the dispersing nozzle was located at a point of 38.10 cm from the ultrasonic source where the intensity was negligible low as can be seen from the axial intensity profiles presented in the previous part.

Figures 7 and 8 are results for water drops in TCE, where water was the light phase and the dispersing nozzle was close to the ultrasonic source. They confirm that the size of the drop may be reduced if the dispersing nozzle is subjected to an intense ultrasonic field.

As mentioned in the previous part, the size of a drop depends on the balance of forces acting upon it during formation. Normally, the drop grows in size at the nozzle tip, and is released when the forces acting in the direction away from the nozzle, mainly the buoyant force, just overcome the interfacial tension force. The normal balance of forces might be disturbed by the longitudinal vibrations as well as the turbulence caused by ultrasonic cavitation. The drop would thus be released prematurely, and consequently would be smaller than the normal size.

A smaller drop size and thus a larger interfacial area of contact can simply be achieved by using a smaller nozzle (1,2). However, a smaller nozzle increases the nonuniformity of the drops and consequently increases the drop coalescence during passage through the column (3). Also, a smaller nozzle may become plugged if there are solids suspended in the liquids (4). Therefore, the use of ultrasonic vibration to reduce the droplet size in a spray column may not be impractical.

By dimensional analysis and analysing the experimental results, an empirical correlation for predicting the decrease in drop size caused by ultrasonic vibration has been obtained and is as follows

$$\Delta D/D_N = 2.78 (\mu_d/D_N \Delta \rho v_N)^{0.66} (D_N \Delta \rho v_N^2/\sigma)^{0.39} (I/I')^{0.89}$$
(1)

where 
$$\triangle D = D_0 - D_1$$
, and  $I < I_c$ .

The continuous phase flow rate and viscosity have no noticeable effect on the droplet size (2,5,6) and should not have any significant effect on  $\Delta D$ . The use of  $\Delta \rho$  instead of  $\rho_c$  and  $\rho_d$  has been found to be better in fitting the experimental data.

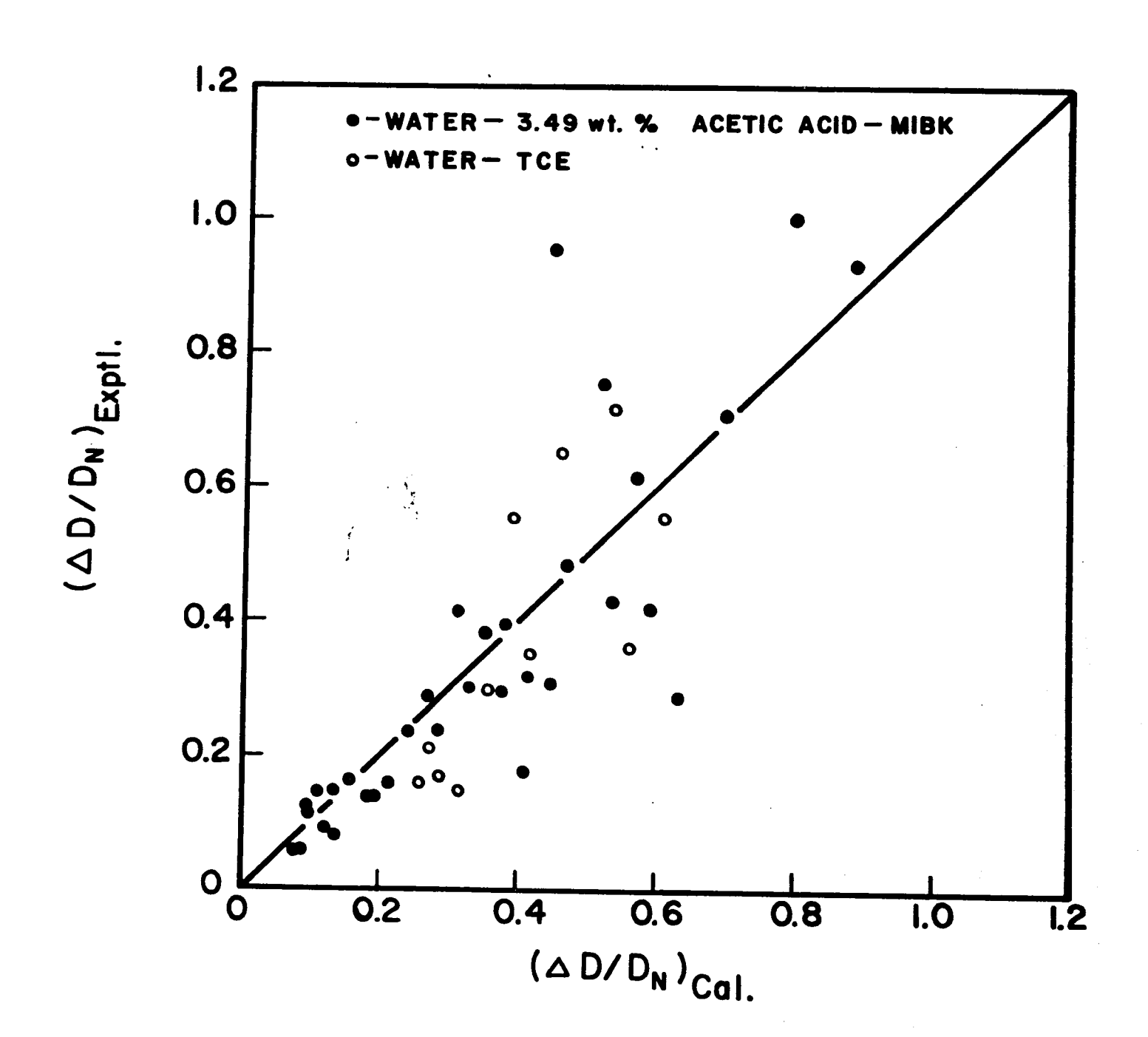
Equation (1) was developed for the 3.49% acetic acid-MIBK-water system with an absolute average deviation of 31.2%. Data for the water-TCE system, which has higher values of interfacial tension, density

difference, and dispersed phase viscosity as can be seen from Table 1, fit the correlation with a deviation of 38.7%. Experimental and calculated values of  $\Delta D/D_N$  for both systems are shown in Figure 11. Detailed data are given in Appendix E. For the water-TCE system, there was no transfer of solute between the dispersed and the continuous phases, whereas for the water-MIBK system, transfer of acetic acid from the drops to the continuous water phase took place. However, since the solute concentration of the MIBK feed was only 3.49%, the effect of solute transfer on the droplet formation would not be significant.

The shape of the drops observed in this investigation was nearly spherical as can be seen from the sample photographs in Figure 1. For a few cases, where the 0.316 cm nozzle was used and the drop size was greater than about 0.5 cm, the shape was ellipsoidal. However, since the relative values instead of absolute size of the droplets were of interest in this study, only the horizontal diameters of the drops were measured and used. For all the cases, no breakup or coalescence of the drops during the rise or fall period was observed.

It has been shown (7,8,9,10) that droplets of the dispersed phase in a spray column normally rest at the interface for a certain time and such a rest time depends on the temperature and physical properties of the system, the drop size, the length of fall, and the disturbance at the interface.

DROP SIZE CORRELATION



From Figures 9 and 10, it is seen that the rest times of drops at the interface for both water-3.49% acetic acid-MIBK solution and water-TCE systems decrease with increasing intensity ratio of the ultrasonic vibration. This is in analogy with the report of Brown and Hanson (11), in which a high energy AC field was shown to cause reduction in the rest time of drops at a liquid-liquid interface, and the rest time was found to decrease with increasing applied field strength.

The reduction of rest time by an electric field was thought (9) to be due to the increase of disturbance at the interface and the polarization of the drops. Ultrasonic vibration would not cause any polarization and its effect on the rest time might be due to the increase of turbulence at the interface. As mentioned earlier, the formation and collapse of cavitation bubbles may cause agitation and turbulence in the liquid. It is quite possible that such turbulence may cause an early rupture of the film which is trapped between the drop and the interface. The trapped film is assumed to cause the existence of the fest.time.

All of the coalescence processes observed in this study were of single-stage, although the viscosity ratios  $\mu_d/\mu_c$  for the systems used, fell in the range in which, according to Charles and Mason (12), multi-stage coalescence should occur. Charles and Mason reported that multi-stage coalescencewould take place if  $\mu_d/\mu_c$  was between 0.02 and 9.

#### CONCLUSIONS

It may be concluded from this investigation that the size of the adispersed phase droplets in a spray column is decreased when the dispersing nozzle is placed in an intense ultrasonic field. Such a decrease in the drop size by ultrasonic vibration depends heavily on the intensity ratio, I/I', which is defined as the ratio of the ultrasonic intensity to the threshold intensity of cavitation. The drops decrease in size with increasing I/I', and disturbance of the normal force balance of the drop, which may cause the drop to be released prematurely, was postulated to be responsible for such a decrease. An empirical correlation in the form of dimensionless groups has been proposed for estimating the decrease of drop size caused by ultrasonic vibration.

For the case where the heavy phase was dispersed, the size of the droplet was not affected by the ultrasonic vibration because in that case the dispersing nozzle was far from the vibration source, and the intensity there was not sufficient to introduce any appreciable effect.

The rest time of drops at the aqueous-organic interface in a spray column may be reduced by applying ultrasonic vibration to the system. The increase in the degree of turbulence at the interface by ultrasonic cavitation, which may cause an early rupture of the film trapped between the drop and the interface, was thought to be the cause.

#### NOMENCLATURE

### Roman Symbols

C\_2 - solute concentration of the MIBK feed, wt.%

D - average drop diameter, cm

 $\mathbf{D}_{\mathbf{N}}$  - nozzle diameter, cm

 $\Delta D$  - diameter difference  $(D_0 - D_I)$ , cm

f - frequency, kc/sec

F - flow rate, ml/sec

I - ultrasonic intensity measured by the thermocouple probe, mv

I' - threshold intensity measured by the thermocouple probe, .mv

I - critical intensity measured by the thermocouple probe, mv

t\_ - rest time of the drop at the interface, sec

 $v_{_{\rm N}}$  - nozzle velocity, cm/sec

### Greek Symbols

μ - viscosity, poise

 $\rho$  - density, g/ml

Δρ - difference in density between continuous and dispersed phase, g/ml

o - interfacial tension, dynes/cm

#### Subscripts

c - continuous phase

d - dispersed phase

I - at an intensity I

m ~ MIBK phase

0 - at zero intensity

### REFERENCES

- 1. Hayworth, C.B., and R.E. Treybal, Ind. Eng. Chem. 42 1174 (1950)
- 2. Null, H.R., and H.F. Johnson, A.I.Ch.E. Journal 4 273 (1958).
- 3. Johnson, H.F., and H. Bliss, Trans. Am. Inst. Chem. Engrs. <u>42</u> 331 (1946)
- 4. Treybal, R.E., "Mass-Transfer Operation", p.372, McGraw-Hill, New York (1955)
- 5. Garwin, L., and B.P. Smith, Chem. Eng. Progr. 49 591 (1953)
- 6. Calderbank, P.H., and I.J.O. Korchinski, Chem. Eng. Sci. 6 65 (1956)
- 7. Nielson, L.E., Wall, R., and G. Adamas, J. Colloid Sci. <u>13</u> 441 (1958)
- 8. Charles, G.E., and S.G. Mason, J. Colloid Sci. 15 236 (1960)
- 9. Brown, A.H., and C. Hanson, Brit. Chem. Eng. <u>11</u> 695 (1966)
- 10. Jeffreys, G.V., and J.L. Hawksley, A.I.Ch.E. Journal 11 413 (1965)
- 11. Brown, A.H., and C. Hanson, Trans. Far. Soc. 61 1754 (1965)
- 12. Charles, G.E., and S.G. Mason, J. Colloid Sci. 15 105 (1960).

#### PART III

#### THE MECHANISM OF EXTRACTION UNDER ULTRASONIC VIBRATION

### INTRODUCTION

In the first experimental part described earlier, the effect of ultrasonic vibration on the extraction efficiency was evaluated in terms of Ka, the product of the overall mass transfer coefficient and the interfacial area of contact. In the present investigation, the dispersed phase holdup in the column was determined, which enabled the calculation of K and a, and the effect of ultrasonic vibration on these two parameters was studied separately. The interfacial area of contact was calculated from the holdup and the average surface area of the drops, the latter being known from the drop size data obtained in the previous experiment, i.e., Part II.

Holdup of the dispersed phase in a spray column can be measured directly by shutting off the feed and effluent simultaneously and noting the fall or rise of the interface level as the dispersed phase droplets clear the column and accumulate at the interface. However, this measurement is not accurate when the amount of holdup is small, since the change in interface level will be very small and therefore subject to considerable error. An indirect method was therefore adopted in which the residence time of the drop in the column is measured and the

holdup is calculated from this residence time and the known dispersed phase flow rate.

The extraction process in a spray column can be divided into three stages as suggested by Licht and Conway<sup>(1)</sup>. The period during which the drops are forming constitutes stage 1. Stage 2 covers the period of rise or fall of the drops through the continuous phase. Stage 3 begins at the end of stage 2 and consists of the coalescence process of the drops at the interface. In this study, experiments were also undertaken to investigate the influence of ultrasonic vibration on the end effect and the transfer of solute during stage 2. By measuring the overall fraction extracted as well as the contact time for stage 2 at various effective column heights, thefraction extracted at stage 2, the end effect, and the effective diffusivity were calcualted by the Johnson-Hamielec method<sup>(2)</sup>.

### APPARATUS AND PROCEDURE

The experimental apparatus and system used in this study were the same as those of the first experimental part.

For measuring the residence time of a drop in the column, a run consisted simply of adjusting the flow rates of both continuous and dispersed phases, the ultrasonic frequency, and the ultrasonic intensity to the desired values, and the time was measured by a stopwatch. The residence time of a drop in the column was taken between the moment of the

detachment of the drop from the nozzle tip and its complete disappearance at the interface. Twenty measurements were made for one run and the mean value was used.

The same procedure was employed to determine the contact time for stage 2, i.e., the time during which the drop rises or falls, except that the timing was from the moment of the detachment of the drop at the nozzle tip to the instant of its arrival at the interface. The contact time for stage 2 is equal to the residence time of the drop in the column minus the rest time of the drop at the interface.

For determining the overall fraction extracted, the procedure and measurement were the same as described in the first experimental part.

#### METHODS OF CALCULATION

By assuming that the drops are spherical, the average volume and average surface area of a single drop may be calculated from the average drop diameter as

$$v_{\rm D} = \pi \ D^3/6 \tag{1}$$

$$S = \pi D^2$$
 (2)

The total holdup of dispersed phase, the total number of drops, and the total transfer area in the column are then respectively,

$$\mathbf{H}_{\mathbf{L}} = \mathbf{F}_{\mathbf{d}} \mathbf{L} \tag{3}$$

$$N_{D} = 6 F_{d}t/\pi D^{3} + 1.0$$
 (4)

$$A = (6 F_d t/\pi D^3 + 1.0) \pi D^2 = 6 F_d t/D + \pi D^2$$
 (5)

where t is the average residence time of a drop in the column, and  $\mathbf{F}_{\mathbf{d}}$  is the dispersed phase flow rate. The interfacial area of contact in the column is then

$$a = (6 F_d t/D + \pi D^2) / V_e$$
 (6)

where  $V_e$  is the effective volume of column.

The overall mass transfer coefficient based on the water phase,  $K_{\mathbf{w}}$ , may be calculated from the value of  $K_{\mathbf{a}}$  obtained in the first experimental part and the corresponding value of "a" calculated by Equation (6)

$$K_{w} = K_{u}a/a \tag{7}$$

The fraction extracted during stage 2, end effect, and effective diffusivity may be calculated by Johnson-Hamielec's equations  $^{(2)}$ , provided that  $E_{82}$  is smaller than 0.50. The equations are

$$E_t = 1.81 (1-E_f) (\pi^2 R .99/D^2)^{-1/2} + (0.0189 + 0.981 E_f)$$
 (8)

$$E_{s2} = (E_t - E_f)/(1 - E_f)$$
 (9)

E<sub>t</sub> is the overall fraction extracted. If based on the water phase, it is equal to  $(C_{w2} - C_{w1})/(C_{w1}^* - C_{w1})$ , but if based on the MIBK phase, it is  $(C_{m2} - C_{m1})/(C_{m2}^* - C_{m2})$ . E<sub>f</sub> represents the end effect, i.e., the fraction extracted during drop formation and coalescence at the interface periods.  $\mathcal{D}$  is the molecular diffusivity and R is a multiplier of  $\mathcal{D}$ . R  $\mathcal{D}$  may be called the effective diffusivity.

Plotting  $E_t$  against the square root of  $\theta$ , the contact time of the drops and the continuous phase during the drop rise or fall period, should yield a straight line whose slope and intercept may be used to determine  $R^{\otimes}$  and  $E_f$  respectively. The fraction extracted during stage 2, i.e.,  $E_s$ , is then calculated by Equation (9).

### RESULTS AND DISCUSSION

The residence time data are summarized in Table 1, and the calculated values of  $K_{\overline{W}}$  and a are plotted versus I/I' in Figures 1 through 9.

For MIBK drops in water, i.e., when MIBK was dispersed in the continuous water phase, the residence time of the drop in the column does not seem to be significantly affected by the ultrasonic vibration.

For a particular nozzle size, the values of t for all different levels

TABLE 1

### SUMMARY OF RESIDENCE TIME DATA

Z = 30.48 cm

 $C_{m2} = 3.49 \text{ wt.}\%$ 

TEMPERATUE: 24.5 - 25.5°C

PRESSURE: Atmosphere

(a) MIBK Drops in Water

 $F_{d} = 0.050 \text{ ml/sec}$ 

 $F_c = 0.043 \text{ ml/sec}$ 

${ t D}_{ extbf{N}}$	1	t, sec		
cm	I/I' = 0	I/I = 1.13	1/1! = 3.60	.1/I' = 5.82
0.079	5.06	5.09	5.11	5.10
0.163	4.79	4.81	4.77	4.84
0.316	4.51	4.50	4.50	4.52

(b) Water Drops in MIBK

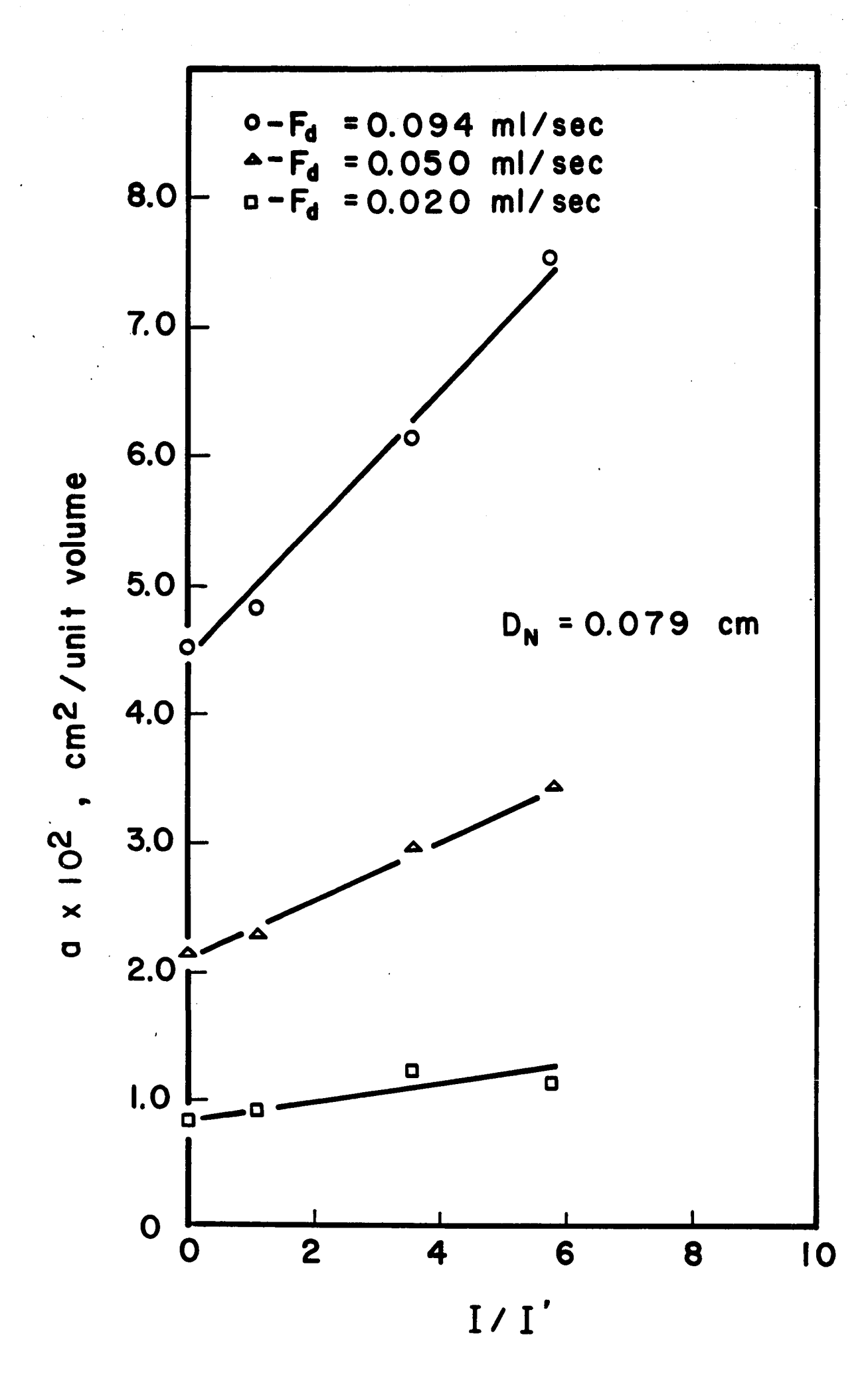
 $F_d = 0.043 \text{ m1/sec}$ 

 $F_c = 0.050 \text{ ml/sec}$ 

$D_{N}$	${ m D}_{ m N}$		t, sec		
	cm '	I/I' = 0	1/1' = 1.13	I/I' = 3.60	1/12 = 5.82
	0.079	5.22	5.14	4.91	4.90 _
<u></u>	0.163	4.60	4.60	4.41	4.39
_	0.316	4.42	4.40	3.70	3.70

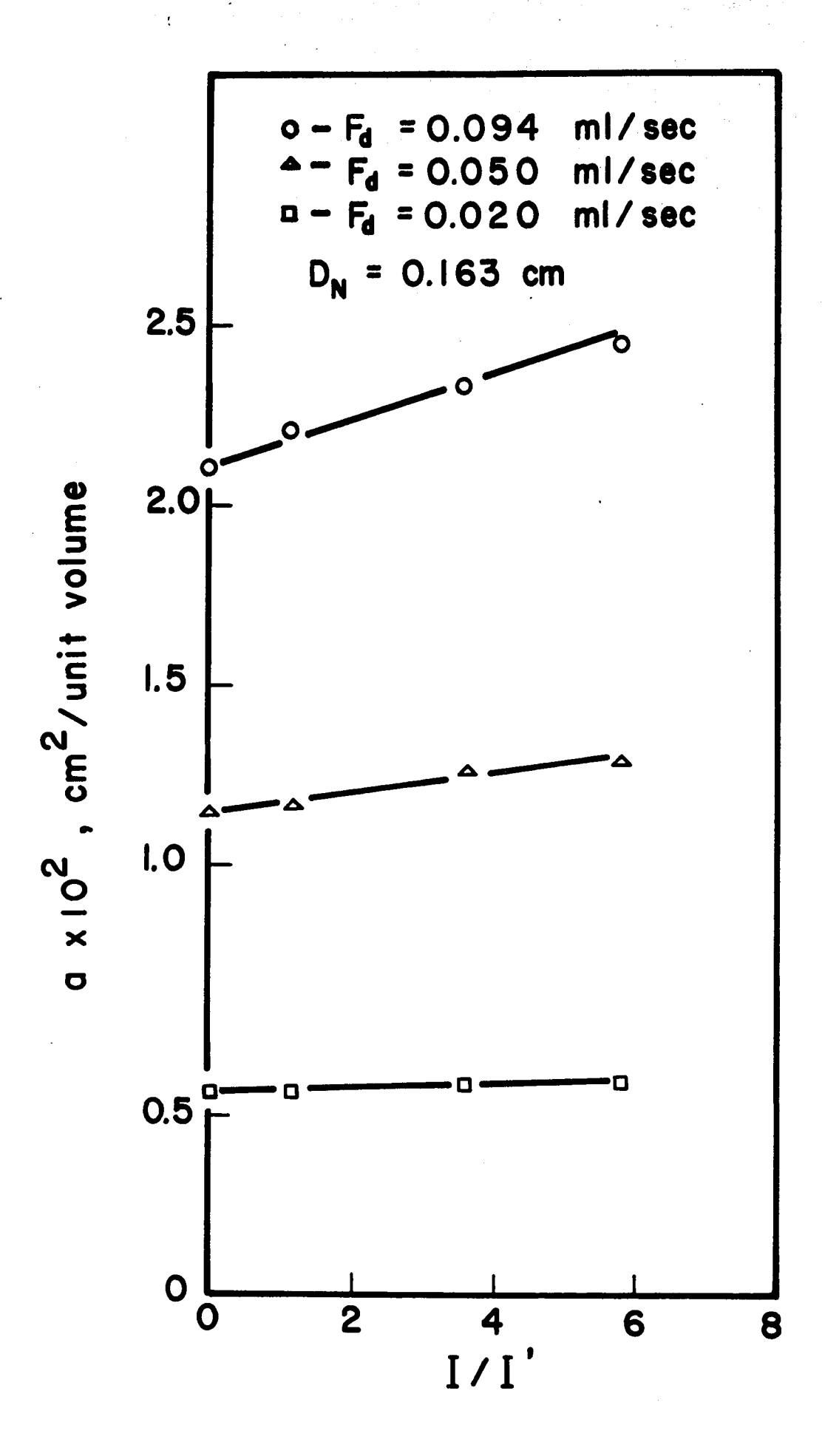
a VERSUS I/I' FOR MIBK PHASE DISPERSED

 $(D_{N} = 0.079 \text{ cm})$ 

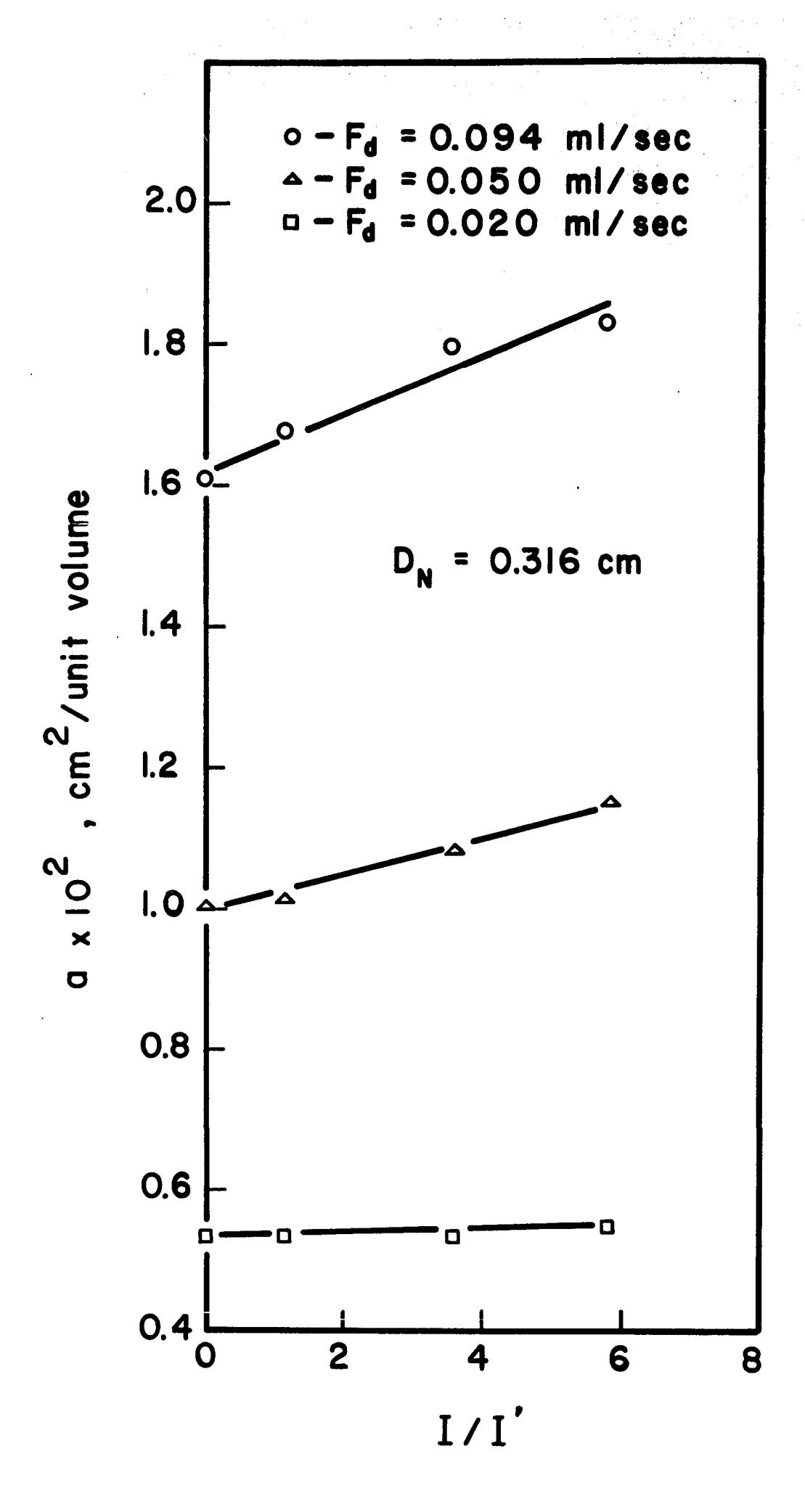


a VERSUS I/I' FOR MIBK PHASE DISPERSED

 $(D_{N} = 0.163 \text{ cm})$ 

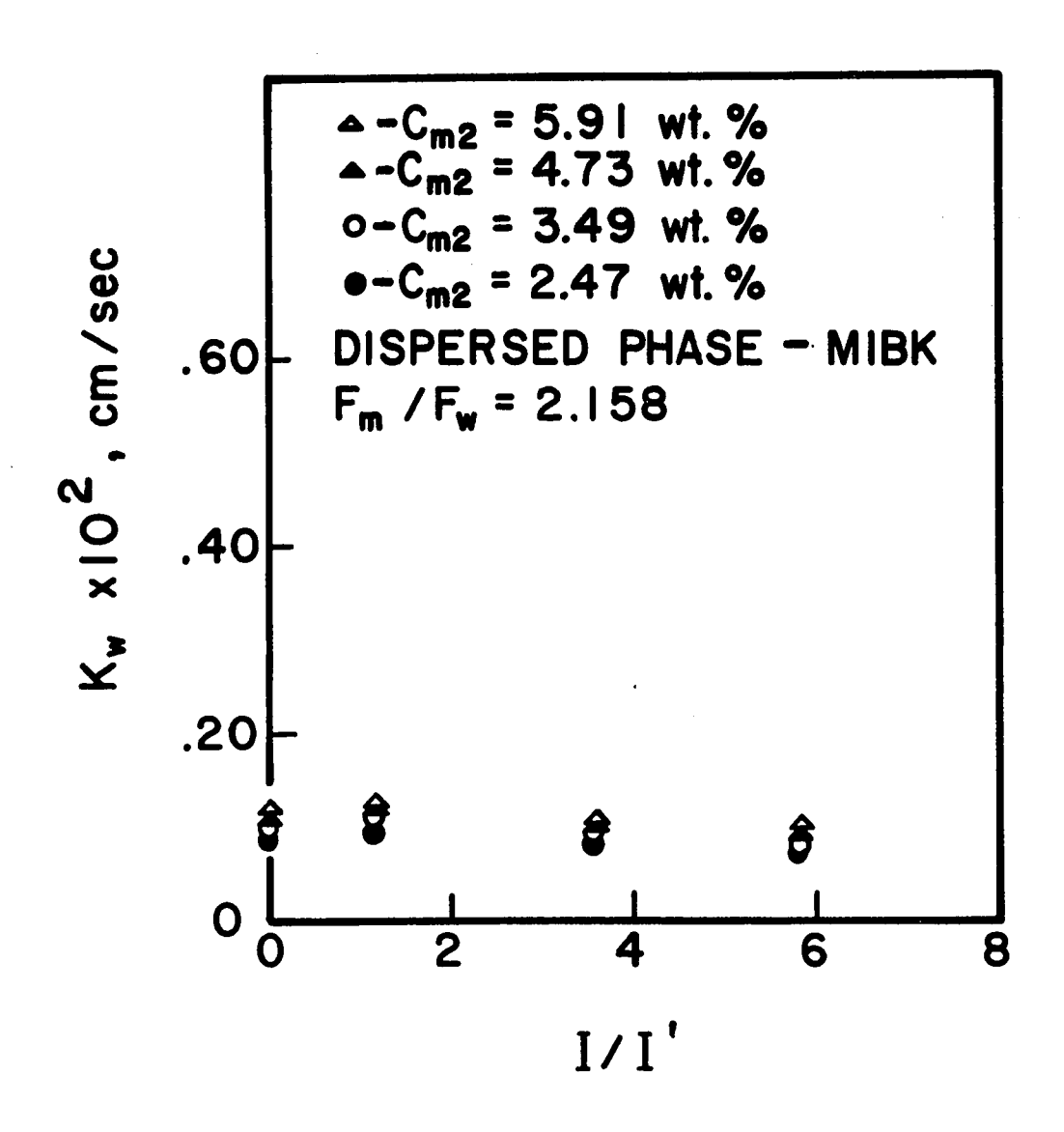


a VERSUS I/I' FOR MIBK PHASE DISPERSED  $(D_{N} = 0.316 \text{ cm})$ 



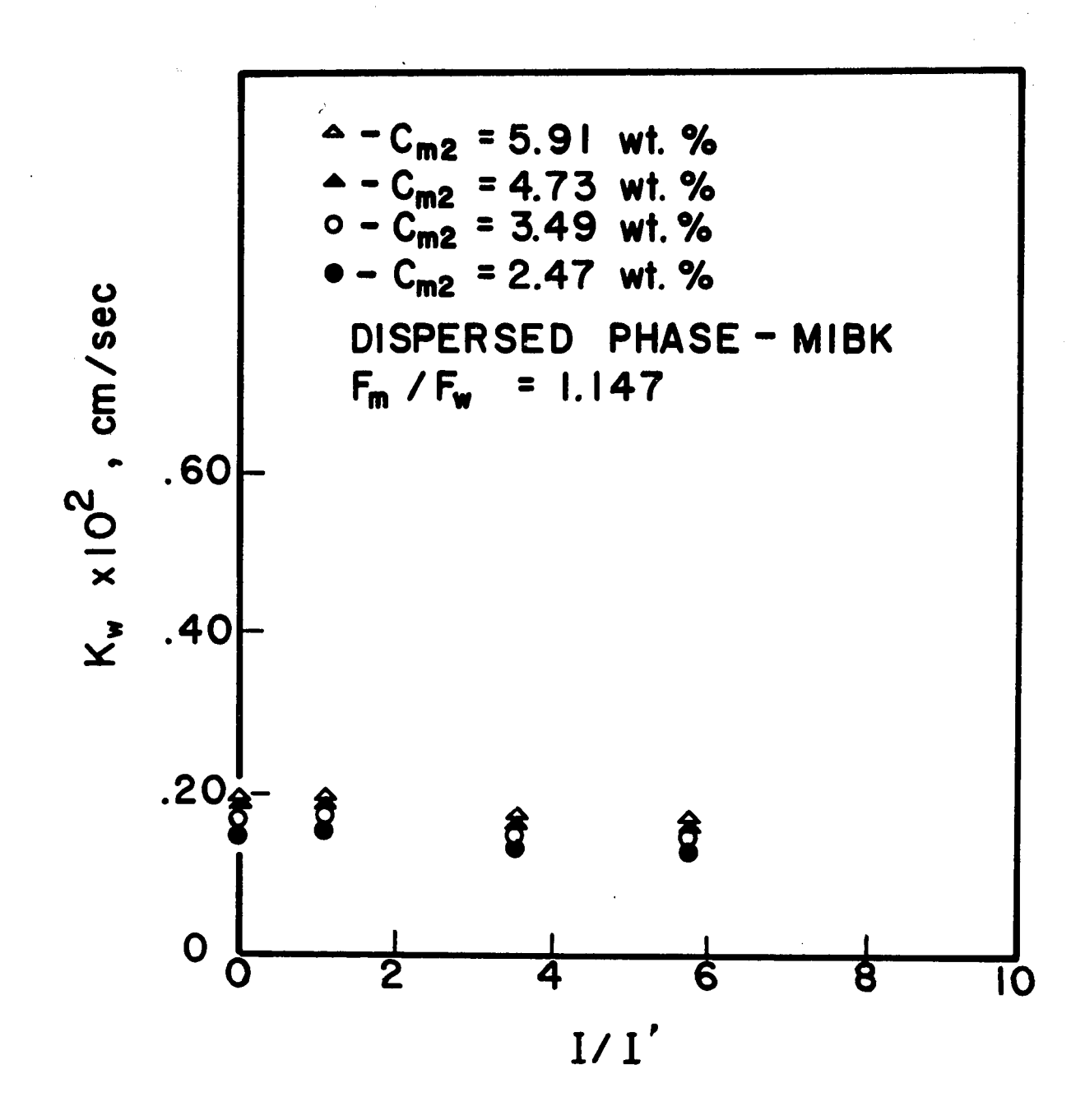
K VERSUS I/I' FOR MIBK PHASE DISPERSED

$$(F_{m}/F_{w} = 2.158)$$

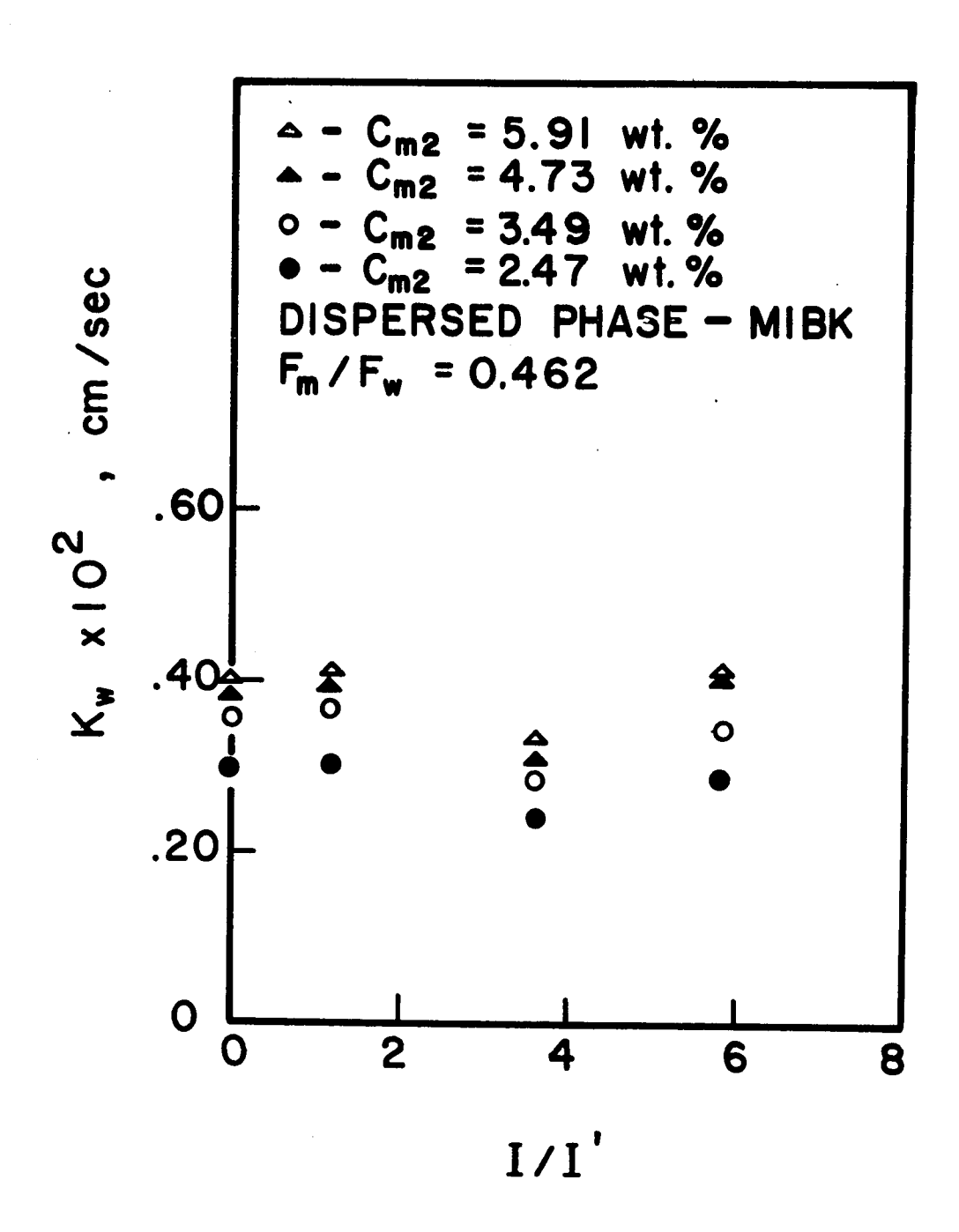


K VERSUS I/I' FOR MIBK PHASE DISPERSED

$$(F_{\rm m}/F_{\rm w} = 1.147)$$

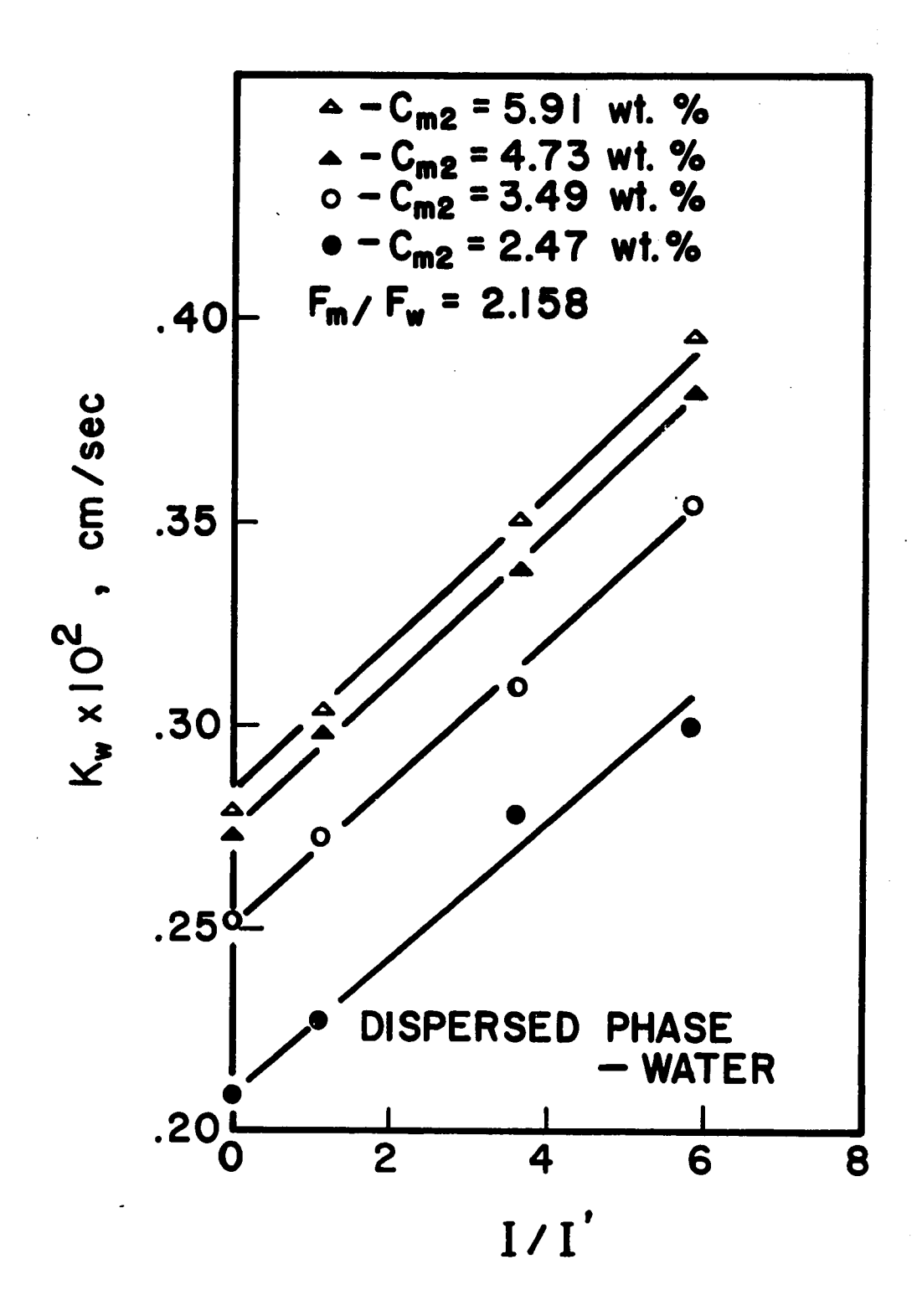


 $K_{\overline{W}}$  VERSUS I/I' FOR MIBK PHASE DISPERSED  $(F_{\overline{M}}/F_{\overline{W}} = 0.462)$ 



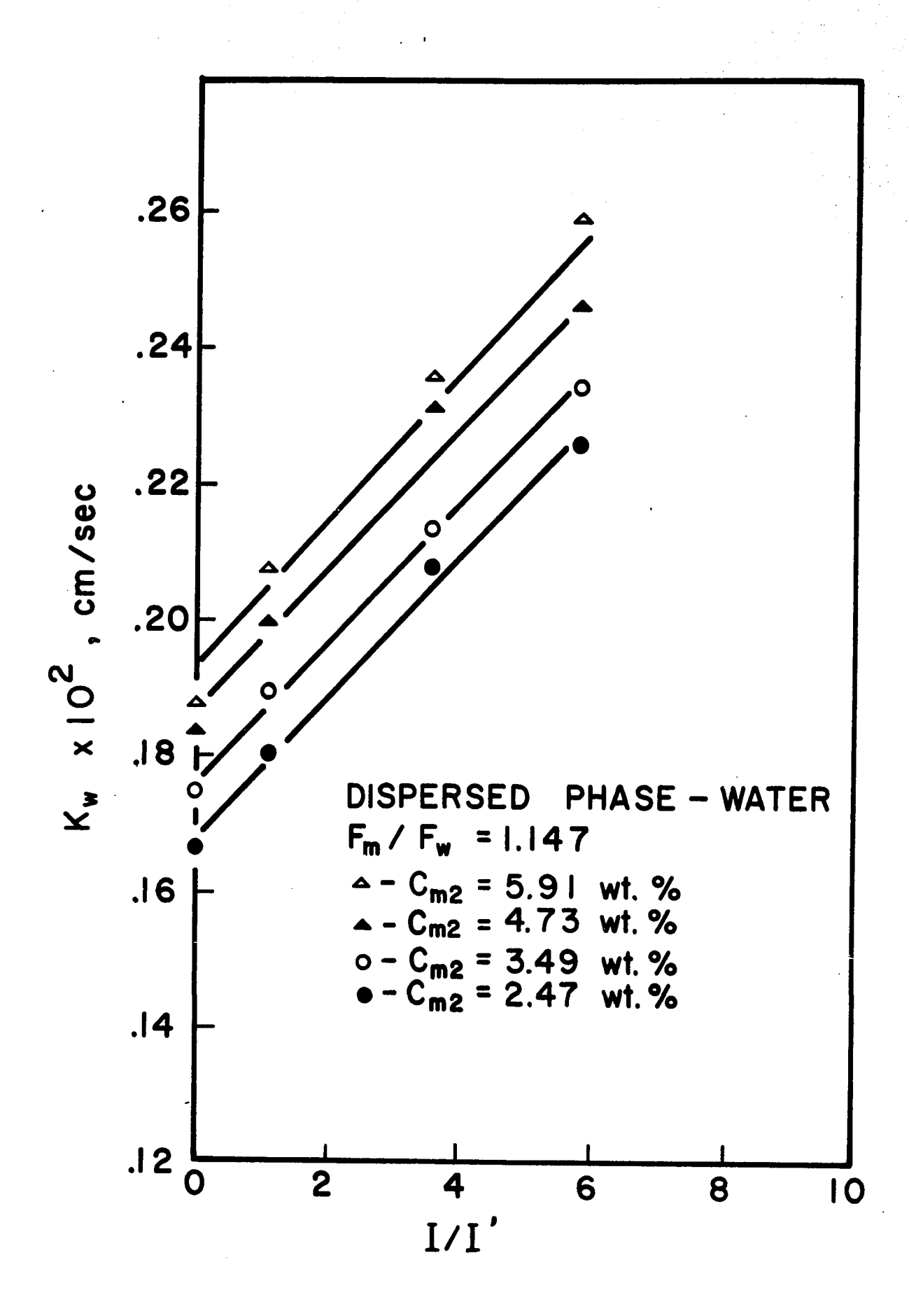
K VERSUS I/I' FOR WATER PHASE DISPERSED

 $(F_{\rm m}/F_{\rm w} = 2.158)$ 



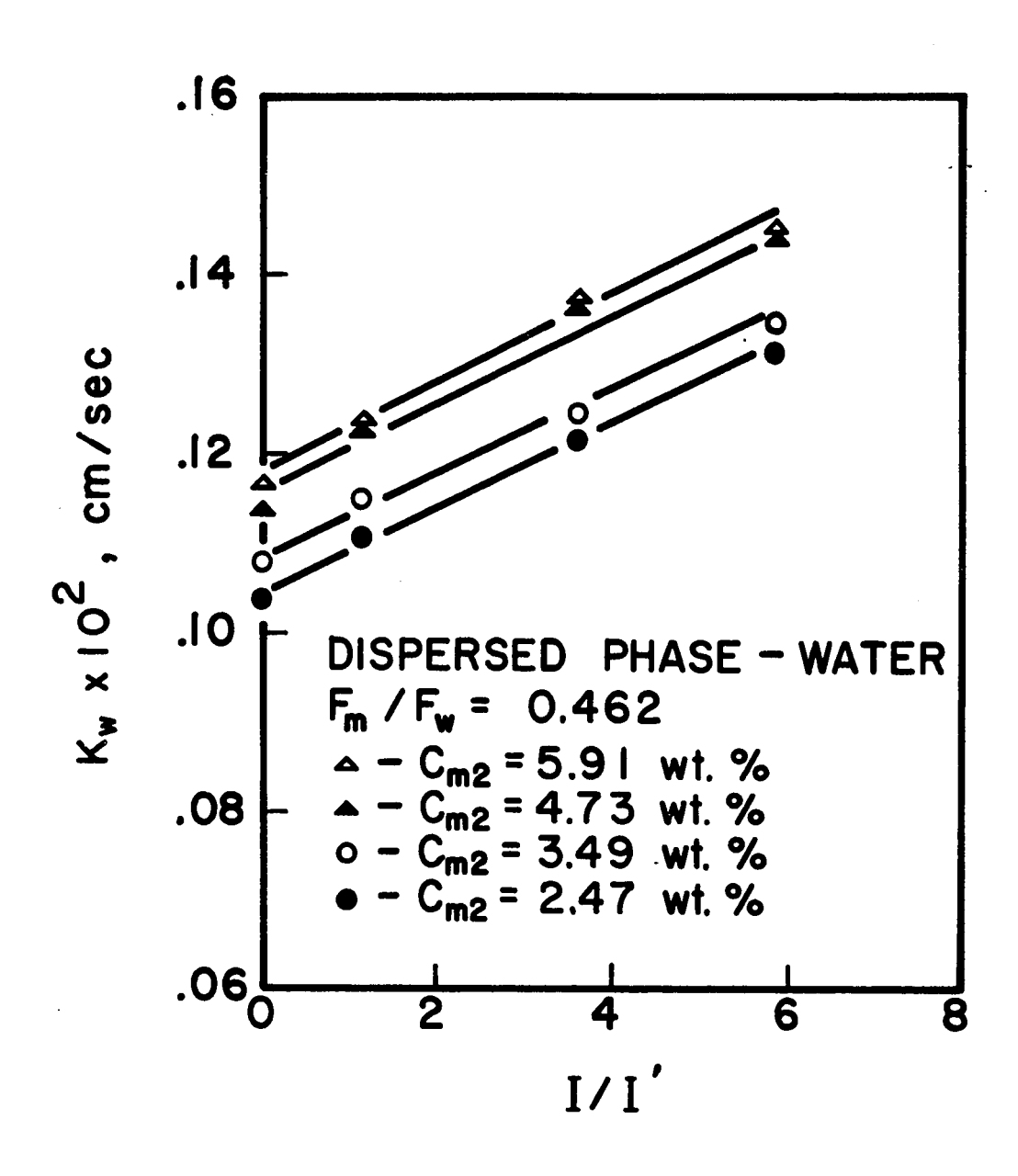
 $K_{\overline{W}}$  VERSUS I/I' FOR WATER PHASE DISPERSED

 $(F_{\rm m}/F_{\rm w} = 1.147)$ 



K VERSUS I/I' FOR WATER PHASE DISPERSED

 $(F_{\rm m}/F_{\rm w} = 0.462)$ 



result from changes in both the droplet velocity and the rest time of the drop at the interface, or either one of these quantities. The droplet velocity as well as the rest time at the interface have been reported by several investigators (3,4,5,6) to be a function of the drop diameter. Accordingly, ultrasonic vibration should have some effect on the value of t, because, when MIBK is dispersed, the dispersing nozzle is close to the ultrasonic source and the drop size decreases with increasing ultrasonic intensity. However, the variation in t may not be detectable by the measuring technique employed in this study.

The interfacial area data caclulated by Equation (6) for MIBK drops in water are presented as plots of "a" versus I/I', using the dispersed phase flow rate as a parameter. As shown in Figures 1,2 and 3, the interfacial area of contact for this case increases with I/I' approximately in a linear fashion. Such an increase is mainly due to the decrease in the average drop diameter.

For the case where the water phase was dispersed, the values of t were slightly reduced by the ultrasonic vibration. This may result from the decrease in the rest time of the drop at the interface, since, when water is dispersed, the interface level is located near the ultrasonic source, and the rest time of the drop at the interface decreases with increasing ultrasonic intensity as found in the previous experimental

part. It was also found in the previous experimental part that the drop sizes were not affected by the ultrasonic vibration when water was the dispersed phase.

TABLE 2

F = 0.050 ml/sec

## INTERFACIAL AREA FOR WATER PHASE DISPERSED

= 0.049 m1/sec

<b>a</b>		0.070 -		ת	==	0.241	cm	
<sup>D</sup> N	=	0.079 c	Sm Sm	ט	_	.0,671		
				 <del></del>				

ı/ı'	0	1.13	3.60	5.82	
a cm²/unit volume	0.0168	0.0165	0.0159	0.0159	

Therefore, the interfacial area of contact for this case does not increase with the ultrasonic intensity but decreases slightly due to a reduction in the value of t. An example is given in Table 2.

The calculated values of  $K_W$  for the MIBK phase dispersed were plotted against I/I', and are shown in Figures 3,4 and 5. No significant change in  $K_W$  was found when the column liquids were subjected to ultrasonic vibration. On the contrary, when water was the dispersed phase,  $K_W$  increased linearly with I/I' as shown in

Figures 6 to 9. Such an increase was due to the increase in turbulence at the interface as postulated in the first experimental part.

Based on the results of this study, the following correlations may be proposed, when I and I' are measured at the dispersing nozzle tip or at the aqueous-organic interface and I is less than the critical intensity for emulsification,  $I_{\alpha}$ .

$$(a)_{\mathsf{T}} = \alpha \left( \mathsf{I}/\mathsf{I}^{\mathsf{T}} \right) + (a)_{\mathsf{O}} \tag{10}$$

$$(K_{w})_{I} = \beta (I/I') + (K_{w})_{0}$$
 (11)

where subscripts I and O refer to an intensity of I and zero intensity respectively.  $\alpha$  and  $\beta$  are constants;  $\alpha$  is a function of the dispersed phase flow rate and nozzle diameter, while  $\beta$  is a function of the dispersed and continuous phase flow rates and is independent of the initial solute concentration. Both  $\alpha$  and  $\beta$  may be a function of the liquid properties and the column geometry. Values of  $\alpha$  and  $\beta$  obtained in this investigation are tabulated in Tables 3 and 4.

The fraction extracted and the effective diffusivity data are summarized in Table 5. The values of  $E_f$  obtained in this investigation are between 63 and 82% of the total extraction which are higher than that reported by others  $^{(7,8)}$ . These high values of  $E_f$  result from the small effective column height; when the column is short, a relatively large persentage of mass transfer will occur at the end.

TABLE 3

### VALUES OF $\alpha$

SYSTEM: Water-Acetic Acid-MIBK

CONTINUOUS PHASE: Water

DISPERSED PHASE: MIBK

EFFECTIVE COLUMN HEIGHT: 30.48 cm

COLUMN DIAMETER: 3.81 cm

F <sub>d</sub>	α <b>x</b> 1	0 <sup>3</sup>	
m1/sec	D <sub>N</sub> = 0.079 cm	$D_{N} = 0.163$ cm	D <sub>N</sub> = 0.316 cm
0.020	0.78	0.07	0.03
0.050	2.20	0.30	0.25
0.094	6.22	0.53	0.41

### TABLE 4

### VALUES OF B

SYSTEM: Water-Acetic Acid-MIBK

CONTINUOUS PHASE: MIBK

DISPERSED PHASE: Water

NOZZLE DIAMETER: 0.079 cm

EFFECTIVE COLUMN HEIGHT: 30.48 cm

COLUMN DIAMETER: 3.81 cm

F <sub>m</sub> /F <sub>w</sub>	2.158	1.147	0.462	
β x 10 <sup>4</sup>	1.67	1.07	0.50	

TABLE 5
FRACTION EXTRACTED DATA

SYSTEM: Water-Acetic Acid-MIBK

TRANSFER OF SOLUTE: From MIBK to Water

NOZZLE DIAMETER: 0.079 cm

TEMPERATURE: 24.5 - 25.5°C

PRESSURE: Atmosphere

(a) CONTINUOUS PHASE: Water

DISPERSED PHASE: MIBK

 $F_d = 0.094 \text{ ml/sec}$ 

 $C_{m2} = 5.91 \text{ wt.}\%$ 

 $F_c = 0.043 \text{ ml/sec}$ 

 $C_{w1} = 0$ 

Z cm	e sec	I/I'	E <sub>t</sub>	E <sub>s2</sub>	E <sub>f</sub>	$\sqrt{\text{R}}$ $(\text{cm}^2/\text{sec})^{1/2}$
30.48 34.29	3.5 3.9	0 0	0.324 0.329	0.144 0.154	0.207	$2:22 \times 10^{-3}$
30.48 34.29	3.5 3.9	5.82 5.82	0.454 0.461	0.208 0.222	0.307	$2.24 \times 10^{-3}$

(b) CONTINUOUS PHASE: MIBK

DISPERSED PHASE: Water

 $F_d = 0.043 \text{ m1/sec}$ 

 $c_{m2} = 5.91 \text{ wt.}\%$ 

 $F_c = 0.050 \text{ ml/sec}$ 

 $C_{w1} = 0$ 

Z cm	e sec	1/1'	Et	E <sub>s2</sub>	Ef	$\sqrt{R_0 \delta}$ $(cm^2/sec)^{1/2}$
30.48 34.29	3.5 3.9	0	0.353 0.359	0.135 0.144	0.252	2.66 x 10 <sup>-3</sup>
30.48 34.29	3.5 3.9	5.82 5.82	0.455 0.459	0.129 0.136	0.374	$2.51 \times 10^{-3}$

For the case where MIBK was dispersed, the increase of  $E_{\rm g2}$  caused by ultrasonic vibration was small, whereas the increase in the end effect,  $E_{\rm f}$ , was 48.31%. Similarly, when water was dispersed, the increase in the overall extraction rate due to ultrasonic vibration was also totally caused by the increase in  $E_{\rm f}$ . These experimental findings confirm the postulation presented in the first experimental part, namely, the imposition of ultrasonic vibration from the bottom of the column mainly affects the dispersing nozzle or the interface. The increase in  $E_{\rm f}$  was due to the increase of extraction rate during the droplet formation period when MIBK was dispersed. On the other hand, when water was dispersed, the increase in  $E_{\rm f}$  was due to the increase in the extraction rate at the interface. For the former case the dispersing nozzle was close to the ultrasonic source, while for the latter, the interface level was near the source.

In regard to the diffusivity during the drop rise or fall period, the change in the values of  $(R \mathcal{B})^{1/2}$  for I/I' = 0 to I/I' = 5.82 were + 0.90% and -5.97% respectively for both cases as seen from Table 5(a) and 5(b). These results indicate that the ultrasonic intensity in the middle of the column is not sufficient to cause any significant effect on the value of  $R \mathcal{B}$ .

The molecular diffusivisty for the system at  $30^{\circ}$ C is  $0.52 \times 10^{-5}$  cm<sup>2</sup>/sec<sup>(9)</sup>, and its square root should therefore be  $2.28 \times 10^{-3}$  cm/sec<sup>1/2</sup>.

Hence, values of (R.S)<sup>1/2</sup> obtained in this investigation are seem to agree quite well with the known value. Obviously, the multiplier R here is nearly unity. The use of such a multiplier R was proposed by Johnson and Hamielec<sup>(2)</sup> for droplets with internal circulation, because the circulation within the drop causes the effective diffusivity to be several times of the molecular diffusivity as reported by Calderbank and Korchinski<sup>(10)</sup>. It has been known <sup>(11,12)</sup> that the internal circulation occurs only when the drop is greater than a critical size. The critical drop size for the present system, as calculated by the equation given by Heertjes et al<sup>(12)</sup>, is about 0.46 cm. Since the droplet sizes encountered in this study were all smaller than 0.25 cm, the drops can be considered to be stagnant internally. And hence the fact R is unity, may thus be justified.

#### CONCLUSIONS

Based on the results obtained in this study, the following conclusions may be drawn:

(1) For the case where the dispersing nozzle is close to the ultrasonic source, the interfacial area of contact between the phases in the column increases with the intensity ratio, I/I'. This increase is due to the reduction in the average drop diameter. Nevertheless, the overall mass transfer coefficient for this case is not significantly affected by the ultrasonic waves propagating from the bottom of the column.

- (2) The very contrary is the case when the interface level in the column is located near the source. The overall mass transfer coefficient increases with the intensity ratio due to the increase in the degree of turbulence at the interface, but the interfacial area of contact decreases slightly with the intensity ratio. The decrease in the interfacial area is due to a reduction in the rest time of drops at the interface and the consequent decrease in the dispersed phase holdup.
- (3) Correlations for estimating the interfacial area of contact as well as the overall mass transfer coefficient in the column for the above two cases may be presented in the following forms

$$(a)_T = \alpha(I/I') + (a)_0$$

$$(K_{\mathbf{w}})_{\mathbf{I}} = \beta(\mathbf{I}/\mathbf{I}') + (K_{\mathbf{w}})_{\mathbf{o}}$$

where  $I < I_c$ .

(4) For the experimental configurations and conditions employed in this study, the ultrasonic intenstiy in the middle of the column is not sufficient to cause any significant change in either the extraction rate or the effective diffusivity during the drops rise or fall period. The ultrasonic vibration affects only the dispersing nozzle or the aqueous-organic interface section depending on their proximity to the source.

#### **NOMENCLATURE**

#### Roman Symbols

- a interfacial area of contact, cm<sup>2</sup>/unit volume
- A total transfer area, cm<sup>2</sup>
- C solute concentration, wt.%
- D average drop diameter, cm
- $\mathbf{D}_{_{\mathbf{N}}}$  nozzle diameter, cm
- 🔊 molecular diffusivity, cm<sup>2</sup>/sec
- E<sub>f</sub> fraction extracted during drop formation and coalescence at the interface periods, dimensionless
- E overall fraction extracted, dimensionless
- E fraction extracted during drop rise or fall period, dimensionless
- F flow rate, ml/sec
- H, total holdup, cm<sup>3</sup>
- I ultrasonic intensity measured by the thermocouple probe, mv
- I' threshold intensity measured by the thermocouple probe, mv
- I critical intensity measured by the thermocouple probe, mv
- K overall mass transfer coefficient, cm/sec
- $N_{\mathrm{D}}$  total number of drops in the column, dimensionless
- R multiplier of the molecular diffusivity, dimensionless
- S average drop surface area, cm<sup>2</sup>
- t residence time of the drop in the column, sec
- V<sub>n</sub> average drop volume, cm<sup>3</sup>
- $V_{\rm p}$  effective column volume, cm<sup>3</sup>
- Z effective column height, cm

### Greek Symbols

- $\alpha$  constant, cm
- β constant, cm
- 6 contact time during drop rise or fall period, sec

#### Subscripts

- c continuous phase
- d dispersed phase
- I at an intensity I.
- m MIBK phase
- O at zero intensity
- w water phase
- feed or effluent at the top of the column
- 2 feed or effluent at the bottom of the column

#### REFERENCES

- 1. Licht, W., and J.B. Conway, Ind. Eng. Chem. 42 1151 (1950)
- 2. Johnson, A.I., and A.E. Hamielec, A.I.Ch.E. Journal 6 145 (1960)
- 3. Hu, S., and R.C. Kintner, A.I.Ch.E. Journal 1 42 (1955)
- 4. Licht, W., and G.S.R. Narasimhamurty, A.I.Ch.E. Journal 1 366 (1955)
- 5. Klee, A.E., and R.E. Treybal, A.I.Ch.E. Journal 2 444 (1956)
- 6. Jeffreys, G.V., and J.L. Hawksley, A.I.Ch.E. Journal 11 413 (1965)
- 7. Sherwood, T.K., Evans, J.E., and J.V.A. Longcor, Ind. Eng. Chem. 31 1144 (1939)
- 8. Treybal, R.E., "Mass Transfer Operation", p. 435, McGraw-Hill, New York (1955)
- 9. Smoot, L.D., and A.L. Babb, Ind. Eng. Chem. Fundamentals 1 (2) 93 (1962)
- 10. Calderbank, P.H., and I.J.O. Korchinski, Chem. Eng. Sci. 6 65 (1956)
- 11. Hughes, R.R., and E.R. Gilliland, Chem. Eng. Progr. 48 497 (1952)
- 12. Heertjes, P.M., Holvi, W.A., and H. Talsma, Chem. Eng. Sci. 3
  122 (1954).

# APPENDIX A

RESULTS OF THE PRELIMINARY INVESTIGATION

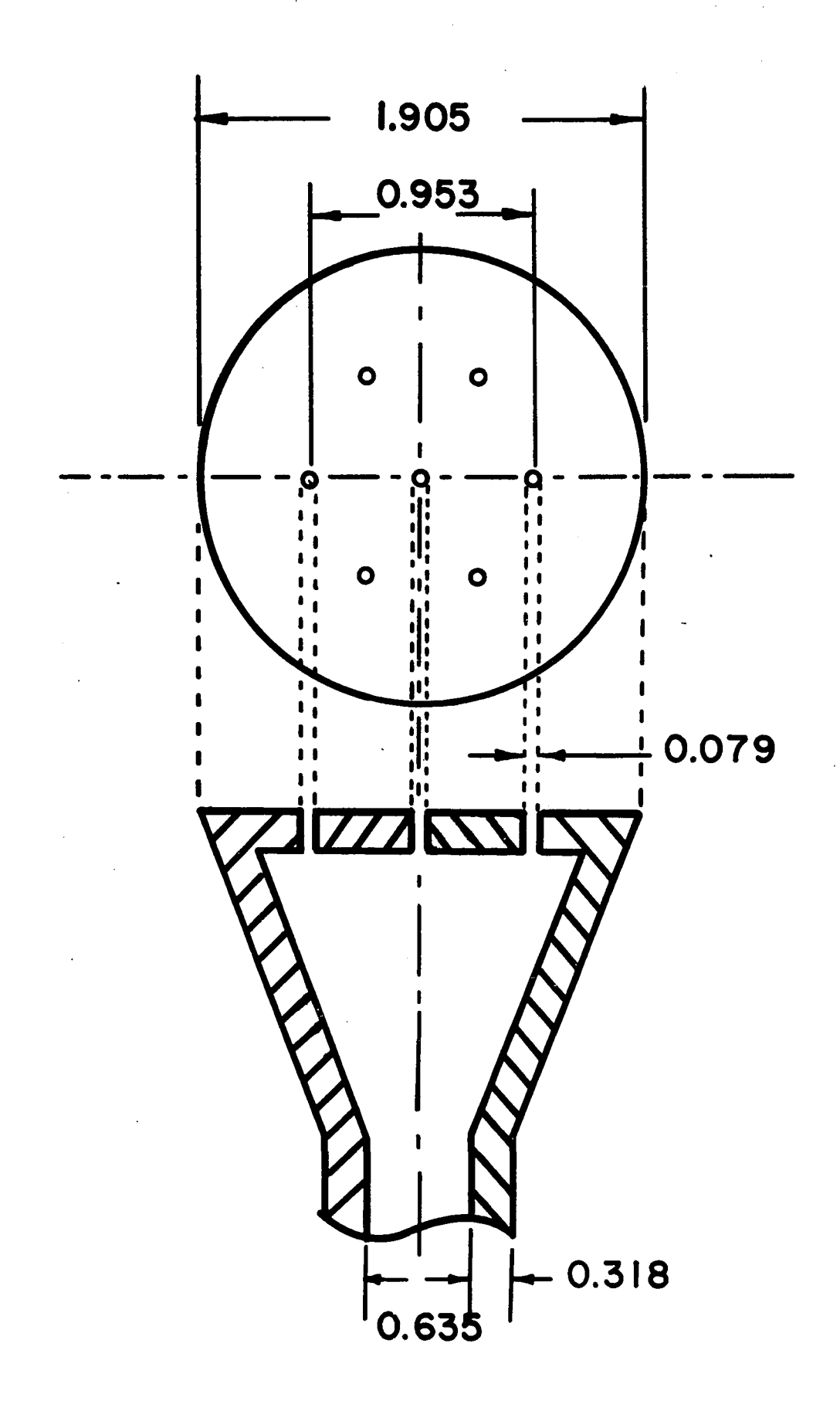
The purpose of this preliminary investigation was to test whether ultrasonic vibration would improve the performance of a liquid-liquid extraction column.

The apparatus, methods of measurement and calculation, and procedure are same as described in Experimental Section Part I except that the dispersing distributor was different and the column was of 7.62 cm I.D. and 60.96 cm long. Details of the distributor dimensions are shown in Figure A-1.

The results obtained are summarized in Table A-1, and are shown in Figures A-2 and A-3. The measuring point for I, the relative ultrasonic intensity in the liquids, was 3.17 cm from the wall, and 12.70 cm from the bottom which was the interface level of the aqueous and organic phases during the operation. The radial intensity profiles at this interface level are shown in Figures A-4 and A-5.

It is seen from Figure A-2 that there is an increase in  $K_W$  a values when the column liquids were subjected to ultrasonic vibration, and that higher ultrasonic intensity gives a further increase in the  $K_W$  a values. In Figure A-3, although the electric power input for Curve 1 is greater than that for Curve 2, the intensity for Curve 1 at the measuring point, i.e., near the center of the column at which most of the mass transfer takes place, is less than that for Curve 2. The fact that the increase in  $K_W$  a for Curve 1 is less than that for Curve 2 could thus be justified. The comparison of two curves in Figure A-3 also indicated the

DETAILS, OF THE CERAMIC DISTRIBUTOR



ALL DIMENSIONS ARE IN cm

TABLE A-1

### EXPERIMENTAL RESULTS (PRELIMINARY INVESTIGATION)

SYSTEM: Water - Acetic Acid - MIBK

TRANSFER OF SOLUTE: From MIBK to Water

CONTINUOUS PHASE: MIBK

DISPERSED PHASE: Water

LOCATION OF INTERFACE LEVEL: 12.70 from the Bottom

LOCATION OF DISPERSING NOZZLE: 53.34 cm from the Bottom

EFFECTIVE COLUMN HEIGHT: 40.64 cm

AQUEOUS FLOW RATE: 0.85 ml/sec

ORGANIC FLOW RATE: 0.75 ml/sec

CONCENTRATION OF AQUEOUS FEED: Zero

TEMPERATURE: 27 - 28°C

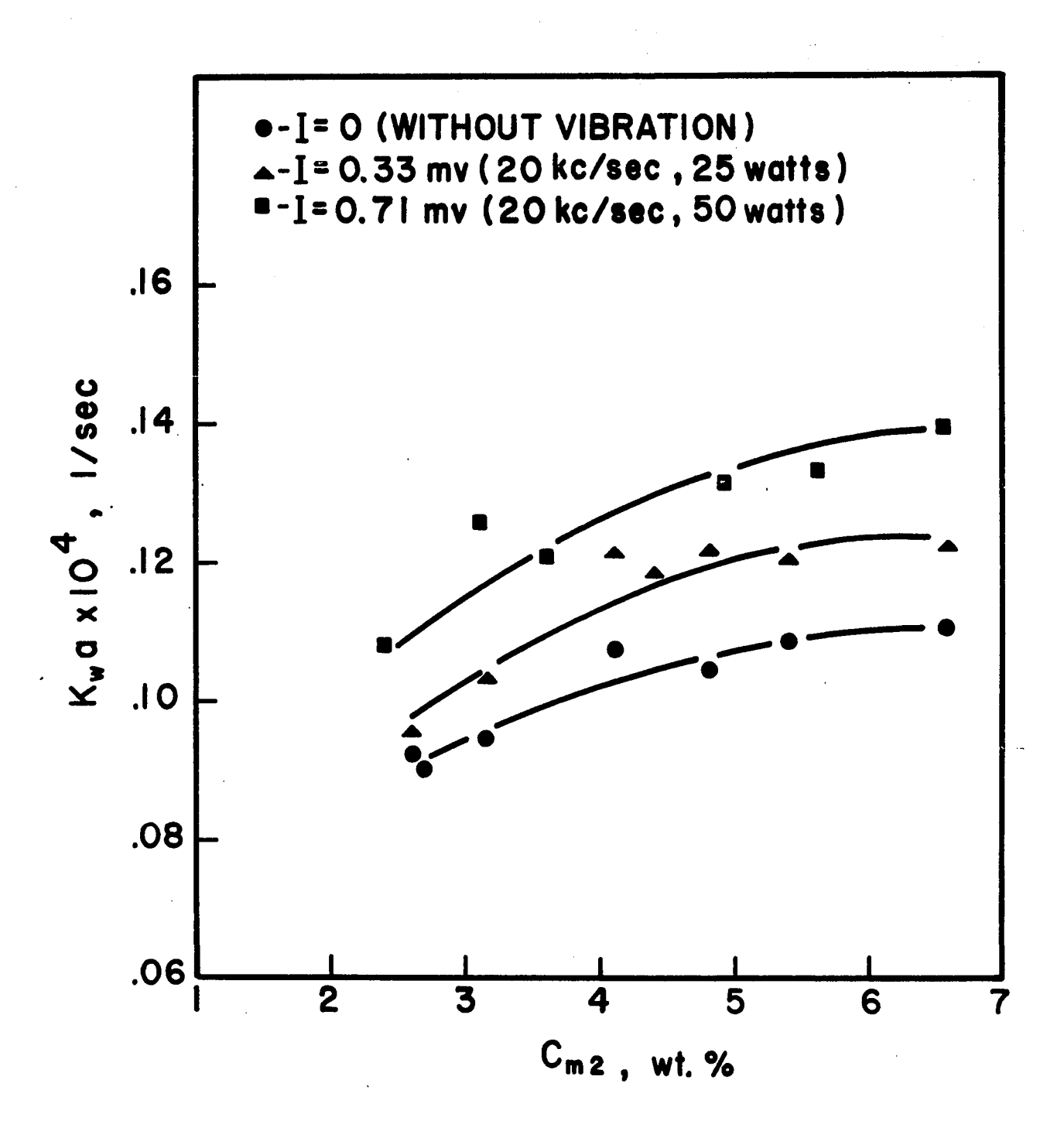
PRESSURE: Atmoshpere

f kc/sec	I mv	C <sub>w2</sub> wt.%	C <sub>m1</sub> wt.%	C <sub>m2</sub>	K <sub>w</sub> a x 10 <sup>4</sup> 1/sec	
	0	1.62	4.63	6.57	1.104	
0	0	1.34	3.82	5.42	1.088	
0	_		3.39	4.79	1.045	
<b>0</b> ·	0	1.15				
0	0	1.04	2.98	4.10	1.080	
0	0	0.75	2.40	3.16	0.947	
Ō	0	0.63	2.06	2.73	0.907	
Ö	0	0.62	1.95	2.61	0.929	
20	0.33	1.75	4.49	6.57	1.225	
20	0.33	1.45	3.69	5.42	1.213	
20	0.33	1.30	3.22	4.79	1.222	
			3.01	4.41	1.195	
20	0.33	1.19	2.01	→ • ~ T	1.173	

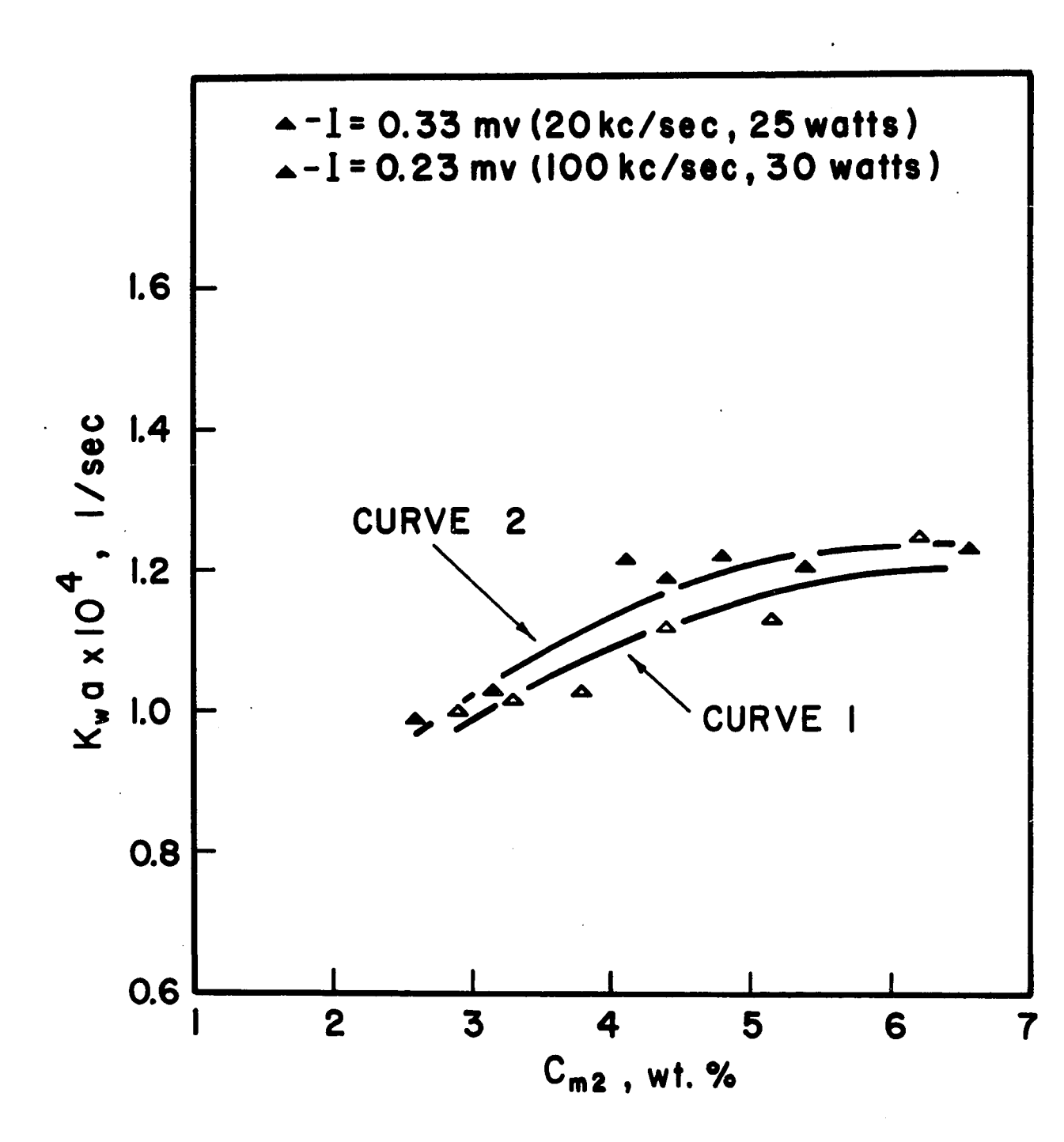
continued...

f kc/sec	I mv	C <sub>w2</sub> wt.%	C <sub>m1</sub>	C <sub>m2</sub> wt.%	K <sub>w</sub> a x 10 <sup>4</sup> 1/sec
20	0.33	0.79	2.21	3.16	1.034
20	0.33	0.63	1.93	2.61	0.954
20	0.71	1.92	4.23	6.54	1.395
20	0.71	1.60	3.71	5.62	1.316
20	0.71	1.40	3.26	4.93	1.304
20	0.71	1.02	2.52	3.62	1.213
20	0.71	0.90	2.01	3.08	1.265
20	0.71	0.65	1.69	2.40	1.088
100	0.23	1.67	4.11	6.18	1.246
100	0.23	1.30	3.49	5.14	1.136
100	0.23	1.14	3.14	4.39	1.121
100	0.23	0.94	2.79	3.78	1.033
100	0.23	0.83	2.47	3.33	1.026
100	0.23	0.72	2.14	2.89	1.006

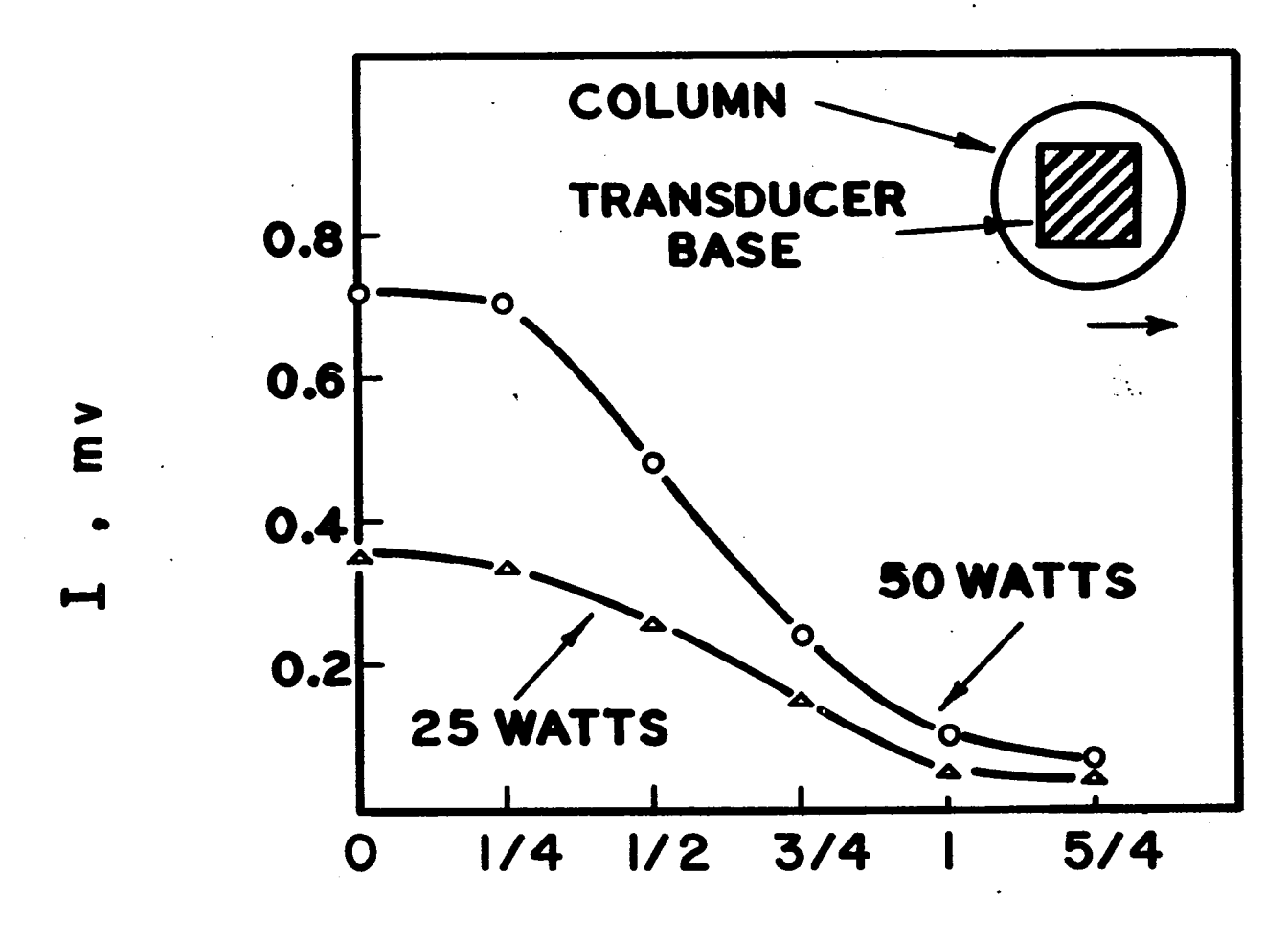
EFFECT OF ULTRASONIC INTENSITY ON  $\mathbf{K}_{\mathbf{W}}\mathbf{a}$ 



EFFECT OF ULTRASONIC FREQUENCY ON  $\mathbf{K}_{\mathbf{W}}\mathbf{a}$ 

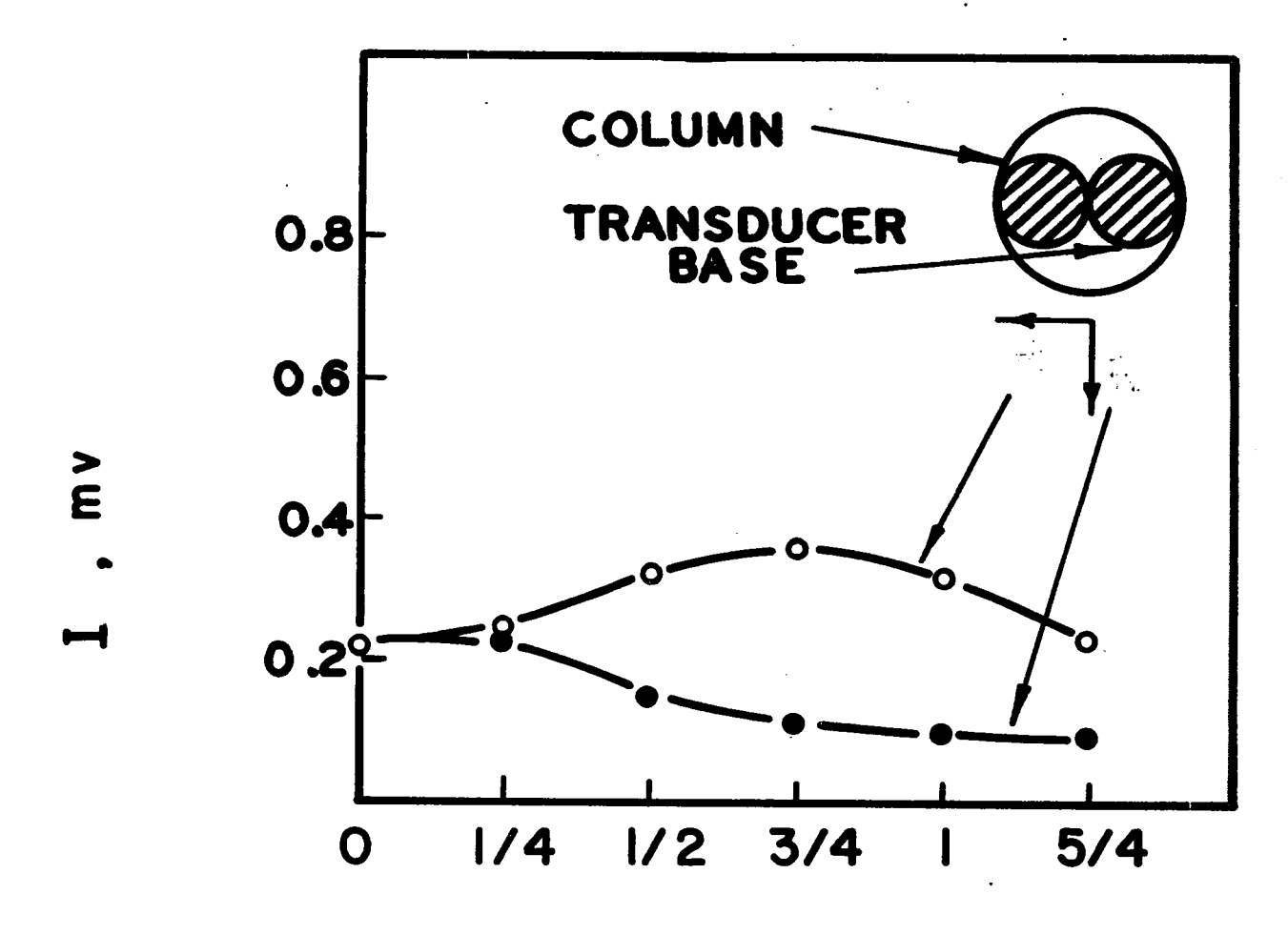


RADIAL INTENSITY PROFILES FOR THE 20 kc TRANSDUCER



DISTANCE FROM THE CENTER X 2.54, cm

RADIAL INTENSITY PROFILES FOR THE 100 kc TRANSDUCER



DISTANCE FROM THE CENTER X 2.54, cm

possibility that frequencies of the vibration may not be an influential factor after all.

From Figures A-4 and A-5, it is observed that the ultrasonic intensity is a maximum along the center axis of the transducer and a minimum along the column wall. In order to have a more uniform radial intensity distribution, the ratio of the cross-sectional area of the column to the area of the transducer base should be as small as possible. Moreover, it would be desirable to locate the center of the transducer along the axis of the column, since most of the mass transfer usually takes place near the center of the column.

APPENDIX B

TRANSDUCERS USED JN THIS WORK

In this work, ultrasonic vibrations were produced by the magnetostrictive and piezoelectric transducers which were made of Ferroxcube 7A2 and barium titanate respectively.

A magnetostrictive material can be used to convert magnetic oscillations into mechanical vibrations due to its ability to change in physical dimensions when subjected to a magnetic field. The actual changes in dimensions produced by this effect are very small, the relative deformation  $d\ell/\ell$  being of the order  $10^{-4}$  to  $10^{-6}$ . Here  $d\ell$  is the change length experienced by a rod of length  $\ell$ .

The magnetostrictive effect is temperature dependent, and as the temperature is increased the material experiences a reduction in its magnetostrictive properties. When the temperature reaches the Curie point of the material, then the material looses its magnetostrictive properties completely. Table B-1 lists some of the important constants for Ferroxcube 7A2.

A material is said to be piezoelectric if it changes in size when electric force is applied to it, the sign of the change being reversed on reversal of the direction of the electric force. The piezoelectric effect is also a function of the temperature. It decreases with rise of temperature, and disappears at the Curie point. The important constants for barium titanate are given in Table B-2.

To produce ultrasonic vibration by use of the magnetostrictive or piezoelectric transducer, the external magnetic field or the oscillatory

current is set to vary at an ultrasonic frequency, thereby causing mechanical vibration to be produced at the same frequency. If the frequency of the oscillatory current or the magnetic field variation is set at the natural frequency of the material being used so that it is at mechanical resonance, then, the pressure amplitude of the vibration becomes quite large. For this reason, the transducers are always operated at resonance. The resonant frequency of the transducer can be approximately calculated by using the formula

$$f_r = v/2\ell$$

where v is the velocity of sound in the material, and  $\ell$  is the length or thickness of the transducer.

TABLE B-1 IMPORTANT CONSTANTS FOR FERROXCUBE 7A2

Composition	Curie Temp.	Sound Velocity	Modulus of Elasticity
Ni-Cu-Co- Ferrous Ferrite	530 <sup>o</sup> C	5700 m/sec	1.5 - 2.5 × 10 <sup>-7</sup> n/m <sup>2</sup>

TABLE B-2 IMPORTANT CONSTANTS FOR BARIUM TITANATE

Density	Curie Temp.	Sound Velocity	Modulus of Elasticity
5.4 x 10 <sup>-3</sup> kg/m <sup>3</sup>	120 <sup>o</sup> c	4460 m/sec	1 10.8 x 10 <sup>-10</sup> n/m <sup>2</sup>

APPENDIX C

ROTAMETER CALIBRATION CURVES

#### FIGURE C-1

ROTAMETER CALIBRATION CURVE FOR DISTILLED WATER AT 25°C

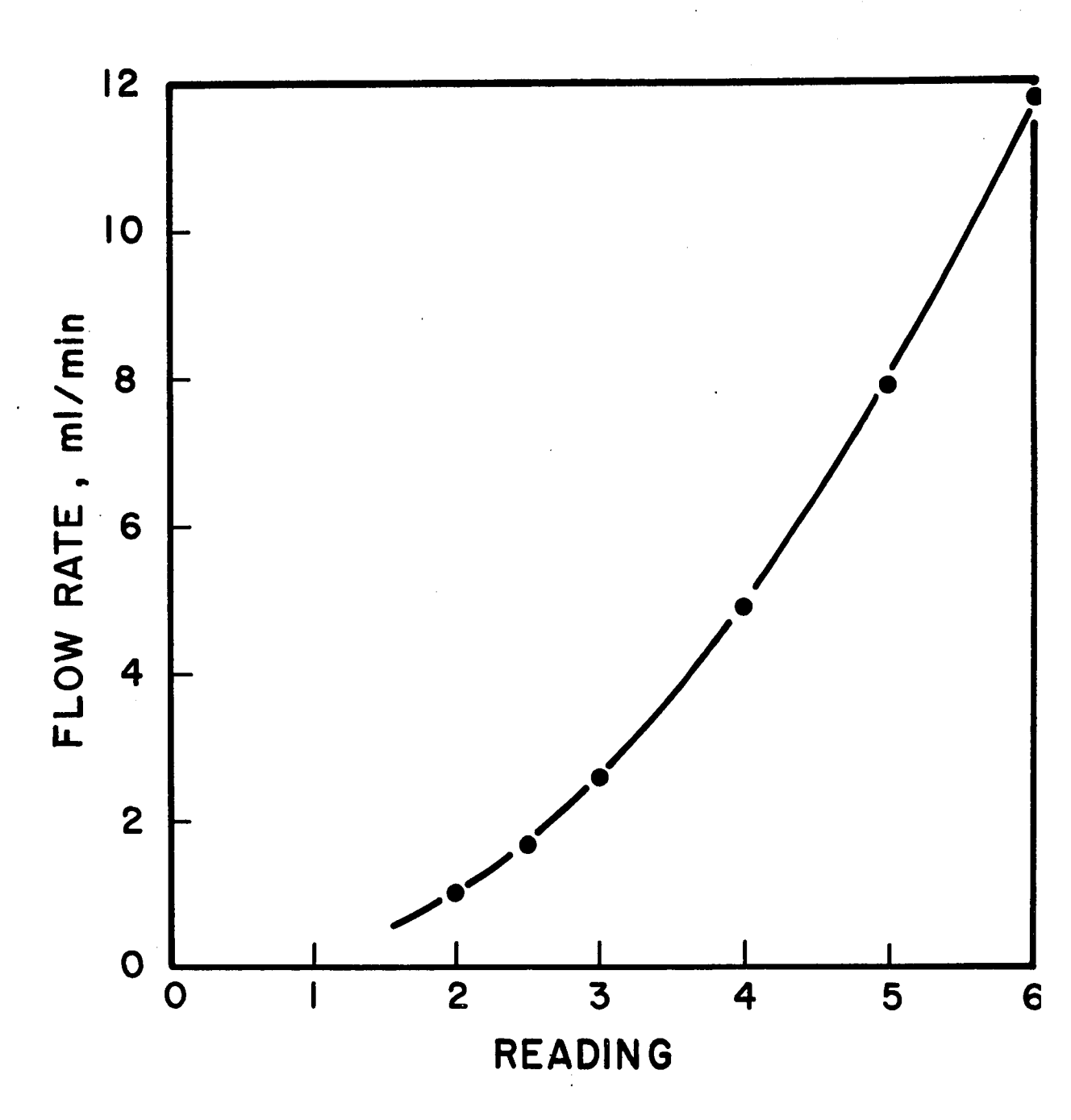
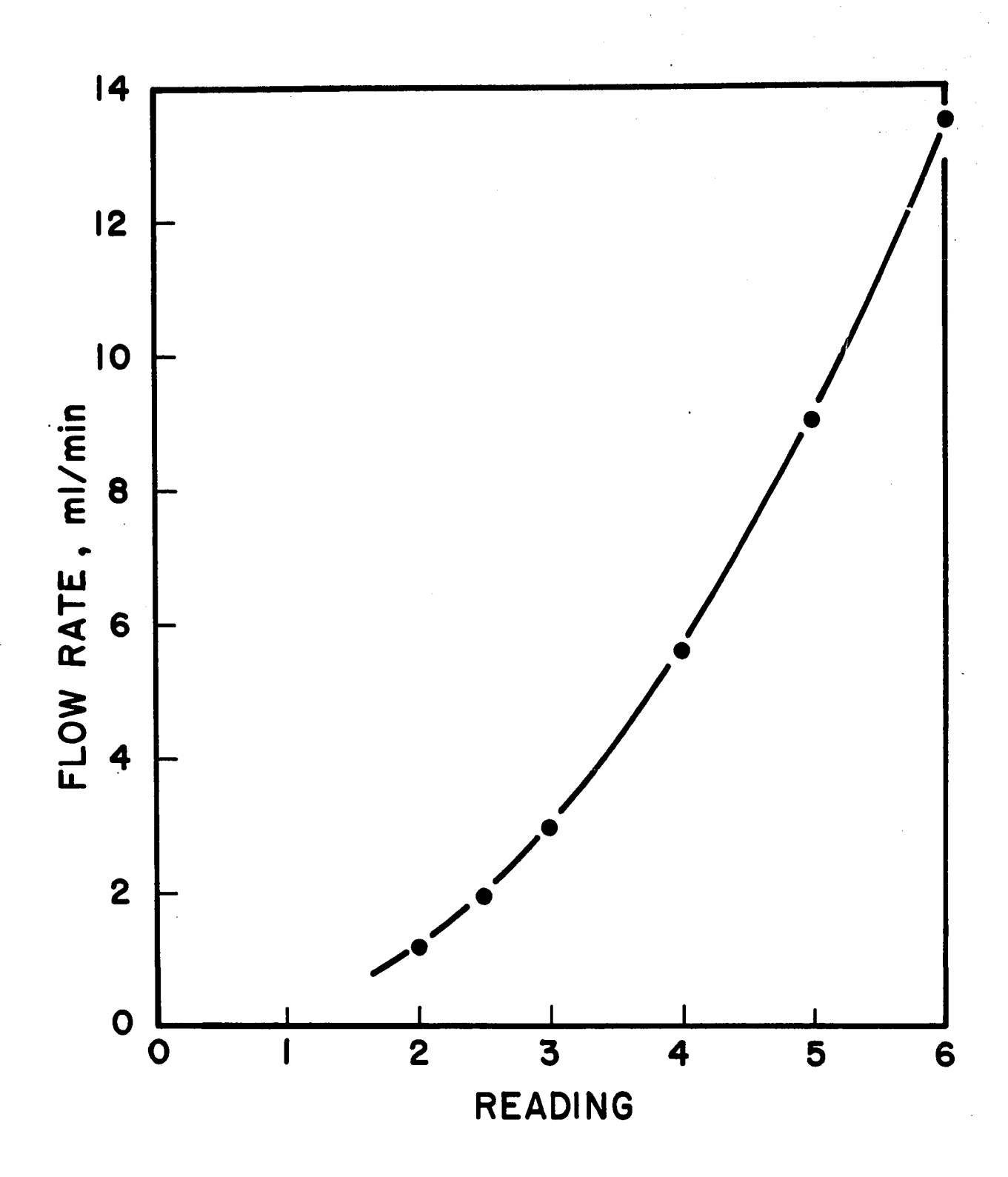


# FIGURE C-2

ROTAMETER CALIBRATION CURVE FOR 10% ACETIC ACID-MIBK SOLUTION AT 25°C



### APPENDIX D

PHYSICAL PROPERTIES OF THE SYSTEM:

WATER-ACETIC ACID-METHYL ISOBUTYL KETONE

## FIGURE D-1

EQUILIBRIUM CURVE FOR WATER-ACETIC ACID-MIBK SYSTEM AT 25°C

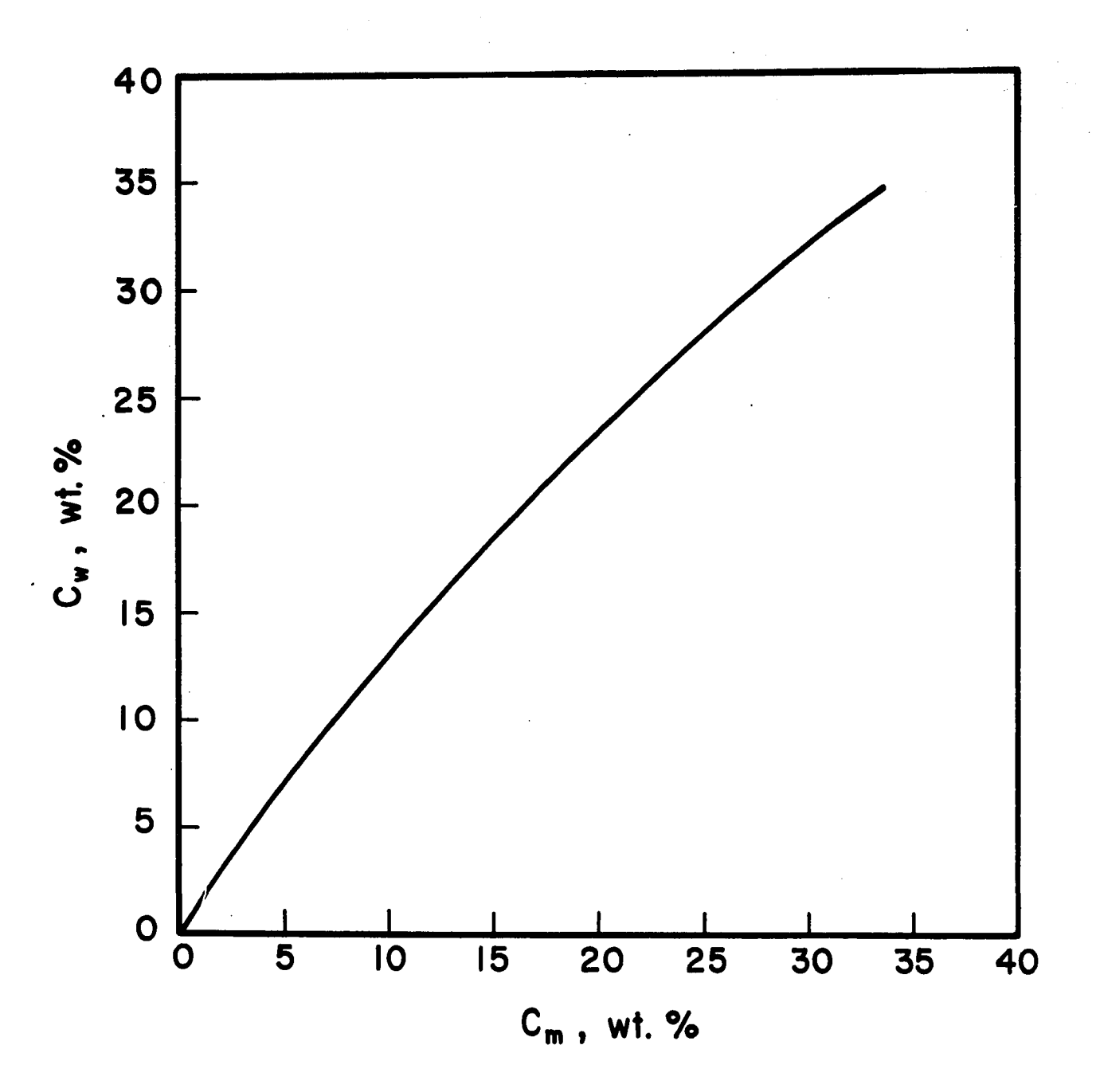


## FIGURE D-2

DENSITY OF ACETIC ACID-MIBK SOLUTION AT 25°C

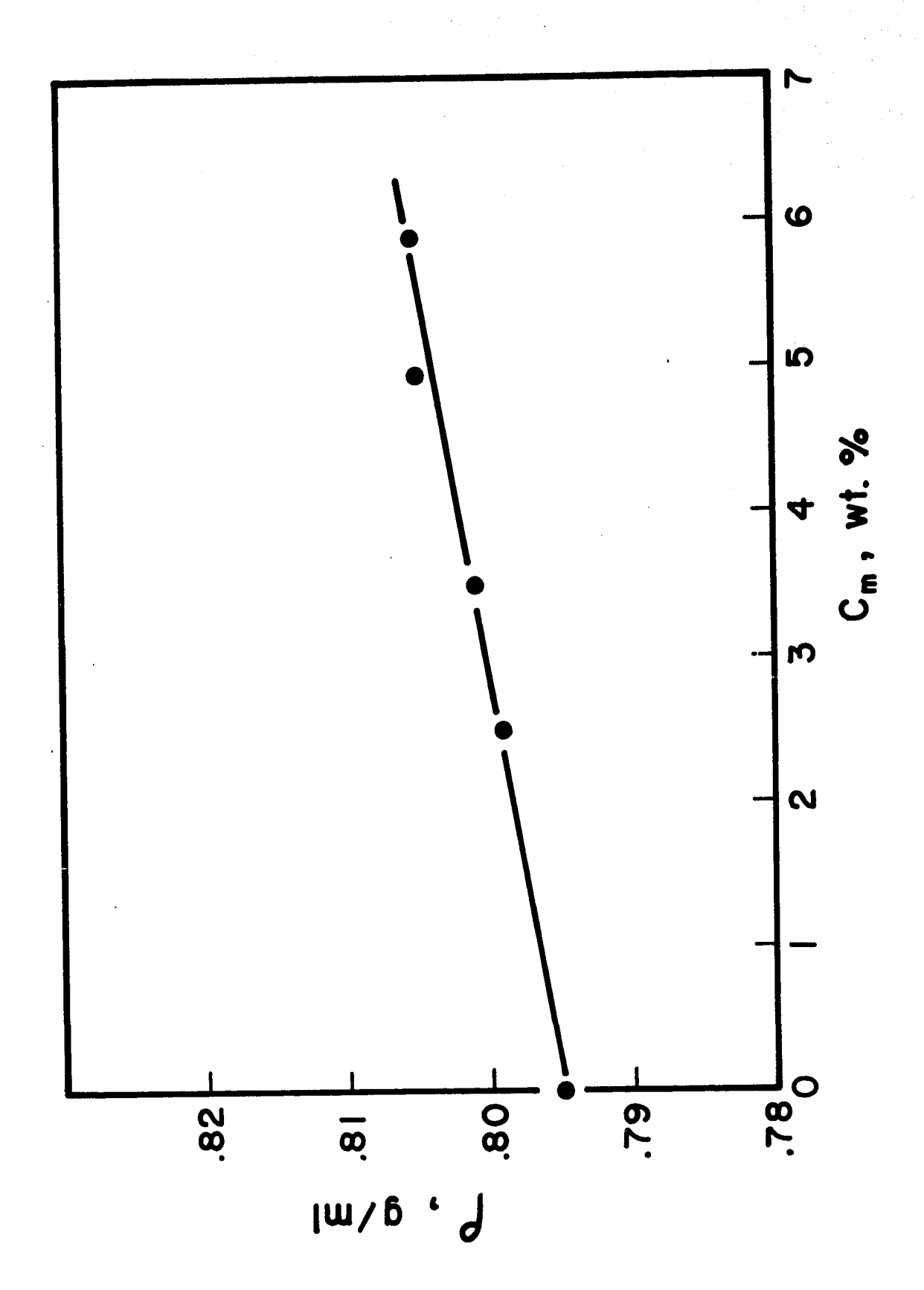


## FIGURE D-3

.VISCOSITY OF ACETIC ACID-MIBK SOLUTION AT 25°C

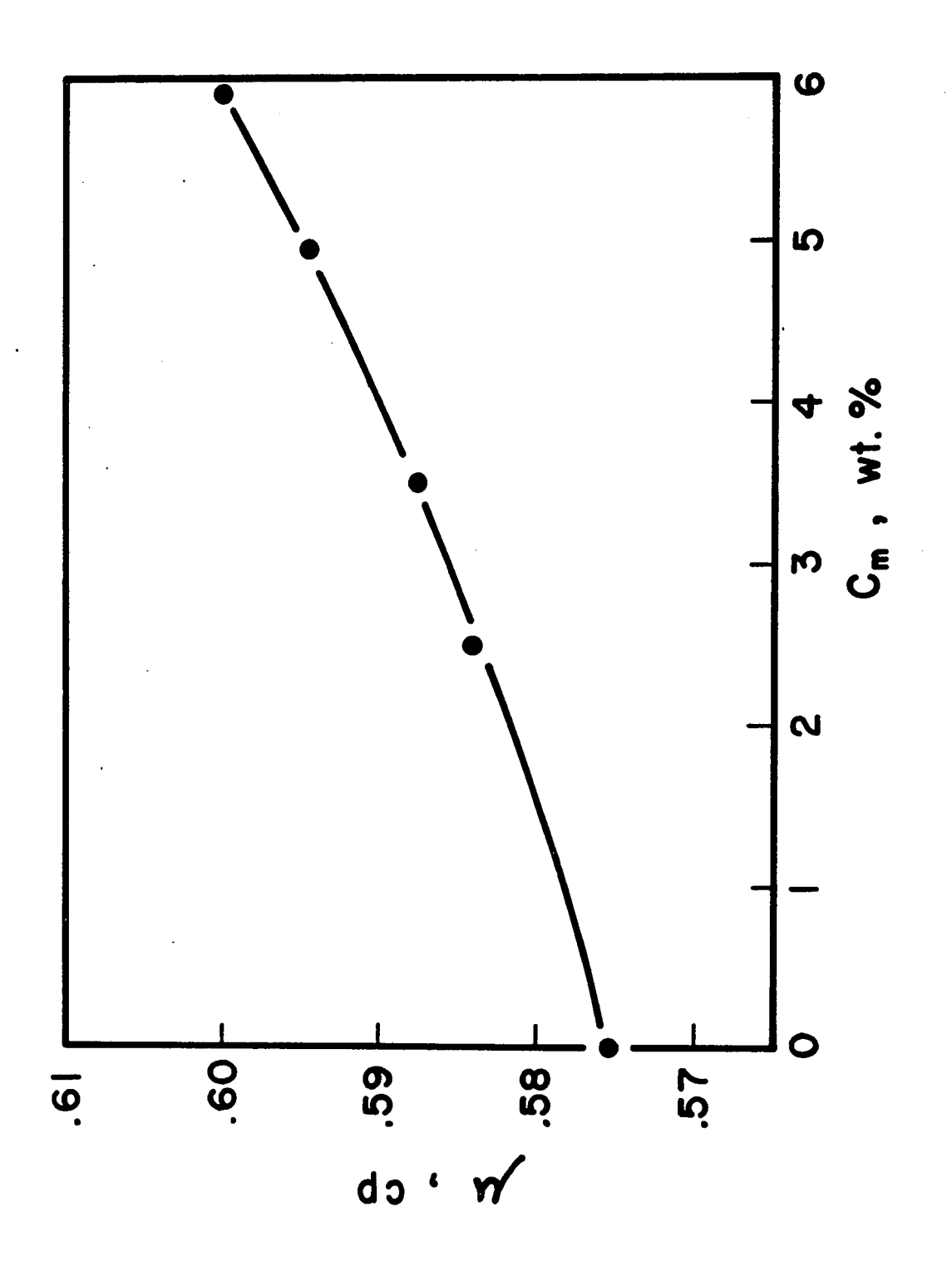
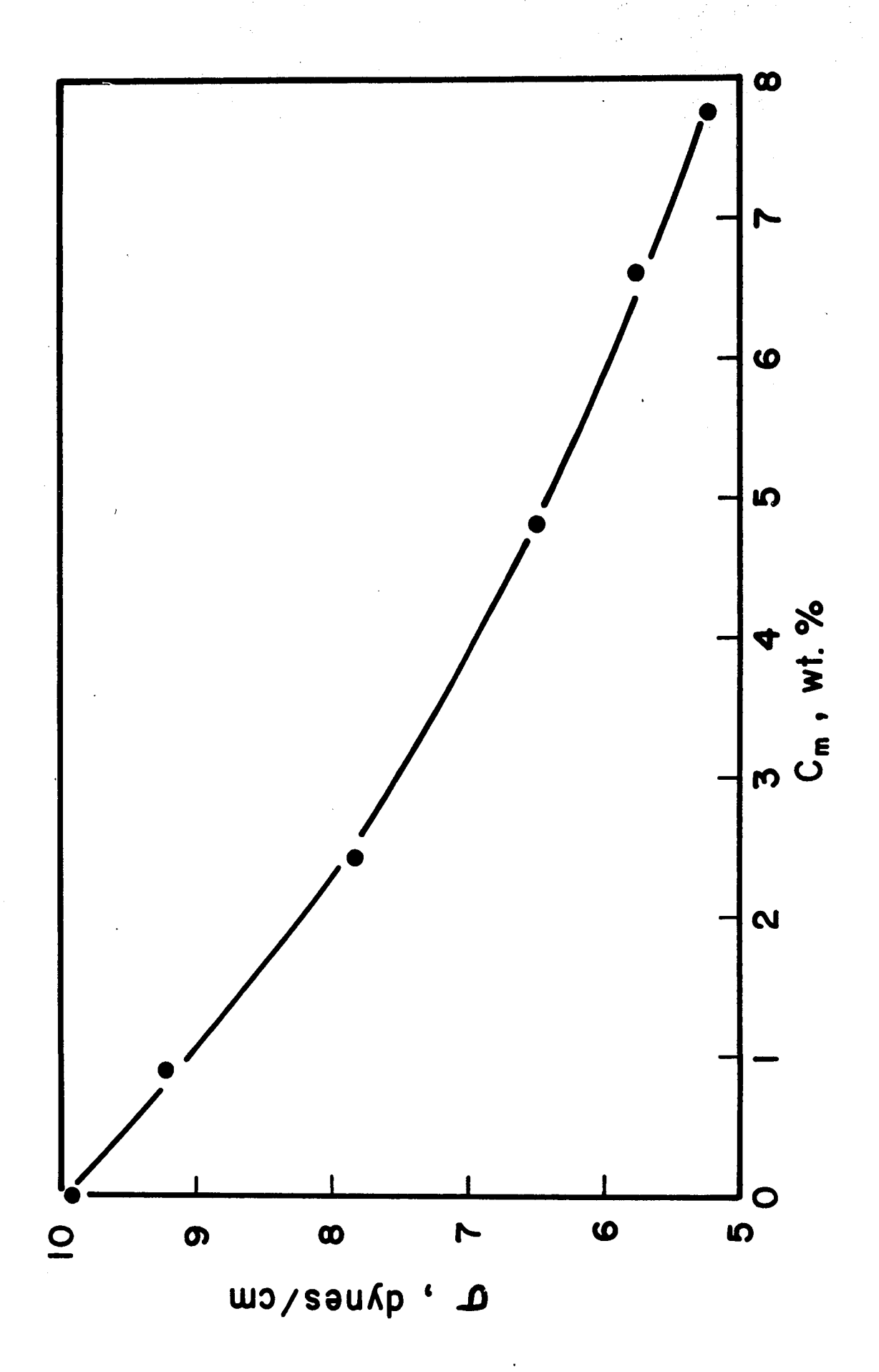


# FIGURE D-4

Interfacial tension of water-acetic acid-mibk system at  $25^{\circ}\mathrm{c}$ 



# APPENDIX E

EXPERIMENTAL AND CALCULATED DATA

TABLE E-1

#### CAPACITY COEFFICIENT DATA

SYSTEM: Water-Acetic Acid-MIBK

TRANSFER OF SOLUTE: From MIBK to Water

EFFECTIVE COLUMN HEIGHT: 30.48 cm

COLUMN DIAMETER: 3.81 cm

CONCENTRATION OF AQUEOUS FEED: Zero

TEMPERATURE: 24.5 - 25.5°C

PRESSURE: Atmosphere

(a) CONTINUOUS PHASE: Water

DISPERSED PHASE: MIBK

LOCATION OF DISPERSING NOZZLE: 7.62 cm from the Bottom

LOCATION OF INTERFACE LEVEL: 38.10 cm from the Bottom

AQUEOUS FLOW RATE: 0.043 ml/sec

ORGANIC FLOW RATE: 0.020 ml/sec

NOZZLE DIAMTER: 0.079 cm

f kc/sec	I mv	C w2 wt,%	Cml wt. %	C <sub>m2</sub> wt. %	K <sub>w</sub> a x 10 <sup>4</sup> 1/sec
0	0	1.40	2.83	5.91	0.336
100	0.17	1.50	2.76	5.91	0.366
40	0.36	1.59	2.47	5.91	0.410
20	0.64	1.71	2.36	5.91	0.454
0 .	0	1.11	2.40	4.73	0.318
100	0.17	1.17	2.23	4.73	0.345
40	0.36	1.25	2.14	4.73	0.379
20	0.64	1.34	1.85	4.73	0.433
0	0	0.81	1.75	3.49	0.304

f	I	C <sub>w2</sub>	C <sub>m1</sub>	C <sub>m2</sub>	Ka x 104
kc/sec	mv	wt. %	wt. %	wt. %	w 1/sec
100	0.17	0.85	1.61	3.49	0.330
40	0.36	0.89	1.56	3.49	0.352
20	0.64	0.94	1.53	3.49	0.376
0	0	0.52	1.29	2.47	0.254
0	0	0.51	1.31	2.47	0.247
100	0.17	0.54	1.26	2.47	0.266
100	0.17	0.55	1.23	2.47	0.271
40	0.36	0.59	1.21	2.47	0.297
40	0.36	0.58	1.17	2.47	0.296
20	0.64	0.61	1.17	2.47	0.313

(b) CONTINUOUS PHASE: Water

DISPERSED PHASE: MIBK

LOCATION OF DISPERSING NOZZLE: 7.62 cm from the Bottom

LOCATION OF INTERFACE LEVEL: 38.10 cm from the Bottom

AQUEOUS FLOW RATE: 0.043 ml/sec

ORGANIC FLOW RATE: 0.050 ml/sec

NOZZLE DIAMETER: 0.079 cm .

f kc/sec	I mv	C w2 wt.%	C <sub>m1</sub>	c <sub>m2</sub>	K a x 10
		W L • /o	wt.%	wt.%	1/sec
0	0	1.97	4.37	5.91	0.412
100	0.17	2.06	4.15	5.91	0.443
40	0.36	2.19	3.96	5.91	0.487
20	0.64	2.43	3.76	5.91	0.563
0	0	1.54	3.30	4.73	0.402
100	0.17	1.66	3.24	4.73	0.443
40	0.36	1.76	3.22	4.73	0.476
20	0.64	1.91	3.14	4.73	0.504
0	0	1.12	2.54	3.49	0.375
100	0.17	1.21	2.52	3.49	0.410
40	0.36	1.29	2.45	3.49	0.449
20	0.64	1.42	2.32	3.49	0.517
0	0	0.74	1.88	2.47	0.321
100	0.17	0.79	1.82	2.47	0.353
40	0.36	0,87	1.76	2.47	0.398
20	0.64	0.94	1.69	2.47	0.444

(c) CONTINUOUS PHASE: Water

DISPERSED PHASE: MIBK

LOCATION OF DISPERSING NOZZLE: 7.62 cm from the Bottom

LOCATION OF INTERFACE LEVEL: 38.10 cm from the Bottom

AQUEOUS FLOW RATE: 0.043 ml/sec

ORGANIC FLOW RATE: 0.094 m1/sec

NOZZLE DIAMETER: 0.079 cm

f kc/sec	I mv	C w2 wt.%	C m1 wt.%	C <sub>m2</sub> wt.%	K <sub>w</sub> a x 10 <sup>4</sup> 1/sec
0	0	2.60	4.61	5.91	0.557
100	0.17	2.75	4.51	5.91	0.606
40	0.36	2.98	4.39	5.91	0.680
20	0.64	3.24	4.29	5.91	0.766
0	0	2.08	3.82	4.73	0.537
100	0.17	2.22	3.75	4.73	0.588
40	0.36	2.37	3.62	4.73	0.648
20	0.64	2.60	3.46	4.73	0.750
0 -	0	1.47	2.84	3.49	0.492
100	0.17	1.57	2.76	3.49	0.539
40	0.36	1.70	2.64	3.49	0.605
20	0.64	1.84	2.55	3.49	0.682
0	. 0	0.97	2.07	2.47	0.424
100	0.17	1.04	2.03	2.47	0.463
40	0.36	1.13	1.99	2.47	0.519
20	0.64	1.25	1.92	2.47	0.594

# TABLE E-1 (eant'd)

(d) CONTINUOUS PHASE: MIBK

DISPERSED PHASE: Water

LOCATION OF DISPERSING NOZZLE: 38.10 cm from the Bottom

LOCATION OF INTERFACE LEVEL: 7.62 cm from the Bottom

AQUEOUS FLOW RATE: 0.043 ml/sec

ORGANIC FLOW RATE: 0.02 ml/sec

NOZZLE DIMATER: 0.079 cm.

f kc/sec	I mv	C w2 wt:.%	C <sub>m1</sub> wt.%	C <sub>m2</sub> wt.%	K <sub>w</sub> a x 10 <sup>4</sup> 1/sec
		W. Ç. <sub>2</sub> ./6	W L • /o	W L . /o	1/860
0	0	0.95	3.72	5.91	0.196
100	0.17	1.00	3.75	5.91	0.206
40	.0.36	1.03	3.50	5.91	0.219
20	0.64	1.10	3.56	5.91	0.235
0	0	0.75	2.95	4.73	0.191
100	0.17	0.80	2.95	4.73	0.203
40	0.36	0.83	2.78	4.73	0.218
20	0.64	0.88	2.79	4.73	0.230
0	0	0.55	2.21	3.49	0.182
100	0.17	0.58	2.27	3.49	0.190
40	0.36	0.59	2.11	3.49	0.199
20	0.64	0.63	2.08	3.49	0.214
0	0	0.40	1.59	2.47	···· 0.175
100	0.17	0.42	1.65	2.47	0.183
40	0.36	0.43	1.53	2.47	0.195
20	0.64	0.46	1.53	2.47	0.210

(e) CONTINUOUS PHASE: MIBK

DISPERSED PHASE: Water

LOCATION OF DISPERSING NOZZLE: 38.10 cm from the Bottom

LOCATION OF INTERFACE LEVEL: 7.62 cm from the Bottom

AQUEOUS FLOW RATE: 0.043 ml/sec

ORGANIC FLOW RATE: 0.050 ml/sec

NOZZLE DIAMTER: 0.079 cm.

f kc/sec	I mv	C w2 wt.%	C ml wt.%	C m2 wt.%	Kax 10 W 1/sec
0	0	1.57	4.35	5.91	0.318
100	0.17	1.71	4.48	5.91	0.344
40	0.36	1.78	4.14	5.91	0.375
20	0.64	1.93	4.13	5.91	0.413
0	0	1.25	3.47	4.73	0.311
100	0.17	1.35	3.61	4.73	0.331
40	0.36	1.43	3.32	4.73	0.369
20	0.64	1.52	3.37	4.73	0.392
0	0	0.91	2.58	3.49	0.295
100	0.17	0.98	2.63	3.49	0.316
40	0.36	1.02	2.49	3.49	0.341
20	0.64	1.10	2.43	3.49	0.374
0	0	0.65	1.84	2.47	0.282
100	0.17	0.69	1.89	2.47	0.299
40	0.36	0.75	1.83	2.47	0.333
20	0.64	0.81	1.82	2.47	0.361

(f) CONTINUOUS PHASE: MIBK

DISPERSED PHASE: Water

LOCATION OF DISPERSING NOZZLE: 38.10 cm from the Bottom

LOCATION OF INTERFACE LEVEL: 7.62 cm from the Bottom

AQUEOUS FLOW RATE: 0.043 ml/sec

ORGANIC FLOW RATE: 0.094 m1/sec

NOZZLE DIMATER: 0.079 cm.

f kc/sec	I mv	Cw2 wt.%	Cm1 wt.%	C <sub>m2</sub> wt.%	K a x 10 <sup>4</sup>
0	0	2.27	4.65	5.91	0.471
100	0.17	2.42	4.74	5.91	0.504
40	0.36	2.60	4.61	5.91	0.559
20	0.64	2.84	4.51	5.91	0.629
0	0	1.81	3.73	4.73	0.461
100	0.17	1.95	3.88	4.73	0.493
40	0.36	2.04	3.62	4.73	0.539
20	0.64	2.27	3.72	4.73	0.608
0	0	1.30	2.84	3.49	0.424
100	0.17	1.36	2.81	3.49	0.451
40	0.36	1.46	2.77	3.49	0.494
20	0.64	1.61	2.69	3.49	0.565
0	. 0	0.83	2.05	2.47	0.353
100	0.17	0.88	2.11	2.47	0.376
40	0.36	0.97	1.99	2.47	0.428
20	0.64	1.07	2.03	2.47	Q.477

(g) CONTINUOUS PHASE: Water

DISPERSED PHASE: !MIBK

LOCATION OF DISPERSING NOZZLE: 7.62 cm from the Bottom

LOCATION OF INTERFACE LEVEL: 38.10 cm from the Bottom

AQUEOUS FLOW RATE: 0.043 ml/sec

$\mathbf{F}_{\mathbf{m}}$	$\mathbf{D_{N}}$	·I	f	Cw2	C <sub>m1</sub>	C <sub>m2</sub>	K <sub>w</sub> a x 10 <sup>4</sup>
m1/sec	cm	mv	kc/sec	wt.%	wt.%	wt.%	1/sec
0.000	0.014		_				
0.020	0.316	~ 0 ,	. O	0.74	1.79	3.49	0.272
0.020	0.316	0.36	40	0.77	1.71	3.49	0.290
0.020	0.163	0	0	0.80	1.68	3.49	0.302
0.020:	0.163	0.36	40	0.88	1.72	3.49	0.335
0.050	0.316	0	0	1.03	2.53	3.49	0.342
0.050	0.316	0.36	40	1.12	2.47	3.49	0.378
0.050	0.163	0	0	1.10	2.57	3.49	0.364
0.050	0.163	0.36	40	1.21	2.40	3.49	0.421
0.094	0.316	Ö	0	1.35	2.82	3.49	0.445
0.094	0.316	0.36	40	1.53	2.74	3.49	0.525
0.094	0.163	0	0	1.42	2.78	3.49	0.323
0.094	0.163	0.36	40	1.62			
0.077	.0. IOJ	0.30	40	1.02	2.69	3.49	0.569

(h) CONTINUOUS PHASE: MIBK

DISPERSED PHASE: Water

LOCATION OF DISPERSING NOZZLE: 38.10 cm from the Bottom

LOCATION OF INTERFACE LEVEL: 7.62 cm from the Bottom

AQUEOUS FLOW RATE: 0.043 m1/sec

F m m1/sec	D <sub>N</sub>	mv	f kc/sec	Cw2 wt.%	C <sub>m1</sub> wt.%	C <sub>m2</sub> wt.%	K <sub>w</sub> a x 10 <sup>4</sup>
0.020	0.316	0	0	0.55	2.18	3.49	0.182
0.020	0.316	0.36	40	0.58	2.14	3.49	0.194
0.020	0.163	0	0	0.56	2.18	3.49	0.187
0.020	0.163	0.36	40	0.59	2.11	3.49	0.200
0.050	0.316	0	0	0.91	2.66	3.49	0.289
0.050	0.316	0.36	40	1.00	2.58	3.49	0.325
0.050	0.163	0	. 0	0.90	2.66	3.49	0.286
0.050	0.163	0.36	40	1.01	2.56	3.49	0.331
0.094	0.316	0	0	1.30	2.84	3.49	0.423
0.094	0.316	0.36	40	1.47	2.76	3.49	0.498
0.094	0.163	0	<b>0</b> ° .	1.30	2.85	3.49	0.425
0.094	0.163	0.36	40	1.46	2.78	3.49	0.492

TABLE E-2

# AXIAL INTENSITY PROFILE DATA

TEMPERATURE: 24.5 - 25.5°C

PRESSURE: Atmosphere

f = 20 kc/sec W*= 42 watts		· ·	f = 40  kc/sec W = 30 watts		f = 100 kc/sec W = 23 Watts	
L x 2.54	I	L x 2.54 cm	I mv	L x 2.54	I mv	
0	1.30	. 0	1.01	0	0.38	
1	1.01	1	0.65	. 1	0.26	
2	0.80	2	0.45	2	0.20	
3	0.64	3	0.36	3	0.17	
4	0.56	. 4	0.34	4	0.19	
5	0.46	5	0.35	- 5	0.13	
6	0.42	6	0.45	6	0.15	
6 7	0.40	7	0.30	7	0.13	
8	0.58	8	0.41	8	0.14	
9	0.38	9	0.31	9	0.1	
10	0.55	10	0.46	10	0.0	
11	0.43	11	0.34	11	0.00	
12	0.57	12	0.23	12	0.0	
13	0.34	13	0.12	13	0.0	
14	0.11	14	0.05	14	0	
15	0.03	15	0.01	15	0	

<sup>\*</sup> W: Power input to the transducer

TABLE E-3

# MASS TRANSFER CORRELATION DATA

(a) CONTINUOUS PHASE: Water

DISPERSED PHASE: MIBK

EFFECTIVE COLUMN HEIGHT: 30.48 cm

COLUMN DIAMETER: 3.81 cm

TRANSFER OF SOLUTE: From MIBK to Water

v <sub>m</sub> /v <sub>w</sub>	$v_{\rm m}/v_{\rm w}$ $c_{\rm i} \rho_{\rm i}/\rho_{\rm w}$ I/I'		$\mu_{\mathbf{w}}^{\prime}/\rho_{\mathbf{w}}^{\mathbf{v}_{\mathbf{w}}^{\mathbf{D}}}$ N	(% Iner.K <sub>w</sub> a) <sub>Exp</sub>	ptl. (% Incr.K a) Cal.	
0.462 0.462 0.462 0.462 0.462 0.462 0.462 0.462 0.462 0.462 1.147	0.0476 0.0476 0.0476 0.0381 0.0381 0.0279 0.0279 0.0279 0.0197 0.0197 0.0197 0.0197	1.13 3.60 5.82 1.13 3.60 5.82 1.13 3.60 5.82 1.13 3.60 5.82 1.13	30.00 30.00 30.00 30.00 30.00 30.00 30.00 30.00 30.00 30.00 30.00	8.97 22.22 35.18 8.57 19.21 36.44 8.42 15.88 23.61 7.15 18.33 25.08 7.53 18.27	6.67 19.84 31.21 6.42 19.11 30.07 6.10 18.15 28.55 5.75 17.12 26.93 7.72	
1.147 1.147	0.0476 0.0381	5.82 1.13	30.00 30.00	36.91 10.00	22.98 36.15 7.44 continued	

TABLE E-3 (cont'd)

v <sub>m</sub> /v <sub>w</sub>	$c_i^{\rho_i/\rho_w}$	1/1'	$\mu_{\mathbf{w}}^{\prime}/ ho_{\mathbf{w}}^{\mathbf{v}_{\mathbf{w}}^{\mathbf{D}}}\mathbf{N}$	(% Incr.Kwa)Expl	l. (% Incr.K <sub>w</sub> a)*
1.147	0.0381	3.60	30.00	18.47	22.14
1.147	0.0381	5.82	30.00	25.41	34.83
1.147	0.0279	1.13	30.00	9.19	7.06
1.147	0.0279	3.60	30.00	19.61	21.03
1.147	0.0279	5.82	30.00	`37 <b>.</b> 59	33.07
1.147	0.0197	1.13	30.00	9.88	6.66
1.147	0.0197	3.60	30.00	24.02	19.83
1.147	0.0197	5.82	30.00	38.41	31.20
2.158	0.0476	1.13	30.00	8.70	8.55
2.158	0.0476	3.60	30.00	21.94	25.46
2.158	0.0476	5.82	30.00	37.39	40.04
2.158	0.0381	1.13	30.00	9.65	8.24
2.158	2.0381	3.60	30.00	20.76	24.53
2.158	0.0381	5.82	30.00	39.68	38.58
2.158	0.0279	1.13	30.00	9.51	7.82
2.158	0.0279	3.60	30.00	22.94	23.28
2.158	0.0279	5.82	30.00	38.65	36.63
2.158	0.0197	1.13	30.00	9.03	7.38
2.158	0.0197	3.60	30.00	22.40	21.97
2.158	0.0197	5.82	30.00	40.03	34.56
2.158	0.0279	3.60	^7.50	17.92	16.87
2.158	0.0279	3.60	14.52	19.71	19.67

TABLE E-3 (cont'd)

/v <sub>w</sub>	c <sub>i</sub> p <sub>i</sub> /p <sub>w</sub>	I/I'	$\mu_{\mathbf{w}}^{\prime}/\mathbf{\rho}_{\mathbf{w}}^{\mathbf{v}}\mathbf{v}_{\mathbf{w}}^{\mathbf{D}}\mathbf{v}_{\mathbf{N}}$	(% Iner.K <sub>w</sub> a) <sub>Exptl</sub> .	(% Iner.Kwa) Cal.
1.147	0.0279	3.60	7.50	10.54	15.23
1.147	0.0279	3.60	14.52	15.45	17.76
0.462	0.0279	3.60	7.50	6.39	13.15
0.462	0.0279	3.60	14.52	10.90	15.33

<sup>\* (%</sup> Incr.  $K_w^a)_{Cal} = 5.06 (I/I')^{0.94} (v_m/v_w)^{0.16} (c_i \rho_i/\rho_w)^{0.17} (\mu_w/\rho_w^v_w^D_N)^{0.23}$ .

TABLE E-3 (cont'd)

(b) CONTINUOUS PHASE: MIBK

DISPERSED PHASE: Water

EFFECTIVE COLUMN HEIGHT: 30.48 cm

COLUMN DIAMETER: 3.81 cm

TRANSFER OF SOLUTE: From MIBK to Water

v <sub>m</sub> /v <sub>w</sub>	$c_{\mathbf{i}}^{} \rho_{\mathbf{i}}^{} / \rho_{\mathbf{w}}^{}$	1/1'	$\mu_{\mathbf{w}}/\rho_{\mathbf{w}}\mathbf{v}_{\mathbf{w}}\mathbf{D}_{\mathbf{N}}$ (2)	% Incr.K <sub>w</sub> a) <sub>Exptl.</sub>	(% Incr.K <sub>w</sub> a) <sub>Cal.</sub>
0.462	0.0476	1.13	30.00	4.74	3.77
0.462	0.0476	3.60	30.00	11.41	11.99
0.462	0.0476	5.82	30.00	19.51	19.34
0.462	0.0381	1.13	30.00	6.01	3.63
0.462	0.0381	3.60	30.00	13.64	11.54
0.462	0.0381	5.82	30.00	20.06	18.65
0.462	0.0279	1.13	30.00	4.12	3.44
0.462	0.0279	3.60	30.00	9.18	10.93
0.462	0.0279	5.82	30.00	17.58	17.67
0.462	0.0197	1.13	30.00	4.16	3.23
0.462	0.0197	3.60	30.00	11.40	10.29
0.462	0.0197	5.82	30.00	19.73	16.64
1.147	0.0476	1.13	30.00	8.14	5.22
1.147	0.0476	3.60	30.00	17.96	16.60
1.147	0.0476	5.82	30.00	29.75	26.84
1.147	0.0381	1.13	30.00	6.60	5.02

TABLE E-3 (cont'd)

v <sub>m</sub> /v <sub>w</sub>	c <sub>i</sub> p <sub>i</sub> /p <sub>w</sub>	1/1'	$\mu_{ m w}/ ho_{ m w}{ m v}_{ m w}{ m D}_{ m N}$	(% Incr.Kwa)Expt	(% Iner.K a)** Cal.
1.147	0.0381	3.60	30.00	18.78	15.97
1.147	0.0381	5.82	30.00	26.22	25.83
1.147	0.0279	1.13	30.00	7.23	4.76
1.147	0.0279	3.60	30.00	15.58	15.13
1.147	0.0279	5.82	30.00	26.99	24.47
1.147	0.0197	1.13	30.00	5.98	4.48
1.147	0.0197	3.60	30.00	18.02	14.25
1.147	0.0197	5782	30.00	27.97	23.03
2.158	0.0476	1.13	30.00	7.00	6.55
2.158	0.0476	3.60	30.00	18.52	20.82
2.158	0.0476	5.82	30.00	33.46	33.66
2.158	0.0381	1.13	30,00	6.94	6.30
2.158	0.0381	3.60	30,00	16.93	20.03
2.158	0.0381	5.82	30,,00	31.92	32.39
2.158	0.0279	1.13	30,,00	6.32	5.97
2.158	0.0279	3.60	30,00	16.38	18.97
2.158	0.0279	5.82	30,,00	33.07	30.68
2.158	0.0197	1.13	30.00	6.69	5.62
2.158	0.0197	3.60	30.00	21.32	17.86
2.158	0.0197	5.82	30.00	35.27	28.88
2.158	0.0279	3.60	7.50	17.73	18.97
2.158	0.0279	3.60	14.52	15.79	18.97

TABLE E-3 (cont'd)

v <sub>m</sub> /v <sub>w</sub>	$c_{i}^{\rho_{i}/\rho_{w}}$	1/1'	$\mu_{_{\mathbf{W}}}/\rho_{_{\mathbf{W}}}v_{_{\mathbf{W}}}D_{_{\mathbf{N}}}$	(% Incr.K <sub>w</sub> a) <sub>Expt</sub>	.1. (% Iner.K <sub>w</sub> a) *** Cal.
1.147	0.0279	3.60	7.50	12.67	15.13
1.147	0.0279	3.60	14.52	15.51	15.13
0.462	0.0279	3.60	7.50	6.65	10.92
0.462	0.0279	3.60	14.52	6.97	10.92

\*\* 
$$(\% \text{ Incr.}_{\mathbf{w}}^{\mathbf{K}})_{\mathbf{Cal}} = 7.44 (\mathbf{I/I'})^{1.00} (\mathbf{v_m/v_w})^{0.36} (\mathbf{c_i} \ \mathbf{\rho_i/\rho_w})^{0.17}$$

.. TABLE E-3 (cont'd)

(c) \* CONTINUOUS PHASE: MIBK

DISPERSED PHASE: Water

EFFECTIVE COLUMN HEIGHT: 40.64 cm

COLUMN DIAMETER: 7.62 cm

TRANSFER OF SOLUTE: From MIBK to Water

v <sub>m</sub> /v <sub>w</sub>	$c_i^{\rho_i/\rho_w}$	1/1'	$\mu_{_{\mathbf{W}}}/\rho_{_{\mathbf{W}}}v_{_{\mathbf{W}}}D_{_{\mathbf{N}}}$	(% Iner.Kwa)Expt1.	(% Incr.K <sub>w</sub> a)** Cal.
0.882	0.0526	3.00	60.67	10.91	12.82
0.882	0.0526	6.45	60.67	28.52	27.60
0.882	0.0434	3.00	60.67	11.35	12.40
0.882	0.0434	6.45	60.67	26.83	22.69
0.882	0.0328	3.00	60.67	13.04	11.81
0.882	0.0328	6.45	60.67	22.20	25.43
0.882	0.0253	3.00	60.67	9.25	11.29
0.882	0.0253	6.45	60.67	23.05	24.31
0.882	0.0209	3.00	60.67	2.69	10.92
0.882	0.0209	6.45	60.67	18.85	23.51
0.882	0.0494	1.54	60.67	12.07	6.52
0.882	0.0351	1.54	60.67	7.71	6.15
0.882	0.0302	1.54	60.67	3.51	5.99
0.882	0.0266	1.54	60.67	6.24	5.86
0.882	0.0231	1.54	60.67	6.09	5.72

<sup>\*</sup> Results of the Preliminary Investigation

<sup>\*\* (%</sup>Incr.K<sub>w</sub>a)<sub>Cal.</sub> = 7.44 (I/I')<sup>1.00</sup>  $(v_m/v_w)^{0.36}$   $(c_i \rho_i/\rho_w)^{0.17}$ .

TABLE E-4

# DROP SIZE DATA

TEMPERATURE: 24.5 - 25.5°C PRESSURE: Atmosphere

(a) SYSTEM: Water - 3.49% Acetic Acid - MIBK Solution

CONTINUOUS PHASE: Water

DISPERSED PHASE: MIBK

LOCATION OF DISPERSING NOZZLE: 7.62 cm from the Bottom

CONTINUOUS PHASE FLOW RATE: 0.043 ml/sec

D <sub>N</sub>	Fd ml/sec	V N cm/sec	f kc/sec	I mv.	D cm	
0.079	0.020	2.408	0	0	0.224	
0.079	0.050	10.133	. <b>O</b>	0	0.212	
0.079	0.094	19.075	0	0	0.185	
0.079	0.151	30.772	0	0	0.157	
0.079	0.020	2.408	100	0.17	0.211	
0.079	0.050	10,133	100	0.17	0.201	
0.079	0.094	19.075	100	0.17	0.174	
0.079	0.151	30.772	100	0.17	0.139	
0.079	0.020	2.408	40	0.36	0.148	
0.079	0.050	10.133	40	0.36	0.152	
0.079	0.094	19.075	40	0.36	0.135	
0.079	0.020	2.408	20	0.64	0.168	
0.079	0.050	10.133	20	0.64	0.132	
0.079	0.094	19.075	20	0.64	0.111	
0.163	0.020	0.958	0	0	0.424	
0.163	0.050	2.380	0	0	0.428	
0.163	0.094	4.481	0	0	0.401	
0.163	0.151	7.228	0	0	0.361	
0.163	0.020	0.958	100	0.17	0.400	
0.163	0.050	2.380	100	0.17	0.412	
0.163	0.094	4.481	100	0.17	0.376	
0.163	0.151	7.228	100	0.17	0.350	
0.163	0.020	0.958	40	0.36	0.356	
			,	<del>-</del>	- · - <del>-</del>	

TABLE E-4 (cont'd)

D N	Fd	$\mathbf{v}_{\mathbf{N}}$	f	·I	D
cm T	m1/sec	cm/sec	kc/sec	mv	cm
0.163	0.050	2.380	40	0.36	0.365
0.163	0.094	4.481	40	0.36	0.352
0.163	0.151	7.228	. 40	0.36	0.331
0.163	0.020	0.958	20	0.64	0.345
0.163	0.050	2.380	20	0.64	0.358
0.163	0.094	4.481	20	0.64	0.333
0.163	0.151	7.228	20	0.64	0.314
0.316	0.020	0.255	0	0	0.466
0.316	0.050	0.633	0	0	0.511
0.316	0.094	1.192	0	0	0.548
0.316	0.151	1.923	01	. 0	0.561
0.316	0.020	0.255	100	0.17	0.448
0.316	0.050	0.633	100	0.17	0.493
0.316	0.094	1.192	100	0.17	0.506
0.316	0.151	1.923	100	0.17	0.525
0.316	0.020	0.255	140	0.36	0.416
0.316	0.050	0.633	40	0.36	0.434
0.316	0.094	1.192	40	0.36	0.456
0.316	0.151	1.923	40	0.36	0.485
0.316	0.020	0.255	20	0.64	0.370
0.316	0.050	0.633	20	0.64	0.384
0.316	0.094	1.192	20	0.64	0.446
0.316	0.151	1.923	20	0.64	0.462

TABLE E-4 (cont'd)

(b) SYSTEM: Water - 3.49% Acetic Acid - MIBK Solution

CONTINUOUS PHASE: MIBK

DISPERSED PHASE: Water

LOCATION OF DISPERSING NOZZLE: 38.10 cm of from the Bottom

CONTINUOUS PHASE FLOW RATE: 0.050 ml/sec .

$^{\mathrm{D}}\mathrm{_{N}}$	$^{\mathbf{F}}\mathbf{d}$	$v_{_{ m N}}$	f	I	D
cm	m1/sec	cm/sec	kc/sec	mv	cm
0.079	0.018	3.572	0	0	0.257
0.079	0.043	5.781	Ō	Ö	0.244
0.079	0.082	8.843	0	0 .	0.226
0.079	0.018	3.572	20	0.64	0.259
0.079	0.043	5.781	20	0.64	0.238
0.079	0.082	8.843	20	0.64	0.227
0.163	0.018	0.839	0	0	0.484
0.163	0.043	1.358	0	0	0.496
0.163	0.082	2.077	0	0	0.504
0.163	0.132	3.913	0	. 0	0.520
0.163	0.018	0.839	20	0.64	0.484
0.163	0.043	1.358	20	0.64	0.489
0.163	0.082	2.077	20	0.64	0.507
0.163	0.132	3.913	20	0.64	0.523
0.316	0.018	0.223	0	0	0.571
0.316	0.043	0.361	0	0	0.565
0.316	0.082	0.553	0	0	0.584
0.316	0.132	1.041	0	0	0.557
0.316	0.018	0.223	20	0.64	0.573
0.316	0.043	0.361	20	0.64	0.552
0.316	0.082	0.553	20	0.64	0.583
0.316	0.132	1.041	20	0.64	0.567

TABLE E-4 (cont'd)

(c) SYSTEM: Water - 1,1,2 Trichloroethane (TCE)

CONTINUOUS PHASE: TCE

DISPERSED PHASE: Water

LOCATION OF DISPERSING NOZZLE: 7.62 cm from the Bottom

CONTINUOUS PHASE FLOW RATE: 0.031 ml/sec.

D N cm	F <sub>d</sub> ml/sec	V <sub>N</sub> cm/sec	f kc/sec	I	D
				mv	cm
0.079	0.018	3.572	0	0	0.323
0.079	0.043	5.781	0	0	0.349
0.079	0.082	8.843	0	0	0.368
0.079	0.018	3.572	20	0.64	0.279
0.079	0.043	5.781	20	0.64	0.320
0.079	0.082	8.843	20	0.64	0.311
0.163	0.018	0.839	0	0	0.466
0.163	0.043	1.358	0	0	0.491
0.163	0.082	2.077	0	0	0.492
0.163	0.132	3.913	0	0	0.536
0.163	0.018	0.839	20	0.64	0.397
0.163	0.043	1.358	20	0.64	0.399
0.163	0.082	2.077	20	0.64	0.434
0.163	0.132	3.913	20	0.64	0.429
0.316	0.018	0.223	0	. 0	0.519
0.316	0.043	0.361	0	0	0.514
0.316	0.082	0.553	0	0	0.505
0.316	0.132	1.041	0	0	0.501
0.316	0.018	0.223	20	0.64	0.469
0.316	0.043	0.361	20	0.64	0.446
0.316	0.082	0.553	20	0.64	0.452
0.316	0.132	1.041	20	0.64	0.454

TABLE E-5

### REST TIME DATA

TEMPERATURE: 24.5 - 25.5°C PRESSURE: Atmosphere

(a) SYSTEM: Water - 3.49 % Acetic Acid - MIBK Solution

CONTINUOUS PHASE: MIBK

DISPERSED PHASE: Water

LOCATION OF INTERFACE LEVEL: 7.62 cm from the Bottom

CONTINUOUS PHASE FLOW RATE: 0.050 ml/sec

DISPERSED PHASE FLOW RATE: 0.043 ml/sec

D <sub>N</sub>	D	f	I	tr
cm	cm	kc/sec	mv	sec
0.079	0.258	0	0	1.704
0:079	0.258	100	0.17	1.602
0.079	0.258	40	0.36	1.401
0.079	0.258	20	0.64	1.402
0.163	0.484	0	0	1.421
0.163	0.484	100	0.17	1.150
0.163	0.484	40	0.36	1.164
0.163	0.484	20	0.64	0.939
0.316	0.572	0	0	1.355
0.316	0.572	100	0.17	1.126
0.316	0.572	40	0.36	0.566
0.316	0.572	20	0.64	0.547

(b) SYSTEM: Water - 1, 1, 2 Trichloroethane (TCE)

CONTINUOUS PHASE: Water

DISPERSED PHASE: TCE

LOCATION OF INTERFACE LEVEL: 7.62 cm from the Bottom

CONTINUOUS PHASE FLOW RATE: 0.043 ml/sec

DISPERSED PHASE FLOW RATE: 0.031 ml/sec

N	D	f.	I	<sup>t</sup> r
m	cm	kc/sec	mv	sec
316	0.572	. 0	^ <b>0</b>	0.625
0.316	0.572	100	0.17	0.427
.316	0.572	40	0.36	0.466
0.316	0.572	20	0.64	0.366

TABLE E-6

# DROPLET CORRELATION DATA

TEMPERATURE: 24.5 - 25.5°C

PRESSURE: Atmosphere

1/1'	μ <sub>d</sub> /D <sub>N</sub> Δρν <sub>N</sub>	$\mu_{ m N}^{}\Delta \rho { m v}_{ m N}^{2}/\sigma$	( $\Delta D/D_N^{\prime})_{\rm Exp}$	ptl. (ΔD/D <sub>N</sub> )* Cal
1.13	0.0904	0.0364	0.165	0.157
3.60	0.0904	0.0364	0.962	0.450
5.82	0.0904	0.0364	0.709	0.696
1.13	0.0362	0.2272	0.139	0.180
3.60	0.0362	0.2272	0.759	0.516
5.82	0.0362	0.2272	1.013	0.800
1.13	0.0192	0.8030	0.139	0.197
3.60	0.0192	0.8030	0.623	0.567
5.82	0.0192	0.8030	0.937	0.878
1.13	0.1866	0.0041	0.147	0.107
3.60	0.1866	0.0041	0.417	0.306
5.82	0.1866	0.0041	0.485	0.474
1.13	0.1000	0.0259	0.483	0.122
3.60	0.0746	0.0259	0.387	0.352
5.82	0.0746	0.0259	0.429	0.544
1.13	0.0397	0.0239	0.153	0.135
3.60	0.0397	0.0914	0.301	0.386
5.82	0.0397	0.0914	0.417	
1.13	0.0347	0.2359		0.598
3.60	0.0247	0.2359	0.067	0.144
5.82	0.0247	0.2359	0.184	0.415
1.13	0.3617		0.288	0.642
3.60		0.0006	0.057	0.075
5.82	0.3617 0.3617	0.0006	0.158	0.215
1.13	0.1447	0.0006	0.304	0.334
3.60	0.1447	0.0036	0.057	0.086
5.82	0.1447	0.0036	0.244	0.247
1.13	0.1447	0.0036 0.0126	0.402 0.133	0.383 0.095

TABLE E-6 (cont'd)

1/1'	$^{\mu}{}_{d}$ / $^{D}{}_{N}$ $\Delta$ pv $_{N}$	$D_{N} \Delta \rho v_{N}^{2} / \sigma$	(\D/D <sub>N</sub> ) <sub>Exp</sub>	otl. (ΔD/D <sub>N</sub> )*
3.60	0.0770	0.0126	0.291	0.272
5.82	0.0770	0.0126	0.323	0.421
1.13	0.0479	0.0324	0.114	0.102
3.60	0.0479	0.0324	0.241	0.292
5.82	0.0479	0.0324	0.313	0.452
5.82	0.3225	0.0003	0.158	0.256
5.82	0.1992	0.0009	0.215	0.276
5.82	0.1301	0.0021	0.168	0.276
5.82	0.0691	0.0074	0.149	0.323
5.82	0.1662	0.0025	0.301	0.364
5.82	0.1027	0.0065	0.564	0.392
5.82	0.0671	0.0153	0.356	0.417
5.82	0.0356	0.0542	0.656	0.459
5.82	0.0325	0.1341	0.557	0.613
5.82	0.0498	0.0573	0.367	0.575
5.82	0.0805	0.0219	0.721	0.535

<sup>\*</sup>  $\Delta D/D_N = 2.78 (\mu_d/D_N \Delta \rho v_N)^{0.66} (D_N \Delta \rho v_N^2/\sigma)^{0.39} (I/I')^{0.89}$ 

TABLE E-7

#### INTERFACIAL AREA DATA

SYSTEM: Water - Acetic Acid - MIBK

CONTINUOUS PHASE: Water

DISPERSED PHASE: MIBK

LOCATION OF DISPERSING NOZZLE: 7.62 cm from the Bottom

EFFECTIVE COLUMN HEIGHT: 30.48 cm

COLUMN DIAMETER : 3.81 cm

SOLUTE CONCENTRATION OF AQUEOUS FEED: Zero

SOLUTE CONCENTRATION OF ORGANIC' FEED: 3.49 wt.%

CONTINUOUS PHASE FLOW RATE: 0.043 ml/sec

TEMPERATURE: 24.5 - 25.5°C

PRESSURE': Atmosphere

D N cm	F d m1/sec	V N cm/sec	1/1'	a x 10 <sup>3</sup> cm <sup>2</sup> /unit volume
0.316	0.020	0.255	0	5.35
0.316	0.050	0.633	Ö	10.01
0.316	0.094	1.192	Ö	16.14
0.316	0.020	0.255	1.13	5.34
0.316	0.050	0.633	1.13	10.13
0.316	0.094	1.192	1.13	16.84
0.316	0.020	0.255	3.60	5.35
0.316	0.050	0.633	3.60	10.70
0.316	0.094	1.192	3.60	17.99
0.316	0.020	0.255	5.82	5.49

TABLE E-7 (cont'd)

D <sub>N</sub> cm	F <sub>d</sub> m1/sec	V <sub>N</sub> cm/sec	I/I'	a x 10 <sup>3</sup> cm <sup>2</sup> /unit volum
				cm / unit volum
0.316	0.050	0.633	5.82	11.50
0.316	0.094	1.192	5.82	18.27
0.163	0.020	0.958	0	5.59
0.163	0.050	2.380	Ö	11.39
0.163	0.094	4.481	ŏ	20.99
0.163	0.020	0.958	1.13	5.65
0.163	0.050	2.380	1.13	11.64
0.163	0.094	4.481	1.13	22.11
0.163	0.020	0.958	3.60	5.86
0.163	0.050	2.380	3.60	12.61
0.163	0.094	4.481	3.60	23.37
0.163	0.020	0.958	5.82	5.94
0.163	0.050	2.380	5.82	12.79
0.163	0.094	4.481	5.82	24.52
0.079	0.020	2.408	0	8.40
0.079	0.050	10.133	Ö	21.25
0.079	0.094	19.075	Ö	45.27
0.079	0.020	2.408	1.13	8.84
0.079	0.050	10.133	1.13	22.35
0.079	0.094	19.075	1.13	48.08
0.079	0.020	2.408	3.60	12.22
0.079	0.050	10.133	3.60	29.28
0.079	0.094	19.075	3.60	61.78
0.079	0.020	2.408	5.82	10.85
0.079	0.050	10.133	5.82	33.63
0.079	0.094	19.075	5.82	75.04

TABLE E-8

### MASS TRANSFER COEFFICIENT DATA

SYSTEM: Water - Acetic Acid - MIBK

TRANSFER OF SOLUTE: From MIBK to Water

EFFECTIVE COLUMN HEIGHT: 30.48 cm

COLUMN DIAMETER: 3.81 cm

SOLUTE CONCENTRATION OF AQUEOUS FEED: Zero

TEMPERATURE: 24.5 - 25.5°C

PRESSURE: Atmosphere

(a) CONTINUOUS PHASE: Water

DISPERSED PHASE: MIBK

LOCATION OF DISPERSING NOZZLE: 7.62 cm from the Bottom

LOCATION OF INTERFACE LEVEL: 38.10 cm from the Bottom

C m2 wt.%	F <sub>m</sub> /F <sub>w</sub>	1/1'	K <sub>w</sub> x 10 <sup>2</sup> cm/sec	
5.91	0.462	0	0.400	
4.73	0.462	0	0.378	
3.49	0.462	0	0.362	
2.47	0.462	0	0.298	
5.91	0.462	1.13	0.414	
4.73	0.462	1.13	0.390	
3.49	0.462	1.13	0.373	
2.47	0.462	1.13	0.304	
5.91	0.462	3.60	0.336	
4.73	0.462	3.60	0.310	
3.49	0.462	3.60	0.288	
2.47	0.462	3.60	0.242	
5.91	0.462	5.82	0.418	
4.73	0.462	5.82	0.399	

TABLE E-8 (cont'd)

C <sub>m2</sub>	F <sub>m</sub> // F	I/I'	$K_{\rm w} \times 10^2$
vt. %	W		cm/sec
3.49	0.462	5.82	0.346
2.47	0.462	5.82	0.289
5.91	1.147	0	0.194
4.73	1.147	0	0.189
3.49	1.147	0	0.177
2.47	1.147	0	0.151
5.91	1.147	1.13	0.198
4.73	1.147	1.13	0.198
3.49	1.147	1.13	0.183
2.47	1.147	1.13	0.158
-5 <b>.</b> 91	1.147	0.36	0.166
4.73	1.147	0.36	0.163
3.49	1.147	0.36	0.153
2.47	1.147	0.36	0.136
5.91	1.147	5.82	0.166
4.73	1.147	5.82	0.158
3.49	1.147	5.82	0.154
2.47	1.147	5.82	0.132
5.91	2.158	0	0.123
4.73	2.158	0	0.119
3.49	2.158	0	0.109
2.47	2.158	0	0.094
5.91	2.158	1.13	0.126
4.73	2.158	1.13	0.122
3.49	2.158	1.13	0.112
2.47	2.158	1.13	0.096
5.91	2.158	3.60	0.110
4.73	2.158	3.60	0.105
3.49	2.158	3.60	0.098
2.47	2.158	3.60	0.084
5.91	2.158	5.82	0.102
4.73	2.158	5.82	0.100
3.49	2.158	5.82	0.091
2.47	2.158	5.82	0.079

(b) CONTINUOUS PHASE: MIBK

DISPERSED PHASE: Water

LOCATION OF DISPERSING NOZZLE: 38.10 cm from the Bottom

LOCATION OF INTERFACE LEVEL: 7.62 cm from the Bottom

C <sub>m2</sub> wt.%	F <sub>m</sub> /F <sub>w</sub>	I/I'	K x 10 <sup>2</sup> cm/sec
5.91	0.462	0	0.117
4.73	0.462	Ö	0.114
3.49	0.462	Ŏ	0.108
2.47	0.462	Ŏ	0.104
5.91	0.462	1.13	0.124
4.73	0.462	1.13	0.123
3.49	0.462	1.13	0.115
2.47	0.462	1.13	0.111
5.91	0.462	3.60	0.138
4.73	0.462	3.60	0.137
3.49	0.462	3.60	0.125
2.47	0.462	3.60	0.123
5.91	0.462	5.82	0.145
4.73	0.462	5.82	0.145
3.49	0.462	5.82	0.135
2.47	0.462	5.82	0.132
5.91	1.147	0	0.189
4.73	1.147	0	0.184
3.49	1.147	0	0.175
2.47	1.147	0	0.167
5.91	1.147	1.13	0.208
4.73	1.147	1.13	0.200
3.49	1.147	1.13	0.191
2.47	1.147	1.13	0.181
5.91	1.147	3.60	0.236
4.73	1.147	3.60	0.232
3.49	1.147	3.60	0.214
2.47	1.147	3.60	0.210
5.91	1.147	5.82	0.260
4.73	1.147	5.82	0.246
3.49	1.147	5.82	0.235
2.47	1.147	5.82	0.227

TABLE E-8 (cont'd)

C m2 rt.%	Fm/F <sub>w</sub>	ı∤ı'	K x 10 <sup>2</sup> cm/sec
5.91	2.158	0	0.280
4.73	2.158	Ö	0.274
3.49	2.158	Ō	0.252
2.47	2.158	0	0.209
5 <b>.</b> 91	2.158	1.13	0.305
4.73	2.158	1.13	0.298
3.49	2.158	1.13	0.273
2.47	2.158	1.13	0.228
5.91	2.158	3.60	0.351
4.73	2.158	3.60	0.339
3.49	2.158	3.60	0.311
2.47	2.158	3.60	0.269
5.91	2.158	5.82	0.396
4.73	2.158	5.82	0.382
3.49	2.158	5.82	0.355
2.47	2.158	5.82	0.300

# APPENDIX F

ANALYSIS OF ERROR IN THE MATERIAL

BALANCE FOR ACETIC ACID

Error in the material balance for acetic acid was calculated by the following equations

$$A_{w} = F_{w} \rho_{w} (C_{w2} - C_{w1})$$

$$A_{m} = F_{m} \rho_{m} (C_{m:1} - C_{m2})$$

$$A_{av} = (A_{w} + A_{m})/2$$
ERROR = 
$$\frac{|A_{w} - A_{m}|}{A_{av}} \times 1.00$$

where A : amount of acetic acid transferred to the water phase, g/sec

 $\mathbf{A}_{\mathbf{m}}$ : amount of acetic acid extracted from the MIBK phase, g/sec

 $\mathbf{A}_{\mathbf{a}\mathbf{v}}$  : average value of  $\mathbf{A}_{\mathbf{w}}$  and  $\mathbf{A}_{\mathbf{m}}$  , g/sec

C: acid concentration, wt. %,

F : flow rate, ml/sec

ρ : density, g/ml

Subscript 8

m = MIBK phase

w = water phase:

1 = inlet

2: = outlet

The average error in the material balance for all the runs is 18.9%. Detailed data are given in Table F-1. If  $F_{\rm m}$  is increased by a factor of 1.22 or  $F_{\rm w}$  is reduced to 82% of its value, the average error is 5.43% as can be seen from Table F-2. The values given in Tables F-1 and F-2 correspond to the data given in Table E-1

25.43

23.58

29.13

28.58

26.44

29.66

26.58

27.38 25.75

TABLE F-1 ERROR IN THE MATERIAL BALANCE FOR ACETIC ACID

	(a)	•	
A <sub>w</sub>	A <sub>m</sub>	Error	
g/sec	g/sec	%	
0.0602	0.0493	19.95	
0.0645	0.0504	24.54	
0.0684	0.0550	21.60	
0.0735	0.0568	25.67	
0.0477	0.0373	24.59	
0.0503	0.0400	22.83	
0.0538	0.0414	25.86	- <u>1</u> -1
0.0576	0.0461	22.26	
0.0348	0.0278	22.31	
0.0366	0.0301	19.42	
0.0383	0.0309	21.37	•
0.0404	0.0314	25.24	
0.0224	0.0189	16.88	
0.0219	0.0186	16.65	
0.0232	0.0194	18.13	•
0.0237	0.0198	17.52	
0.0254	0.0202	22.87	
0.0249	0.0208	18.10	•
0.0262	0.0208	23.09	
	(ъ)		
A <sub>w</sub>	A <sub>m</sub>	Error	
g/sec	g/sec	%	
0.0847	0.0616	31.59	
0.0886	0.0704	22.87	
0.0942	0.0750	18.78	
0.1045	0.0860	19.41	· · · · · · ·
0.0662	0.0572	14.62	•
0.0714	0.0596	17.79	
0.0757	0.0604	22.46	
0.0737	0.0004	22.40	

0.0636

0.0380

0.0388

0.0416

0.0468

0.0236

0.0260

0.0284 0.0312

0.0821

0.0482

0.0520

0.0555 ·

0.0611

0.0318

0.0340

0.0374 0.0404

(c)

A W g/sec		A m g/sec		Error %	
0.1118		0.0978		13.40	
0.1183		0.1053		11.60	
0.1281		0.1143		11.41	
0.1393		0.1218		13.40	
0.0894		0.0684		26.61	
0.0955		0.0737		25.73	
0.1019		0.0835		19.89	•
0.1118		0.0955		15.72	
0.0632	•	0.0489		25.57	
0.0675		0.0549		20.61	
0.0731		0.0639		13.40	
0.0791	•	0.0707	W.	11.26	•
0.0417		0.0301		32.40	•
0.0447	•	0.0331	•	29.90	
0.0486		0.0361	· .	29.51	
0.0538		0.0414	• •	26.05	

(d) .

A <sub>w</sub> .		A <sub>m</sub>		•		Error	
g/sec		g/sec	•		•	%	
0.0409		0.0350				15.31	
0.0430		0.0346		•.	• • •	21.76	
0.0443	•	0.0386		:		13.83	
0.0473		0.0376				22.85	
0.0323	•	0.0285			٠,	12.42	•
0.0344		0.0285				18.83	
0.0357		0.0312				13.43	
0.0378		0.0310	•			19.74	
0.0237		0.0205			•	14.37	
0.0249	· ·	0.0195		•		24.38	
0.0254	•	0.0221				13.87	•
0.0271	•	0.0226			• • •	18.25	
0.0172		0.0141				19.95	
0.0181	•	0.0131				31.69	
0.0185		0.0150		•		20.58	
0.0198		0.0150				27.23	• • •

A <sub>w</sub> . g/sec		A <sub>m</sub> g/sec	Error %
0.0675		0.0624	7.87
0.0735		0.0572	24.98
0.0765		0.0708	7.79
0.0830		0.0712	15.29
0.0538		0.0504	6.43
0.0581		0.0448	25.77
0.0615		0.0564	8.64
0.0654		0.0544	18.30
0.0391		0.0364	7.23
0.0421		0.0344	20.22
0.0439		0.0400	9.21
0.0473		0.0424	10.93
0.0280	· · •	0.0252	10.35
0.0297		0.0232	24.48
0.0323		0.0256	22.99
0.0348		0.0260	29.03
· · · · · · · · · · · · · · · · · · ·	(f) (		
A <sub>w</sub> g/sec	(f) \	A <sub>m</sub> g/sec	Error %
g/sec 0.0976	(f) \	0.0948	% 2.97
g/sec 0.0976 0.1041	(£)	0.0948 0.0880	% 2.97 16.74
0.0976 0.1041 0.1118	(£)	0.0948 0.0880 0.0978	% 2.97 16.74 13.40
0.0976 0.1041 0.1118 0.1221	(£)	0.0948 0.0880 0.0978 0.1053	2.97 16.74 13.40 14.81
0.0976 0.1041 0.1118 0.1221 0.0778	(£)	0.0948 0.0880 0.0978 0.1053 0.0752	% 2.97 16.74 13.40 14.81 3.44
0.0976 0.1041 0.1118 0.1221 0.0778 0.0839	(£)	0.0948 0.0880 0.0978 0.1053 0.0752 0.0639	2.97 16.74 13.40 14.81 3.44 26.97
0.0976 0.1041 0.1118 0.1221 0.0778 0.0839 0.0877	(£)	0.0948 0.0880 0.0978 0.1053 0.0752 0.0639 0.0835	% 2.97 16.74 13.40 14.81 3.44 26.97 4.96
0.0976 0.1041 0.1118 0.1221 0.0778 0.0839 0.0877 0.0976	(£)	0.0948 0.0880 0.0978 0.1053 0.0752 0.0639 0.0835 0.0760	% 2.97 16.74 13.40 14.81 3.44 26.97 4.96 24.96
0.0976 0.1041 0.1118 0.1221 0.0778 0.0839 0.0877 0.0976 0.0559	(£)	0.0948 0.0880 0.0978 0.1053 0.0752 0.0639 0.0835 0.0760 0.0489	% 2.97 16.74 13.40 14.81 3.44 26.97 4.96 24.96 13.40
0.0976 0.1041 0.1118 0.1221 0.0778 0.0839 0.0877 0.0976 0.0559 0.0585	(£)	0.0948 0.0880 0.0978 0.1053 0.0752 0.0639 0.0835 0.0760 0.0489 0.0511	% 2.97 16.74 13.40 14.81 3.44 26.97 4.96 24.96 13.40 13.40
0.0976 0.1041 0.1118 0.1221 0.0778 0.0839 0.0877 0.0976 0.0559 0.0585 0.0628	(£)	0.0948 0.0880 0.0978 0.1053 0.0752 0.0639 0.0835 0.0760 0.0489 0.0511 0.0541	2.97 16.74 13.40 14.81 3.44 26.97 4.96 24.96 13.40 13.40 14.77
0.0976 0.1041 0.1118 0.1221 0.0778 0.0839 0.0877 0.0976 0.0559 0.0585 0.0628 0.0692	(£)	0.0948 0.0880 0.0978 0.1053 0.0752 0.0639 0.0835 0.0760 0.0489 0.0511 0.0541	2.97 16.74 13.40 14.81 3.44 26.97 4.96 24.96 13.40 13.40 14.77
0.0976 0.1041 0.1118 0.1221 0.0778 0.0839 0.0877 0.0976 0.0559 0.0559 0.0585 0.0628 0.0692 0.0357	(£)	0.0948 0.0880 0.0978 0.1053 0.0752 0.0639 0.0835 0.0760 0.0489 0.0511 0.0541 0.0602 0.0316	2.97 16.74 13.40 14.81 3.44 26.97 4.96 24.96 13.40 13.40 14.77 14.02 12.21
0.0976 0.1041 0.1118 0.1221 0.0778 0.0839 0.0877 0.0976 0.0559 0.0585 0.0692 0.0357 0.0378	(£)	0.0948 0.0880 0.0978 0.1053 0.0752 0.0639 0.0835 0.0760 0.0489 0.0511 0.0541 0.0602 0.0316 0.0271	2.97 16.74 13.40 14.81 3.44 26.97 4.96 24.96 13.40 13.40 14.77 14.02 12.21 33.18
0.0976 0.1041 0.1118 0.1221 0.0778 0.0839 0.0877 0.0976 0.0559 0.0559 0.0585 0.0628 0.0692 0.0357	(£)	0.0948 0.0880 0.0978 0.1053 0.0752 0.0639 0.0835 0.0760 0.0489 0.0511 0.0541 0.0602 0.0316	2.97 16.74 13.40 14.81 3.44 26.97 4.96 24.96 13.40 13.40 14.77 14.02 12.21

(g)

A <sub>w</sub> g/sec	A m g/sec	Error %
0.0318	0.0272	15.66
0.0331	0.0285	15.03
0.0344	0.0290	17.17
0.0378	0.0283	28.78
0.0443	0.0384	14.25
0.0482	0.0408	16.55
0.0473	0.0368	24.97
0.0520	0.0436	17.63
0.0581	0.0504	14.14
0.0658	0.0564	15.37
0.0611	0.0534	13.40
0.0700	0.0602	14.64
	(h)	
A w g/sec	A m g/sec	Error %
g/sec	A m g/sec	%
g/sec 0.0237	Amg/sec	% 12.06
g/sec 0.0237 0.0243	A m g/sec 0.0210 0.0216	% 12.06 14.35
0.0237 0.0243 0.0241	A m g/sec 0.0210 0.0216 0.0210	% 12.06 14.35 13.85
0.0237 0.0243 0.0241 0.0254	A m g/sec 0.0210 0.0216 0.0210 0.0221	% 12.06 14.35 13.85 13.87
0.0237 0.0243 0.0241 0.0254 0.0391	Amg/sec  0.0210 0.0216 0.0210 0.0221 0.0332	% 12.06 14.35 13.85 13.87 16.40
0.0237 0.0243 0.0241 0.0254 0.0391 0.0430	Amg/sec  0.0210 0.0216 0.0210 0.0221 0.0332 0.0364	% 12.06 14.35 13.85 13.87 16.40 16.62
0.0237 0.0243 0.0241 0.0254 0.0391 0.0430 0.0387	Amg/sec  0.0210 0.0216 0.0210 0.0221 0.0332 0.0364 0.0332	% 12.06 14.35 13.85 13.87 16.40 16.62 15.30
0.0237 0.0243 0.0241 0.0254 0.0391 0.0430 0.0387 0.0434	Amg/sec  0.0210 0.0216 0.0210 0.0221 0.0332 0.0364 0.0332 0.0372	% 12.06 14.35 13.85 13.87 16.40 16.62 15.30 15.45
0.0237 0.0243 0.0241 0.0254 0.0391 0.0430 0.0387 0.0434 0.0559	Amg/sec  0.0210 0.0216 0.0210 0.0221 0.0332 0.0364 0.0332 0.0372 0.0489	% 12.06 14.35 13.85 13.87 16.40 16.62 15.30 15.45 13.40
0.0237 0.0243 0.0241 0.0254 0.0391 0.0430 0.0387 0.0434	Amg/sec  0.0210 0.0216 0.0210 0.0221 0.0332 0.0364 0.0332 0.0372	% 12.06 14.35 13.85 13.87 16.40 16.62 15.30 15.45

TABLE F-2 ERROR IN THE MATERIAL BALANCE FOR ACETIC ACID

# IF F IS INCREASED BY A FACTOR OF 1.22

(a)

A <sub>w</sub>	A <sub>m</sub>		Error	
g/sec	g/sec		%	
0.0602	0.0601		0.13	
0.0645	0.0615		4.78	
0.0684	· 0.0672		1.80	
0.0735	0.0693		5.93	
0.0477	0.0455		4.82	
0.0503	0.0488		3.05	:
0.0538	0.0506		6.12	•
0.0576	0.0562		2.46	
0.0348	0.0340			
0.0366	0.0340		2.52	•
0.0383			0.40	
	0.0377		1.57	
0.0404	0.0383		5.49	
0.0224	0.0230		2.97	
0.0219	0.0226		3.20	· ·
0.0232	0.0236		1.70	
0.0237	0.0242		2.32	
0.0254	0.0246		3.10	
0.0249	0.0254		1.73	
0.0262	0.0254	•	3.31	
	(b)			

A w g/sec		A m g/sec	J	Error %
0.0847		0.0752		11.96
0.0886	• • • • • • • • • • • • • • • • • • • •	0.0859		3.08
0.0942	,	0.0952		1.05
0.1045		0.1049	• .	0.41
0.0662		0.0700		5.24
0.0714		0.0727		1.85
0.0757	•	0.0737		2.67
0.0821		0.0776	•	5.68
0.0482		0.0464		3.81
0.0520		0.0473		9.45

continued.

### TABLE F-2 (continued)

(b)

	(0)			
	A <sub>m</sub>		Error	
g/sec	g/sec		%	
0.0555	0.0508		8.88	
0.0611	0.0571		6.71	
0.0318	0.0288			•
0.0340	0.0317		9.99	
0.0374	0.0347		6.85 7.67	•
0.0404	0.0381		6.00	
	(c)		•	
A <sub>w</sub>	A <sub>m</sub>		Error	
g/sec	m g/sec		%	
	0/		/9	· .
0.1118	0.1193		6.46	
0.1183	0.1284		8.26	
0.1281	0.1395		8.45	• . • • • • •
0.1393	0.1486		6.46	
0.0894	0.0835		6.88	
0.0955	0.0899		5.99	
0.1019	0.1018		0.07	
0.1118	0.1165		4.13	
0.0632	0.0596		5.82	
0.0675	0.0670	•		
0.0731	0.0780		0.80	
0.0791	0.0760		6.46	
0.0417			8.61	
0.0447	0.0367		12.79	,
0.0486	0.0404	• •	10.23	
	0.0440		9.83	·
0.0538	0.0505		6.32	
	(d)			
A. W	A <sub>m</sub>		Error	**************************************
g/sec	g/sec			•
,,,,,,,,,,,,,,,,,,,,,,,,,,,,,,,,,,,,,,,	g/ Bec	<u>-</u>	%	•
0.0409	0.0428	•	4.54	
0.0430	0.0422	•	1.97	
0.0443	0.0470		6.03	. ,
0.0473	0.0459			•
0.0323	0.0348		3.07	
.0344	0.0348	•	7.45	
.0357	0.0348		1.00	
	0.0301		6.44	

continued...

continued...

TABLE F-2 (continued)

(d)

A <sub>w</sub>	A <sub>m</sub>	Error
g/sec	g/sec	8
0.0378	0.0379	0.08
0.0237	0.0250	
0.0249	0.0238	5.49
0.0254	0.0256	4.62
0.0271	0.0275	5.99
0.0172	0.0172	1.59
0.0181	0.0160	0.13
0.0185	0.0184	12.06
0.0198	0.0184	0.77 7.51
	(e)	
A	A <sub>m</sub>	Error
~	m	
g/sec	g/sec	%
0.0675	0.0761	12.00
0.0735	0.0698	5.23
0.0765	0.0864	
0.0830	0.0869	12.07
0.0538	0.0615	4.56 13.43
0.0581	0.0547	
0.0615	0.0688	6.02 11.23
0.0654	0.0664	1.53
0.0391	0.0444	12.63
0.0421	0.0420	0.41
0.0439	0.0488	10.66
0.0473	0.0517	8.94
0.0280	0.0307	
0.0297	0.0283	9.52
0.0323	0.0312	4.71 3.21
0.0348	0.0317	9.35
	(f)	
A <sub>w</sub>	A <sub>m</sub>	Error
g/sec	m ~/soc	
B/ 000	g/sec	%
0.0976	0.1156	16.87
0.1041	0.1073	3.10
0.1118	0.1193	6.46
0.1221	0.1284	5.05
o <b>.</b> 0778	0.0917	16.41
•		

continued....

TABLE F-2 (continued)

(f)

A w g/sec		A m g/sec		Error %	
0.0839		0.0780		7.25	
0.0877		0.1018		14.89	
.0.0976		0.0927		5.20	
0.0559		0.0596		6.46	•
0.0585		0.0624		6.46	
0.0628		0.0661		5.09	
0.0692	•	0.0734		5.84	***
0.0357		0.0385		7.66	•
0.0378	and the second of the second	0.0330		13.58	
0.0417		0.0440		5.43	
0.0460		0.0404		13.07	•
	**************************************	(g)	•		
A		A <sub>m</sub>		Error	
g/sec		. ш			
&/ sec		g/sec		%	
0.0318		0.0332		4.20	
0.0331		0.0348	•	4.82	
0.0344		0.0353	•	2.67	
0.0378		0.0346	•	9.09	
0.0443		0.0469	•	5.61	•
0.0482	A CONTROL OF THE CONT	0.0498	•	3.30	•
0.0473		0.0449	•	5.21	
0.0520	•	0.0532		2.21	
0.0581		0.0615	• ,	5.72	
0.0658	•	0.0688		4.48	
0.0616		0.0651	•	6.46	
0.0697		0.0734		5.22	•
<del></del>	•	(h)		•	
A <sub>w</sub>		Δ		Error	
	•	A <sub>m</sub>	•		
g/sec		g/sec		%	
0.0237		0.0256		7.81	
0.0249		0.0264		5.51	
0.0241		0.0256		6.01	
0.0254		0.0269		5.99	
0.0391		0.0405		3.45	•

## TABLE F-2 (continued)

(h)

A <sub>w</sub> g/sec		A m g/sec		Error %	
0.0430		0.0444		3.22	
0.0387		0.0405		4.56	
0.0434	1 2 × 4	0.0454		4.40	
0.0559		0.0596		6.46	
0.0632		0.0670		5.78	
0.0559	 	0.0587		4.91	
0.0628		0.0651		3.69	

#### SUMMARY AND CONTRIBUTIONS TO KNOWLEDGE

This thesis project is the first study concerning the application of ultrasonic vibration to a continuous countercurrent liquid-liquid extraction process. Single-drop extraction experiments were carried out in a spray column with an ultrasonic vibration source at the bottom, using water-acetic acid-MIBK as a test system. The effect of ultrasonic vibration on the overall extraction efficiency, droplet size, coalescence of the drops at the interface, interfacial area of contact, and the overall mass transfer coefficient were investigated. The results may be briefly summarized as follows:

- (1) The overall extraction efficiency, calculated in terms of the capacity coefficient, was increased by the imposition of ultrasonic vibration. The capacity coefficient increased with the intensity ratio; a term proposed for correlating the data and defined as the ratio of ultrasonic intensity to the threshold intensity of cavitation, the latter being a function of the frequency. Nevertheless, there was a practical limit in the ultrasonic intensity beyond which emulsification would occur.
- (2) For the case where the light liquid was dispersed, i.e., when the dispersing nozzle was located close to the ultrasonic source, the increase in the capacity coefficient was mainly due to a decrease in the interfacial area of contact. On the other hand, when the heavy liquid

was dispersed and the aqueous-organic interface was near the ultrasonic source instead of the dispersing nozzle, the increase in the capacity coefficient was primarily due to an increase in the degree of turbulence at the aqueous-organic interface, reducing the resistance to mass transfer there and hence increasing the mass transfer coefficient. This increase of turbulence at the interface by ultrasonic vibration was verified by the decrease of rest time of the drops at the interface. For both cases, the extraction rate during the drop rise or fall period was found not to be affected significantly by the ultrasonic vibration.

(3) The percent increase in the capacity coefficient, caused by ultrasonic vibration for both cases mentioned above, may be calculated by the following empirical equations.

For light liquid dispersed,

% Increase in 
$$K_w a = 5.06 (I/I')^{0.94} (v_m/v_w)^{0.16} (c_i \rho_i/\rho_w)^{0.17} (\mu_w/\rho_w v_w D_N)^{0.23}$$
;

and for heavy liquid dispersed,

% Increase in 
$$K_w a = 7.44 (I/I')^{1.00} (V_m/V_w)^{0.36} (C_i \rho_i/\rho_w)^{0.17}$$

where  $I < I_c$ .

These correlations are applicable to systems having values of physical properties similar to that of water-acetic acid-MIBK.

(4) The decrease in the average drop diameter, ΔD, as the dispersing nozzle is subjected to an intense ultrasonic field, can be estimated by the following correlation

$$\Delta D/D_N = 2.78 (\mu_d/D_N \Delta \rho v_N)^{0.66} (D_N \Delta \rho v_N^2/\sigma)^{0.39} (I/I')^{0.89}$$

where I and I' are measured at the dispersing nozzle tip, and I < I  $_{
m c}$  .

(5) The interfacial area of contact, a, and the overall mass transfer coefficient, K, in a spray-type liquid-liquid extraction column under ultrasonic vibration may be represented by the following linear equations respectively.

$$(a)_{I} = \alpha(I/I') + (a)_{0}$$
 (I < I<sub>c</sub>)

$$(K)_{I} = \beta(I/I') + (K)_{0}$$
  $(I < I_{c})$ 

#### SUGGESTIONS FOR FUTURE WORK

The results of this study indicate that the application
of ultrasonic vibration to a continuous countercurrent liquid-liquid
extraction process may be promising, and thus further studies with regard
to this aspect are justified. It is suggested that the following areas
of investigation may form a suitable basis for future research:

- (1) An investigation into the optimum design of an ultrasonic vibration column: The experimental design used in the present study is not ideal, since the vibration affects either the dispersing nozzle or the aqueous-organic interface section only. If arrangement can be made in such a way that the ultrasonic source comes from both the top and the bottom of the column, or even along the column by making use of cylindrical transducers, the increase in the extraction efficiency is believed to be much more encouraging. A thorough study along this line is a necessary step towards developing an ultrasonic vibration column.
- (2) An investigation into the methods of lifting the intensity limit: As shown in the present study, there exists an upper limit in the ultrasonic intensity beyond which emulsification will occur in liquids, making the separation in the column difficult. A better understanding of the emulsification phenomenon caused by ultrasonic vibration in order to lift such an intensity limit will be an interesting subject of research.

- (3) An investigation into the effect of ultrasonic vibration on the flooding characteristics of an extraction column: It has been known from the performance of pulsed columns that pulsing lowers the flooding limit and hence the maximum throughput of the column. Ultrasonic vibration is believed to have a similar effect on the flooding limit. A systematic study on this subject will provide a useful information for the design of an ultrasonic vibration column.
- (4) An investigation into the effect of ultrasonic vibration on the axial mixing of an extraction column: Axial mixing is known to reduce the extraction rates by destruction of the true countercurrent concentration differences between the liquids. As the column liquids are subjected to an intense ultrasonic field, the degree of axial mixing in the column probably will be affected by the imposition of ultrasonic vibration. An understanding of this phenomenon will help in evaluating the performance of an ultrasonic vibration column.
- (5) An investigation into the development of a generalized mass transfer correlation for an ultrasonic vibration column: By using systems with different values of physical properties and studying the enhancement of mass transfer rate by ultrasonic vibration, it may be possible to develop a generalized correlation for predicting the mass transfer rate in an ultrasonic vibration column.